โครงการการเรียนการสอนเพื่อเสริมประสบการณ์

ลักษณะเฉพาะของทัวร์มาลีนเพื่อเป็นตัวบ่งชี้แหล่งกำเนิดทางภูมิศาสตร์ และการปรับปรุงคุณภาพ

โดย

นางสาวเลอพร พงษ์สามารถ
เลขประจำตัวนิสิต 5932729423

โครงการนี้เป็นส่วนหนึ่งของการศึกษาระดับปริญญาตรี
ภาควิชาธรณีวิทยา คณะวิทยาศาสตร์ จุฬาลงกรณ์มหาวิทยาลัย
ปีการศึกษา 2562

ลักษณะเฉพาะของทัวร์มาลีนเพื่อเป็นตัวบ่งชี้แหล่งกำเนิดทางภูมิศาสตร์และการปรับปรุงคุณภาพ

นางสาวเลอพร พงษ์สามารถ

โครงงานนี้เป็นส่วนหนึ่งของการศึกษาตามหลักสูตรวิทยาศาสตร์บัณฑิต

ภาควิชาธรณีวิทยา คณะวิทยาศาสตร์ จุฬาลงกรณ์มหาวิทยาลัย

ปีการศึกษา 2562

CHARACTERISTICS OF TOURMALINE FOR INDICATOR OF GEOGRAPHIC ORIGIN

AND QUALITY ENHANCEMENT

MISS LERPORN PONGSAMART

A Project Submitted in Partial Fulfillment of the Requirements

for the Degree of Bachelor of Science Program in Geology

Department of Geology, Faculty of Science, Chulalongkorn University

Academic Year 2019

หัวข้อโครงงาน	ลักษณะเฉพาะของทัวร์มาลีนเพื่อเป็นตัวบ่งชี้แหล่งกำเนิดทางภูมิศาสตร์และการปรับปรุงคุณภาพ
โดย	นางสาวเลอพร พงษ์สามารถ
สาขาวิชา	ธรณีวิทยา
อาจารย์ที่ปรึกษาโครงงานหลัก	ศาสตราจารย์ ดร.จักรพันธ์ สุทธิรัตน์

วันที่ส่ง

___/___/_____

วันที่อนุมัติ

___/___/_____

ลงชื่อ__________________________

(ศาสตราจารย์ ดร.จักรพันธ์ สุทธิรัตน์)

อาจารย์ที่ปรึกษาโครงงาน

Project title	CHARACTERISTICS OF TOURMALINE FOR INDICATOR OF GEOGRAPHIC ORIGIN AND QUALITY ENHANCEMENT
By	Miss Lerporn Pongsamart
Field of Study	Geology
Project Advisor	Professor Dr. Chakkaphan Sutthirat

Date of submission

___/___/_____

Date of approval

___/___/_____

Sign______________________________

Professor Dr. Chakkaphan Sutthirat

Project Advisor

เลอพร พงษ์สามารถ : ลักษณะเฉพาะของทัวร์มาลีนเพื่อเป็นตัวบ่งชี้แหล่งกำเนิดทางภูมิศาสตร์และการปรับปรุงคุณภาพ. (CHARACTERISTICS OF TOURMALINE FOR INDICATOR OF GEOGRAPHIC ORIGIN AND QUALITY ENHANCEMENT) อ.ที่ปรึกษาโครงการหลัก: ศาสตราจารย์ ดร.จักรพันธ์ สุทธิรัตน์, 141 หน้า.

งานวิจัยนี้มีจุดประสงค์หลักเพื่อศึกษาลักษณะเฉพาะของพลอยทัวร์มาลีนจากแหล่งสำคัญ ประกอบด้วย บราซิล โมซัมบิก ไนจีเรีย และมาดากัสการ์ รวมถึงศึกษาการเปลี่ยนแปลงลักษณะทางกายภาพของพลอยทัวร์มาลีนที่ผ่านการฉายรังสีแกมมา โดยการใช้เครื่องมือวิเคราะห์ขั้นพื้นฐาน และขั้นสูงจาก ICA GemLab เพื่อพัฒนาฐานข้อมูลในการตรวจสอบแหล่งกำเนิดพลอยทัวร์มาลีน

ตัวอย่างพลอยทัวร์มาลีนที่ใช้ในการศึกษาครั้งนี้จำนวน 84 ตัวอย่าง มีลักษณะค่อนข้างใส มีรอยแตกภายในค่อนข้างมาก และมีมลทินภายในที่เห็นชัด ไม่แสดงการเรืองแสงภายใต้แสงเหนือม่วง และพบมลทินภายในชัดเจน ประกอบด้วยผลึกแร่หลากชนิด มลทินรอยแตกสมาน มลทินของไหล และมลทินท่อการเติบโต

ผลวิเคราะห์จากเครื่องมือขั้นสูง แสดงลักษณะแถบสเปคตรัมการดูดกลืนช่วงแสงเหนือม่วง-มองเห็น-ใต้แดง พบสาเหตุการดูดกลืนจากแมงกานีส วาเนเดียม เหล็ก และทองแดง นอกจากการดูดกลืนแสงในช่วงใต้แดงพบการดูดกลืนที่มีลักษณะคล้ายคลึงกัน สำหรับผลวิเคราะห์องค์ประกอบเคมีจากเครื่องEDXRF ไม่สามารถใช้ในการจำแนกชนิดพลอยทัวร์มาลีนและบ่งชี้แหล่งที่มาทางภูมิศาสตร์ได้ จำเป็นต้องมีการวิเคราะห์ด้วยเครื่องมือประเภทอื่นต่อไป

การวิเคราะห์พลอยทัวร์มาลีนที่ผ่านการอาบรังสีแกมมาพบการเปลี่ยนแปลงสีซึ่งเป็นผลจากการย้ายอิเล็กตรอนในระหว่างธาตุทรานสิชัน การดูดกลืนแสงในช่วงใต้แดงมีการเปลี่ยนแปลงเล็กน้อย ส่วนลักษณะอื่นๆ เช่น มลทินภายใน และองค์ประกอบทางเคมีไม่มีการเปลี่ยนแปลงใดที่จะใช้บ่งบอกการอาบรังสีได้

ภาควิชา ธรณีวิทยา ลายมือชื่อนิสิต ____________________

สาขาวิชา ธรณีวิทยา ลายมือชื่ออ.ที่ปรึกษาโครงการ ____________________

ปีการศึกษา 2562

5932729423: MAJOR GEOLOGY
KEYWORD: TOURMALINE / GAMMA IRRADIATION / MINERAL INCLUSIONS

LERPORN PONGSAMART: CHARACTERISTICS OF TOURMALINE FOR INDICATOR OF GEOGRAPHIC ORIGIN AND QUALITY ENHANCEMENT. ADVISOR: PROF. CHAKKAPHAN SUTTHIRAT, Ph.D., 141 pp.

The objective of this research is to study the characteristics of tourmalines from Brazil, Mozambique, Nigeria, and Madagascar, as well as their physical changes after gamma ray irradiation. Basic equipment and advanced analytical techniques based at the ICA Gem Lab were used for this study. The main aim of this study is to develop database for further identification of geographic origin.

Most of 84 tourmaline samples under this study are transparent with abundant internal fractures and inclusions. They are inert without luminescence under UV lamp. Unknown solid inclusions are found in some samples whereas heal fissure, liquid veil, and growth tube are often found in most samples.

Based on advanced analyses, strong absorptions caused by Mn, V, Fe, and Cu can be clearly observed in UV-Vis-NIR spectrum. For infrared absorption spectrum, all samples show similar pattern. EDXRF chemical analysis could not be used for tourmaline classification and geographic origin determination. Other techniques should be applied for further analyses.

Color of tourmaline after gamma irradiation was changed as a result of charge transfer transition. Infrared absorbance shows a slightly change. Other characteristics include impurities and chemical composition are quite similar to the untreated tourmaline samples.

Department ___Geology___ Student's Signature ____________________

Field of Study ___Geology___ Advisor's Signature ____________________

Academic Year ___2562___

ACKNOWLEDGEMENTS

This report has been accomplished with the gratitude and encouragement of many people. Finally, I would like to thank my advisor, Professor Dr. Chakkaphan Sutthirat and ICA Gem Lab. This report would not have been succeeded without them.

I would like to thank all lectures at Department of Geology, Faculty of Science, Chulalongkorn University for giving me background knowledge, suggestion, and experiences in the past three years.

To my family and friends, I would like to thank for their support, encouragement, and believing in me. And I appreciate all support from others that I have not mentioned here too.

Lerporn Pongsamart

Project Author

CONTENTS

LIST OF CONTENTS (Continued)

LIST OF FIGURES

LIST OF FIGURES (Continued)

LIST OF FIGURES (Continued)

LIST OF FIGURES (Continued)

LIST OF FIGURES (Continued)

LIST OF TABLES

CHAPTER 1

INTRODUCTION

1.1 Background

Tourmaline is recognized as an important and stunning gemstone due to its color variability and unique color zoning. Each tourmaline crystal may contain geochemical fingerprints that can elucidate an astonishing array of geological processes (Dutrow, 2018). Gem tourmalines have been produced from many countries, particularly Brazil, Madagascar, Mozambique, and Nigeria. Their wide range of color variety includes black, brown, green, yellow, blue, pink, red, violet, and colorless (Bačík et al., 2015).

The chemical formula of tourmaline is $XY_3Z_6(BO_3)_3T_6O_{18}(W)_3V$ which is very complex. Tourmaline is mineralogically considered as a supergroup because of various chemical composition possible in the structure leading to numerous species that can be used as gemstone such as elbaite, fluor-elbaite, fluor-liddicoatite, dravite-uvite, etc (Sun et al., 2019). Because each species of tourmaline can provide more than one color, their variety or trade name are widely used (Table 1.1).

Table 1.1 Partial list of tourmaline varieties, color, and probable species from Pezzotta and Laurs (2011).

Variety	Color	Species
Chrome	Deep green	Dravite-uvite
Verdelite	Green	Elbaite, fluor-elbaite, fluor-liddicoatite
Rubellite	Pink and red	Elbaite, fluor-elbaite, fluor-liddicoatite, rossmanite
Paraiba	Neon blue	Elbaite, liddicoatitic tourmaline
Indicolite	Blue	Elbaite, fluor-elbaite, fluor-liddicoatite

Due to complex mineral chemistry, various color varieties can be generated by some particular elements. Green tourmaline is characterized by two varieties, depending on the transition element impurities. Chrome tourmaline is related to V^{3+}, Cr^{3+} and verdelite is related to Fe^{2+}, Fe^{3+}, Fe^{2+}-Ti^{4+} IVCT (Pezzotta and Laurs, 2011), which can be found in East Africa (Kaewtip and Limtrakun, 2016).

Bright blue with green hue variety, called Paraiba-type tourmaline, becomes the most popular variety after it has demanded in the world gem market, and prices escalated rapidly (Laurs et al., 2008). Bright blue to green "Paraiba"type (Cu-bearing) tourmaline is now mined in Brazil, Nigeria, and Mozambique (Abduriyim et al, 2006). Paraiba tourmaline is a rare variety which has higher price than the other similar color varieties with similar colors but lacking of Cu such as indicolite.

Fine red to pinkish hue variety, called Rubellite, is one of the most attractive tourmalines. The color of this variety is caused by Mn^{3+} (Pezzotta and Laurs, 2011). High quality rubellite is very rare; therefore, color enhancement by gamma irradiation are normally required. The color of the tourmaline undertaken gamma irradiation may yield various shades of pink depending on properties of stone (Phichaikamjornwut et al., 2019).

This study focuses on characterization of tourmaline from various geographic sources. In addition, physical characteristics changing of tourmaline after gamma ray irradiation is also determined for green and pink tourmalines.

1.2 Objectives

1.2.1 To study the characteristics of tourmaline from Brazil, Mozambique, Nigeria, and Madagascar.

1.2.2 To study the changing of physical characteristics of tourmaline after undertaken gamma ray irradiation.

1.3 Hypothesis

1.3.1 Tourmalines from Brazil, Mozambique, Nigeria, and Madagascar have different specific characteristics which can be detected their sources.

1.3.2 After gamma ray irradiation, the physical characteristics of tourmaline are changed and determinable.

1.4 Scope of Study

Eighty-five tourmaline samples from Brazil, Mozambique, Nigeria, Madagascar, and unknown source in East Africa are provided by Dr. Dietmar Schwarz, former director of the ICA GemLab. These samples will be examined for physical, chemical, and optical properties.

1.5 Study Area

Brazil: Most of tourmalines are primarily associated with pegmatites and hydrothermal veins whereas their secondary deposits have been accumulated in alluvium, colluvium and Plio-Pleistocene paleo-alluvium (Figure 1.1).

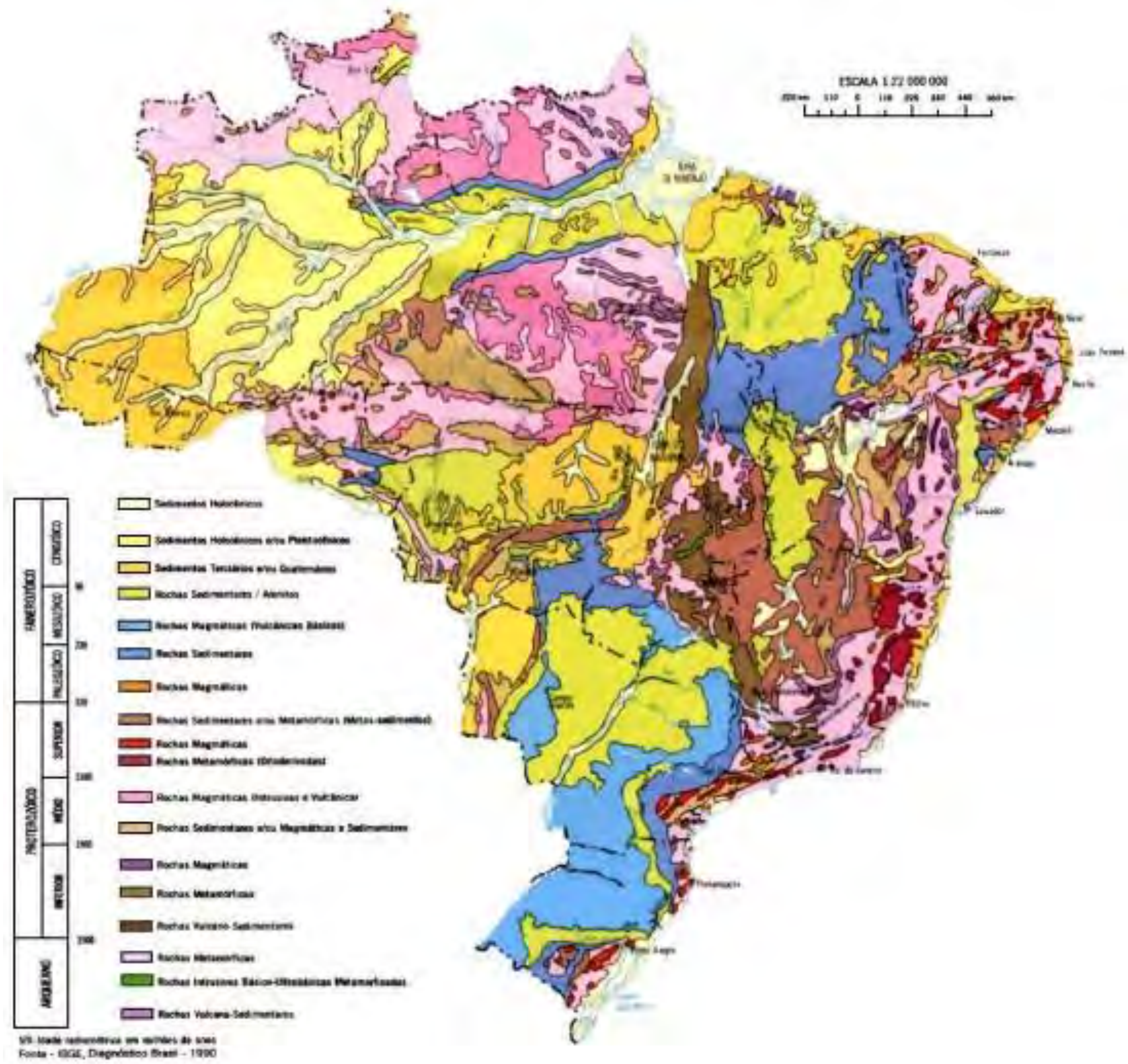

Figure 1.1 Geological map of Brazil (IBGE, 1990).

Mozambique: The main tourmaline mining areas are in Nampula, the northeastern of Mozambique. Migmatite has been reported as basement which is intruded by granitoids and granitic pegmatites. However, Cu-bearing tourmaline has only been found in secondary deposit typically situated on the top of weathered biotite gneiss bedrock (Figure 1.2).

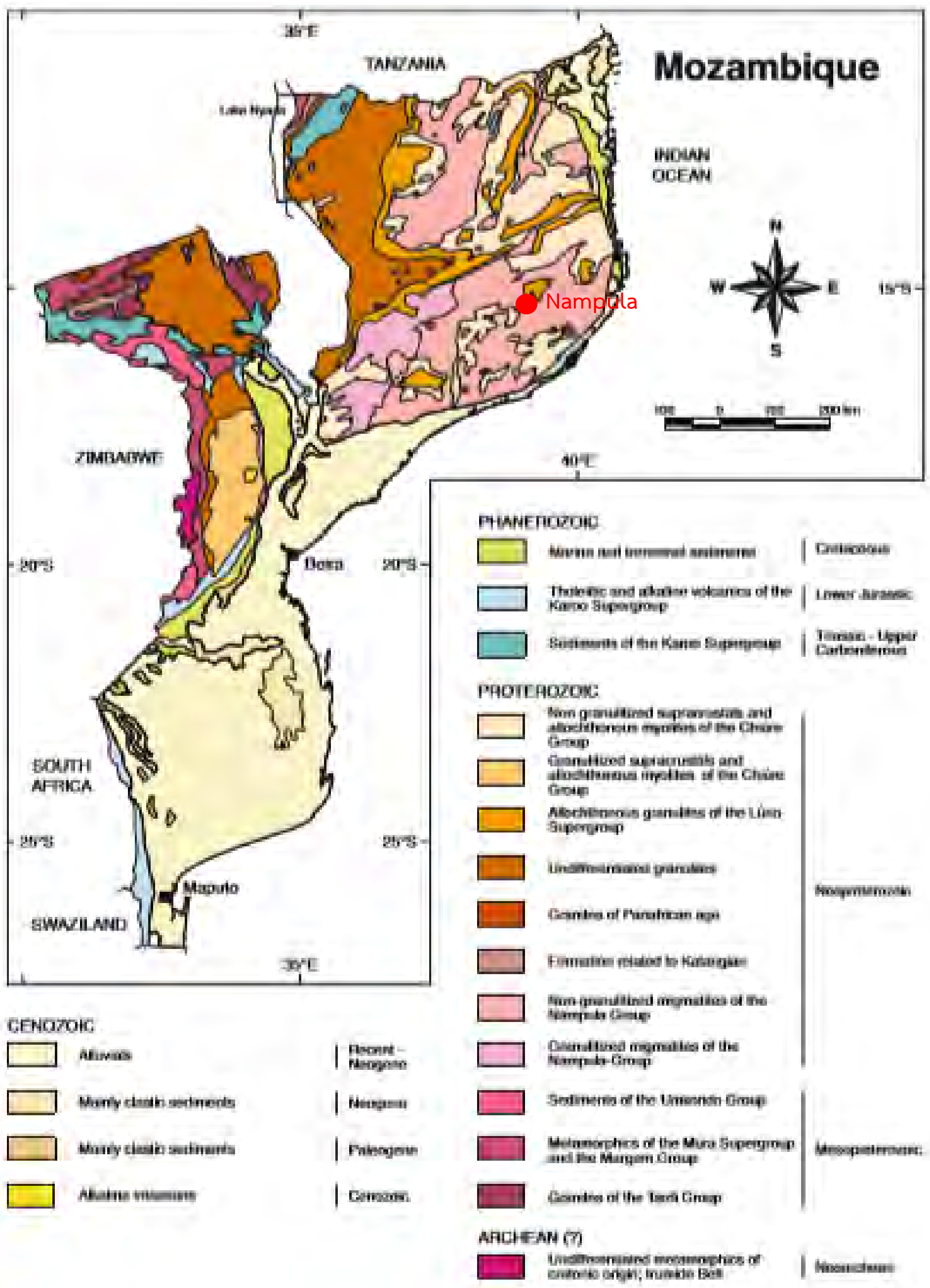

Figure 1.2 Geological overview of Mozambique and the location of Nampula (*Schlüter, 2006*).

Nigeria: Jos, the main tourmaline deposit, is located in the Middle Belt of Nigeria in which is situated within the Pan African mobile belt. Most of the gemstones such as aquamarine, emeralds, sapphire, ruby, and tourmaline have occurred in pegmatite and quartz vein within the basement complex and younger granite (Figure 1.3).

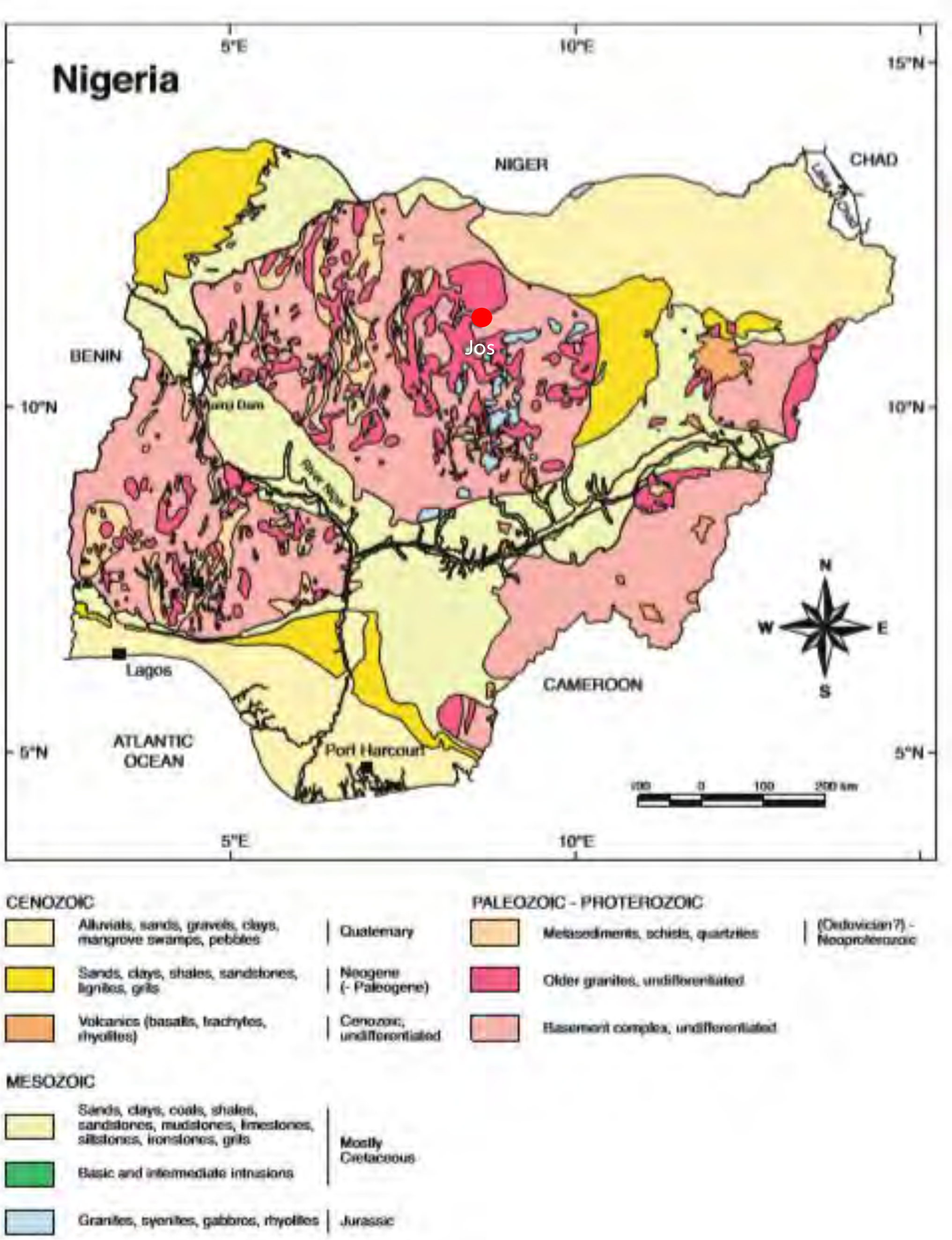

Figure 1.3 Geological overview of Nigeria and the location of Jos (*Schlüter*, *2006*).

Madagascar: Tourmaline in Madagascar are usually found in pegmatite. Many gem-bearing pegmatites in central Madagascar are hosted by rocks of the Itremo Group which is characterized particularly by lower unit of gneiss and upper unit of quartzite, schist, and marble (Figure 1.4).

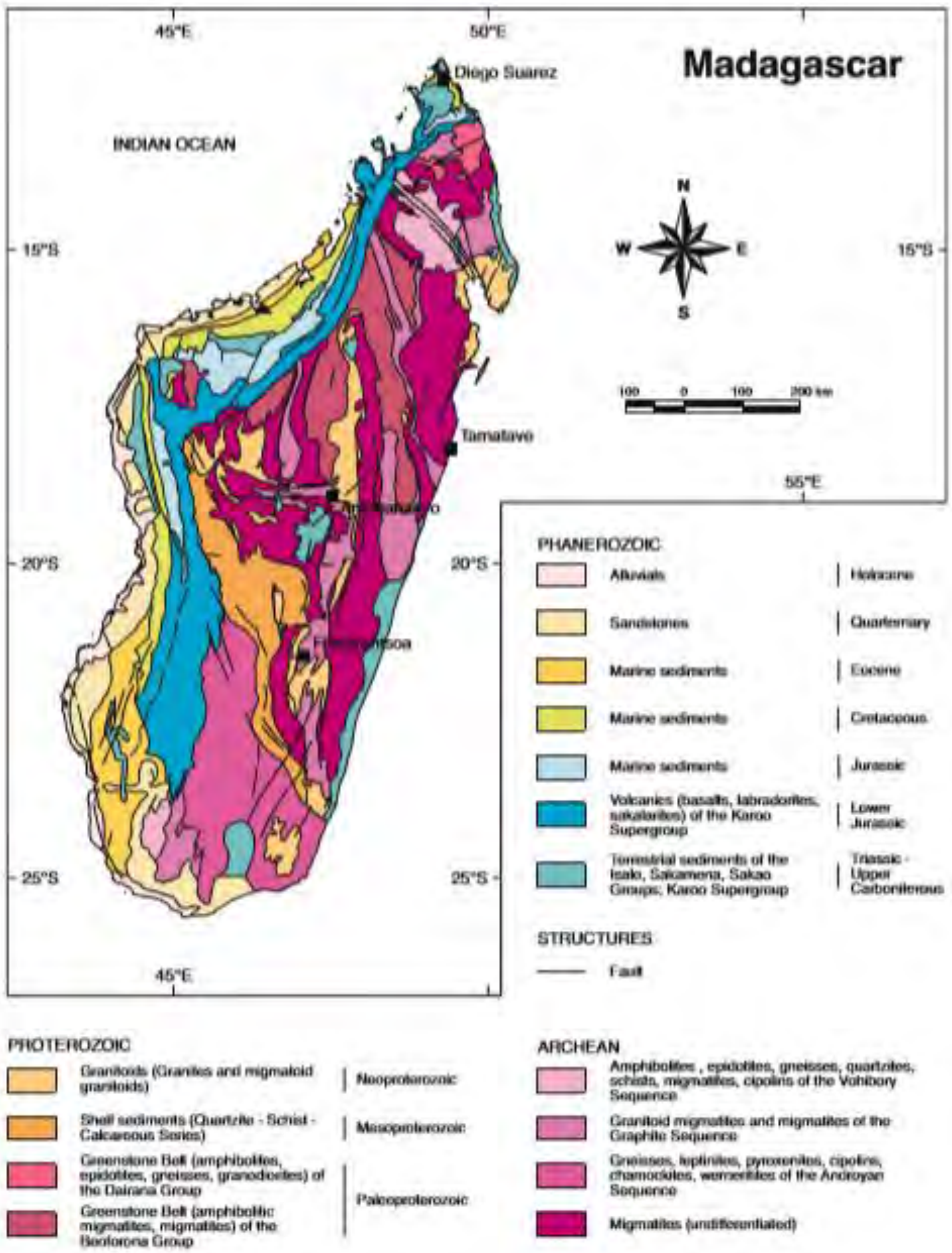

Figure 1.4 Geological overview of Madagascar (*Schlüter*, 2006).

East Africa: Some tourmaline samples were collected from unknown specific locations in East Africa between Tanzania and Madagascar. However, the main gemstone belt of East Africa is located in the Neoproterozoic Mozambique belt which is also the main production of ruby, sapphire, garnet and other gemstones. This terrane appears to have undertaken high pressure and high temperature metamorphism (Figure 1.5).

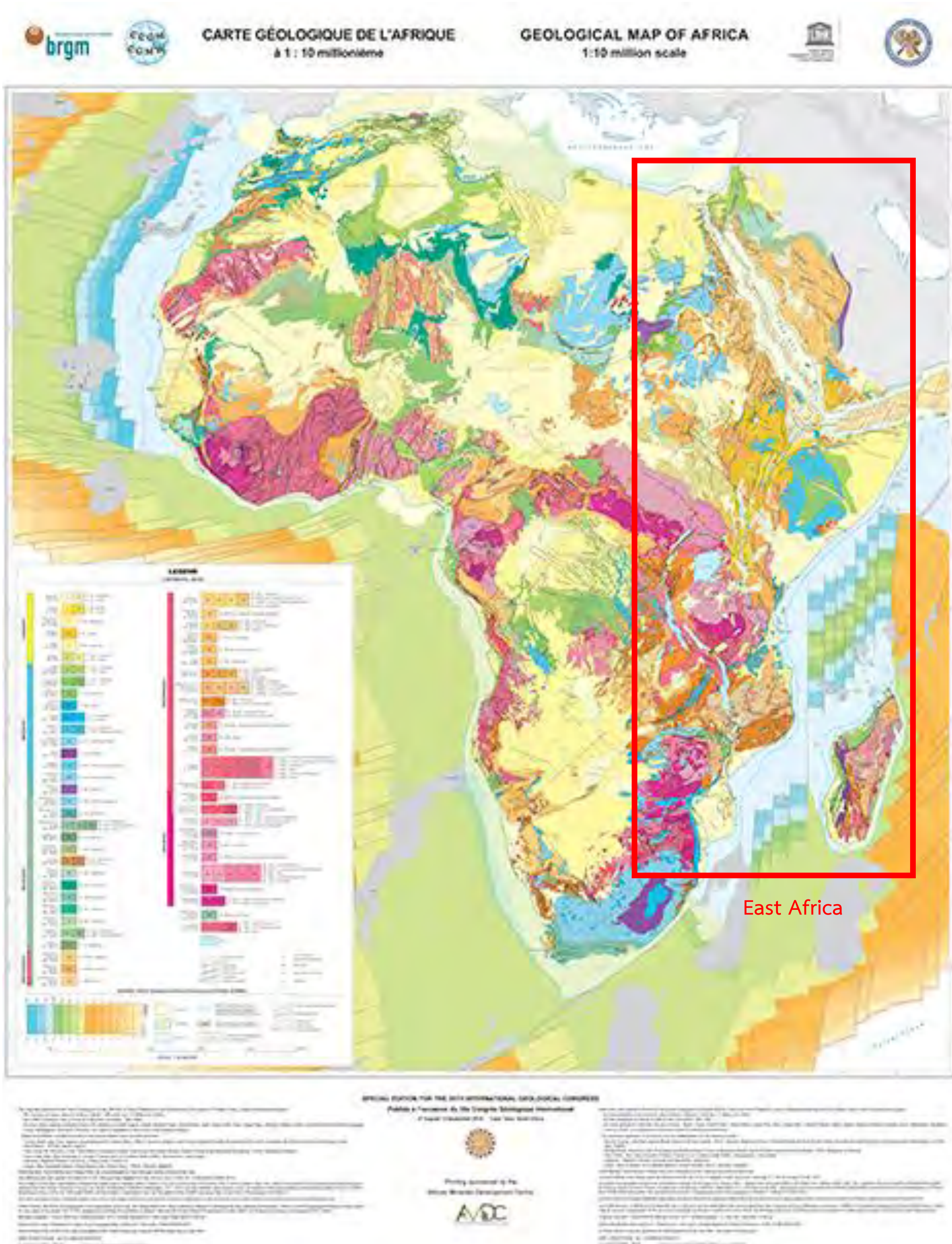

Figure 1.5 Geologic map of Africa and the location of East Africa (Thiéblemont et al., 2016).

1.6 Expected Output

1.6.1 The characteristics of tourmalines from Brazil, Mozambique, Nigeria, and Madagascar.

1.6.2 The changing of physical characteristics of gamma ray irradiated treatment in tourmaline.

CHAPTER 2

RELATED RESEARCH

2.1 Tourmaline

Based on mineralogical classification, tourmaline group is boro-silicate mineral which has very complex chemical compositions leading to various colors. However, Its ideal chemical formula can be defined as $XY_3Z_6(BO_3)_3T_6O_{18}(W)_3V$ in which X site is suitable for Na^+, K^+, Ca^{2+}, or vacant, Y site is designed for Mg^{2+}, Fe^{2+}, Mn^{2+}, Al^{3+}, Fe^{3+}, Mn^{3+}, Cr^{3+}, or Li^+, Z site is more available for Al^{3+}, Mg^{2+}, Fe^{3+}, Cr^{3+}, or V^{3+}, T site is allocated for Si and Al whereas W and V sites are defined for anions such as O^{2-} or OH^- in the W site and O^{2-}, OH^-, or F^- in the V site, respectively. In general, each of the six silicon atoms is surrounded by four oxygen atoms forming a tetrahedral T site which shares two oxygens with the others nearby; consequently a hexagonal ring of Si_6O_{18} is accordingly constructed. Three octahedral Y sites situated on such hexagonal rings combine with BO_3 group whereas the distorted Z sites are slightly smaller octahedra and shared edges to form brucite-like fragments. OH is located at the center of the hexagonal rings and at the corner of the brucite-like fragments of three oxygen atoms (see Figure 2.1 published by Ahn et al., 2013).

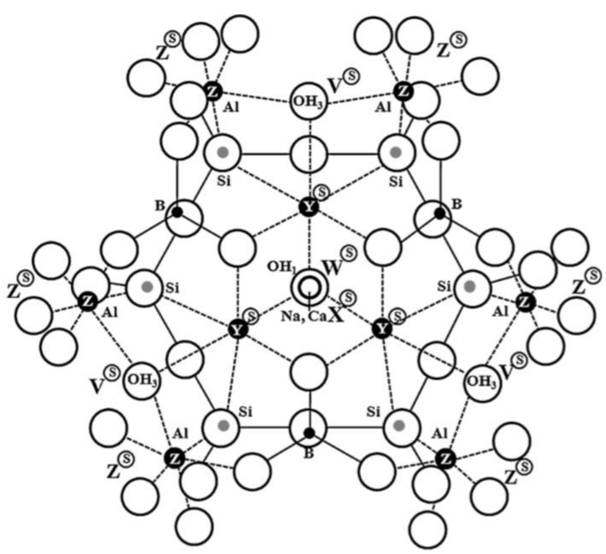

Figure 2.1 Tourmaline structure showing the relative position of X (Na^+, K^+, Ca^{2+}, or vacancies), Y (Mg^{2+}, Fe^{2+}, Mn^{2+}, Al^{3+}, Fe^{3+}, Mn^{3+}, Cr^{3+}, or Li^+), Z (Al^{3+}, Mg^{2+}, Fe^{3+}, or Cr^{3+}), W (O^{2-} or OH^-), and V (O^{2-}, OH^-, or F^-) sites ((s)) containing Si_6O_{18} and BO_3 structures (Ahn et al., 2013).

Tourmaline can be found in igneous, metamorphic, and sedimentary rocks. The tourmalines in igneous rocks, mostly magmatic and pegmatitic environments, are usually characterized by elbaite and fluorliddicoatite species. On the other hand, the metamorphic tourmalines are dravite-uvite species (Pezzotta and Laurs, 2011). Tourmaline species cannot be classified by only color appearance which may be led to color varieties and trade names. For example, a green tourmaline can be a uvite, dravite, chromium-dravite, vanadium-dravite, some other species (Table 2.1). Recently, tourmalines have been described into 33 species (Tables 2.2, 2.3, and 2.4) (Sun et al., 2018).

Table 2.1 Partial list of tourmaline colors, varieties, causes of color, and probable species from Pezzotta and Laurs (2011).

Color	Varietal name	Cause of color	Probable tourmaline species
Colorless	Achroite	No or minor chromophores	Elbaite, fluor-elbaite, fluor-liddicoatite, rossmanite
Pink and red	Rubellite	Mn^{3+}, Mn^{3+}+Fe, or Mn^{2+}-Mn^{3+} IVCT Natural radiation	Elbaite, fluor-elbaite, fluor-liddicoatite, rossmanite
Yellow, yellow-green	Canary	Mn^{2+}, Mn^{2+}-Ti^{4+} IVCT	Elbaite, fluor-elbaite, fluor-liddicoatite
Green	Verdelite	Fe^{2+}, Fe^{3+}, Fe^{2+}-Ti^{4+} IVCT	Elbaite, fluor-elbaite, fluor-liddicoatite
Green (deep)	Chrome	V^{3+}, Cr^{3+}	Dravite-uvite
Blue	Indicolite	Fe^{2+}, Fe^{2+}-Fe^{3+} IVCT	Elbaite, fluor-elbaite, fluor-liddicoatite
Blue (neon)	Paraiba-type	Cu^{2+}	Elbaite, liddicoatitic tourmaline
Brown	-	Fe^{2+}-Ti^{4+} IVCT	Dravite, elbaite, liddicoatitic tourmaline
Black	-	High concentrations of Fe^{2+}, Mn^{2+}, and/or Ti^{4+}	Schorl, elbaite, liddicoatitic tourmaline

Paraiba-type tourmaline is the trade name of a blue copper-bearing tourmaline which contains Cu and Mn from wherever country of origin (Laurs et al., 2008). Nowadays, most of Paraiba tourmaline has been mined in Brazil, Nigeria, and Mozambique in which they are mostly identified as elbaite of alkali group. Moreover, some of them are also classified as liddicoatite of calcic group which their geographic origins are not clearly known (Katsurada and Sun, 2017). The other causes of blue color in tourmaline may be influenced by Fe^{2+}, Fe^{2+}-Fe^{3+} inter valence charge transfer (IVCT) which these tourmalines are called Indicolite in the trade (Pezzotta and Laurs, 2011).

TABLE 2.2 IMA-CMNMC-approved tourmaline species (alkali group) from Sun et al. (2018).

General formula	(X)	(Y_3)	(Z_6)	T_6O_{18}	$(BO_3)_3$	$(V)_3$	(W)
Alkali group (23 species)							
Subgroup 1	*R^{1+}	$R^{2+}{}_3$	$R^{3+}{}_6$	$R^{4+}{}_6O_{18}$	$(BO_3)_3$	**$S^{1-}{}_3$	S^{1-}
Dravite	Na	Mg_3	Al_6	Si_6O_{18}	$(BO_3)_3$	$(OH)_3$	(OH)
Fluor-dravite	Na	Mg_3	Al_6	Si_6O_{18}	$(BO_3)_3$	$(OH)_3$	(F)
Schorl	Na	Fe_3	Al_6	Si_6O_{18}	$(BO_3)_3$	$(OH)_3$	(OH)
Fluor-schorl	Na	Fe_3	Al_6	Si_6O_{18}	$(BO_3)_3$	$(OH)_3$	(F)
Tsilaisite	Na	Mn_3	Al_6	Si_6O_{18}	$(BO_3)_3$	$(OH)_3$	(OH)
Fluor-tsilaisite	Na	Mn_3	Al_6	Si_6O_{18}	$(BO_3)_3$	$(OH)_3$	(F)
Chromium-dravite	Na	Mg_3	Cr_6	Si_6O_{18}	$(BO_3)_3$	$(OH)_3$	(OH)
Subgroup 2	R^{1+}	$R^{1+}{}_{1.5}R^{3+}{}_{1.5}$	$R^{3+}{}_6$	$R^{4+}O_{18}$	$(BO_3)_3$	$S^{1-}{}_3$	S^{1-}
Elbaite	Na	$Li_{1.5}Al_{1.5}$	Al_6	Si_6O_{18}	$(BO_3)_3$	$(OH)_3$	(OH)
Fluor-elbaite	Na	$Li_{1.5}Al_{1.5}$	Al_6	Si_6O_{18}	$(BO_3)_3$	$(OH)_3$	(F)
Subgroup 3 (Y-Z order/disorder)	R^{1+}	$R^{3+}{}_3$ to $R^{2+}{}_2R^{3+}$	$R^{3+}{}_4R^{2+}{}_2$ to $R^{3+}{}_6$	$R^{4+}O_{18}$	$(BO_3)_3$	$S^{1-}{}_3$	S^{2-}
Oxy-dravite	Na	Al_2Mg	Al_5Mg	Si_6O_{18}	$(BO_3)_3$	$(OH)_3$	(O)
Oxy-schorl	Na	$Fe^{2+}{}_2Al$	Al_6	Si_6O_{18}	$(BO_3)_3$	$(OH)_3$	(O)
Povondraite	Na	$Fe^{3+}{}_3$	$Fe^{3+}{}_4Mg_2$	Si_6O_{18}	$(BO_3)_3$	$(OH)_3$	(O)
Bosiite	Na	$Fe^{3+}{}_3$	Al_4Mg_2	Si_6O_{18}	$(BO_3)_3$	$(OH)_3$	(O)
Chromo-alumino-povondraite	Na	Cr_3	Al_4Mg_2	Si_6O_{18}	$(BO_3)_3$	$(OH)_3$	(O)
Oxy-chromium dravite	Na	Cr_3	Cr_4Mg_2	Si_6O_{18}	$(BO_3)_3$	$(OH)_3$	(O)
Oxy-vanadium dravite	Na	V_3	V_4Mg_2	Si_6O_{18}	$(BO_3)_3$	$(OH)_3$	(O)
Vanadio-oxy-chromium-dravite	Na	V_3	Cr_4Mg_2	Si_6O_{18}	$(BO_3)_3$	$(OH)_3$	(O)
Vanadio-oxy-dravite	Na	V_3	Al_4Mg_2	Si_6O_{18}	$(BO_3)_3$	$(OH)_3$	(O)
Maruyamaite	K	$MgAl_2$	Al_5Mg	Si_6O_{18}	$(BO_3)_3$	$(OH)_3$	(O)
Oxy-vanadium-dravite	Na	V_3	V_4Mg_2	Si_6O_{18}	$(BO_3)_3$	$(OH)_3$	(O)
Subgroup 4	R^{1+}	$R^{1+}R^{3+}{}_2$	$R^{3+}{}_6$	$R^{4+}{}_6O_{18}$	$(BO_3)_3$	$S^{1-}{}_3$	S^{2-}
Darrellhenryite	Na	$LiAl_2$	Al_6	Si_6O_{18}	$(BO_3)_3$	$(OH)_3$	(O)
Subgroup 5	R^{1+}	$R^{3+}{}_3$	$R^{3+}{}_6$	$R^{4+}{}_6O_{18}$	$(BO_3)_3$	$S^{2-}{}_3$	S^{1-}
Olenite	Na	Al_3	Al_6	Si_6O_{18}	$(BO_3)_3$	$(O)_3$	(OH)
Fluor-buergerite	Na	$Fe^{3+}{}_3$	Al_6	Si_6O_{18}	$(BO_3)_3$	$(O)_3$	(F)

* R is a generic designation of a cation of the indicated charge.

**S is a generic designation of an anion of the indicated charge.

TABLE 2.3 IMA-CMNMC-approved tourmaline species (calcic group) from Sun et al. (2018).

General formula	(X)	(Y_3)	(Z_6)	T_6O_{18}	$(BO_3)_3$	$(V)_3$	(W)
Calcic group (6 species)							
Subgroup 1	R^{2+}	R^{2+}_3	$R^{3+}_5R^{2+}$	$R^{4+}_6O_{18}$	$(BO_3)_3$	S^{1-}_3	S^{1-}
Uvite	Ca	Mg_3	Al_5Mg	Si_6O_{18}	$(BO_3)_3$	$(OH)_3$	(OH)
Fluor-uvite	Ca	Mg_3	Al_5Mg	Si_6O_{18}	$(BO_3)_3$	$(OH)_3$	(F)
Feruvite	Ca	Fe^{2+}_3	Al_5Mg	Si_6O_{18}	$(BO_3)_3$	$(OH)_3$	(OH)
Subgroup 2	R^{2+}	$R^{1+}_2R^{3+}$	R^{3+}_6	$R^{4+}_6O_{18}$	$(BO_3)_3$	S^{1-}_3	S^{1-}
Fluor-liddicoatite	Ca	Li_2Al	Al_6	Si_6O_{18}	$(BO_3)_3$	$(OH)_3$	(F)
Subgroup 3	R^{2+}	R^{2+}_3	R^{3+}_6	$R^{4+}_6O_{18}$	$(BO_3)_3$	S^{1-}_3	S^{2-}
Lucchesiite	Ca	Fe^{2+}_3	Al_6	Si_6O_{18}	$(BO_3)_3$	$(OH)_3$	(O)
Subgroup 4	R^{2+}	R^{2+}_3	R^{3+}_6	$R^{4+}_5R^{3+}O_{18}$	$(BO_3)_3$	S^{1-}_3	S^{1-}
Adachiite	Ca	Fe^{2+}_3	Al_6	Si_5AlO_{18}	$(BO_3)_3$	$(OH)_3$	(OH)

* R is a generic designation of a cation of the indicated charge.

**S is a generic designation of an anion of the indicated charge.

TABLE 2.4 IMA-CMNMC-approved tourmaline species (X-site vacant group) from Sun et al. (2018).

General formula	(X)	(Y_3)	(Z_6)	T_6O_{18}	$(BO_3)_3$	$(V)_3$	(W)
X-site vacant group (4 species)							
Subgroup 1	□***	$R^{2+}R^{3+}_3$	R^{3+}_6	$R^{4+}_6O_{18}$	$(BO_3)_3$	S^{1-}_3	S^{1-}
Magnesio-foitite	□	Mg_2Al	Al_6	Si_6O_{18}	$(BO_3)_3$	$(OH)_3$	(OH)
Foitite	□	Fe^{2+}_2Al	Al_6	Si_6O_{18}	$(BO_3)_3$	$(OH)_3$	(OH)
Subgroup 2	□	$R^{1+}R^{3+}_2$	R^{3+}_6	$R^{4+}_6O_{18}$	$(BO_3)_3$	S^{1-}_3	S^{1-}
Rossmanite	□	$LiAl_2$	Al_6	Si_6O_{18}	$(BO_3)_3$	$(OH)_3$	(OH)
Subgroup 3	□	$R^{1+}R^{3+}_2$	R^{3+}_6	$R^{4+}_6O_{18}$	$(BO_3)_3$	S^{1-}_3	S^{2-}
Oxy-foitite	□	Fe^{2+}_2Al	Al_6	Si_6O_{18}	$(BO_3)_3$	$(OH)_3$	(O)

* R is a generic designation of a cation of the indicated charge.

**S is a generic designation of an anion of the indicated charge.

***X-site vacancy □

2.2 The Significant Deposit

Gem-quality tourmalines can be found in many deposits around the world with various geologic settings. However, they are usually found in cavities of granitic pegmatites that are typically emplaced in the continental crust at moderate to shallow depth. The ages of tourmaline-bearing pegmatites are variable. Many large pegmatitic fields in Brazil, Namibia, Mozambique, and Madagascar appear to have formed during the latest stages of the tectono-metamorphic Pan-African event about 500-550 million years ago involving the Gondwana supercontinent; Although, some of tourmaline-bearing pegmatites may have formed more recently. Gem-quality tourmaline can be found in metamorphic rocks such as chrome tourmaline from Tanzania. Tourmalines are highly resistant to physical and chemical weathering, they have also accumulated in eluvial and alluvial deposits in Madagascar.

Inclusions in tourmaline can reflect the environment of its original formation; they may be fingerprint for specific deposit. For example, blue Paraiba-type tourmaline from Brazil has native copper inclusions. Some mineral inclusions such as quartz, zircon, albite, muscovite, lepidolite, pyrite, monazite, fluorapatite, pyrochlore-group minerals, topaz, manganotantalite, and hydroxyl herderite can be found in tourmaline because most of them relate to pegmatitic paragenesis. Moreover, trapped fluids are more commonly found in tourmaline. These fluid inclusions have appeared in negative crystals, capillary-like tubes, heal fractures, and growth tubes. Other inclusions generally contain single-phase gas, two phases aqueous liquid and gas inclusions, and fluid trapped during tourmaline development (Pezzotta and Laurs, 2011).

Pan-African belt, a tectono-thermal or thermo-tectonic event, had taken place about 600-450 Ma with emplacement of granites and pegmatites of the Precambrian (Schlüter, 2006); these rock formations have been discovered surrounding older cratons. This concept relates to the Gondwana continent (see Figure 2.2). The term Pan-Africa is used to describe magmatic, metamorphic, and tectonic activity of Neoproterozoic to earliest Paleozoic age, especially the continent that was a part of Gondwana. One of the mobile belts contains poly-deformed high-grade metamorphic assemblages, exposed in middle to lower crustal levels, it has been grouped as Mozambique Belt of East Africa and Madagascar (Kröner and Stern, 2004).

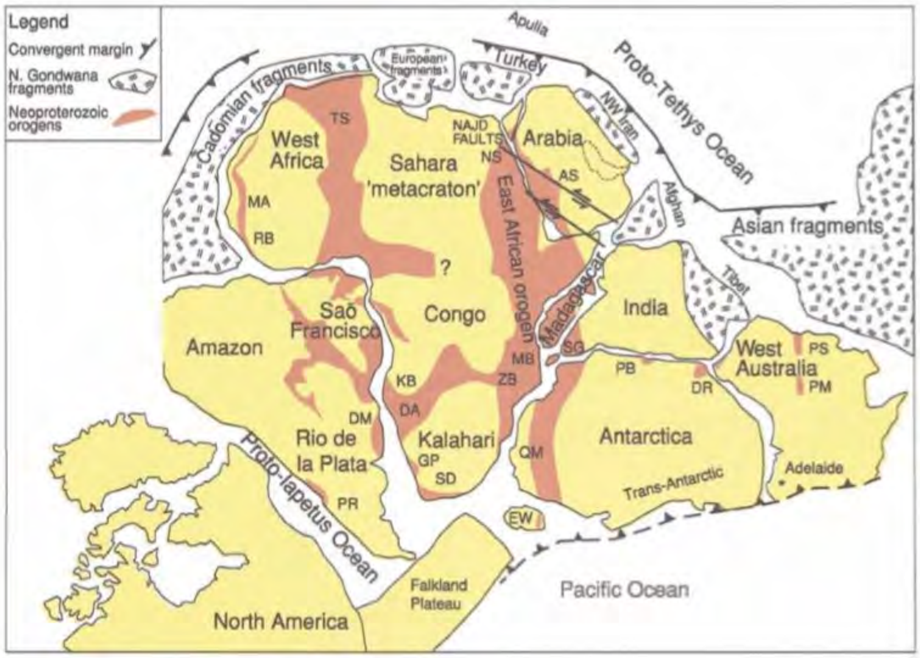

Figure 2.2 Map of Gondwana at the end of Neoproterozoic time (~540 Ma) showing the general arrangement of Pan-African belts. AS, Arabian Shield; BR, Brasiliano; DA, Darnara; DM, Dom Feliclano; DR, Denman Darling; EW, Eilsworth-Whitrnore Mountains; GP, Gariep; KB, Kaoko; MA, Mauretanides; MB, Mozarnbique Belt; NS, Nubian Shield; PM, Peterman Ranges; PB, Pryolz Bay; PR, Parnpean Ranges; PS, Paterson; QM, Queen Maud Land; RB, Rokelides; SD, Saldania; SG, Southern Granulite Terrane; TS, Trans- Sahara Belt; WB, West Congo; ZB, Zarnbezi (Kröner and Stern, 2004).

Brazil

In Brazil, gem-quality tourmaline has mainly occurred in the Northeast Sub-province, East Sub-province, and Central Sub-province (Figure 2.3) in which relate to granitic rocks, associated pegmatites, and hydrothermal deposit (Barreto and Schulze, 2010).

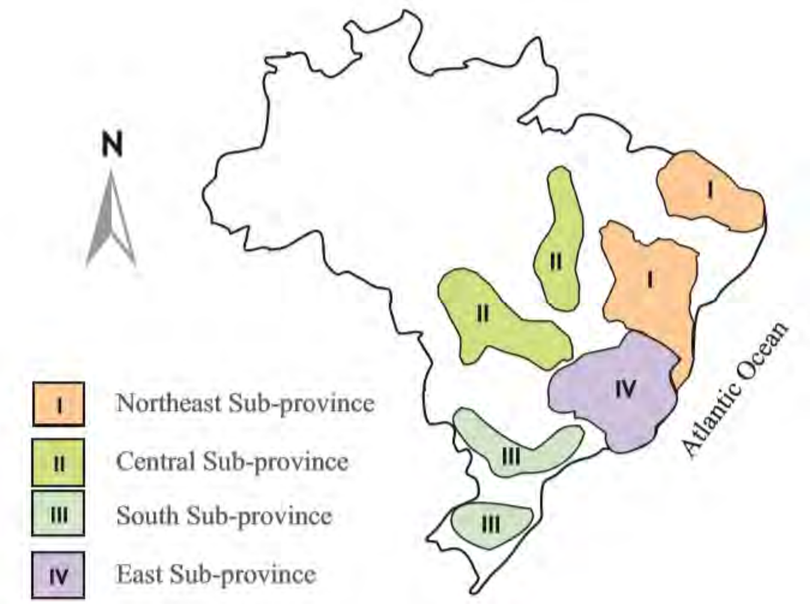

Figure 2.3 Gemological sub-provinces in Brazil (Brito Barreto and Bretas Bittar, 2010).

Geology of northeastern Brazil is complicated. It consists of Archean and Early Proterozoic gneisses and migmatite, Late Proterozoic igneous and metamorphic rocks. Regional deformation in this area had produced widespread metamorphism, folding, faulting, and several periods of granitic magmatism. The most recent tectonic cycles is represented by the Brasiliano-Pan-African Orogeny, between 650 and 480 Ma. This geologic event led to the separation of South America from Africa prior to intrusions of granitic bodies and pegmatites in the latter stages. The pegmatites typically form tabular-, lens-, or dike-like bodies which larger pegmatites contain mainly quartz, feldspar, and mica. On the other hand, smaller pegmatites contain more complex of mineralization; quartz core were formed at the central zones and often surrounded by gem and rare-element minerals such as spodumene, garnet, and tourmaline. Source of copper in Paraiba-type tourmaline is still unknown, but it may have derived from underlying copper-bearing rocks and incorporated into the pegmatitic magmas (Shigley et al., 2001).

Eastern Brazilian Pegmatite Province (EBP) has exposed within a large region, the EBP pegmatite is the main productions of gems such as aquamarine, tourmalines, topaz, quartz, etc. (Pedrosa-Soares et al., 2009).

In central Brazil, tourmaline-bearing pegmatites occur in different landscapes such as flat to hilly terrain, tops and slopes of hills or mountain. The pegmatite bodies have formed as round to NE-SW elongated shapes which can be separated into two groups, the southern group and the northern group. However, both groups present similar mineral assemblages; kaolinite, quartz, microcline, and muscovite are found as essential composition whereas accessory minerals contain beryl, Fe-Mn oxides, and colorful tourmaline. Only altered wall zone is observed *in situ* in the northern pegmatites (Almeida Queiroz and Botelho, 2018).

East Africa

East African Orogen contains Arabian–Nubian Shield in the north and the Mozambique Belt in the south (Figure 2.4), these orogenic belts are partly referred to Pan-African tectono-thermal activity in the Mozambique Belt; it related with deformation in the Arabian-Nubian Shield as well as magmatism, and metamorphism. Both belts present some differences of lithology, metamorphic grade, and the level of exposure; the Mozambican rocks have been interpreted as lower crustal compared to the Arabian-Nubian Shield. The East African Orogeny, 800-650 Ma, appears to be responsible to the construction of Gondwana (Kusky et al., 2003).

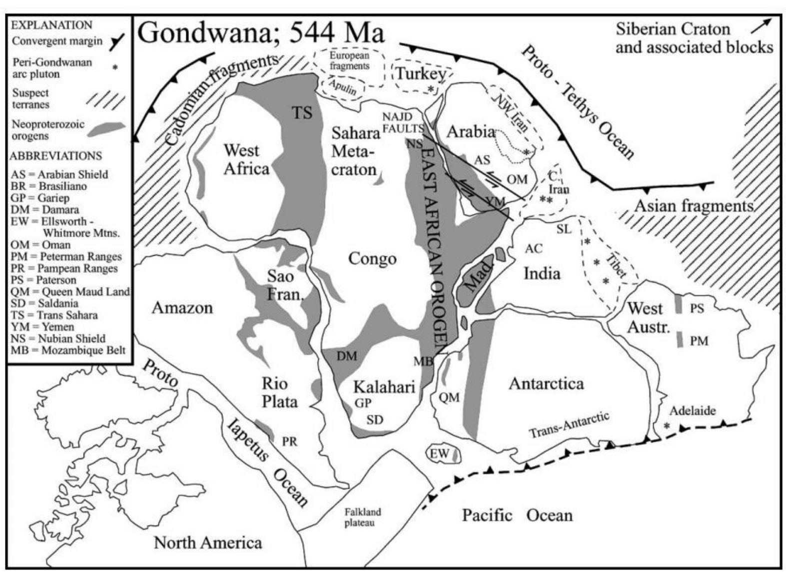

Figure 2.4 Map of Gondwana at the end of Neoproterozoic time showing the general arrangement of different tectonic elements (Kusky et al., 2003).

East African Rift System (EARS) has formed a narrow, elongated system of normal faults, connected to the worldwide system of oceanic rifts through the Afar Triangle to Gulf of Aden and the Red Sea (Figure 2.5). The EARS is composed of two main rifts, the eastern and the western branches. The eastern branch is a volcanic-rich system located in the Kenya and Ethiopian Rifts; it has probably begun in early Miocene or early Paleogene. The western branch has begun during late Miocene, and related less volcanism than the eastern branch (Figure 2.6) (Morley et al., 1999).

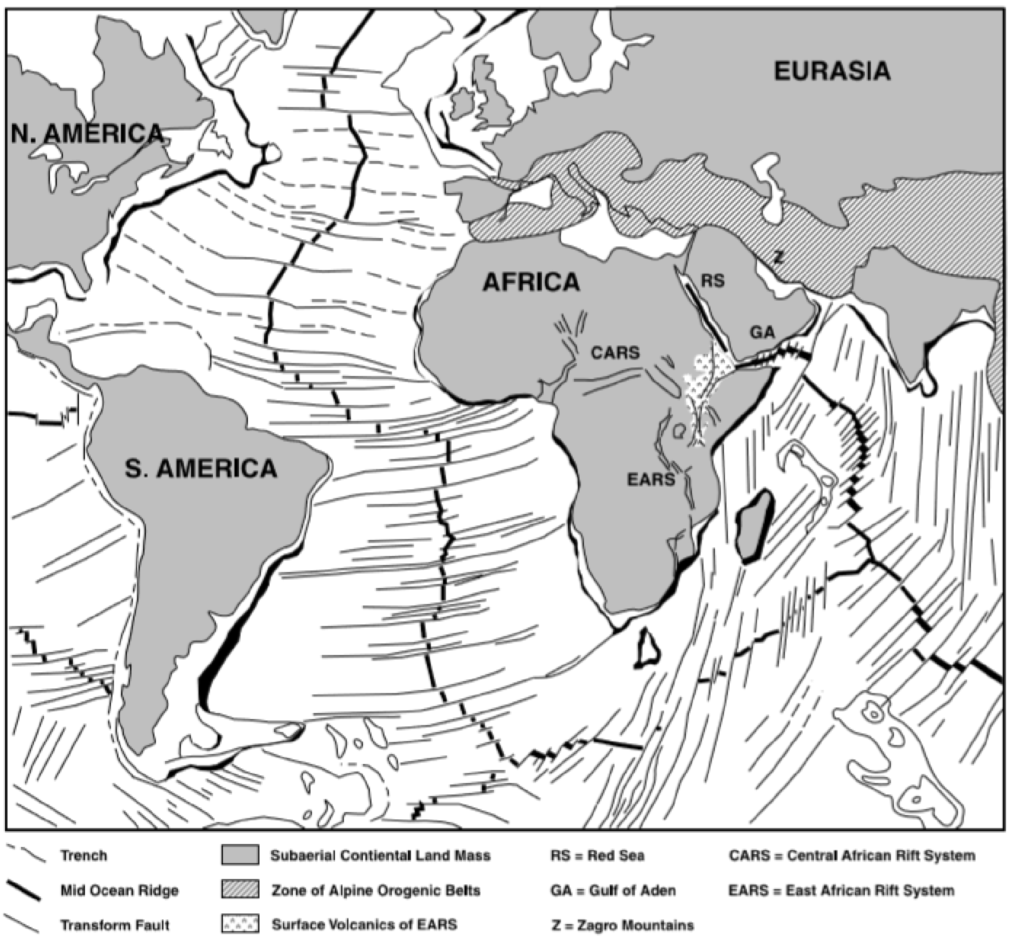

Figure 2.5 Simplified map of the rift systems surrounding Africa (Morley et al., 1999).

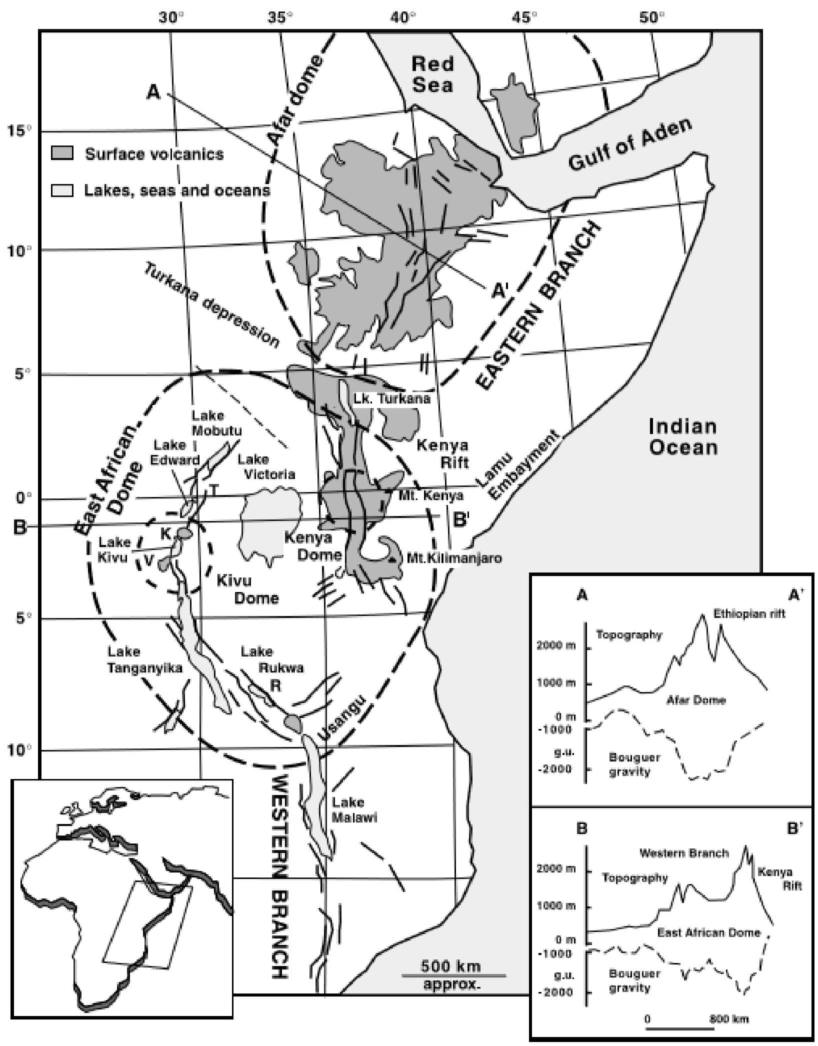

Figure 2.6 Distribution of topographic domes with relation to rift structure in East Africa. Western branch volcanic centers; R= Rungwe, T= Toro-Ankole, V= Virunga, K= South Kivu (Morley et al., 1999).

Gemstone belt of East Africa located in the Neoproterozoic Mozambique belt between Tanzania and Madagascar is mainly composed of ruby, sapphire, garnet, tourmaline and several other gemstones that appear to have originated at high pressures and high temperatures (Guillou-Frottier et al., 2008). The Mozambique Belt is divided into the Mozambique, Niassa, and Central Zambezi tectonic provinces. The biggest gem deposit in Mozambique located in in the northern part of the country can be divided into two regions, northwestern and northeastern regions. They consists of medium- to high-grade gneisses and voluminous granitoids which are represented by the Mecuburi Group, the Muaguibe Group and Nampula Group (Schlüter, 2005).

Nampula in Mozambique

The basement rocks in the Nampula area have formed part of the Mozambique Belt, 1100-800 Ma, which consists of metamorphosed gneisses or migmatites significantly deformed during the Pan-African tectonic event. Subsequently, these rocks were intruded by granitoids and rare-element granitic pegmatites during 600-410 Ma, and spread from Mediterranean Sea down to central Mozambique and became one of the most important sources of rare metals, industrial minerals, and gemstones (e.g., beryl and tourmaline). Tourmaline-bearing layer which is a paleoplacer set on the weathered biotite gneiss bedrock, and covered by a reddish brown to black tropically weathered horizon. The Cu-bearing tourmaline has only been found as waterworn pebbles in secondary deposit (Laurs et al., 2008).

Jos in Nigeria

The basement rocks of Jos Plateau in central-northern Nigeria are young granite that is represented by alkali feldspar granites associated with rhyolites, minor gabbros, and syenites. This young granite formed between Neoproterozoic to early Paleozoic, being elongated trending in north-south direction, and parallel to the main Pan-African trends which is controlled by earlier structures (Schlüter, 2006). Many pegmatites occurred in the area consist of major minerals (e.g., K-feldspar, albite, and quartz) and accessory tourmaline. Mineral assemblages and ages of these pegmatites are similar to pegmatite in Brazil (Akintola and Adekeye, 2008).

Madagascar

Basement rocks of Madagascar are part of the Mozambique orogenic belt (or East African Orogen) which were part of the Gondwana supercontinent. The Pan-African orogeny occurred about 600-450 Ma and the last magmatic cycle of this event occurred about 570-455 Ma which related to granitic plutons and pegmatite fields. Many gemstone deposits in the Mozambique Belt are associated with gem-bearing pegmatites intruded at shallow depths, which is represented by the central Madagascar (Dirlam, 2002).

2.3 Color Enhancement

Colors of tourmaline were caused by chemical composition. The deep purplish pink to the purplish red tourmaline in Rubellite has been highly valued with vivid color. Therefore, gamma irradiation has been applied for color treatment of pale pink tourmaline to change into vivid pink color (Phichaikamjornwut et al., 2019). Pale pink tourmaline may be changed to vivid pink color due to the steady formation of Mn^{3+}. Because the d^4 configuration of Mn^{3+} ions is stimulated by band absorption of visible light between 390 and 510 nm as d-d into d-d transitions (Ahn et al., 2013).

CHAPTER 3

METHODOLOGY

3.1 Literature Reviews

Previous researches related to pink, purple, blue, and green tourmalines from Brazil, Mozambique, Nigeria, Madagascar, and East Africa were reviewed and focused on characteristics and general properties of tourmaline, sample preparation for laboratory and gamma ray irradiation. Data analysis from various equipment and laboratory were also investigated.

3.2 Sample Collection and Preparation

Total of 85 samples of natural tourmalines are from Brazil, Mozambique, Nigeria, Madagascar and East Africa. Brazilian materials include fifty rough and faceted samples in various colors containing pink, blue, green, and purple. Thirteen rough tourmalines with pink, blue, and green are from Nampula in Mozambique. Four rough stones are from Jos in Nigeria. Only one faceted green tourmaline is surely from Madagascar; whereas other sixteen faceted green tourmalines are told as East African samples. These samples were owned by Dr. Dietmar Schwarz.

Twelve samples including four rough green tourmalines from Brazil, seven rough green and pale pink tourmalines from Nampula in Mozambique, and only rough light blue tourmaline from Jos in Nigeria, were cut and polished into two pieces. One half of each sample was treated by gamma irradiation (300 kGy) for 2 times (Figure 3.1).

Figure 3.1 Selected twelve tourmalines from Brazil, Mozambique, and Nigeria were cut into 2 pieces which one piece (on the right) of each sample was treated by gamma irradiation (300 kGy) for 2 times.

3.3 Physical Property

Specific gravity was determined for all samples using a hydrostatic balance (Figure 3.2). Weighing the samples in air and in water before the specific gravity is determined by the ratio of weight in air to difference between weight in air and weight in water. Short wave and long wave UV lamps or UV-colorscope (Figure 3.3) was used to observe fluorescence. Refractive indices of all samples were measured with a refractometer (Figure 3.4) using a monochromatic light source and determining the critical angle of total reflection as a shadow edge on the contacted surface between RI liquid and a prism. And internal features of all samples were observed under a gemological microscope which includes optical natural light, transmitted light, reflected light, and dark-field illumination (Figure 3.5).

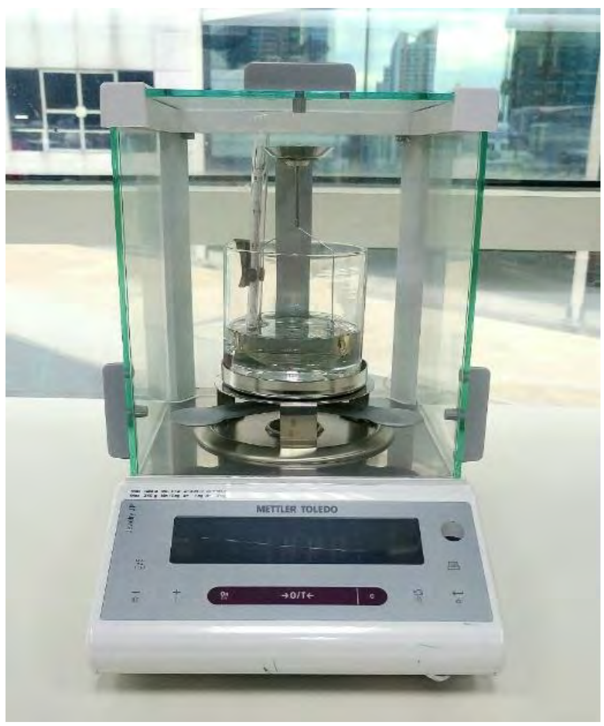

Figure 3.2 Hydrostatic balance at ICA GemLab.

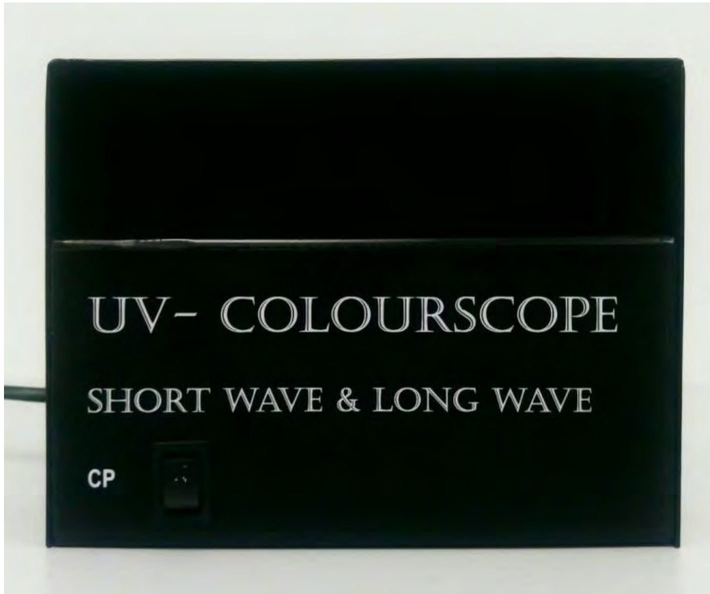

Figure 3.3 UV-Colorscope at ICA GemLab.

Figure 3.4 Refractometer at ICA GemLab.

Figure 3.5 Gemological microscope at ICA GemLab.

3.4 Optical Property

UV-Vis-NIR spectra of tourmaline samples in region of 280-880 nm were measured using Jasco V-770 UV-Vis-NIR spectrophotometer (Figure 3.6). Its attached double beam and single monochromator can measure the wide ranges of UV to NIR within single scan. Infrared (IR) spectra related to the OH stretching are usually acquired for natural tourmaline which the studied samples were investigated using Fourier Transform Infrared (FTIR, model Nicolet iS50) Spectrophotometer (Figure 3.7). The spectral region from 7,000 to 3,500 cm^{-1} was measured for natural samples which the region of 5,500-3,000 cm^{-1} was specifically focused for comparison in the gamma-irradiated samples.

Figure 3.6 UV-Vis-NIR Spectrophotometer model Jasco V-770 at ICA GemLab.

Figure 3.7 Fourier Transform Infrared Spectrophotometer (FTIR) model Nicolet iS50 at ICA GemLab.

3.5 Chemical Composition

Chemical analyses of all tourmaline samples were obtained from Energy-Dispersive X-ray Fluorescence (EDXRF) Spectrometer model ARL QUANT’X (Figure 3.8).

Figure 3.8 Energy-Dispersive X-ray Fluorescence (EDXRF) model ARL QUANT’X at ICA GemLab.

3.6 Data Analysis, Discussion and Conclusion

All results collected from analytical equipment and advanced instruments are analyzed, discussed and concluded on the characteristics of tourmalines from Brazil, Nampula in Mozambique, Jos in Nigeria, and Madagascar and the changing of physical characteristics of gamma ray irradiated treatment in tourmaline.

CHAPTER 4

RESULTS

4.1 General Properties

Physical properties of all tourmaline samples are reported in Appendix A. Refractive indices (R.I.) of 50 samples from Brazil were measured at n_o=1.638-1.641 and n_e=1.620-1.624 with birefringence of 0.017-0.019. Specific gravity (S.G.) varied from 3.029 to 3.238. Twelve tourmaline samples from Nampula in Mozambique yielded R.I. of n_o=1.638-1.641 and n_e=1.619-1.623 with birefringence of 0.017-0.019 and S.G. of 3.024-3.144. Four samples from Jos in Nigeria gave R.I. of n_o=1.639-1.641 and n_e=1.621-1.623 with birefringence of 0.017-0.019 and S.G. of 3.023-3.102. Only one sample from Madagascar presented R.I. of n_o=1.640 and n_e=1.620 with birefringence of 0.020 and S.G. of 3.132. Seventeen samples from East Africa obtained R.I. of n_o=1.638-1.640 and n_e=1.619-1.623 with birefringence of 0.017-0.020, and S.G. of 3.037-3.132. In addition, all the samples were inert in LWUV and SWUV.

4.2 Microscopic Characteristics

The common inclusions found in tourmaline samples from Brazil, Nampula in Mozambique, Jos in Nigeria, and East Africa are composed of cracks (Figures 4.1 and 4.2), liquid veils (Figures 4.3 and 4.4), and growth tubes (Figure 4.5). Yellow to reddish brown stains in growth tubes can be found in tourmaline samples from Brazil and Nampula in Mozambique (Figure 4.6). Moreover, minute particles (Figure 4.7) were found in tourmaline samples from all sources.

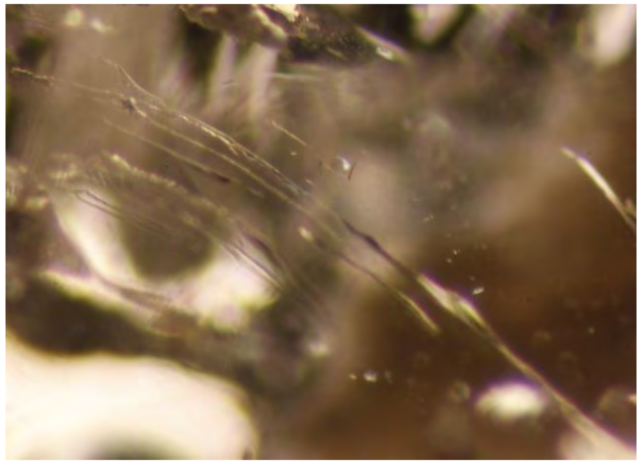

Figure 4.1 Cracks, 5.0X in sample TPBRA050 from Brazil.

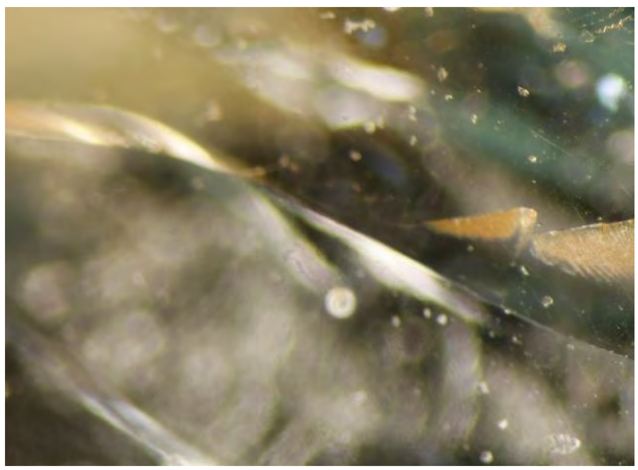

Figure 4.2 Cracks, 2.5X in sample TPNIG003 from Jos in Nigeria.

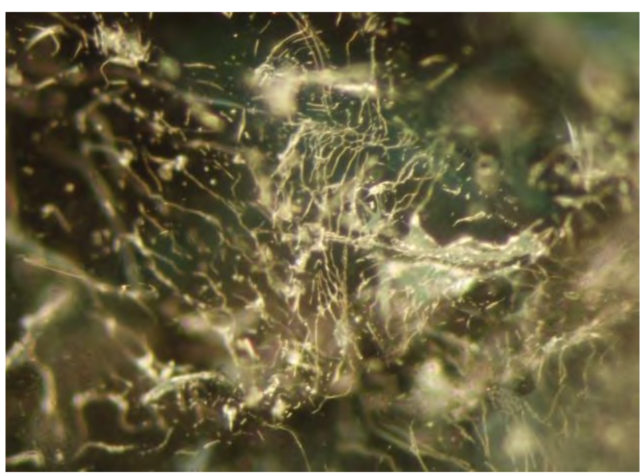

Figure 4.3 Liquid veils, 5.0X in sample TPBRA037 from Brazil.

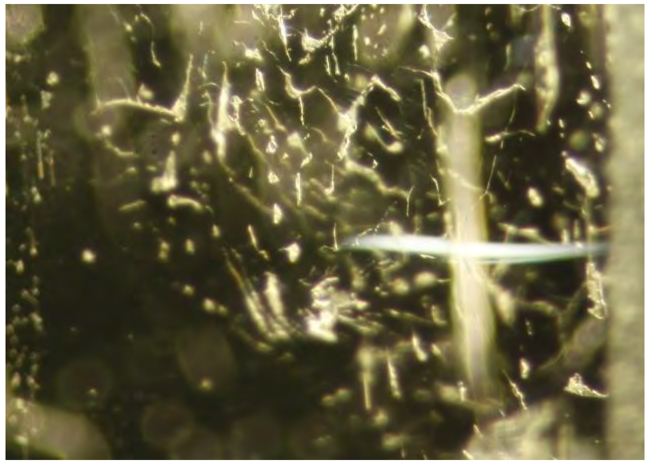

Figure 4.4 Liquid veils, 2.5X in sample TPMOZ006 from Nampula in Mozambique.

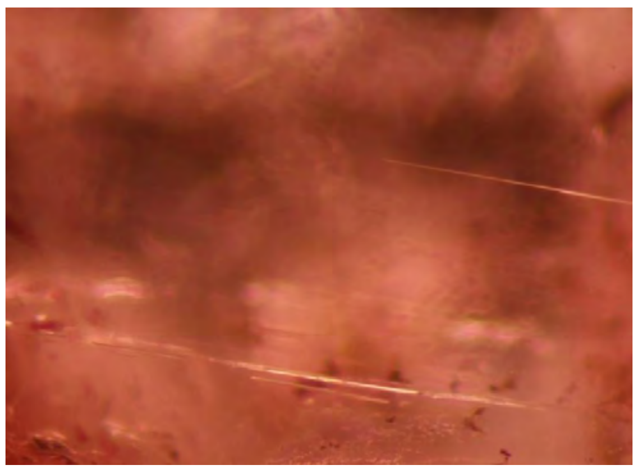

Figure 4.5 Growth tubes, 5.0X in sample TPBRA019 from Brazil.

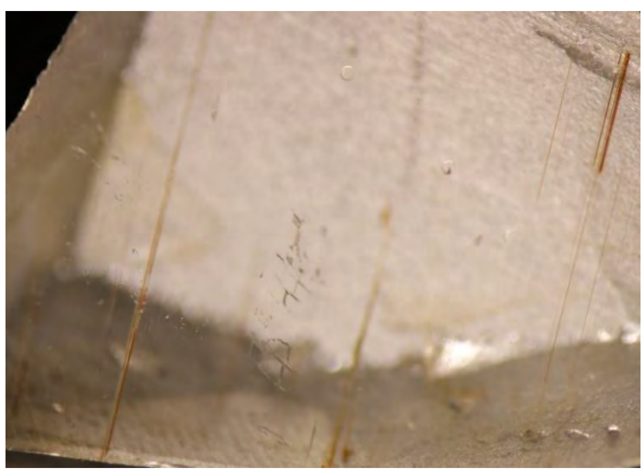

Figure 4.6 Yellowish brown stains in growth tubes, 1.25X

in sample TPMOZ001 from Nampula in Mozambique.

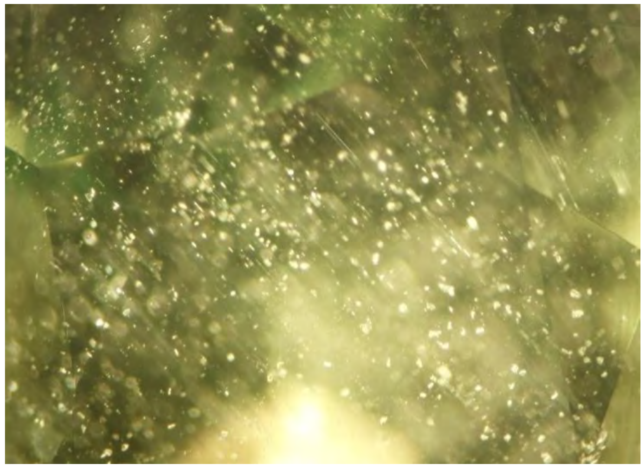

Figure 4.7 Minute particles, 2.0X in sample TPEA001 from Madagascar.

Secondary fluid inclusions were described as “fingerprint” inclusions (Figures 4.8 and 4.9); they can be found in tourmaline samples from Brazil, Mozambique, Nigeria, and East Africa.

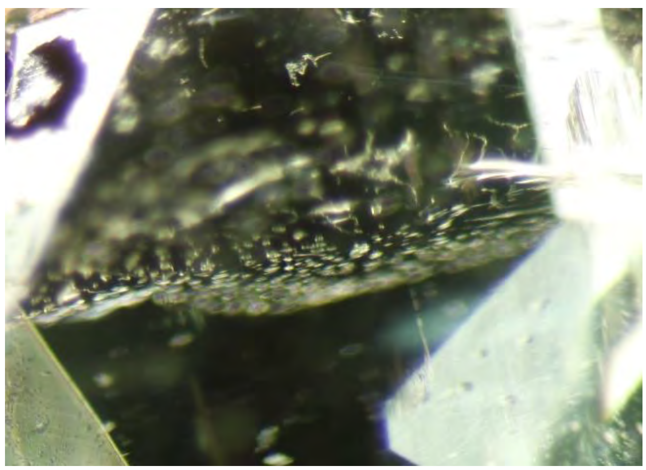

Figure 4.8 Fingerprint inclusions, 2.5X in sample TPBRA031 from Brazil.

Figure 4.9 Fingerprint inclusions 1.25X in sample TPMOZ007 from Nampula in Mozambique.

One of the most crucial inclusions in samples from Brazil and Mozambique is heal fissures (Figures 4.10 and 4.11); which often occur as “trichites” (Figures 4.12 and 4.13). They are fluid-filled cavities connected as networks of thin capillaries. The capillaries were irregular and coarse, wispy, or thread-like form. The cavities were typically flattened and irregularly shaped. In some fissures, isolated two-phase (liquid-gas) inclusions were abundant (Figures 4.14 and 4.15).

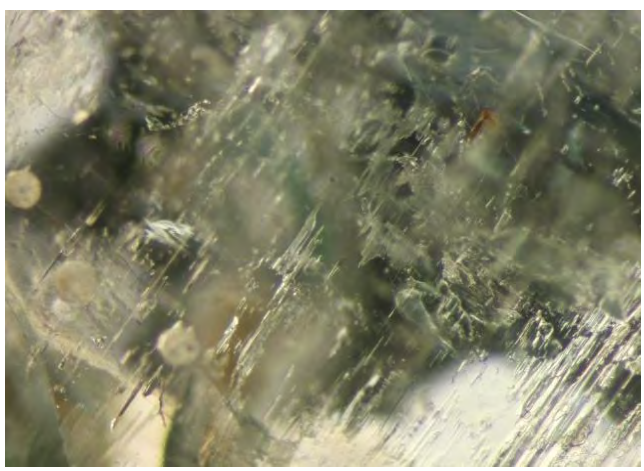

Figure 4.10 Heal fissures, 5.0X in sample TPBRA032 from Brazil.

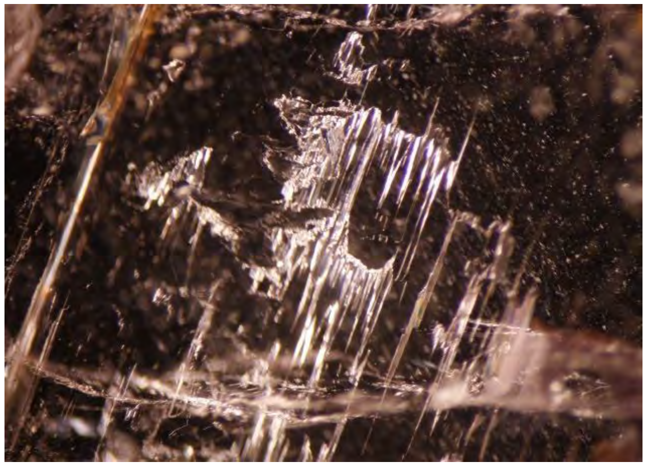

Figure 4.11 Heal fissures, 1.25X in sample TPMOZ010-A from Nampula in Mozambique.

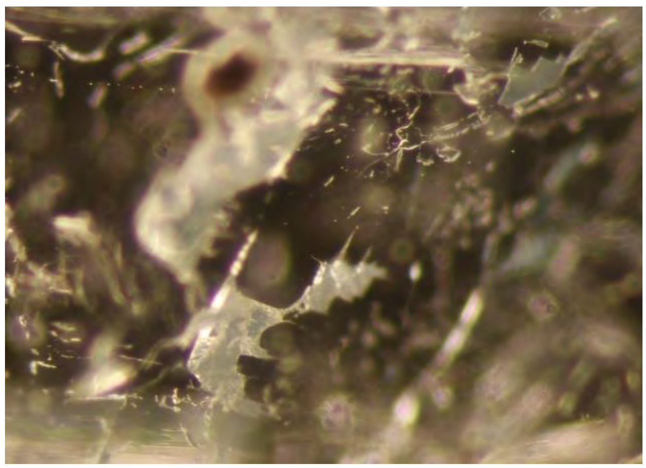

Figure 4.12 Trichites, 5.0X in sample TPBRA029 from Brazil.

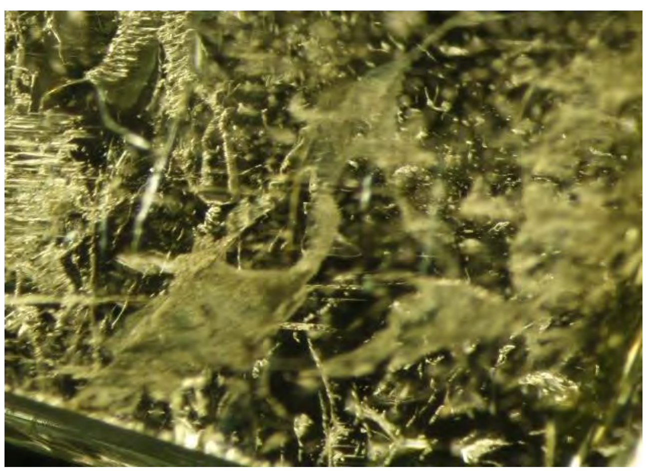

Figure 4.13 Trichites, 1.25X in sample TPMOZ004-A from Nampula in Mozambique.

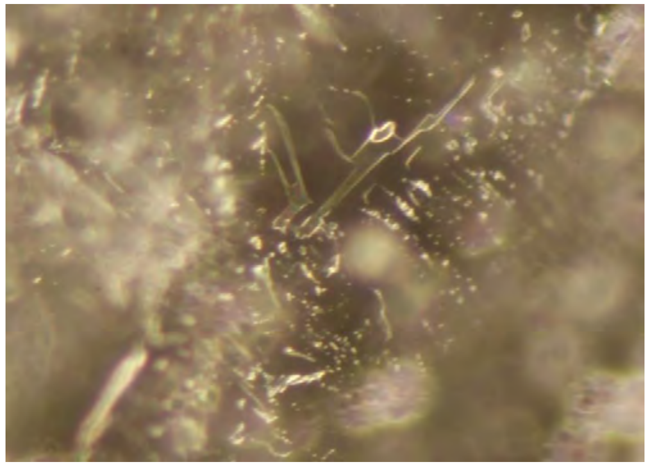

Figure 4.14 Two-phase inclusions in fissures, 5.0X in sample TPBRA026 from Brazil.

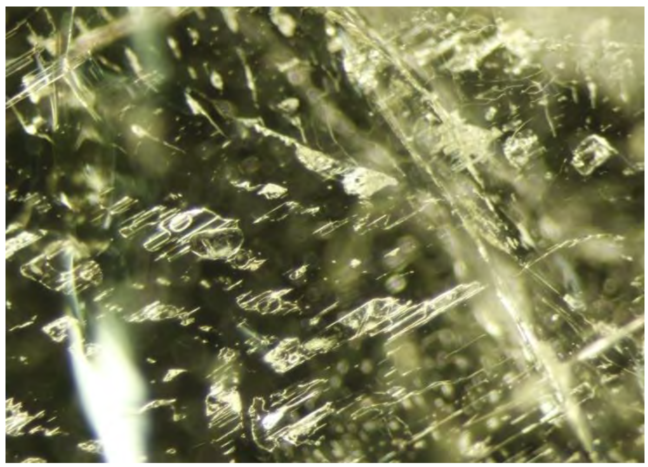

Figure 4.15 Two-phase inclusions in fissures, 5.0X in sample TPMOZ009-A from Nampula in Mozambique.

There are some solid inclusions (unknown minerals) (Figures 4.16-4.27) in samples from Brazil, Mozambique, and Nigeria. Iron strain (Figures 4.28 and 4.29) can be found in samples from all sources except the sample from Madagascar.

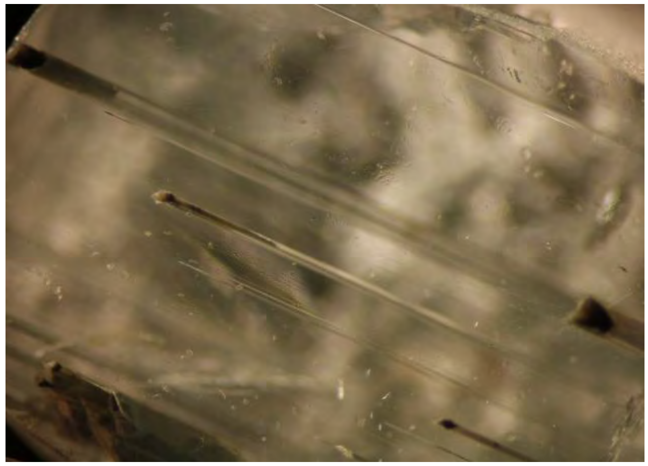

Figure 4.16 Solid inclusions, 3.2X in sample TPBRA016 from Brazil.

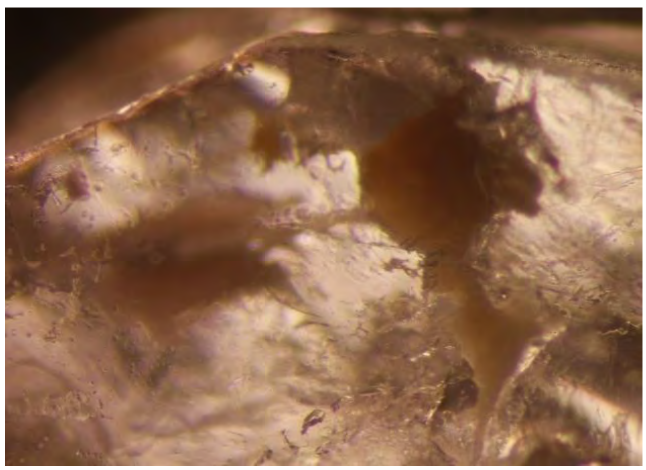

Figure 4.17 Solid inclusions, 5.0X in sample TPBRA022 from Brazil.

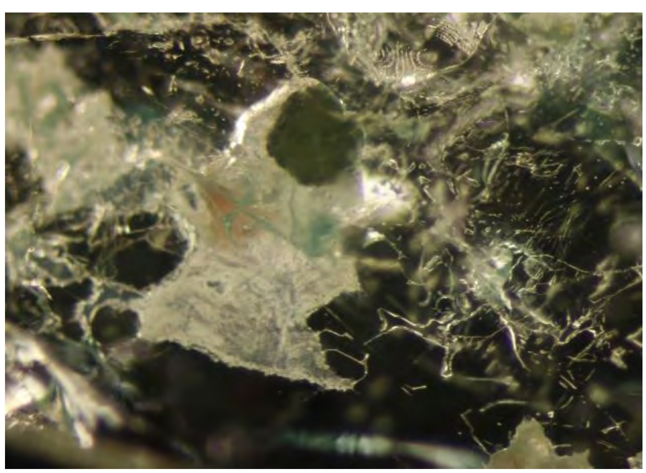

Figure 4.18 Solid inclusions, 5.0X in sample TPBRA022 from Brazil.

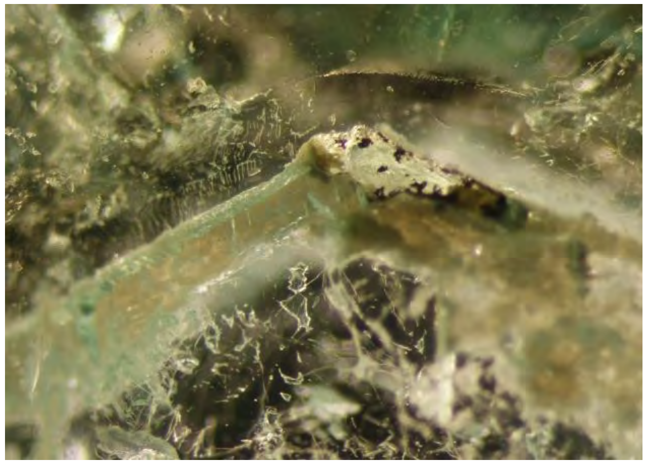

Figure 4.19 Solid inclusions, 4.0X in sample TPBRA036 from Brazil.

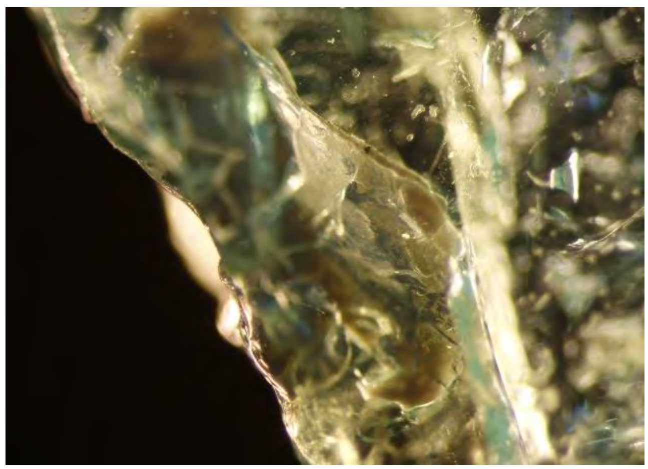

Figure 4.20 Solid inclusions, 2.5X in sample TPBRA037 from Brazil.

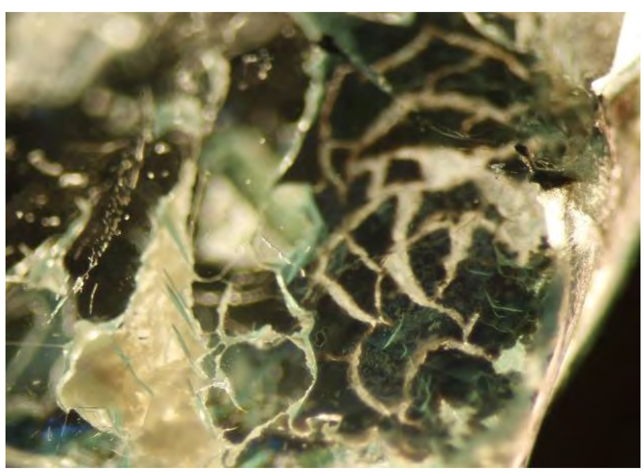

Figure 4.21 Solid inclusions, 2.5X in sample TPBRA037 from Brazil.

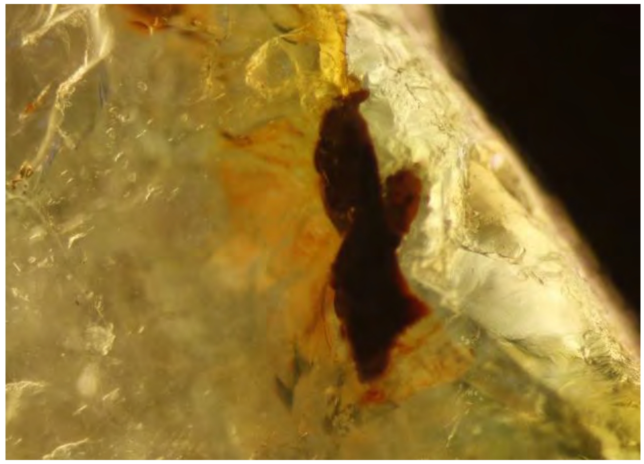

Figure 4.22 Solid inclusions, 2.5X in sample TPBRA042 from Brazil.

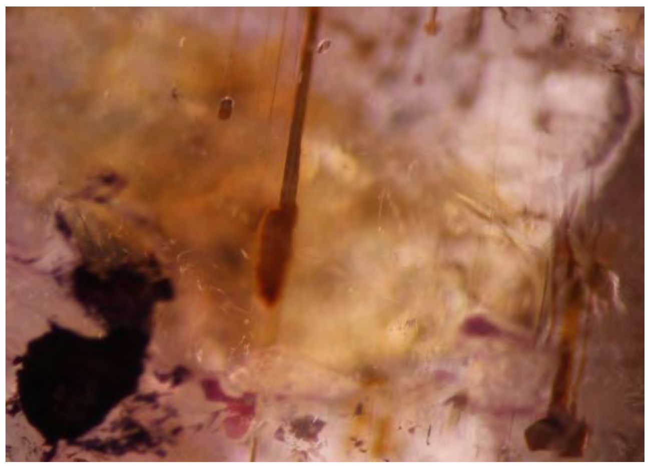

Figure 4.23 Solid inclusions, 2.5X in sample TPMOZ005 from Nampula in Mozambique.

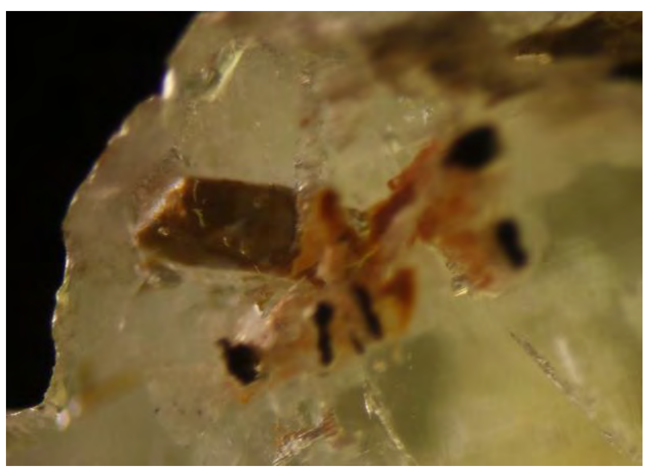

Figure 4.24 Solid inclusions, 2.0X in sample TPMOZ011 from Nampula in Mozambique.

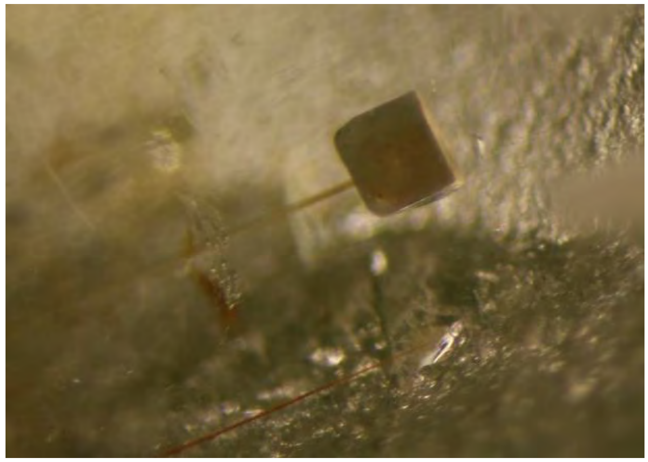

Figure 4.25 Solid inclusions, 2.5X in sample TPMOZ011 from Nampula in Mozambique.

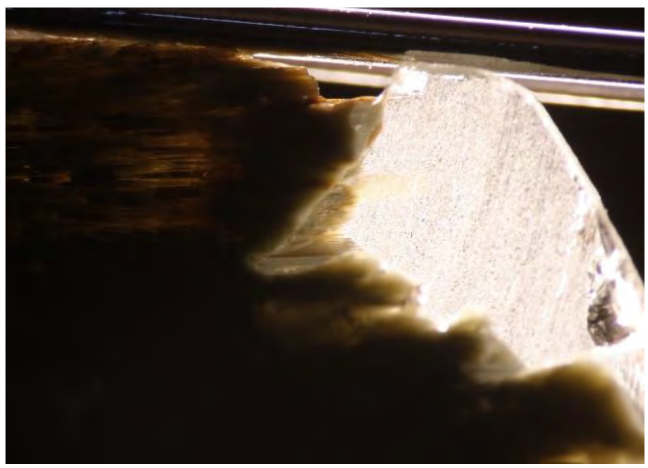

Figure 4.26 Solid inclusions, 1.25X in sample TPNIG002-A from Jos in Nigeria.

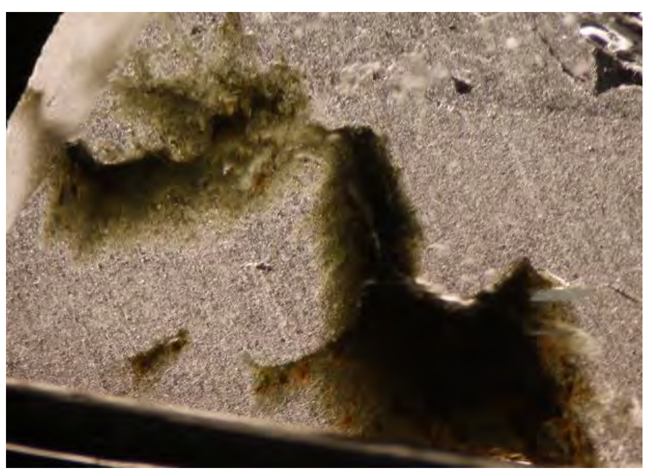

Figure 4.27 Solid inclusions, 1.0X in sample TPNIG002-B from Jos in Nigeria.

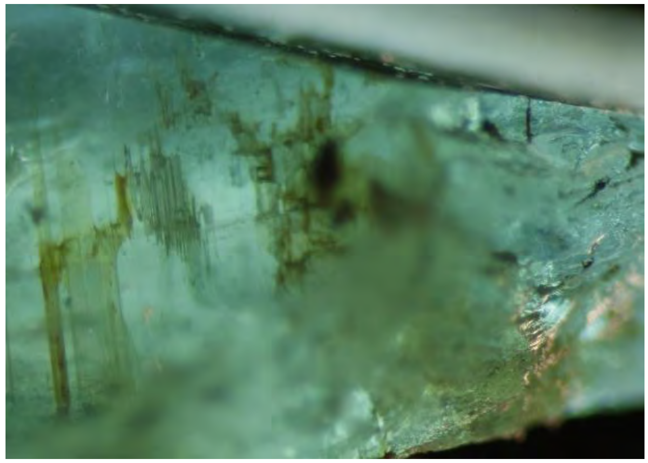

Figure 4.28 Iron strain, 3.2X in sample TPBRA043 from Brazil.

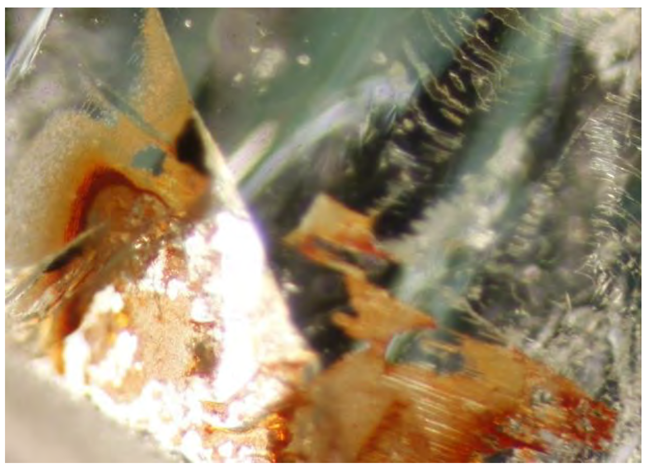

Figure 4.29 Iron strain, 2.5X in sample TPNIG003 from Jos in Nigeria.

For gamma irradiated tourmaline samples, growth tubes and yellowish-brown growth tubes were still remained (Figure 4.30). Liquid and two-phase inclusions were also unaltered (Figures 4.31 and 4.32). Crack, fissure, trichite, iron strain, minute particle, and fingerprint inclusions are still observed in these treated samples (Figures 4.33 and 4.34).

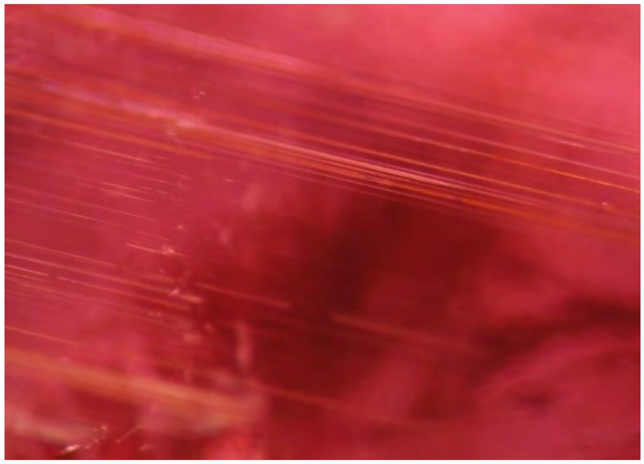

Figure 4.30 Growth tubes and yellowish-brown growth tubes

in gamma irradiated sample, 2.0X in sample TPMOZ002-B from Nampula in Mozambique.

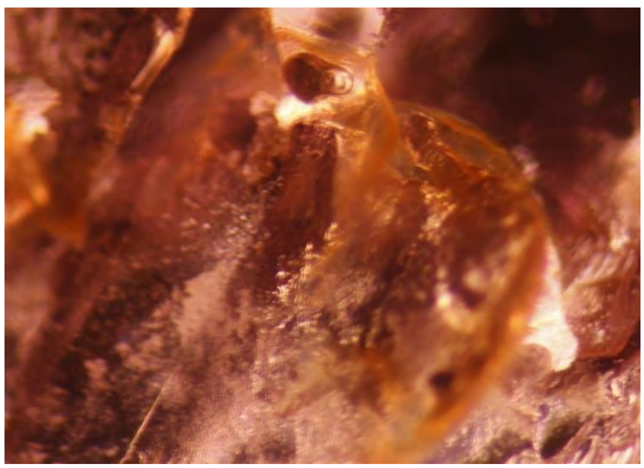

Figure 4.31 Two-phase inclusion (top) and iron strain

in gamma irradiated sample, 4.0X in sample TPBRA038-B from Brazil.

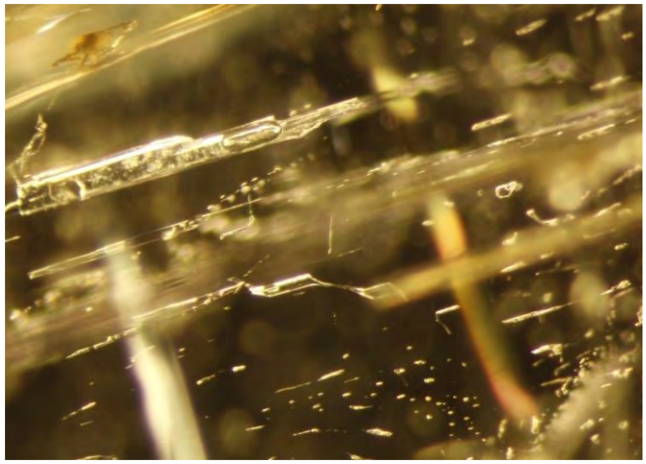

Figure 4.32 Two-phase inclusion in fissures and minute particles in gamma irradiated sample, 4.0X in sample TPBRA038-B from Brazil.

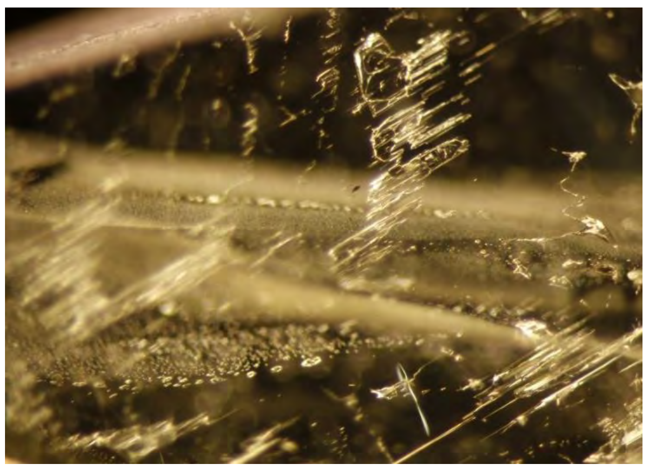

Figure 4.33 Fissures and fingerprint inclusions in gamma irradiated sample, 3.2X in sample TPMOZ009-B from Nampula in Mozambique.

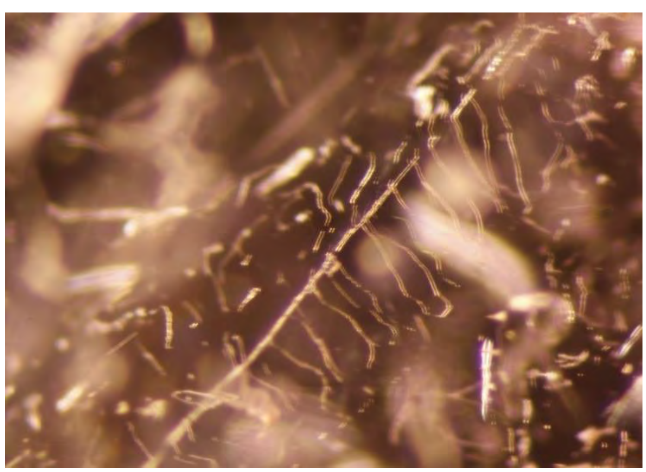

Figure 4.34 Liquid veil in gamma irradiated sample, 5.0X in sample TPNIG001-B from Jos in Nigeria.

In addition, there are unknown inclusions (Figures 4.35-4.40) in some untreated and gamma-irradiation treated samples. The unknown inclusions in treated samples may have already occurred before gamma irradiation.

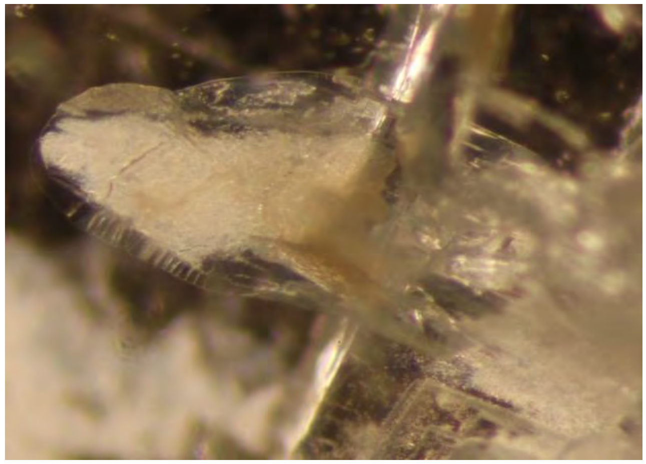

Figure 4.35 Unknown inclusion, 5.0X in sample TPBRA014 from Brazil.

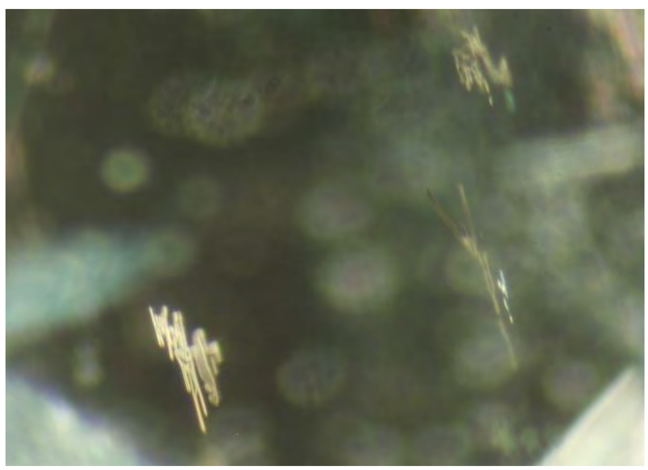

Figure 4.36 Unknown inclusion, 5.0X in sample TPBRA031 from Brazil.

Figure 4.37 Unknown inclusion, 5.0X in sample TPBRA050 from Brazil.

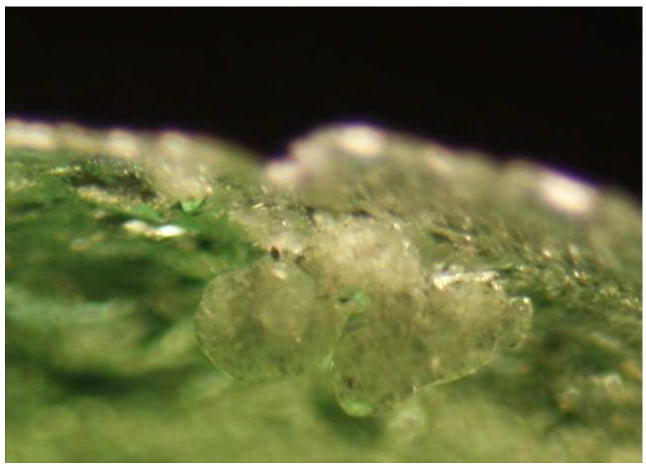

Figure 4.38 Unknown inclusion, 2.0X in sample TPEA005 from East Africa.

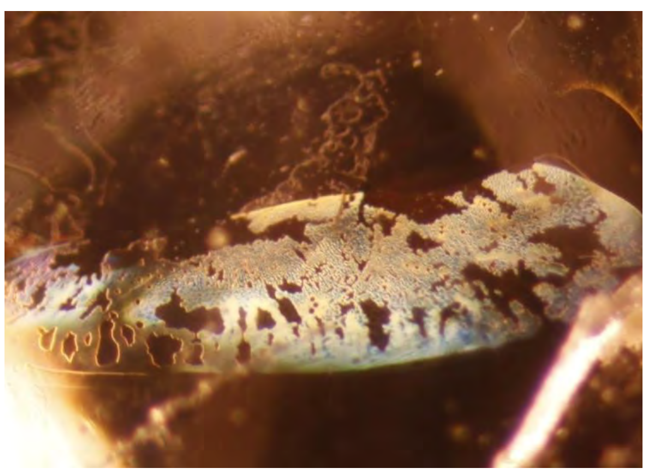

Figure 4.39 Unknown inclusion in gamma irradiated sample, 3.2X in sample TPBRA040-B from Brazil.

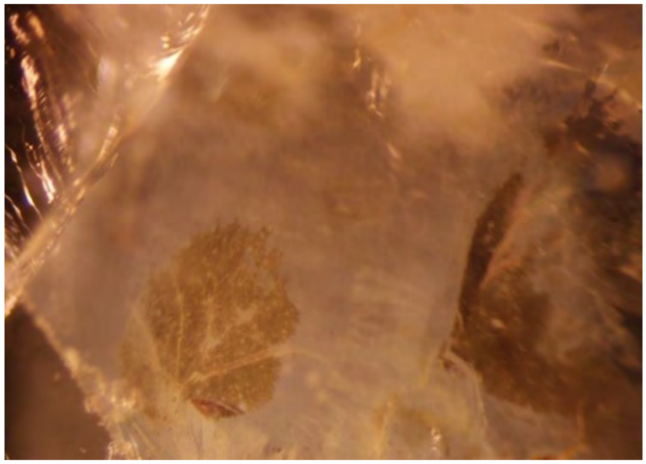

Figure 4.40 Unknown inclusion in gamma irradiated sample,

2.0X in sample TPMOZ011-B from Nampula in Mozambique.

4.3 UV-Vis-NIR Absorption Spectroscopy

Absorption spectra of all samples are provided in Appendix B. The spectra of the same color tourmalines from Brazil, Mozambique, Nigeria, Madagascar and East Africa present similar spectral pattern. Pink tourmalines show a strong absorption band between 510 and 530 nm (Figure 4.41). An absorption band at 515-520 nm is observed in purple samples (Figure 4.42). Presences of Mn^{3+} ions are responsible for these absorption bands. Most of the purple samples show two distinctive absorption bands centered at 390-400 and 685-700 nm, caused by Mn^{2+} and Cu^{2+}, respectively. In addition, pink samples also exhibit a broad absorption between 680 and 715 nm due to Fe^{2+} (Figure 4.43) or Cu^{2+} (Figure 4.41).

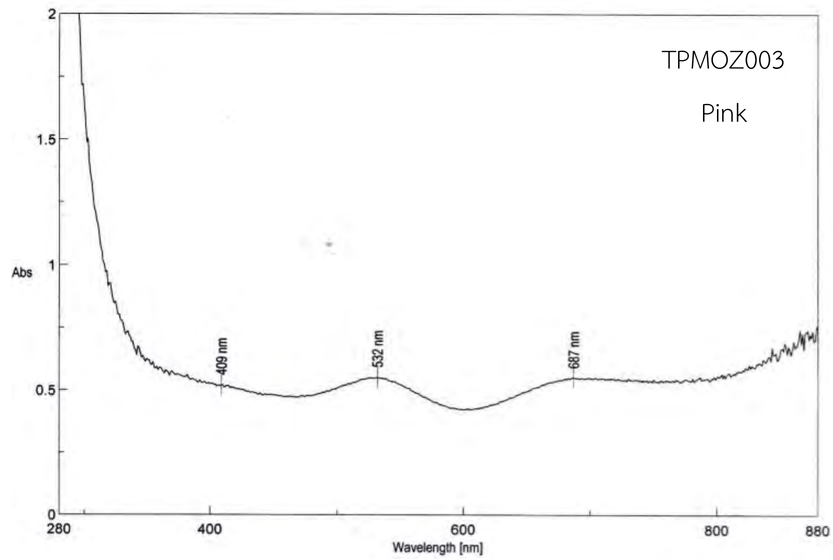

Figure 4.41 Absorption spectrum of natural pink tourmaline from Mozambique.

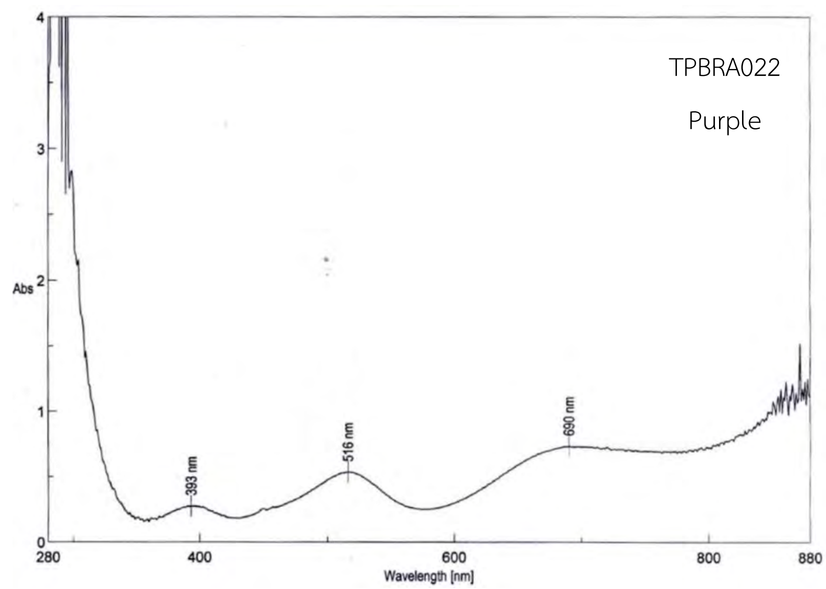

Figure 4.42 Absorption spectrum of natural purple tourmaline from Brazil.

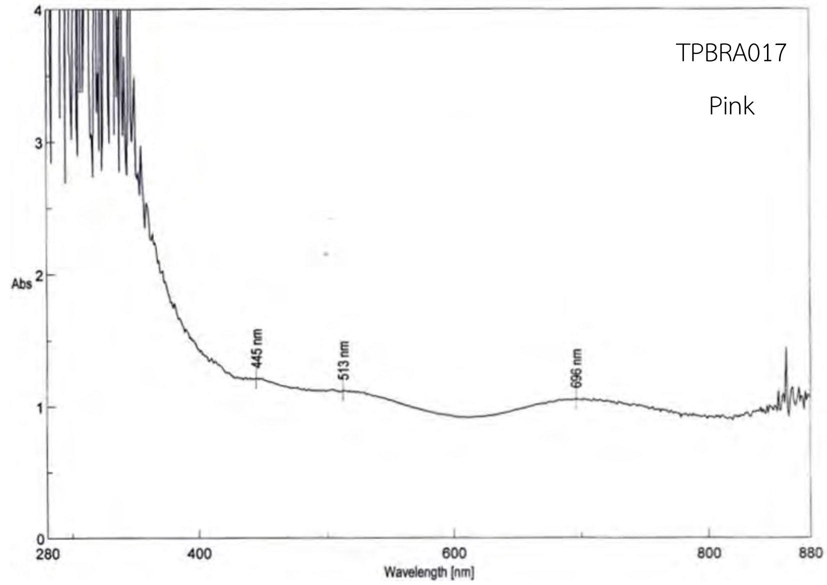

Figure 4.43 Absorption spectrum of natural pink tourmaline from Brazil.

Most of the absorption bands in blue samples from Brazil and Nigeria show the highest absorbance between 690-715 nm caused by Cu^{2+}. Absorption bands also occur at 390-395 and 500-520 nm due to Mn^{2+} and Mn^{3+}, respectively (Figure 4.44). Blue samples from Nampula in Mozambique and some blue samples from Brazil usually show an absorption band due to copper (Figure 4.45). On the other hand, colorless samples from Mozambique and Nigeria show a very low absorption of broad band at 692 nm due to Cu^{2+} (Figure 4.46).

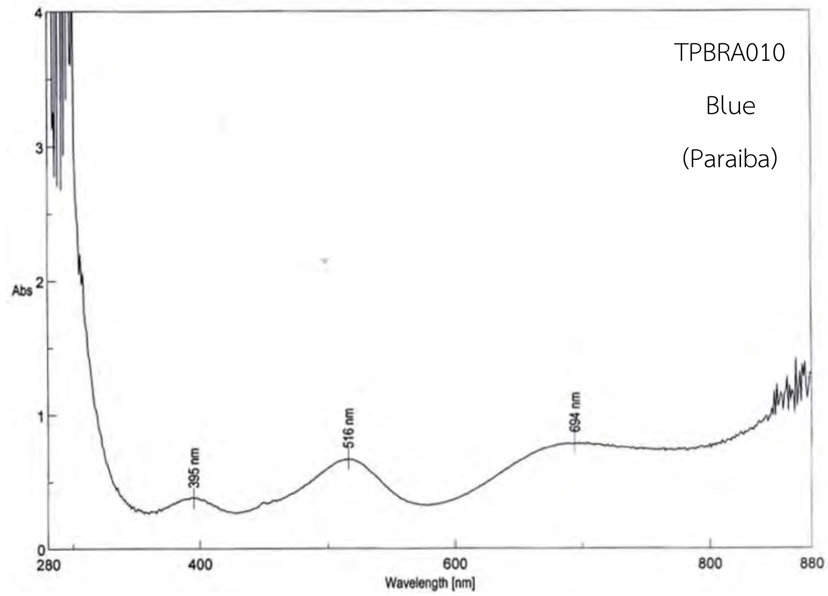

Figure 4.44 Absorption spectrum of natural blue tourmaline from Brazil.

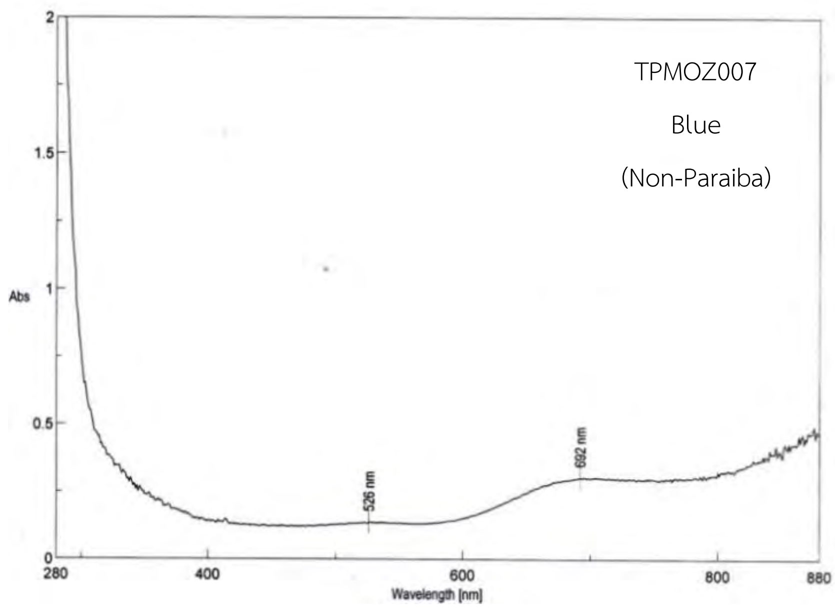

Figure 4.45 Absorption spectrum of natural blue tourmaline from Mozambique.

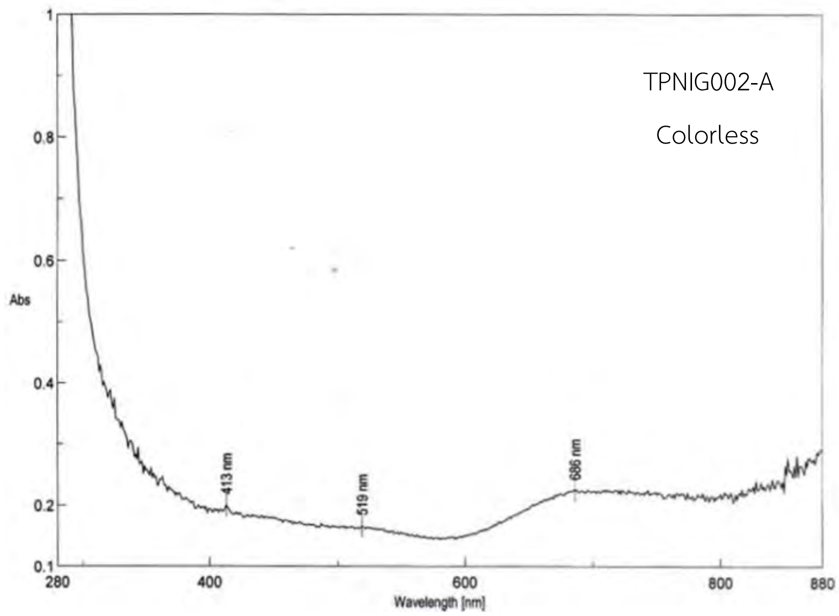

Figure 4.46 Absorption spectrum of natural colorless tourmaline from Jos in Nigeria.

Absorption spectrum of green samples from Madagascar and East Africa show absorption bands at 400-430 and 600-615 nm caused by Mn^{2+} and V^{3+}, respectively (Figure 4.47). However, the absorption spectrum of green samples from Brazil, Mozambique, and East Africa display only a broad band at 690-720 nm due to Cu^{2+} (Figure 4.48) or Fe^{2+} (Figure 4.49).

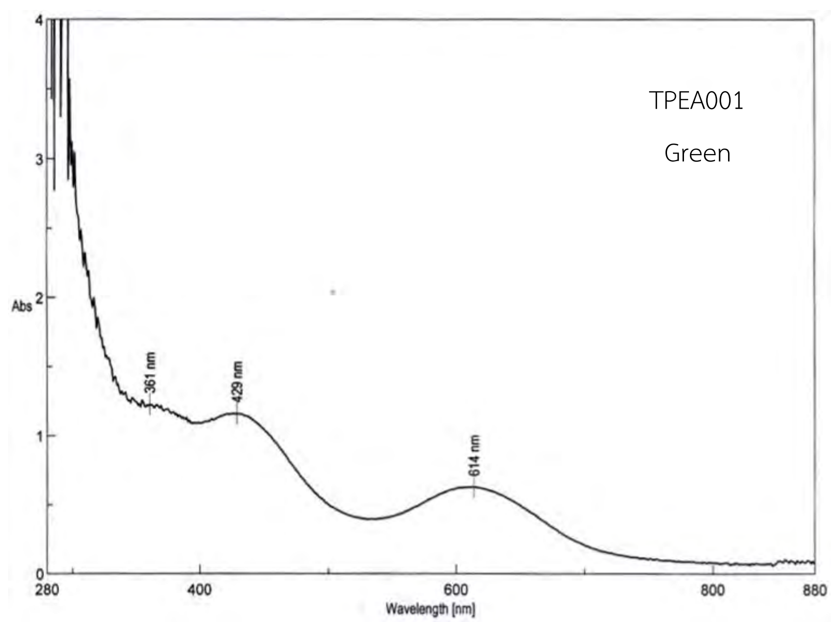

Figure 4.47 Absorption spectrum of natural green tourmaline from Madagascar.

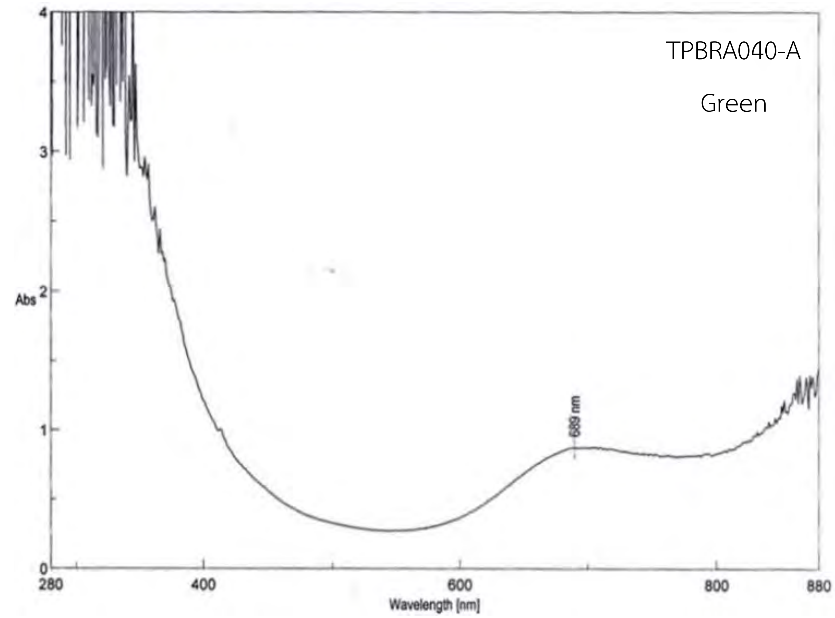

Figure 4.48 Absorption spectrum of natural green tourmaline from Brazil.

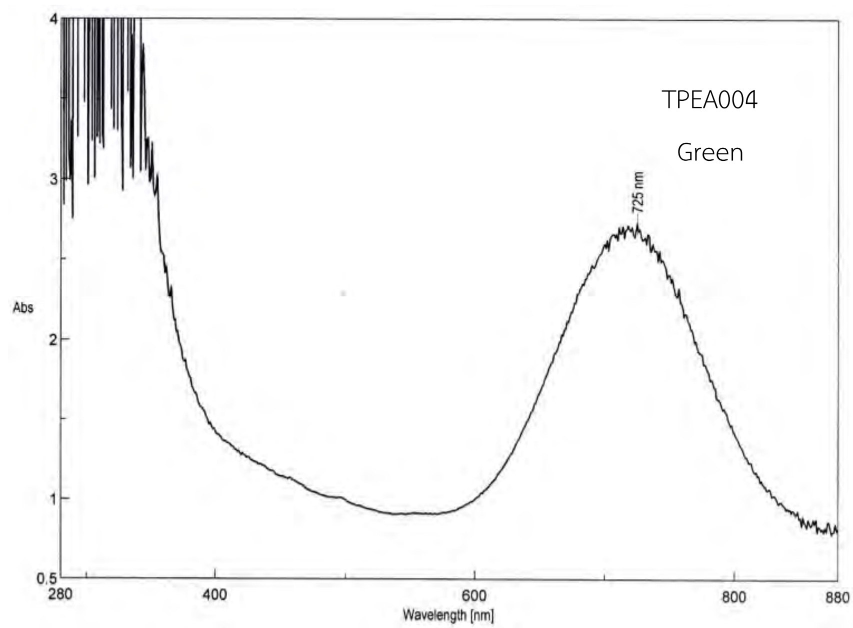

Figure 4.49 Absorption spectrum of natural green tourmaline from East Africa.

UV-Vis-NIR spectra of the untreated light pink samples from Mozambique display the absorption bands at 510-520 and 680-720 nm related to Mn^{3+} and Fe^{2+}, respectively (Figure 4.50). The untreated green samples from Brazil and Mozambique show only a broad absorption band at 690-720 nm due to Fe^{2+} or Cu^{2+} (Figures 4.51 and 4.52). An untreated light blue sample from Nigeria shows three absorption bands due to Mn^{2+}, Mn^{3+}, and Cu^{2+} (Figure 4.53).

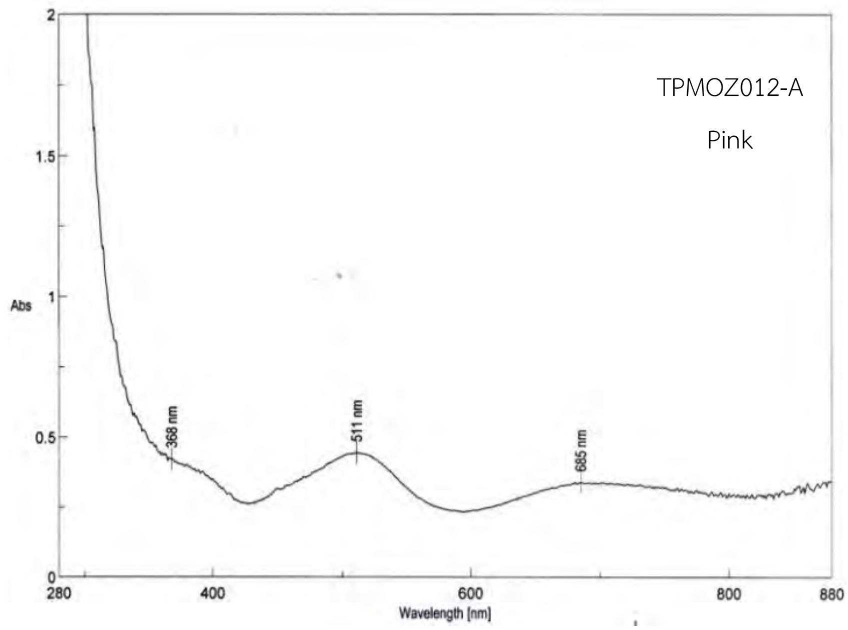

Figure 4.50 Absorption spectrum of untreated pink tourmaline from Mozambique.

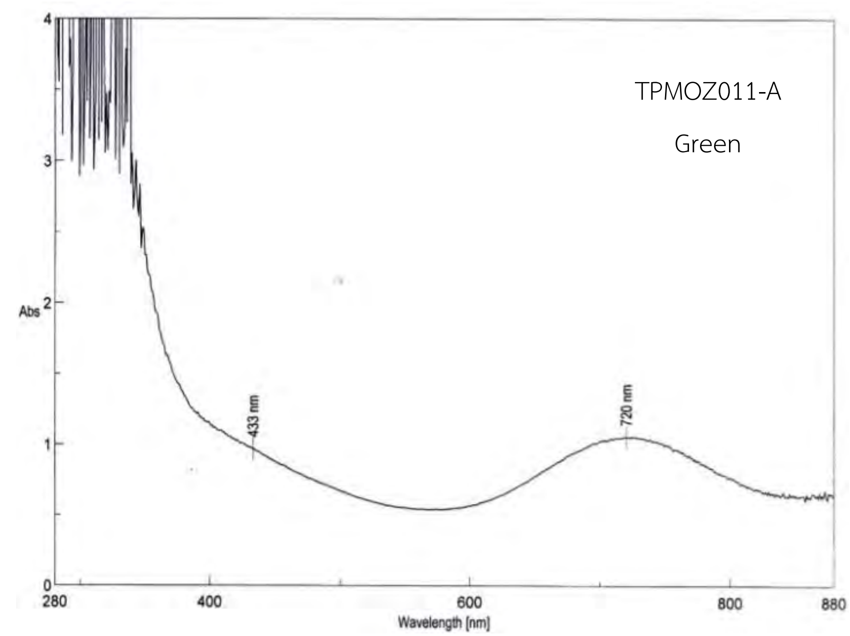

Figure 4.51 Absorption spectrum of untreated green tourmaline from Mozambique.

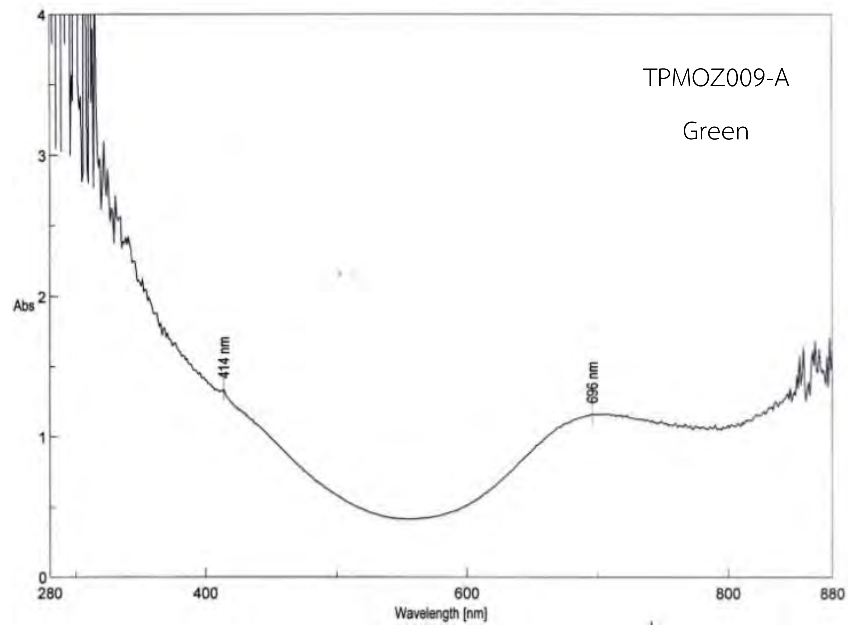

Figure 4.52 Absorption spectrum of untreated green tourmaline from Mozambique.

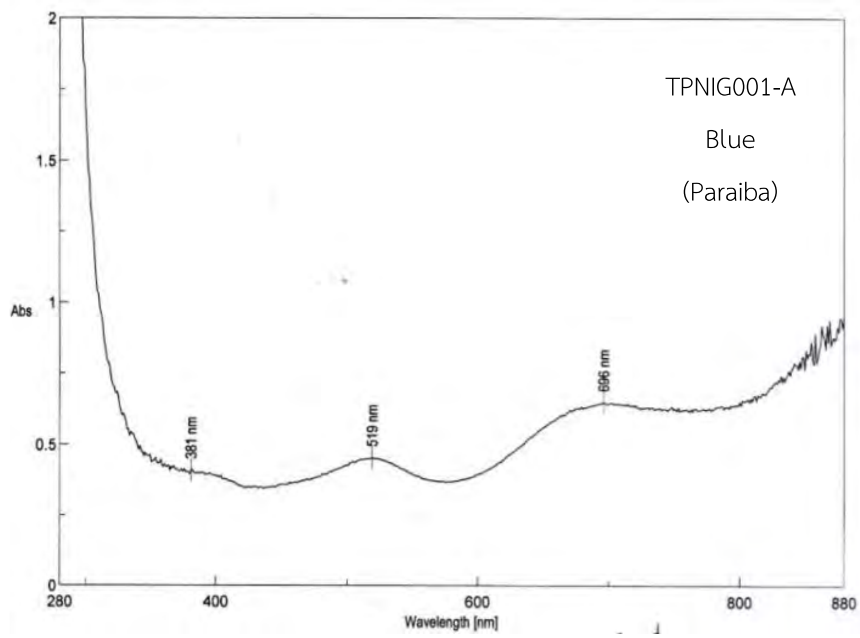

Figure 4.53 Absorption spectrum of untreated light blue tourmaline from Nigeria.

For the first gamma ray treatment, light pink sample is changed to vivid pink which show similar absorption band related to Mn^{3+} with decreased absorption band of Fe^{2+} (Figure 4.54). Most of the green samples changed to pale pink color which present absorption band of Mn^{3+} at 510-520 nm and the decreasing of broad absorption due to Cu^{2+} (Figure 4.55). Two green samples from Mozambique were still unchanged. The absorption bands of the light blue sample due to Mn^{2+} and Mn^{3+} are increased but the absorption band of Cu^{2+} is decreased when both samples are turned to pale pink color (Figure 4.56).

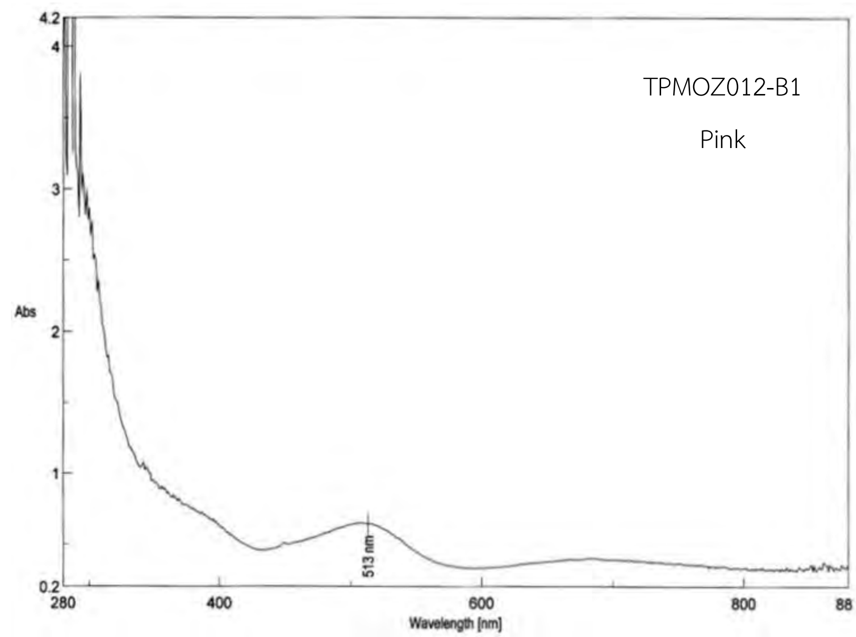

Figure 4.54 Absorption spectrum of first gamma ray irradiated pink tourmaline from Mozambique.

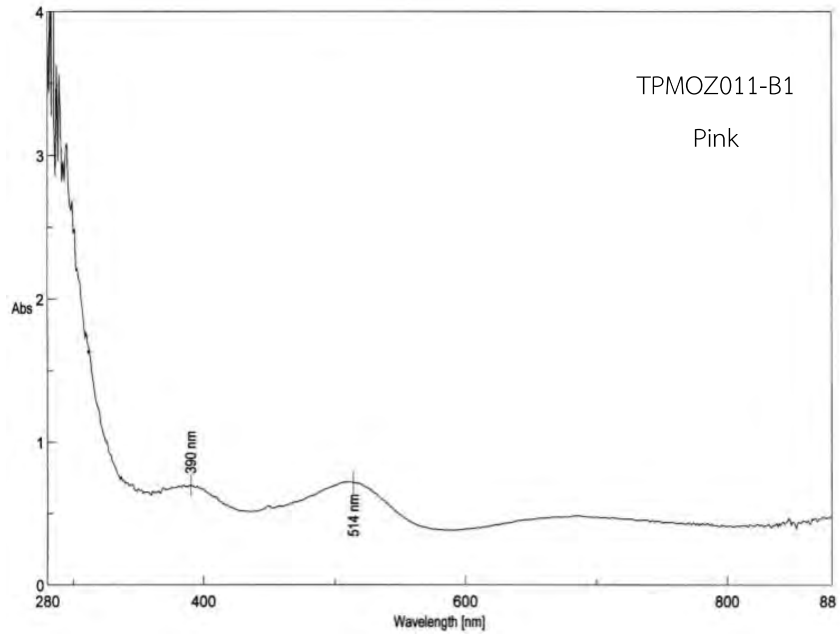

Figure 4.55 Absorption spectrum of first gamma ray irradiated green tourmaline from Mozambique.

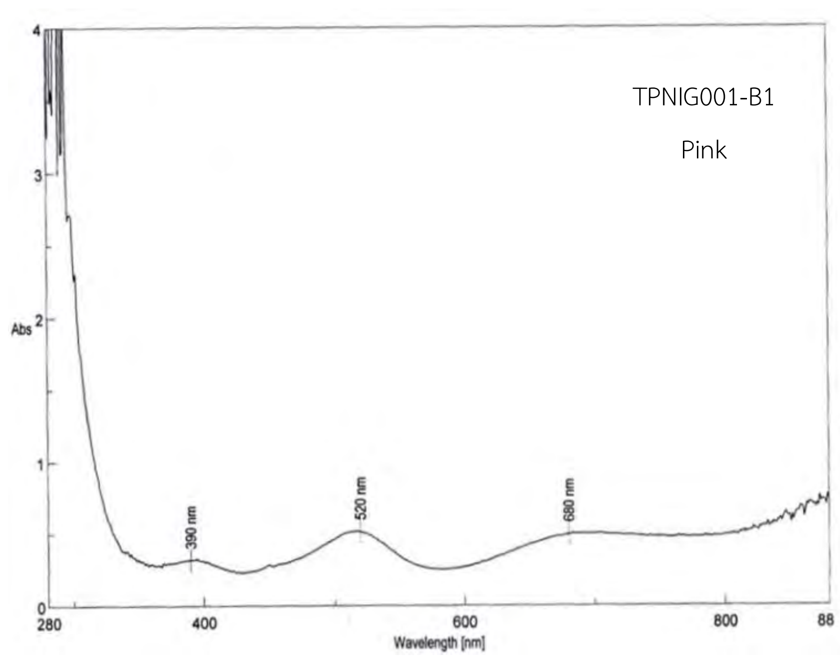

Figure 4.56 Absorption spectra of first gamma ray irradiated blue tourmaline from Nigeria.

After the second time of gamma irradiation, pink samples from Mozambique turn to vivid pink color which their absorption bands of Mn^{3+} and Fe^{2+} tend to be increased and decreased, respectively (Figure 4.57). Green samples changed to pale pink after the 1st radiation and turned to vivid pink after the 2nd radiation present distinctively increasing absorption band of Mn^{3+} (Figure 4.58). Two green samples from Mozambique changed to pale green with decreased absorption band of Cu^{2+} (Figure 4.59). Absorption bands of blue sample turned to pale pink and vivid pink after the 1st and 2nd radiation, respectively, which is caused by increasing adsorption of Mn^{3+} (Figure 4.60).

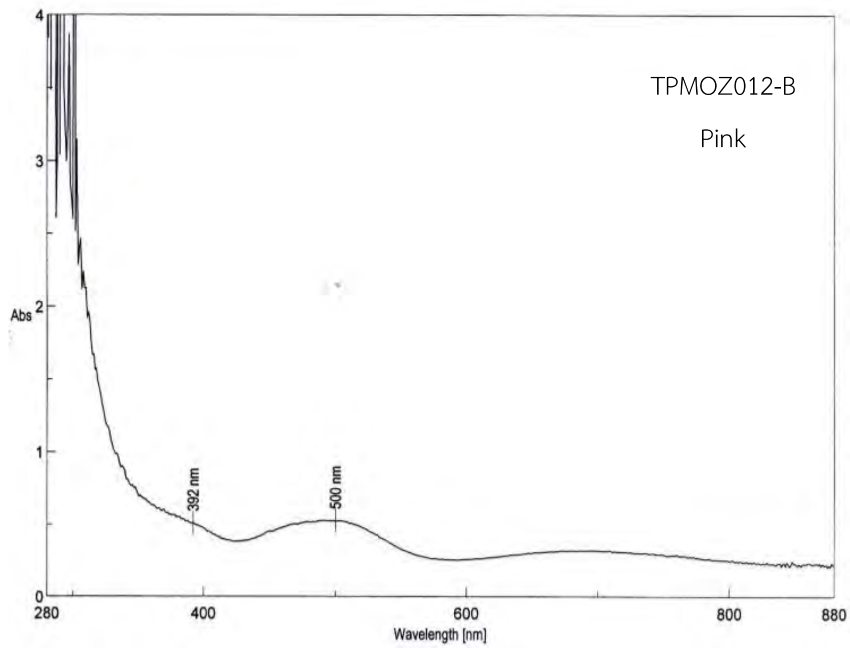

Figure 4.57 Absorption spectrum of second gamma ray irradiated pink tourmaline from Mozambique.

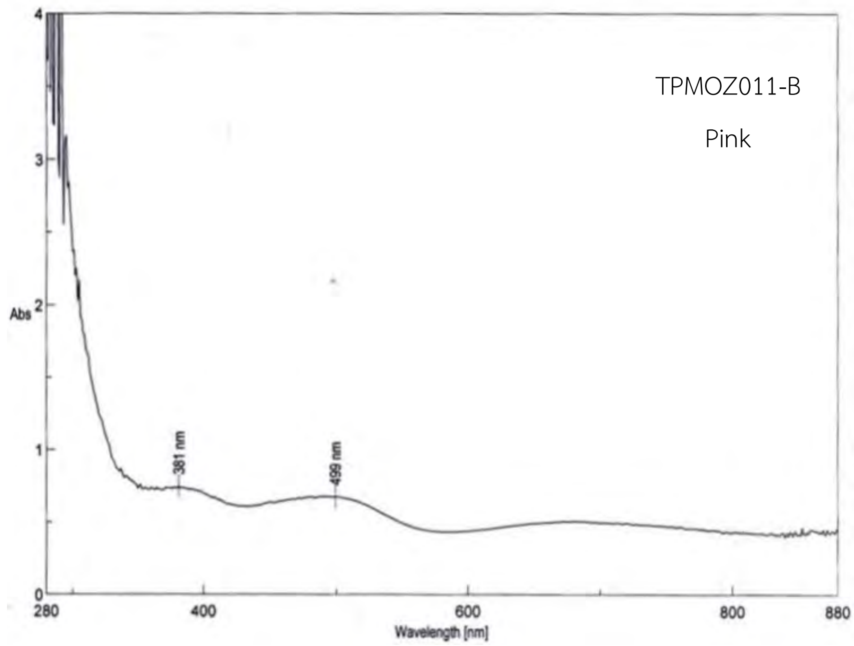

Figure 4.58 Absorption spectrum of second gamma ray irradiated green tourmaline from Mozambique.

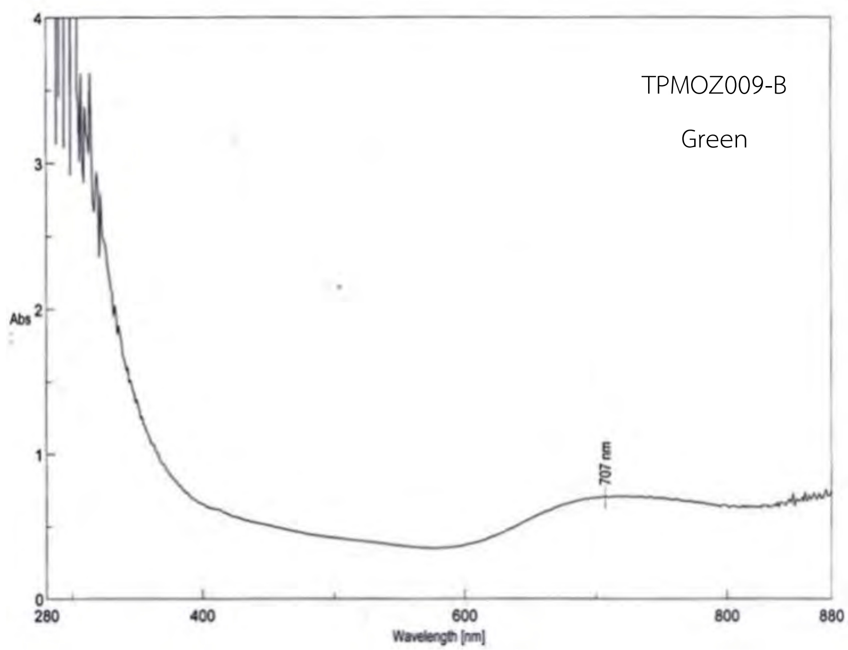

Figure 4.59 Absorption spectrum of second gamma ray irradiated green tourmaline from Mozambique.

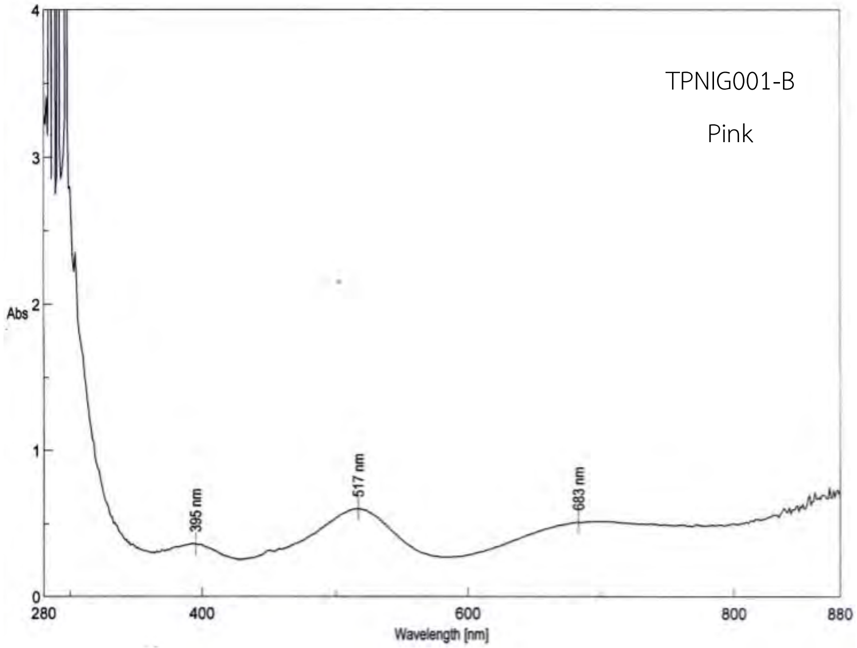

Figure 4.60 Absorption spectrum of second gamma ray irradiated blue tourmaline from Nigeria.

4.4 Fourier Transformed Infrared Spectroscopy

Infrared spectra of all samples are similarly present and reported in Appendix C. They are characterized by broad bands at about 6990, 6770 cm^{-1} related to OH stretching and 4600, 4540, 4440, 4345, 3900 cm^{-1} related to M-OH bonding where M can be Al, Fe, Mn, and others cations (Saeseaw et al., 2009) (Figure 4.61).

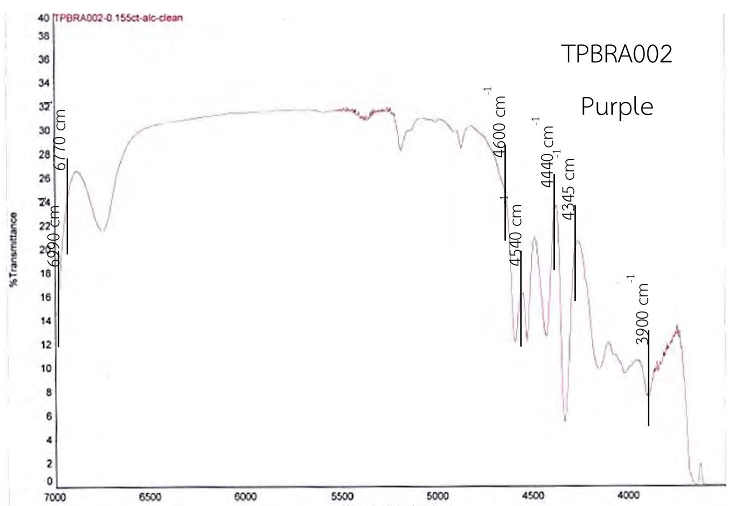

Figure 4.61 Representative FTIR spectrum commonly present in all tourmaline samples.

FTIR spectra of natural and gamma-irradiated tourmaline samples from Brazil, Mozambique, and Nigeria are displayed in Figures 4.62, 4.63, and 4.64, respectively. For natural samples (displayed as blue lines), the absorption bands are grouped as a function of vibrational assignments, such as hydroxyl vibrations region and combination modes of M-OH bonds which are located in the near-infrared spectral range, 4800-4000 cm^{-1}, whereas stretching vibrations present at 4000-3000 cm^{-1}. Weak absorption bands around 4600 cm^{-1} related to Al-OH1 bending and stretching vibrations in Y-site are observable in all samples.

After gamma irradiation (displayed as red line), all bands still remained at the same wave number. The baselines of all treated samples also remain at the same level. Except the strong absorption band around 3700-3400 cm^{-1}, the blue line of Brazil sample tends to be lower than the red line. However, the blue lines of Mozambique and Nigeria samples tend to be higher than the red lines.

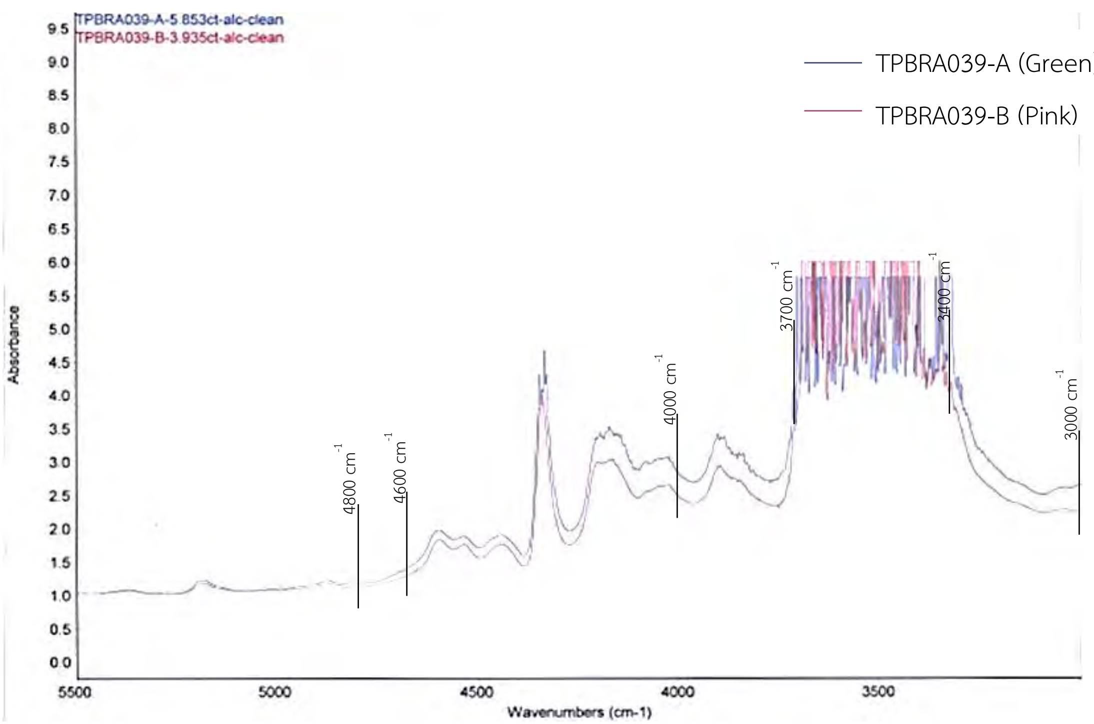

Figure 4.62 Representative FTIR spectrum of natural and gamma-treated tourmaline sample TPBRA039 from Brazil.

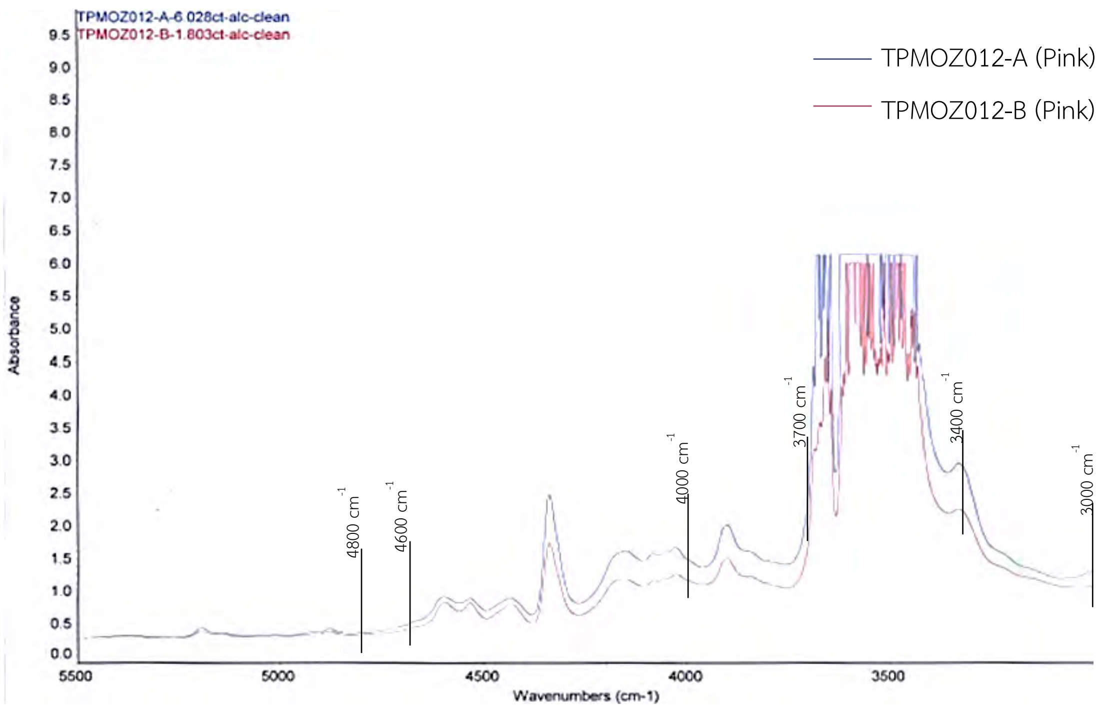

Figure 4.63 Representative FTIR spectrum of natural and gamma-treated tourmaline sample TPMOZ012 from Nampula in Mozambique.

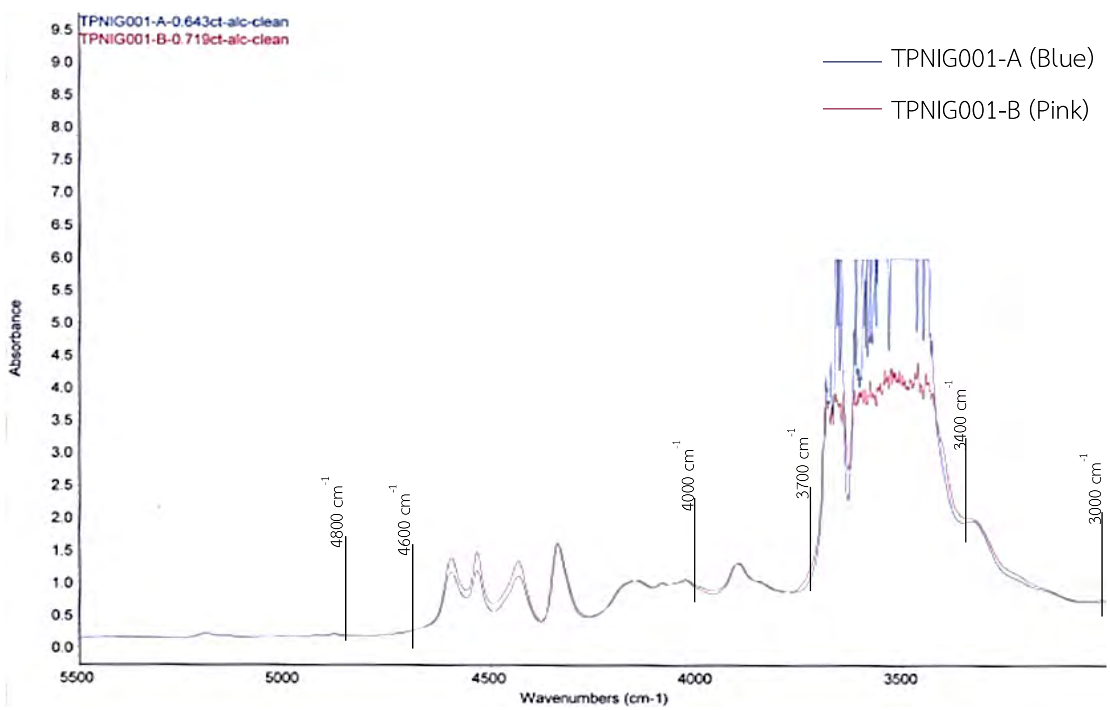

Figure 4.64 Representative FTIR spectrum of natural and gamma-treated tourmaline sample TPNIG001 from Jos in Nigeria.

4.5 Chemical Composition

Major chemical compositions, resulted from Semi-quantitative EDFXF analysis, of tourmaline samples are summarized in Table 4.1. Tourmaline samples from Brazil contain 34.43 to 44.34 wt% Al_2O_3, 26.42 to 38.24 wt% SiO_2, 0.21 to 1.11 wt% MgO, and ≤1.01 wt% Fe_2O_3. Tourmaline samples from Nampula in Mozambique present 38.25 to 43.83 wt% Al_2O_3, 32.53 to 34.68 wt% SiO_2, 0.33 to 0.49 wt% MgO, and 0.00 to 0.31 wt% Fe_2O_3. Tourmaline samples from Jos in Nigeria have similar chemical compositions compared to those from Brazil and Nampula, Mozambique; they present 39.97 to 43.02 wt% Al_2O_3, 32.90 to 34.75 wt% SiO_2, 0.32 to 0.49 wt% MgO, and 0.01 to 2.62 wt% Fe_2O_3. Only one from Madagascar yields 34.03 wt% Al_2O_3, 31.79 wt% SiO_2, uncommonly high content of 11.32 wt% MgO, with low Fe_2O_3 content (0.03 wt%). Samples from East Africa range widely between 25.41 to 40.450 wt% Al_2O_3, 30.18 to 36.08 wt% SiO_2, 0.32 to 15.91 wt% MgO, and 0.00 to 4.38 wt% Fe_2O_3.

Table 4.1 Summary of major and minor contents (wt%), based semi-quantitative EDXRF analysis, of all tourmaline samples from Brazil, Nampula in Mozambique, Jos in Nigeria, Madagascar, and East Africa.

Sample	Brazil	Nampula in Mozambique	Jos in Nigeria	Madagascar	East Africa
SiO_2	26.42-38.24	32.53-34.69	32.90-34.75	31.79	30.18-36.08
TiO_2	0.00-0.14	0.00-0.19	0.00-0.15	0.45	0.02-1.65
Al_2O_3	34.43-44.34	38.25-43.83	39.97-43.02	34.03	25.41-40.45
Fe_2O_3	0.00-1.01	0.00-0.31	0.01-2.62	0.03	0.00-4.38
MnO	0.00-4.77	0.10-5.81	0.25-1.90	0.04	0.01-3.79
MgO	0.21-1.11	0.33-0.49	0.32-0.49	11.32	0.32-15.91
CaO	0.04-1.09	0.08-0.48	0.52-1.10	1.50	0.34-5.16
Na_2O	0.94-3.59	2.21-3.00	2.05-2.37	2.18	1.20-3.22
K_2O	0.00-0.15	0.01-0.06	0.03-0.05	0.11	0.03-0.13
P_2O_5	0.00-0.41	0.00-0.27	0.00-0.01	0.00	0.00-0.40
BaO	0.00-0.01	0.00-0.01	0.00-0.01	0.00	0.00-0.12
Rb_2O	0.00-0.01	0.00	0.00-0.02	0.00	0.00
SrO	0.00	0.00	0.00-0.01	0.01	0.00-0.52
Nb_2O_5	0.00	0.00	0.00	0.00	0.00
PbO_2	0.00-0.09	0.00-0.03	0.02-0.25	0.00	0.00-0.16
Ga_2O_3	0.00-0.13	0.04-0.11	0.03-0.05	0.00	0.00-0.05
ZnO	0.00-3.10	0.00-0.06	0.00-0.12	0.01	0.00-0.48
CuO	0.00-3.49	0.14-0.79	0.32-0.45	0.00	0.00-0.01
Ni_2O_3	0.00-0.01	0.00	0.00	0.00	0.00
V_2O_3	0.00-0.01	0.00-0.01	0.00-0.01	0.36	0.00-0.71
Cr_2O_3	0.00-0.12	0.00-0.03	0.00	0.01	0.00-0.20
CoO	0.00	0.00-0.01	0.00	0.00	0.00-0.01
W	0.00-0.04	0.00	0.00	0.00	0.00-0.01
SnO_2	0.00-0.01	0.00-0.01	0.00	0.00	0.00-0.02
Ce	0.00-0.02	0.00-0.01	0.00	0.03	0.00-0.08

CHAPTER 5

DISCUSSION AND CONCLUSION

All of tourmaline samples from Brazil, Nampula in Mozambique, and Jos in Nigeria yielded refractive indices (R.I.) of n_o= 1.638-1.641 and n_e= 1.619-1.624, birefringence of 0.017-0.020, specific gravity (S.G.) of 3.023-3.238, They are significantly inert in long-wave ultraviolet (LWUV) and short-wave ultraviolet (SWUV).

The common inclusions are composed of crack, liquid veil, minute, fingerprints, heal fissure, iron strain, and growth tube. Yellow to reddish brown growth tubes are found in samples from Brazil and Nampula in Mozambique. Two-phase inclusions and solid inclusion are found in some tourmaline samples, none of these inclusions can be used as the indicator of origin determination. In addition, inclusions in gamma irradiated tourmaline samples are quite similar to the natural stones.

Tourmaline has various colors depending on the transition metals present as impurities in its structure. Moreover, charge interactions between cations and anions are also important to be considered. The cause of color in tourmaline samples were analyzed by UV-Vis-NIR absorption spectrum. The following conclusions were obtained:

Pink color

Manganese (Mn^{3+}) ions in the high state, distorted octahedral sites are responsible for pink and red-pink tourmaline called rubellite (Maneewong et al., 2016) which is evidenced by absorption band at 510-530 nm.

Purple color

These colors are the result of Mn^{3+} and Cu^{2+}, which relate to pink and blue colors (Laurs et al., 2008), evidenced by absorption bands at 515-520 nm and 685-700 nm, respectively.

Blue color

The absorption band in the vicinity of 690-715 nm is due to the presence of Fe^{2+} or Cu^{2+}, which causes a greenish blue color (Abduriyim et al., 2006). Moreover, most of blue tourmaline samples are obtained from Cu^{2+} which combines with Mn^{3+} yielding absorption band at 500-520 nm. Thses are characteristics of Paraiba-type tourmaline (Laurs et al., 2008).

Green color

Green color of tourmaline is a result of V^{3+} on the octahedral coordinated aluminum-sites (Z-sites), evidenced by absorption band at 600-615 nm which is called as chrome tourmaline. Result of Fe^{2+} d-d transitions or Fe^{2+}-Ti^{4+} IVCT evidenced by absorption band at 690-720 nm is called as verdelite (Pezzotta and Laurs, 2011). In addition, the cause of green color in some tourmaline samples is due to Cu^{2+} indicated by absorption band at 690-720 nm (Laurs et al., 2008).

Darker and vivid color

The darker color is formed by high absorbance in all regions of the visible spectra caused by Fe^{2+}-Fe^{3+} IVCT, Fe^{2+} d-d transition, and Fe^{2+}-Ti^{4+} IVCT. In addition, vivid color relates to the higher absorption band that is caused by metal ions in the structure (Bačík et al., 2015).

Lighter color and colorless

Mn^{2+} from d-d transition at the octahedral site, may cause pale color in some samples which show an additional band of Mn^{2+}-Ti^{4+} IVCT, with lower absorbance compared to the darker sample as suggested by Phichaikamjornwut et al. (2019). In comparison between vivid pink and light pink tourmaline samples, the light pink samples usually show higher absorption band at 510-520 nm and lower absorption band at 370-400 nm due to Mn^{3+} and Mn^{2+}, respectively. On the other hand, colorless samples yield very low absorbance.

Effect of gamma irradiation

All light pink tourmaline samples were changed to vivid pink after gamma irradiation. Absorption band of Mn^{2+}, Fe^{3+} were decreased whereas absorption band of Mn^{3+} was increased evidenced by absorption bands at 370-400 nm, 510-520 nm, and 690-720 nm due to Mn^{2+}, Mn^{3+}, and Fe^{3+}, respectively (see Figures 4.50 and 4.57).

Cu^{2+} or Fe^{2+} ions which cause blue or green color in tourmaline are decreased. Mn^{3+} absorption is developed by gamma ray irradiation and consequently leads to dramatic change from green or blue to pink. Mn^{3+} ions are responsible for pink to red color evidenced by comparison between untreated (blue or green) and gamma-irradiated (pink) tourmaline samples. Gamma-irradiated samples have lower absorption band at 690-700 nm and higher absorption band at 510-520 nm due to Cu^{2+} or Fe^{2+} and Mn^{3+}, respectively (see Figures 4.53 and 4.60). Green tourmaline changed to pink is also due to Fe^{2+} -> Fe^{3+} transition after irradiation, a green sample from Nampula in Mozambique which its color was caused by Fe^{2+} is changed to pink, as a result of decreasing absorption band of Fe^{2+} at 720 nm. Color alteration may occur differently depending on impurities and their quantities (Ahn et al., 2013). For example, green samples, caused by Cu^{2+}, from Brazil can be changed to pink color, but green samples, also caused by Cu^{2+}, from Nampula in Mozambique were only changed to pale green (see Figures 4.52 and 4.59).

FTIR spectrum of natural tourmaline samples from Brazil, Mozambique, and Nigeria present similar bands at 4800-4000 cm^{-1} and 4000-3000 cm^{-1}, which relate to M-OH bonds and OH-stretching (Saeseaw et al., 2009). These bands are common in tourmaline and cannot be used as indicator of geographic origin. In comparison between FTIR spectra of untreated tourmaline samples and gamma-irradiated one, most of the band are similar, except the OH band at 3676-3415 cm^{-1} was decreased after gamma irradiation. Liquid inclusions in the samples might be slightly changed (Phichaikamjornwut et al., 2019). In this study, OH band after gamma irradiation of tourmaline samples from Nampula, Mozambique and Jos, Nigeria were decreased, but those of tourmaline samples from Brazil were increased.

Chemical analyses from EDXRF Spectrometer could not be used for tourmaline classification and geographic origin determination. Hence, Electron Probe Micro-Analyzer (EPMA) and Laser Ablation-Inductively Coupled Plasma-Mass Spectrometer (LA-ICP-MS) are required for both prospects.

REFERENCES

Abduriyim, A., Kitawaki, H., Furuya, M., Schwarz, D., 2006. Paraiba-type copper-bearing tourmaline from Brazil, Nigeria, and Mozambique: chemical fingerprinting by LA-ICP-MS. Gems & Gemology, Vol. 42, No. 1, pp. 4-21.

Abduriyim, A., Kitawaki, H., 2006. Applications of laser ablation-inductive coupled plasma-mass spectrometry (LA-ICP-MS) to gemology. Gems & Gemology, Vol 42, No. 2, pp. 98-118.

Ahn, Y., Seo, J., Park, J., 2013. Electronic and vibrational spectra of tourmaline – The impact of electron beam irradiation and heat treatment. Vibrational Spectroscopy, Vol. 65, pp. 165-175.

Akintola, O.F., Adekeye, J.I.D., 2008. Mineralization potentials of pegmatites in the Nasarawa area of central Nigeria. Earth Sci. Res. J., Vol. 12, No. 2, pp. 213-234.

Almeida Queiroz, H., Botelho, N.F., 2018. The Mata Azul pegmatitic field, Tocantins/ Goiás, central Brazil: geology, genesis and mineralization. Brazilian Journal of Geology, Vol. 43, No. 3, pp. 435-456.

Ashwal, L.D., Tucker, R.D., 1999. Geology of Madagascar: A Brief Outline. International Association for Gondwana Research, Vol. 2, No. 3, pp. 335-339.

Bačík, P., Fridrichová, J., *Stubna, J.,* Antal, P., 2015. Application of spectroscopic methods in mineralogical and gemological research of gem tourmalines. Acta Slovaca, Vol. 7, No. 1, pp. 1-9.

Barreto, S.B., Schulze, S.M.B.B., 2010. The gemstone deposits of Brazil: occurrences, production and economic impact. Boletín de la Sociedad GeolóGica Mexicana, Vol. 62, No. 1, pp. 123-140.

Dirlam, D.M., Laurs, B.M., Pezzotta, F., Simmons, W.B., 2002. Liddicoatite tourmaline from Anjanabonoina, Madagascar. Gems & Gemology, Vol. 38, No. 1, pp. 28-53.

Dutrow, B.L., 2018. Tourmaline: a gemstone's guide to geologic evolution of the Earth's crust. Gems & Gemology, Vol. 54, No. 3, pp. 256-257.

Guillou-Frottier, L., Burov, E., Le Goff, E., Deschamps, Y., Bouchot, V., 2008. Plume head-cratonic blocks interactions and gemstones in east Africa. Réunion des Sciences de la Terre, RST 2008, Apr 2008, Nancy, France; https://hal-brgm.archives-ouvertes.fr/hal-01132943.

Jenkins, A., Larsen, R.A., 2004. Gemstone identification using Raman spectroscopy. Spectroscopy, Vol. 19, No. 4, pp. 20-25.

Kaewtip, M., Limtrakun, P., 2016. Gemological and chemical characteristics of green tourmaline from Madagascar, Mozambique, and Tanzania. Walailak J Sci & Tech, Vol. 13, No. 12, pp. 985-992.

Katsurada, Y., Sun, Z., 2017. Cuprian liddicoatite tourmaline. Gem & Gemology, Vol. 53, No. 1, pp. 1-8.

Kröner, A., Stern, R.J., 2004. Pan-African orogeny. Encyclopedia of Geology, Vol. 1, pp. 1-12.

Kusky, T.M., Abdelsalam, M., Tucker, R.D., Stern, R.J., 2003. Evolution of East African and related orogens, and the assembly of Gondwana. Precambrian Research, Vol. 123, pp. 81-85.

Laurs, B.M., Zwaan, J.C., Breeding, C.M., Simmons, W.B., Beaton, D., Rijsdijk, K.F., Befi, R., Falster, A.U., 2008. Copper-bearing (Paraiba-type) tourmaline from Mozambique. Gem & Gemology, Vol. 44, No. 1, pp. 294-320.

Maneewong, A., Pangza, K., Jangsawang, N., Charoennam, T., 2016. Effect of heat treatment and electron beam irradiation tourmaline: UV-Visible, EPR, and Mid-IR spectroscope analyses. Walailak J Sci & Tech, Vol.13, pp. 993-1003.

Manutchehr-Danai, M., 2005. Dictionary of gems and gemology. New York, NY: springer Berlin Heidelberg.

Merkel, P.B., Breeding, C.M., 2009. Spectral differentiation between copper and iron colorants in gem tourmalines. Gems & Gemology, Vol. 45, No. 2, pp. 112-119.

Morley, C.K., Ngenoh, D.K., Ego, J.K., 1999. Introduction to the East African rift system. Geoscience of Rift System – Evolution of East Africa: AAPG in Geology, No. 44, pp. 1-18.

Pedrosa-Soares, A., Chaves, M., Scholz, R., 2009. Eastern Brazilian pegmatite province. Field Trip Guide, pp. 1-28.

Pezzotta, F., Laurs, B.M., 2011. Tourmaline: the kaleidoscopic gemstone. Elements, Vol. 7, pp. 333-338.

Phichaikamjornwut, B., Pongkrapan, S., Intarasiri, S., Bootkul, D., 2019. Conclusive comparison of gamma irradiation and heat treatment for color enhancement of Rubellite from Mozambique.

Vibrational Spectroscopy, Vol. 103, 102926.

Proctor, K., 1985. Gem pegmatites of Minas Gerais, Brazil: the tourmaline of the Araçuaí Districts. Gems & Gemology, Vol. 21, No. 1, pp. 1-19.

Reddy, B.J., Frost, R.L., Martens, W.N., Wain, D.L., Kloprogge, J.T., 2007. Spectroscopic characterization of Mn-rich tourmalines. Vibrational Spectroscopy, Vol. 44, No. 1, pp. 42-49.

Schlüter, T., 2006. Geological Atlas of Africa. New York, NY: Springer Berlin Heidelberg.

Schmetzer, K., Bernhardt, H.J., Dunaigre, C., Krzemnicki, M.S., 2007. Vanadium-bearing gem-quality tourmalines from Madagascar. J. Gemm., Vol. 30, pp. 413-433.

Saeseaw, S., Scarratt, K., Emmett, J., L., 2009. The potential for diffusing copper into tourmaline preparation for initial experimentation. Bangkok, BKK: GIA Laboratory.

Shigley, J.E., Cook, B.C., Laurs, B.M., Oliveira Bernardes, M., An update on “Paraíba” tourmaline from Brazil. Gems & Gemology, Vol. 37, pp. 260-276.

Silva, S.F., Moura, M.A., Queiroz, H.A., Ardisson, J.D., 2018. Chemical and spectroscopic characterization of tourmalines from the Mata Azul pegmatite field, Central Brazil. Journal of Geosciences, Vol. 68, pp. 155-165.

Sun, Z., Palke, A.C., Breeding, C.M., Dutrow, B.L., 2019. A new method for determining gem tourmaline species by LA-ICP-MS. Gems & Gemology, Vol. 55, No. 1, pp. 2-17.

Thiéblemont, D., Liégeois, J.P., Fernandez-Alonso, M., Ouabadi, A., Le Gall, B., Maury, R., Jalludin, M., Vidal, M., Ouattara Gbélé, C., Tchaméni, R., Michard, A., Nehlig, P., Rossi, P., Chêne, F., 2016. Geological map of Africa at 1:10M scale, CGMW-BRGM 2016.

Thongnopkun, P., Ekgasit, S., 2005. FTIR Spectra of faceted diamonds and diamond simulants. Diamond & Related Materials, Vol. 14, pp. 1592-1599.

APPENDIX A

FIGURES OF TOURMALINE SAMPLES FROM BRAZIL,

MOZAMBIQUE, NIGERIA, MADAGASCAR, AND EAST AFRICA

FIGURES OF GAMMA RAY IRRADIATED TOURMALINE SAMPLES

GENERAL PROPERTIES OF TOURMALINE SAMPLES

FIGURES OF TOURMALINE SAMPLES FROM BRAZIL

FIGURES OF TOURMALINE SAMPLES FROM BRAZIL

*Corundum

FIGURES OF TOURMALINE SAMPLES FROM BRAZIL

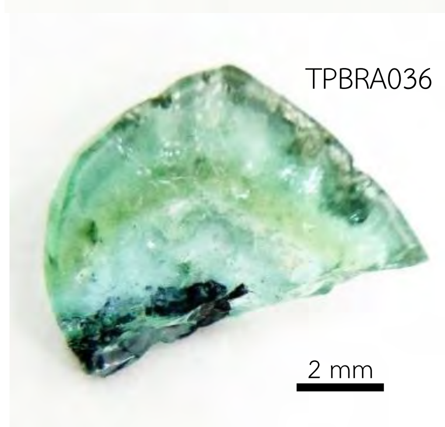

FIGURES OF TOURMALINE SAMPLES FROM BRAZIL

FIGURES OF TOURMALINE SAMPLES FROM BRAZIL

FIGURES OF TOURMALINE SAMPLES FROM MOZAMBIQUE

TPMOZ001

TPMOZ002-A

TPMOZ003

TPMOZ004-A

TPMOZ005

TPMOZ006

TPMOZ007

TPMOZ008

TPMOZ009-A

TPMOZ010-A

TPMOZ011-A

TPMOZ012-A

FIGURES OF TOURMALINE SAMPLES FROM MOZAMBIQUE

FIGURES OF TOURMALINE SAMPLES FROM NIGERIA

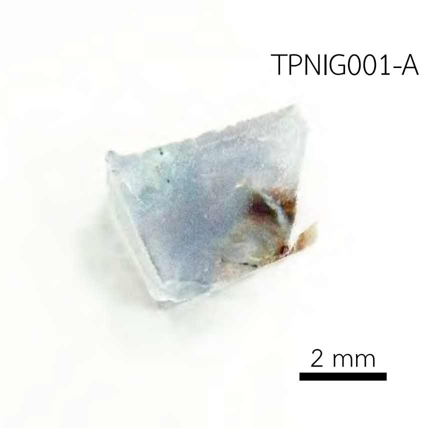

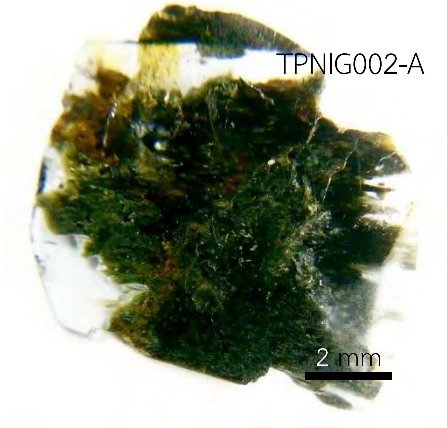

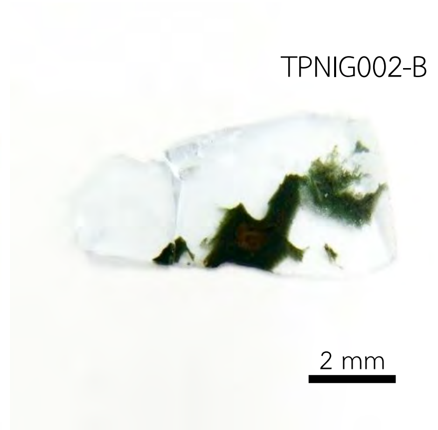

FIGURES OF TOURMALINE SAMPLES FROM MADAGASCAR

TPEA001

FIGURES OF TOURMALINE SAMPLES FROM EAST AFRICA

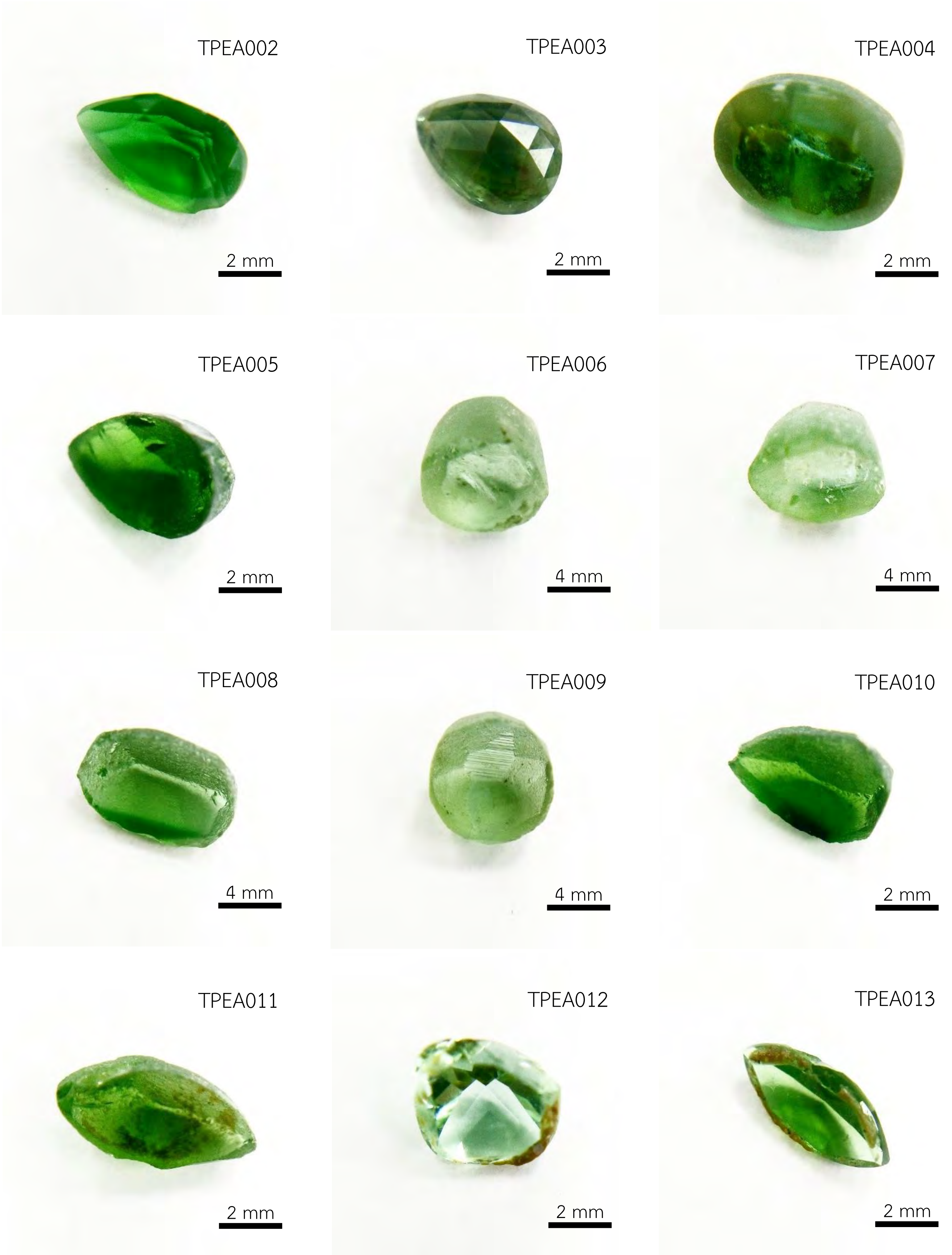

FIGURES OF TOURMALINE SAMPLES FROM EAST AFRICA

FIGURES OF GAMMA RAY IRRADIATED TOURMALINE SAMPLES

GENERAL PROPERTIES OF TOURMALINE SAMPLES FROM BRAZIL

Sample	Color	Luster	Transparency	Weight (ct)	SG (g/cm^3)	RI		Birefringence	Fluorescence	
						n_o	n_e		LW	SW
TPBRA001	Purple	Vitreous	Transparent	0.151	3.146	1.639	1.620	0.019	Inert	Inert
TPBRA002	Purple	Vitreous	Transparent	0.155	3.163	1.640	1.622	0.018	Inert	Inert
TPBRA003	Purple	Vitreous	Transparent	0.177	3.105	1.640	1.622	0.018	Inert	Inert
TPBRA004	Blue	Vitreous	Transparent	0.221	3.069	1.640	1.622	0.018	Inert	Inert
TPBRA005	Blue	Vitreous	Transparent	0.278	3.055	1.640	1.622	0.018	Inert	Inert
TPBRA006	Blue	Vitreous	Transparent	0.196	3.111	1.640	1.622	0.018	Inert	Inert
TPBRA007	Blue	Vitreous	Transparent	0.199	3.109	1.639	1.622	0.017	Inert	Inert
TPBRA008	Blue	Vitreous	Transparent	0.222	3.217	1.639	1.622	0.017	Inert	Inert
TPBRA009	Blue	Vitreous	Transparent	0.278	3.124	1.638	1.620	0.018	Inert	Inert
TPBRA010	Purple	Vitreous	Transparent	0.181	3.175	1.640	1.622	0.018	Inert	Inert
TPBRA012	Blue	Vitreous	Translucent	0.149	3.041	1.639	1.622	0.017	Inert	Inert
TPBRA013	Blue	Vitreous	Transparent	0.225	3.041	1.639	1.622	0.017	Inert	Inert
TPBRA014	Blue	Vitreous	Transparent	0.185	3.033	1.639	1.622	0.017	Inert	Inert
TPBRA015	Blue	Vitreous	Transparent	0.169	3.130	1.640	1.622	0.018	Inert	Inert
TPBRA016	Blue	Vitreous	Transparent	0.199	3.062	1.640	1.622	0.018	Inert	Inert
TPBRA017	Pink	Vitreous	Translucent	0.162	3.176	1.640	1.622	0.018	Inert	Inert
TPBRA018	Blue	Vitreous	Transparent	0.259	3.083	1.639	1.622	0.017	Inert	Inert
TPBRA019	Pink	Vitreous	Transparent	0.179	3.086	1.641	1.623	0.018	Inert	Inert
TPBRA020	Blue	Vitreous	Transparent	0.167	3.036	1.639	1.621	0.018	Inert	Inert
TPBRA021	Colorless	Vitreous	Transparent	0.118	4.069	1.770	1.760	0.010	Inert	Inert
TPBRA022	Purple	Vitreous	Transparent	0.134	3.116	1.639	1.621	0.018	Inert	Inert
TPBRA023	Purple	Vitreous	Transparent	0.267	3.034	1.639	1.622	0.017	Inert	Inert
TPBRA024	Purple	Vitreous	Transparent	0.223	3.055	1.640	1.622	0.018	Inert	Inert
TPBRA025	Purple	Vitreous	Transparent	0.137	3.114	1.640	1.622	0.018	Inert	Inert
TPBRA026	Blue	Vitreous	Transparent	0.194	3.031	1.638	1.621	0.017	Inert	Inert
TPBRA027	Blue	Vitreous	Transparent	0.232	3.093	1.638	1.621	0.017	Inert	Inert
TPBRA028	Blue	Vitreous	Transparent	0.209	3.167	1.641	1.622	0.019	Inert	Inert
TPBRA029	Blue	Vitreous	Transparent	0.150	3.191	1.638	1.621	0.017	Inert	Inert

GENERAL PROPERTIES OF TOURMALINE SAMPLES FROM BRAZIL

Sample	Color	Luster	Transparency	Weight (ct)	SG (g/cm^3)	RI		Birefringence	Fluorescence	
						n_o	n_e		LW	SW
TPBRA030	Blue	Vitreous	Transparent	0.155	3.100	1.639	1.621	0.018	Inert	Inert
TPBRA031	Green	Vitreous	Transparent	0.152	3.234	1.640	1.623	0.017	Inert	Inert
TPBRA032	Greenish Blue	Vitreous	Transparent	0.203	3.123	1.641	1.623	0.018	Inert	Inert
TPBRA033	Greenish Blue	Vitreous	Transparent	0.234	3.162	1.639	1.621	0.018	Inert	Inert
TPBRA034	Blue	Vitreous	Transparent	0.136	3.238	1.638	1.620	0.018	Inert	Inert
TPBRA035	Blue	Vitreous	Transparent	0.307	3.133	1.639	1.622	0.017	Inert	Inert
TPBRA036	Blue, Green	Vitreous	Transparent	0.650	3.081	1.641	1.623	0.018	Inert	Inert
TPBRA037	Blue, Green	Vitreous	Transparent	1.019	3.069	1.639	1.621	0.018	Inert	Inert
TPBRA038-A	Green	Vitreous	Transparent	0.955	3.061	1.639	1.621	0.018	Inert	Inert
TPBRA038-B	Pink	Vitreous	Transparent	0.982	3.068	1.640	1.622	0.018	Inert	Inert
TPBRA039-A	Green	Vitreous	Transparent	5.853	3.079	1.640	1.622	0.018	Inert	Inert
TPBRA039-B	Pink	Vitreous	Transparent	3.935	3.077	1.641	1.622	0.019	Inert	Inert
TPBRA040-A	Green	Vitreous	Transparent	2.795	3.102	1.640	1.623	0.017	Inert	Inert
TPBRA040-B	Pink	Vitreous	Transparent	3.223	3.093	1.641	1.621	0.020	Inert	Inert
TPBRA041-A	Green	Vitreous	Transparent	1.433	3.088	1.641	1.624	0.017	Inert	Inert
TPBRA041-B	Pink	Vitreous	Transparent	1.388	3.064	1.640	1.621	0.019	Inert	Inert
TPBRA042	Fancy	Vitreous	Transparent	1.260	3.081	1.640	1.622	0.018	Inert	Inert
TPBRA043	Greenish Blue	Vitreous	Transparent	0.428	3.101	1.640	1.621	0.019	Inert	Inert
TPBRA044	Blue	Vitreous	Transparent	0.315	3.029	1.639	1.621	0.018	Inert	Inert
TPBRA046	Blue	Vitreous	Transparent	0.345	3.053	1.638	1.620	0.018	Inert	Inert
TPBRA049	Blue	Vitreous	Transparent	0.439	3.049	1.640	1.621	0.019	Inert	Inert
TPBRA050	Blue	Vitreous	Transparent	0.187	3.169	1.640	1.622	0.018	Inert	Inert
TPBRA051	Purple	Vitreous	Transparent	0.227	3.027	1.639	1.621	0.018	Inert	Inert
TPBRA052	Purple	Vitreous	Transparent	0.337	3.120	1.640	1.622	0.018	Inert	Inert
TPBRA053	Purple	Vitreous	Transparent	0.338	3.101	1.640	1.622	0.018	Inert	Inert
TPBRA054	Purple	Vitreous	Transparent	0.390	3.047	1.639	1.620	0.019	Inert	Inert
TPBRA055	Purple	Vitreous	Transparent	0.391	3.055	1.640	1.622	0.018	Inert	Inert

GENERAL PROPERTIES OF TOURMALINE SAMPLES FROM MOZAMBIQUE

Sample	Color	Luster	Transparency	Weight (ct)	SG (g/cm^3)	RI		Birefringence	Fluorescence	
						n_o	n_e		LW	SW
TPMOZ001	Colorless	Vitreous	Transparent	0.693	3.108	1.640	1.622	0.018	Inert	Inert
TPMOZ002-A	Pink	Vitreous	Transparent	3.530	3.075	1.638	1.621	0.017	Inert	Inert
TPMOZ002-B	Pink	Vitreous	Transparent	2.301	3.072	1.640	1.622	0.018	Inert	Inert
TPMOZ003	Pink	Vitreous	Transparent	1.013	3.024	1.640	1.622	0.018	Inert	Inert
TPMOZ004-A	Green	Vitreous	Transparent	1.910	3.111	1.640	1.622	0.018	Inert	Inert
TPMOZ004-B	Green	Vitreous	Transparent	1.086	3.121	1.640	1.623	0.017	Inert	Inert
TPMOZ005	Pink	Vitreous	Transparent	0.631	3.078	1.641	1.623	0.018	Inert	Inert
TPMOZ006	Green	Vitreous	Transparent	0.865	3.100	1.640	1.622	0.018	Inert	Inert
TPMOZ007	Blue	Vitreous	Transparent	1.132	3.093	1.640	1.622	0.018	Inert	Inert
TPMOZ008	Blue	Vitreous	Transparent	1.332	3.090	1.640	1.623	0.017	Inert	Inert
TPMOZ009-A	Green	Vitreous	Transparent	1.283	3.122	1.640	1.623	0.017	Inert	Inert
TPMOZ009-B	Green	Vitreous	Transparent	0.852	3.144	1.641	1.622	0.019	Inert	Inert
TPMOZ010-A	Pink	Vitreous	Transparent	1.737	3.053	1.640	1.621	0.019	Inert	Inert
TPMOZ010-B	Pink	Vitreous	Transparent	0.985	3.069	1.638	1.619	0.019	Inert	Inert
TPMOZ011-A	Green	Vitreous	Transparent	1.290	3.042	1.640	1.623	0.017	Inert	Inert
TPMOZ011-B	Pink	Vitreous	Transparent	2.487	3.048	1.639	1.621	0.018	Inert	Inert
TPMOZ012-A	Pink	Vitreous	Transparent	6.028	3.035	1.640	1.623	0.017	Inert	Inert
TPMOZ012-B	Pink	Vitreous	Transparent	1.803	3.040	1.639	1.622	0.017	Inert	Inert
TPMOZ013-A	Pink	Vitreous	Translucent	0.900	3.041	1.640	1.621	0.019	Inert	Inert
TPMOZ013-B	Pink	Vitreous	Transparent	1.159	3.042	1.639	1.621	0.018	Inert	Inert

GENERAL PROPERTIES OF TOURMALINE SAMPLES FROM NIGERIA

Sample	Color	Luster	Transparency	Weight (ct)	SG (g/cm^3)	RI		Birefringence	Fluorescence	
						n_o	n_e		LW	SW
TPNIG001-A	Blue	Vitreous	Transparent	0.643	3.033	1.641	1.623	0.018	Inert	Inert
TPNIG001-B	Pink	Vitreous	Transparent	0.719	3.060	1.639	1.622	0.017	Inert	Inert
TPNIG002-A	Colorless	Vitreous	Transparent	2.250	3.023	1.640	1.623	0.017	Inert	Inert
TPNIG002-B	Blue	Vitreous	Transparent	0.448	3.102	1.639	1.622	0.017	Inert	Inert
TPNIG003	Blue	Vitreous	Transparent	0.700	3.070	1.640	1.621	0.019	Inert	Inert

GENERAL PROPERTIES OF TOURMALINE SAMPLES FROM MADAGASCAR

Sample	Color	Luster	Transparency	Weight (ct)	SG (g/cm^3)	RI		Birefringence	Fluorescence	
						n_o	n_e		LW	SW
TPEA001	Green	Vitreous	Transparent	0.476	3.132	1.640	1.620	0.020	Inert	Inert

GENERAL PROPERTIES OF TOURMALINE SAMPLES FROM EAST AFRICA

Sample	Color	Luster	Transparency	Weight (ct)	SG (g/cm^3)	RI		Birefringence	Fluorescence	
						n_o	n_e		LW	SW
TPEA002	Green	Vitreous	Transparent	0.383	3.039	1.638	1.619	0.019	Inert	Inert
TPEA003	Green	Vitreous	Transparent	0.451	3.132	1.640	1.622	0.018	Inert	Inert
TPEA004	Green	Vitreous	Transparent	1.826	3.054	1.640	1.622	0.018	Inert	Inert
TPEA005	Green	Vitreous	Transparent	0.597	3.062	1.639	1.622	0.017	Inert	Inert
TPEA006	Green	Vitreous	Transparent	1.174	3.081	1.640	1.622	0.018	Inert	Inert
TPEA007	Green	Vitreous	Transparent	0.549	3.050	1.639	1.619	0.020	Inert	Inert
TPEA008	Green	Vitreous	Transparent	0.549	3.075	1.639	1.622	0.017	Inert	Inert
TPEA009	Green	Vitreous	Transparent	0.692	3.103	1.639	1.622	0.017	Inert	Inert
TPEA010	Green	Vitreous	Transparent	0.522	3.035	1.639	1.622	0.017	Inert	Inert
TPEA011	Green	Vitreous	Transparent	0.567	3.082	1.639	1.621	0.018	Inert	Inert
TPEA012	Green	Vitreous	Transparent	0.616	3.065	1.640	1.623	0.017	Inert	Inert
TPEA013	Green	Vitreous	Transparent	0.328	3.037	1.638	1.619	0.019	Inert	Inert
TPEA014	Green	Vitreous	Transparent	0.551	3.061	1.638	1.619	0.019	Inert	Inert
TPEA015	Green	Vitreous	Transparent	0.426	3.087	1.639	1.620	0.019	Inert	Inert
TPEA016	Green	Vitreous	Transparent	0.565	3.104	1.639	1.620	0.019	Inert	Inert
TPEA017	Green	Vitreous	Transparent	0.271	3.080	1.638	1.619	0.019	Inert	Inert

APPENDIX B

UV-VIS-NIR ABSORPTION SPECTRA OF NATURAL TOURMALINE SAMPLES

AND GAMMA RAY IRRADIATED TOURMALINE SAMPLES

UV-VIS-NIR ABSORPTION SPECTRA OF NATURAL TOURMALINE SAMPLES FROM BRAZIL

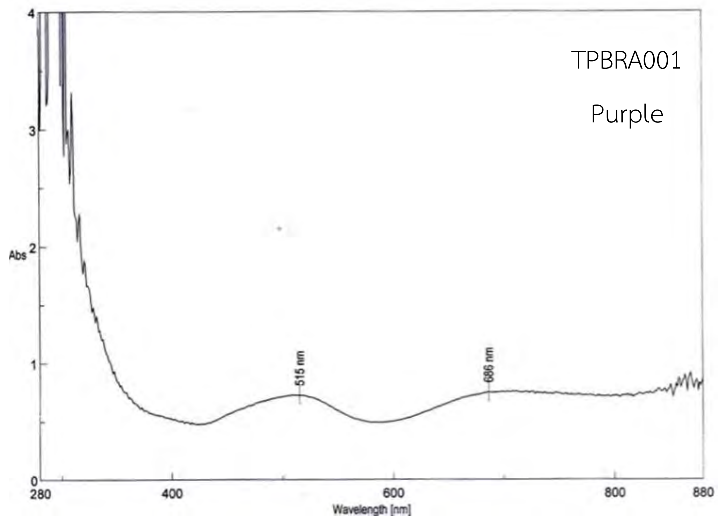

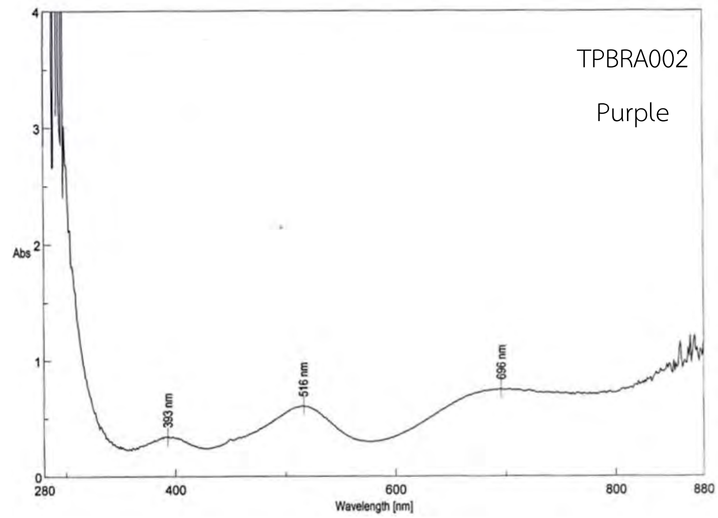

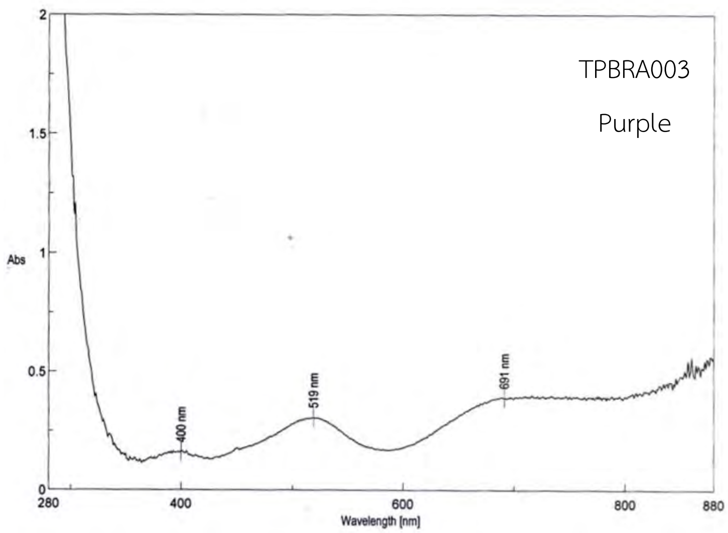

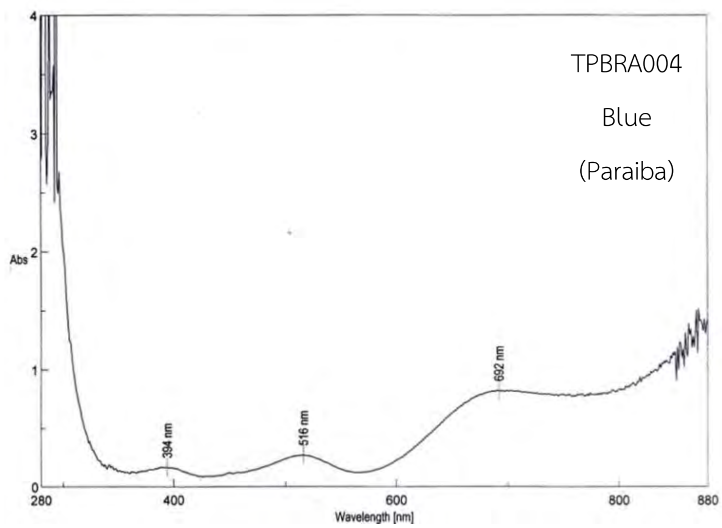

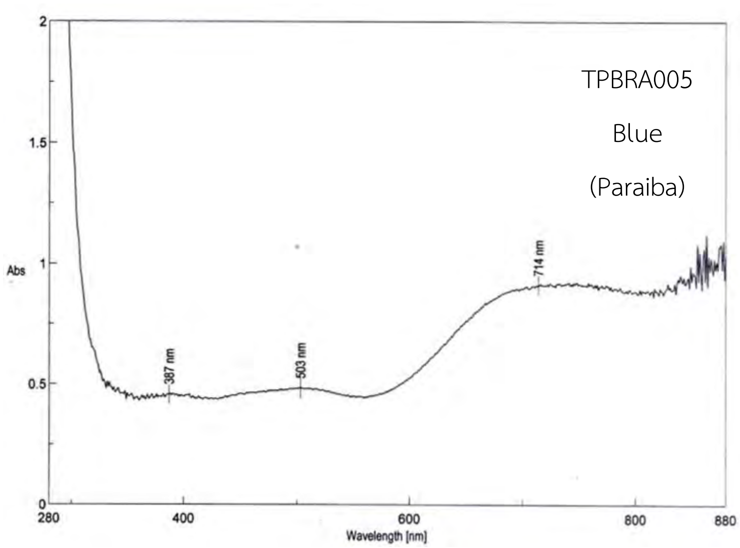

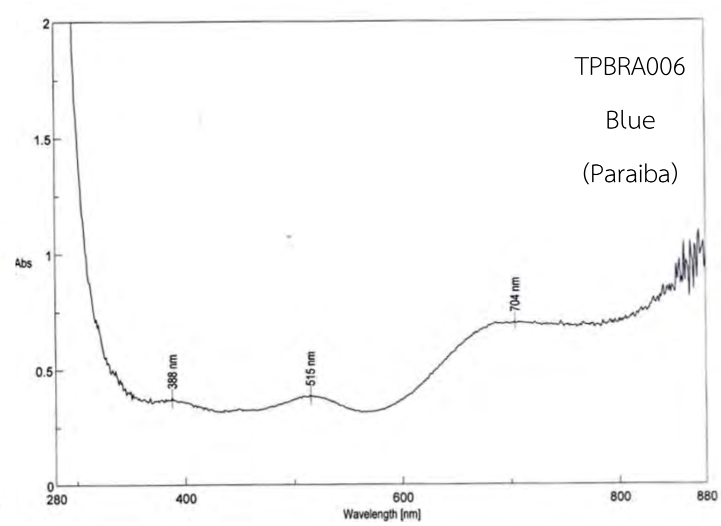

UV-VIS-NIR ABSORPTION SPECTRA OF NATURAL TOURMALINE SAMPLES FROM BRAZIL

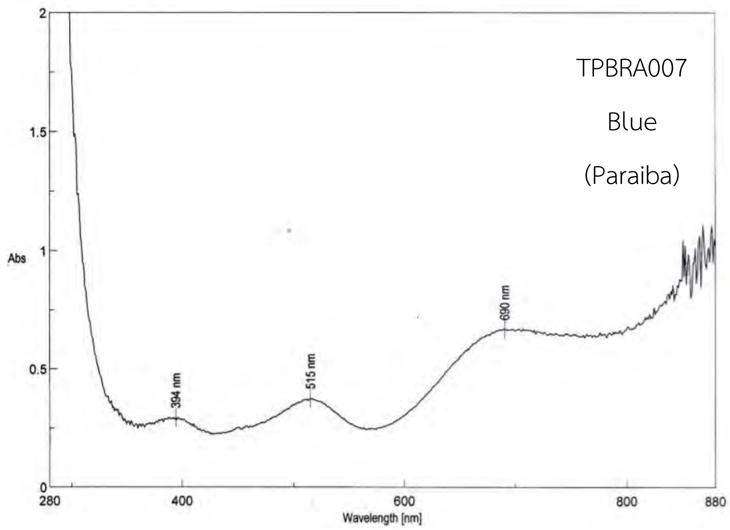

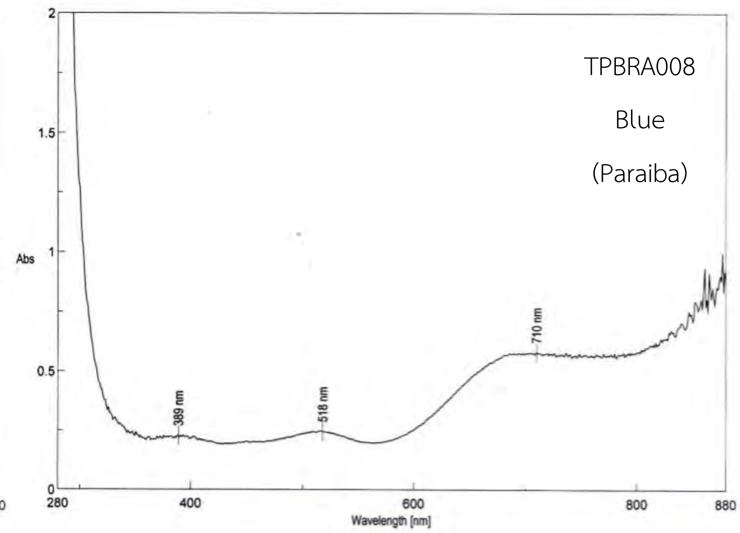

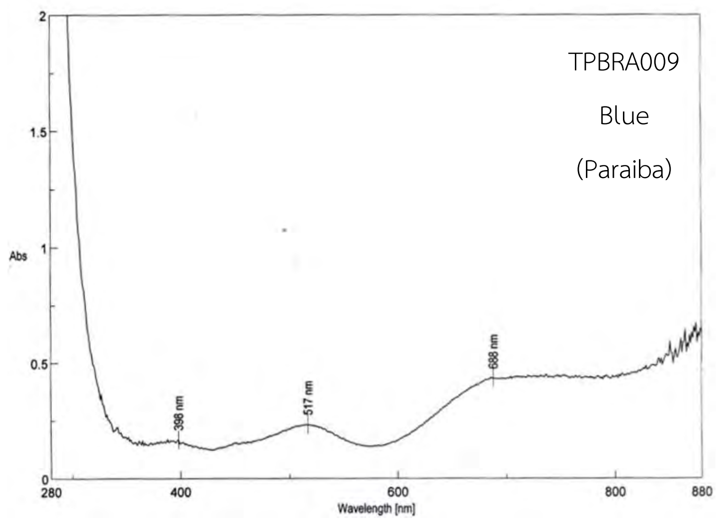

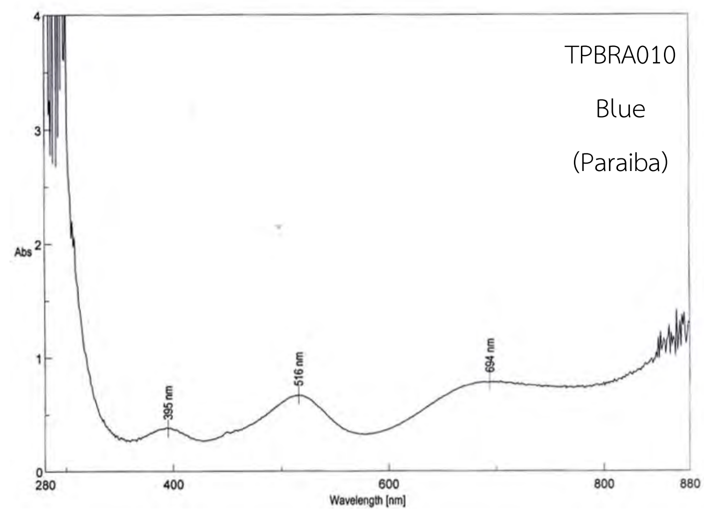

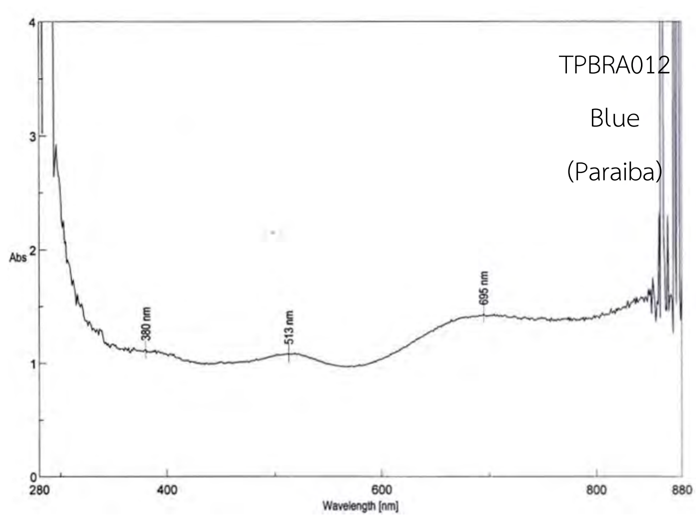

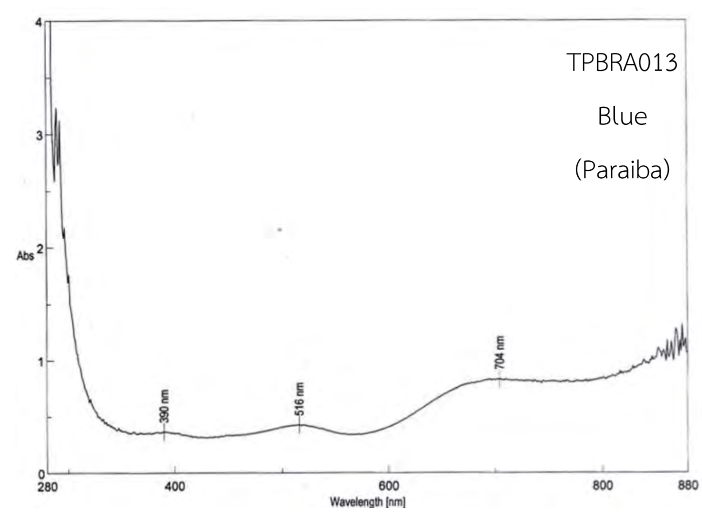

UV-VIS-NIR ABSORPTION SPECTRA OF NATURAL TOURMALINE SAMPLES FROM BRAZIL

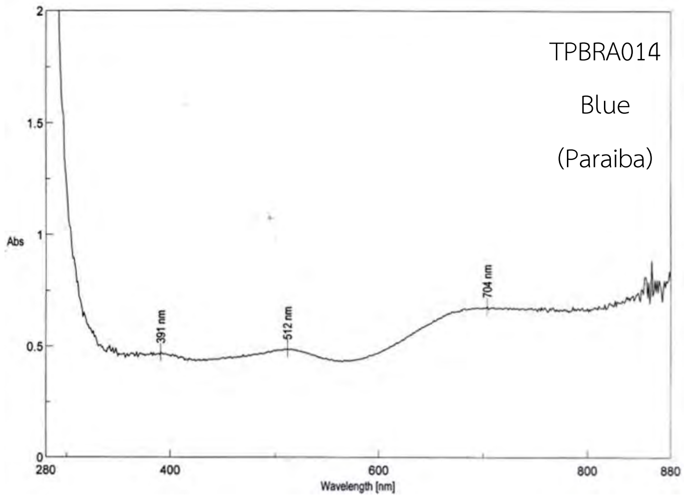

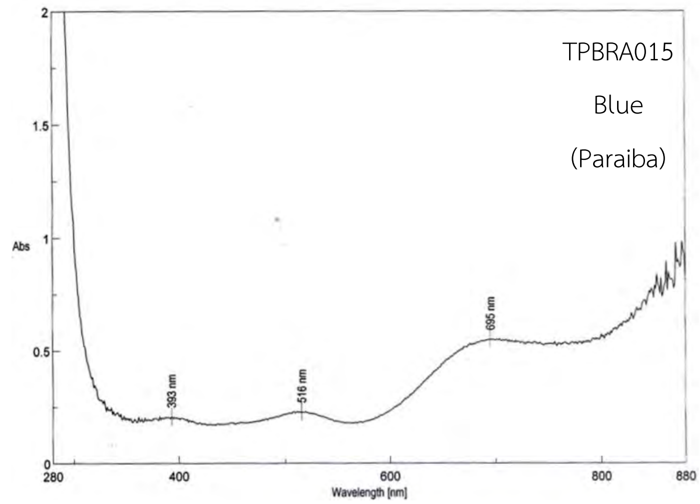

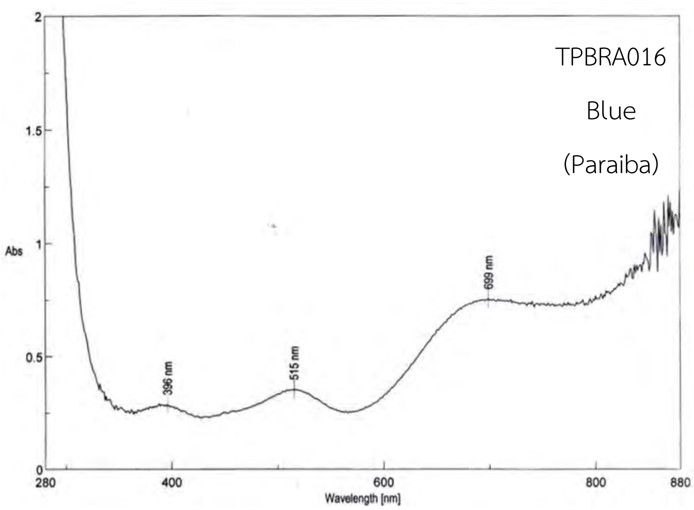

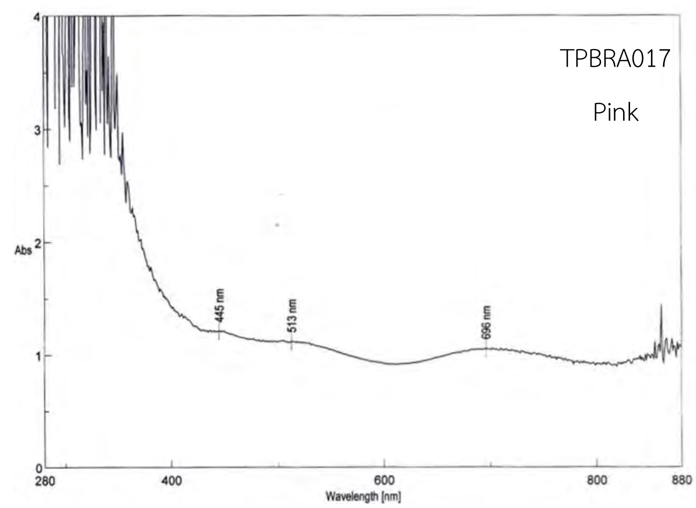

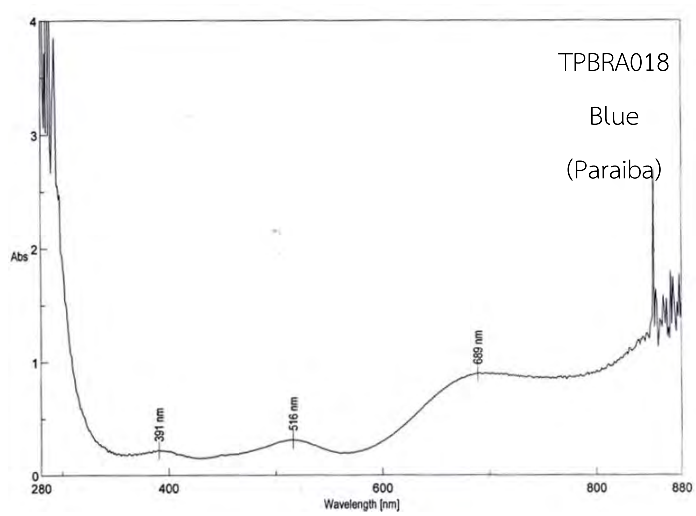

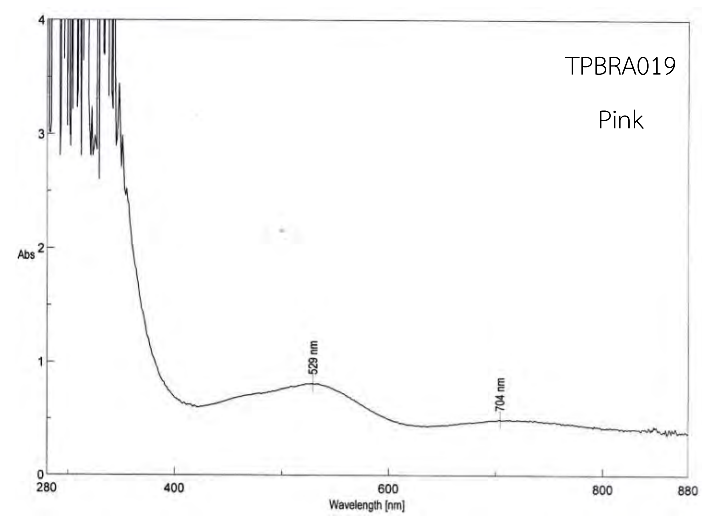

UV-VIS-NIR ABSORPTION SPECTRA OF NATURAL TOURMALINE SAMPLES FROM BRAZIL

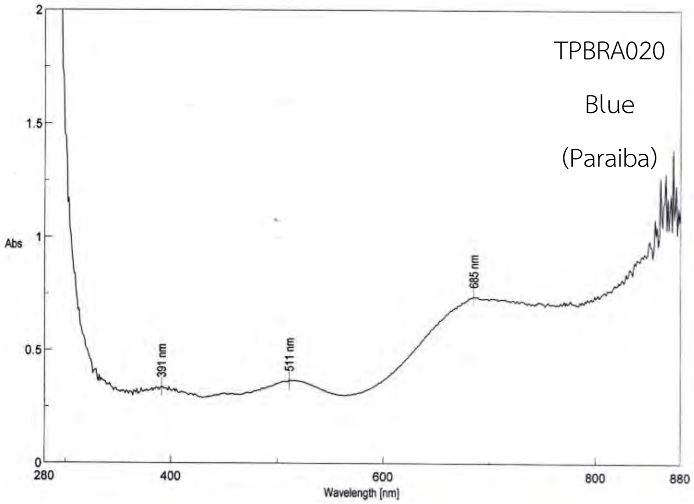

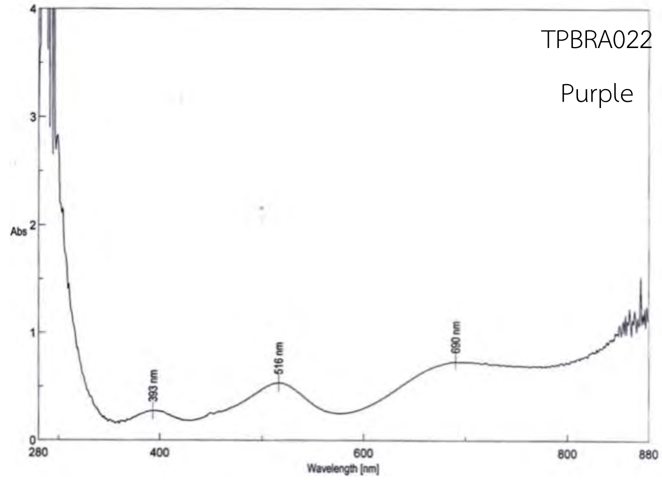

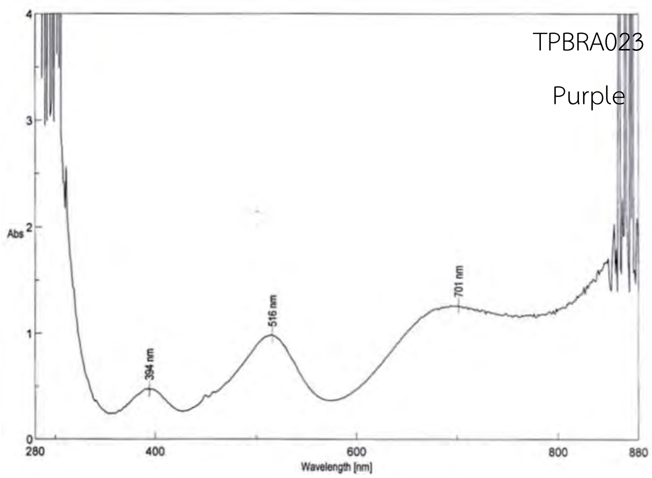

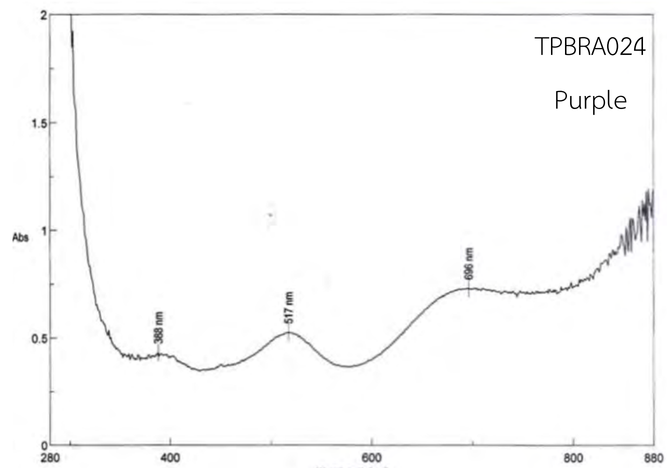

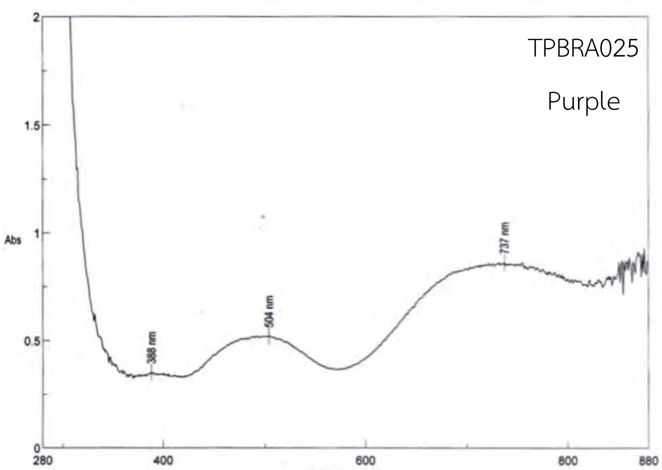

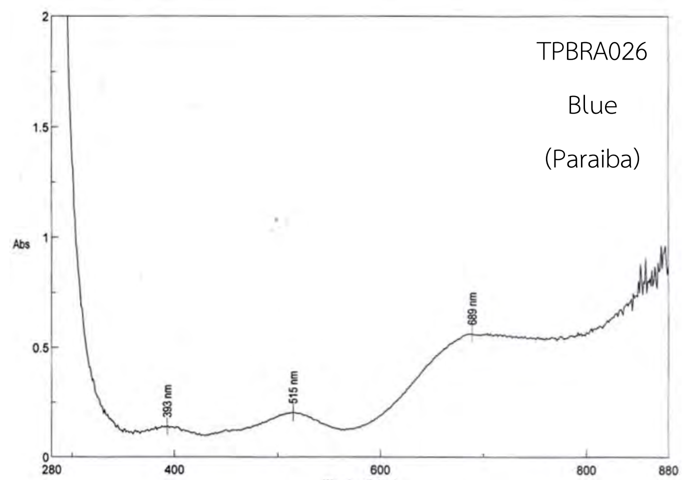

UV-VIS-NIR ABSORPTION SPECTRA OF NATURAL TOURMALINE SAMPLES FROM BRAZIL

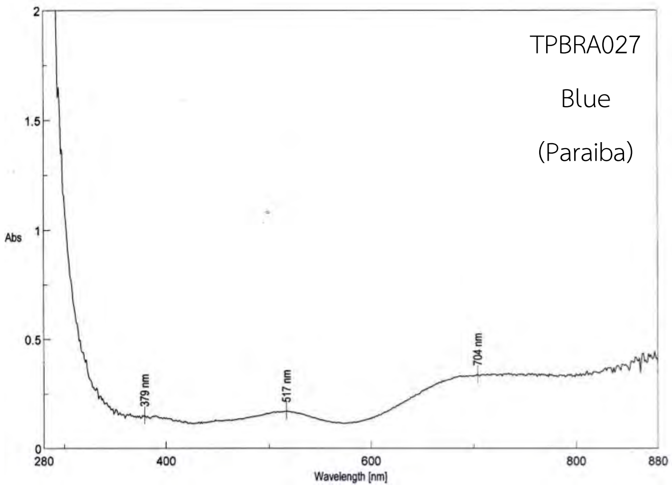

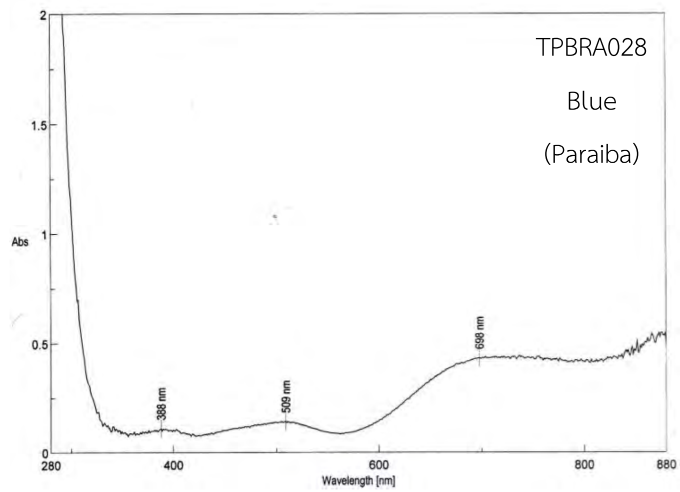

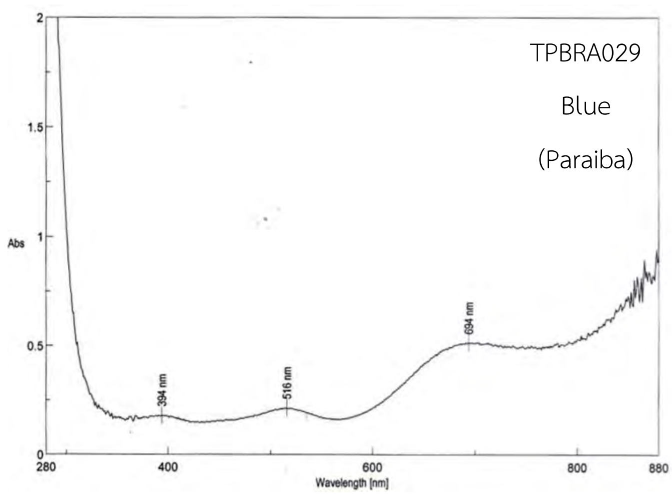

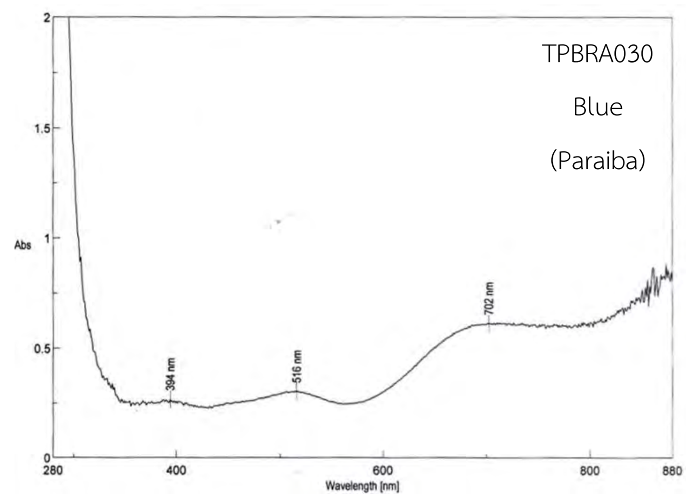

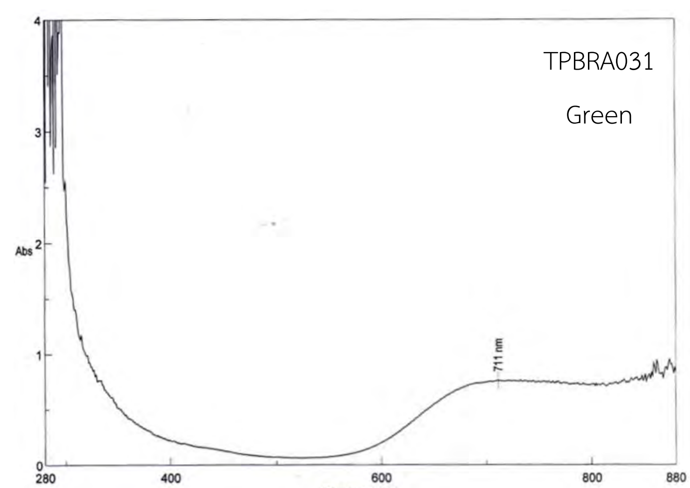

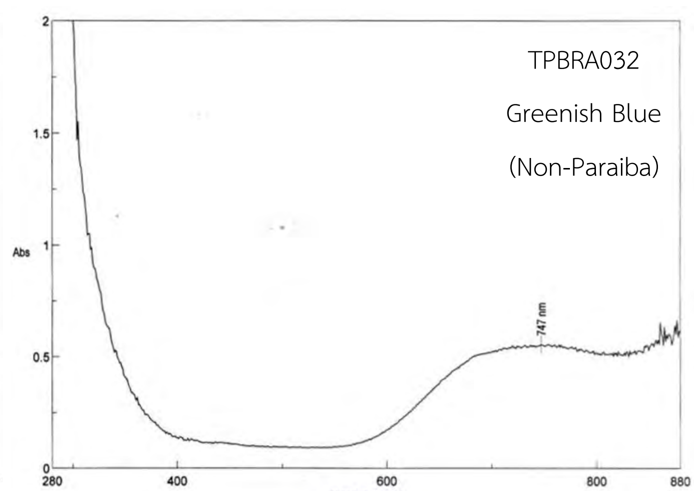

UV-VIS-NIR ABSORPTION SPECTRA OF NATURAL TOURMALINE SAMPLES FROM BRAZIL

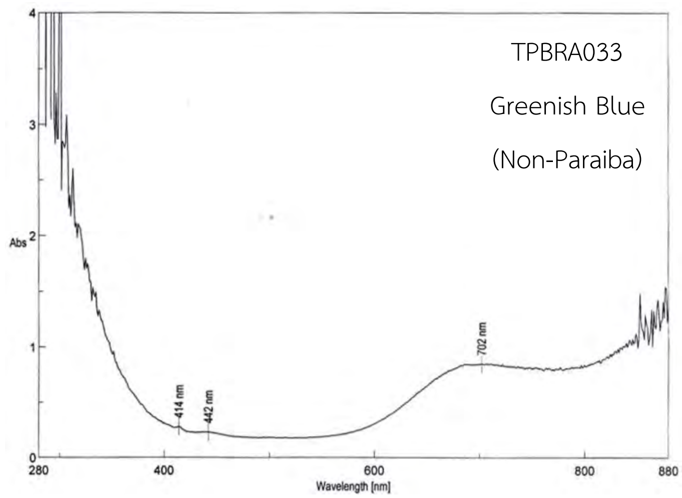

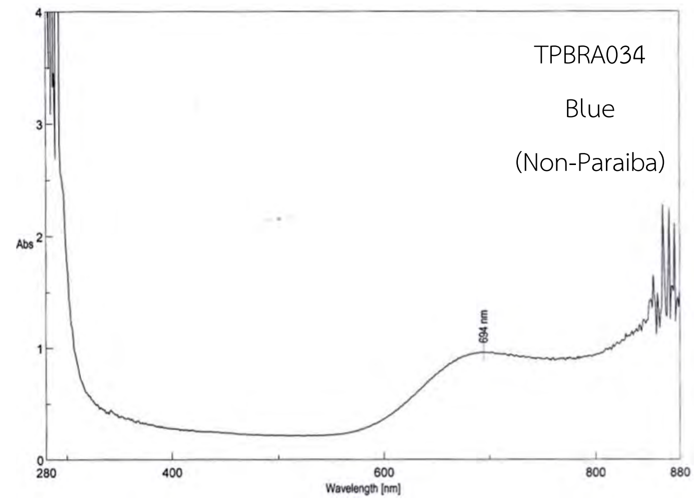

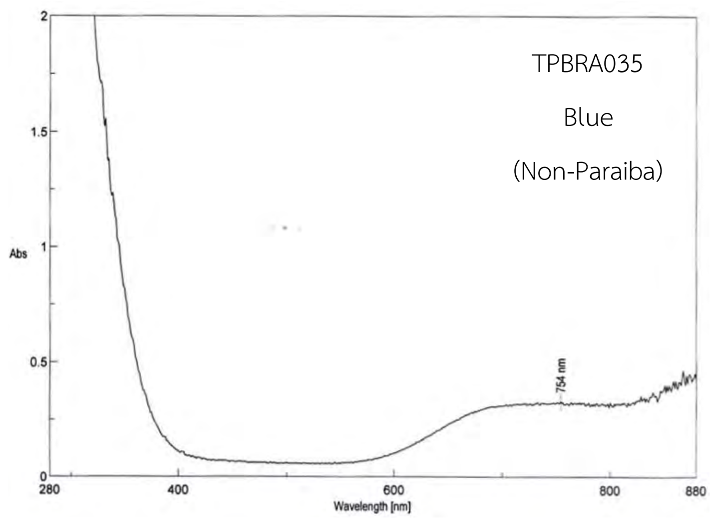

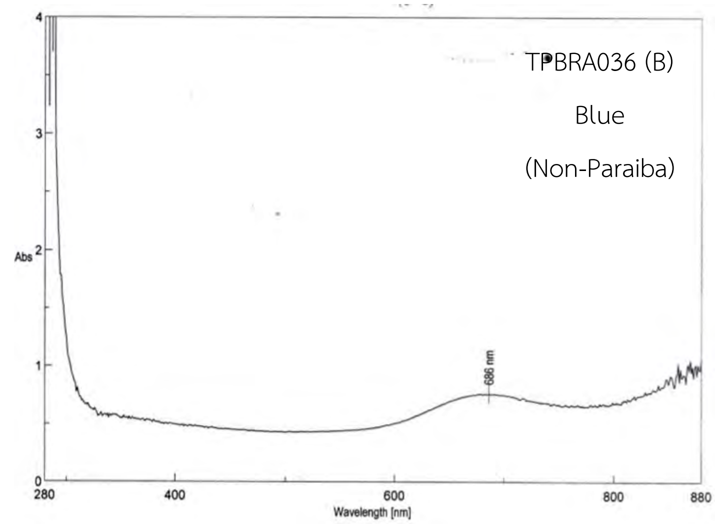

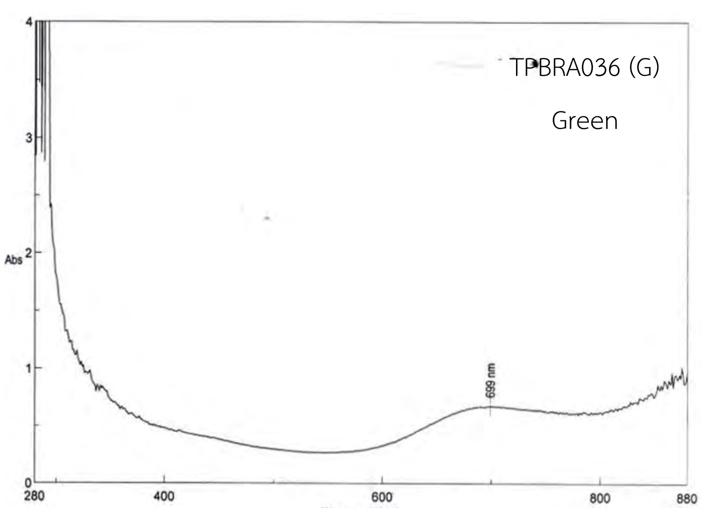

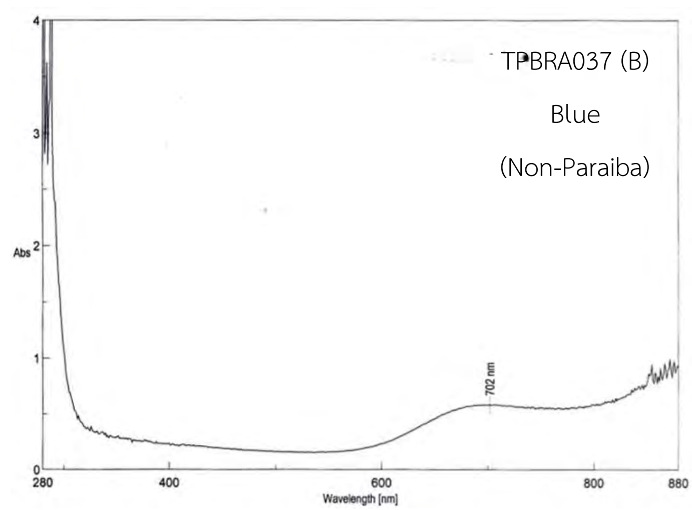

UV-VIS-NIR ABSORPTION SPECTRA OF NATURAL TOURMALINE SAMPLES FROM BRAZIL

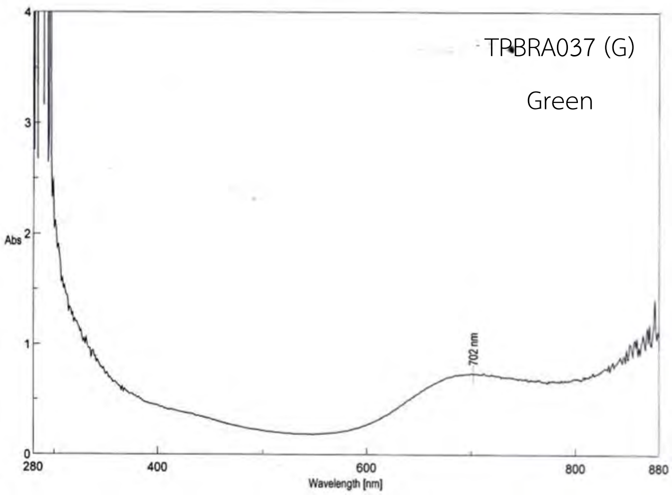

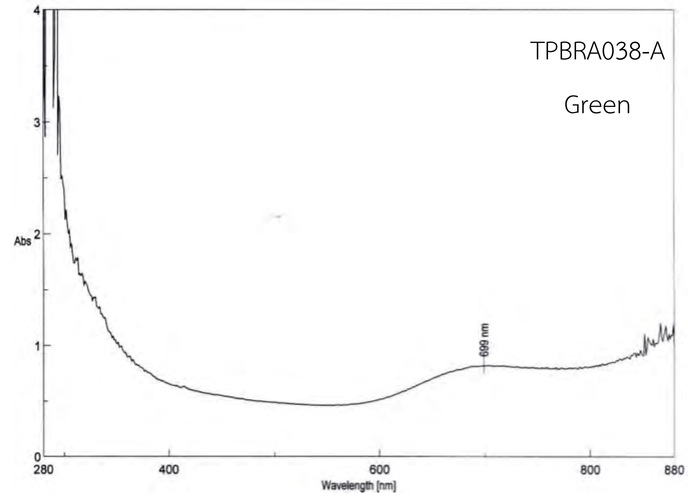

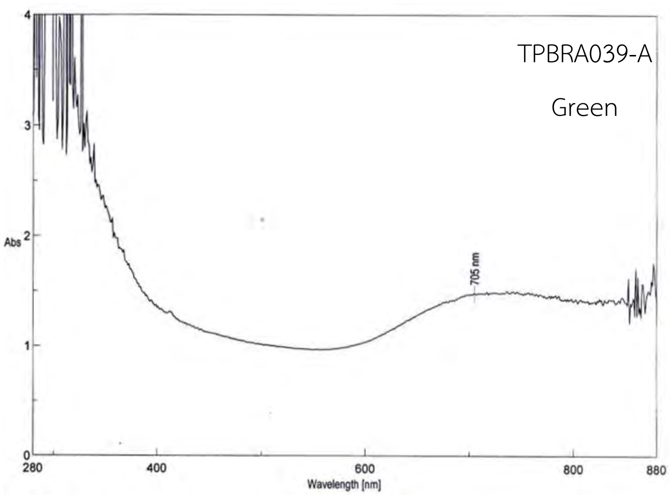

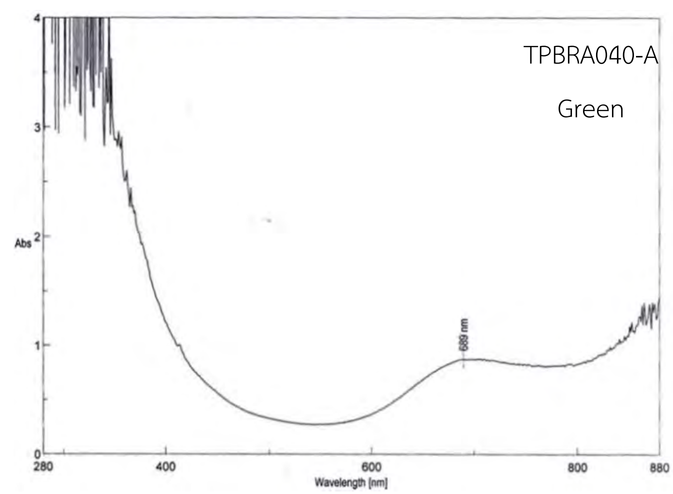

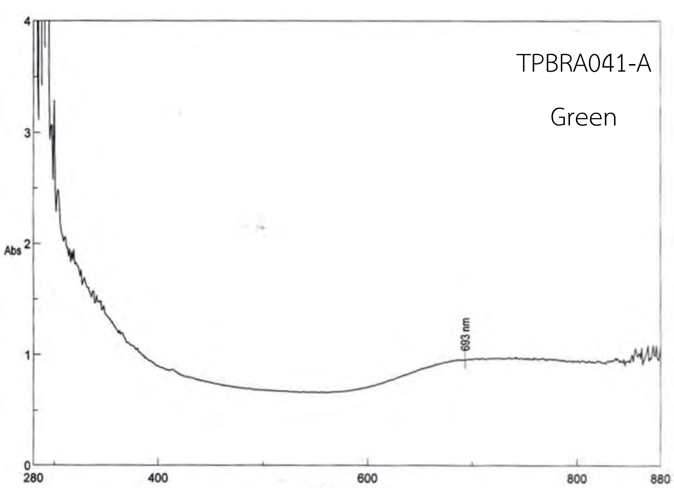

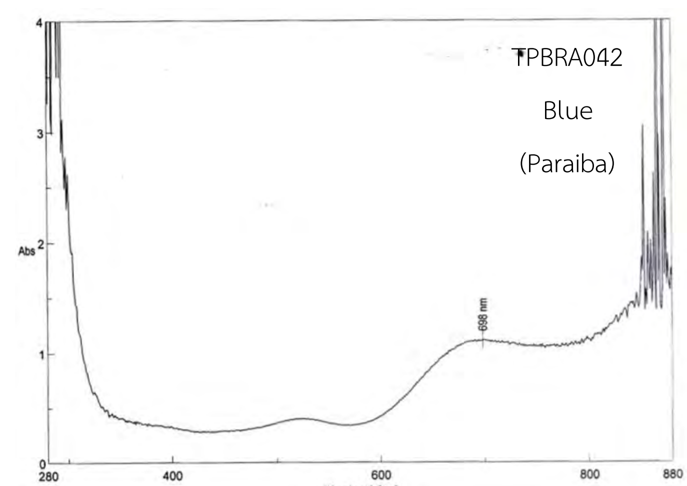

UV-VIS-NIR ABSORPTION SPECTRA OF NATURAL TOURMALINE SAMPLES FROM BRAZIL

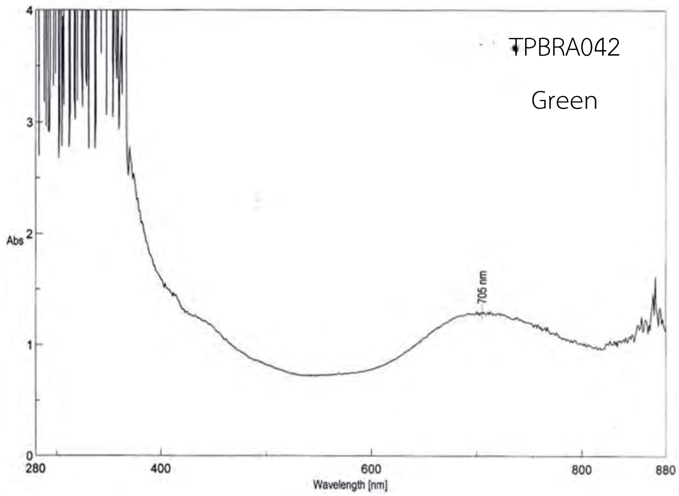

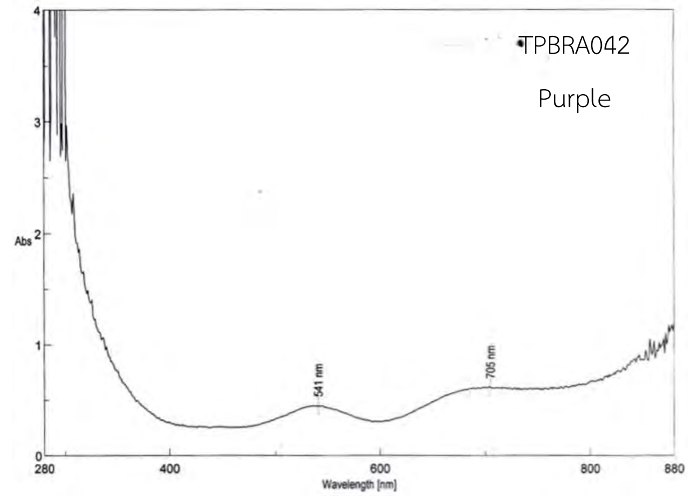

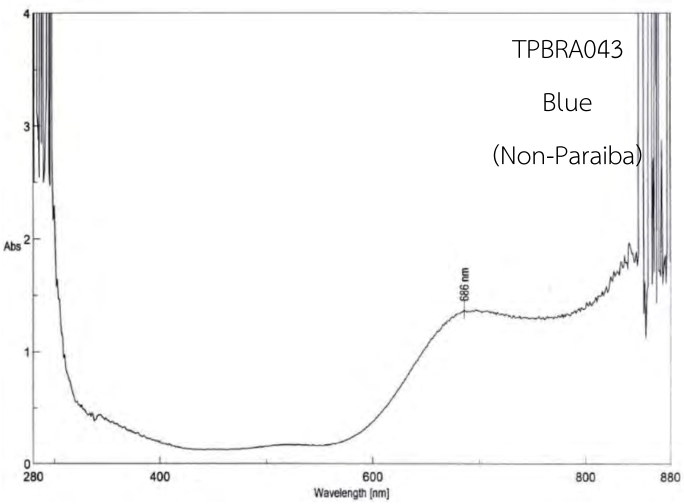

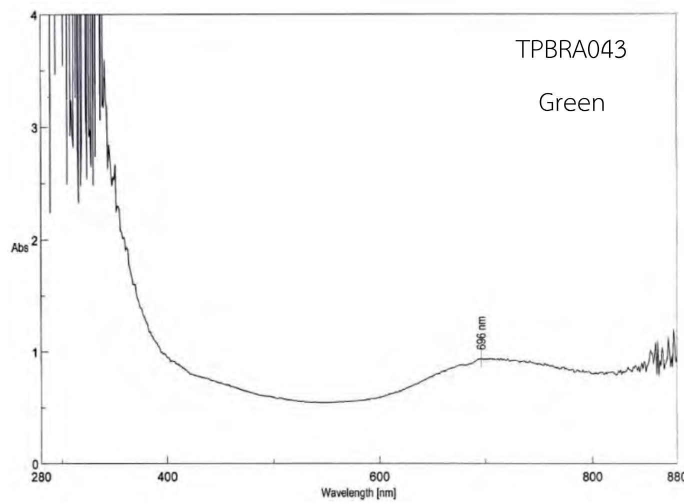

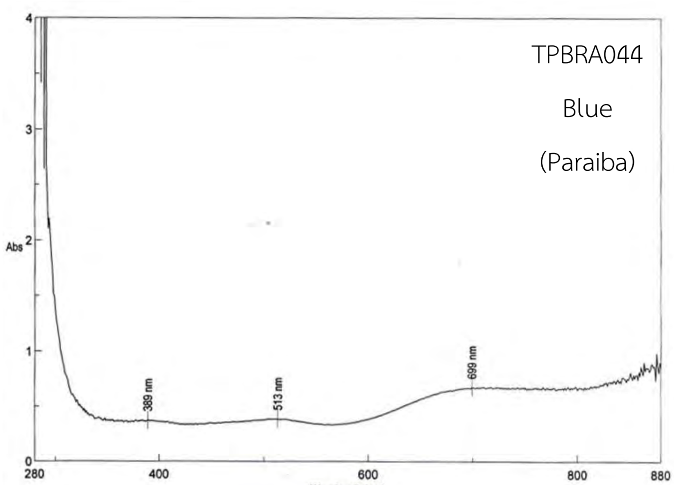

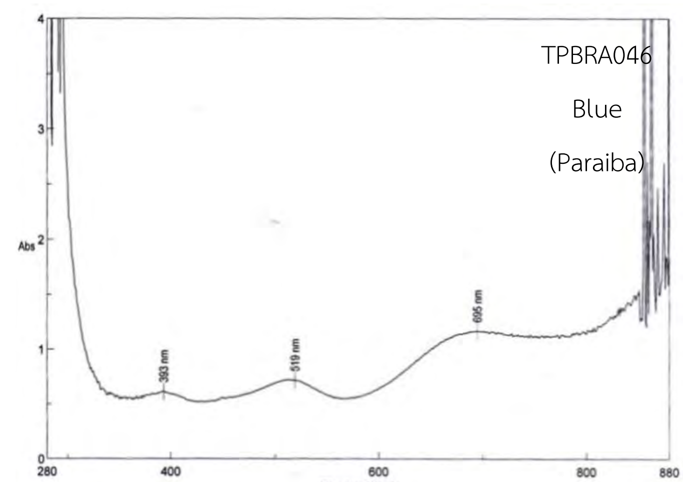

UV-VIS-NIR ABSORPTION SPECTRA OF NATURAL TOURMALINE SAMPLES FROM BRAZIL

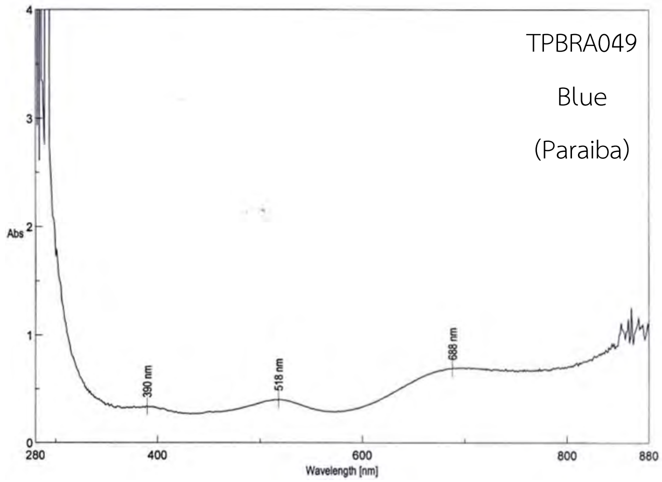

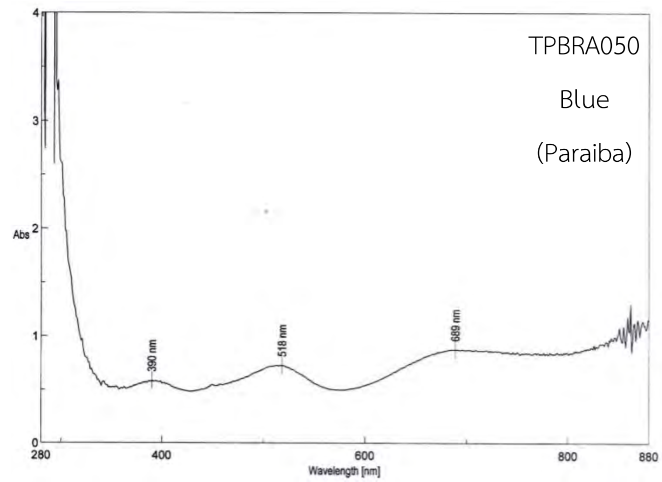

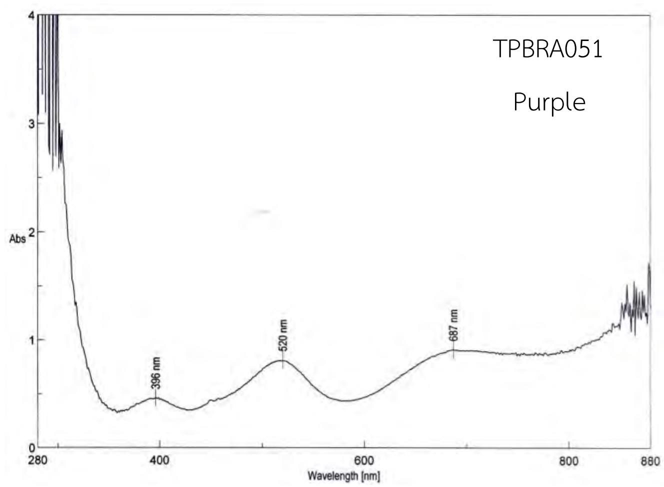

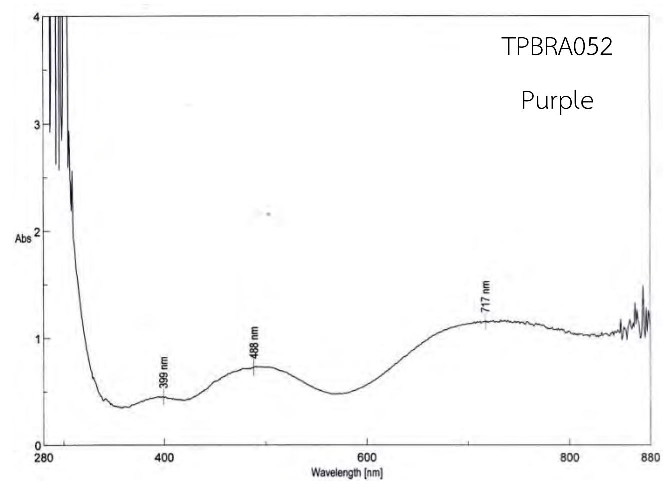

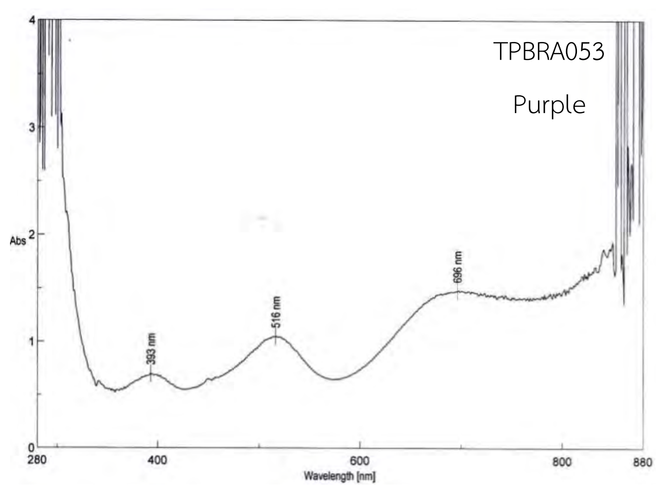

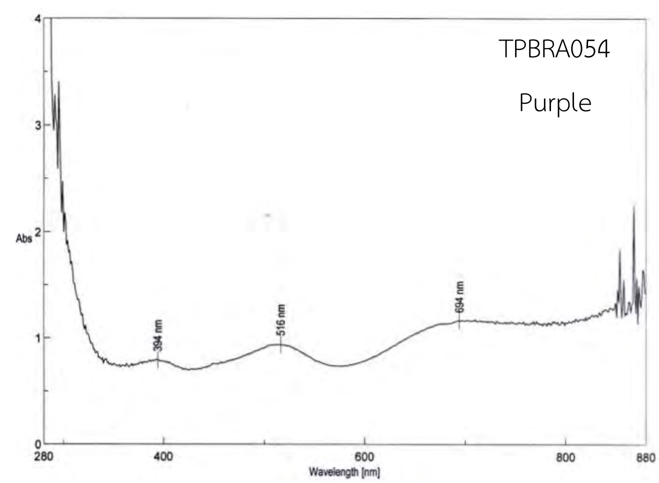

UV-VIS-NIR ABSORPTION SPECTRA OF NATURAL TOURMALINE SAMPLES FROM BRAZIL

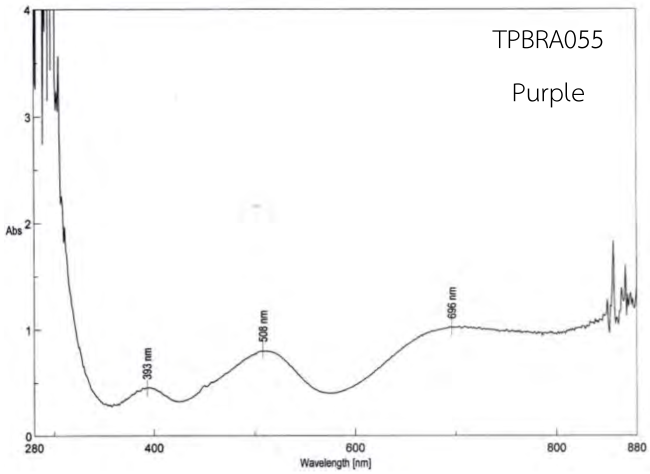

UV-VIS-NIR ABSORPTION SPECTRA OF NATURAL TOURMALINE SAMPLES FROM MOZAMBIQUE

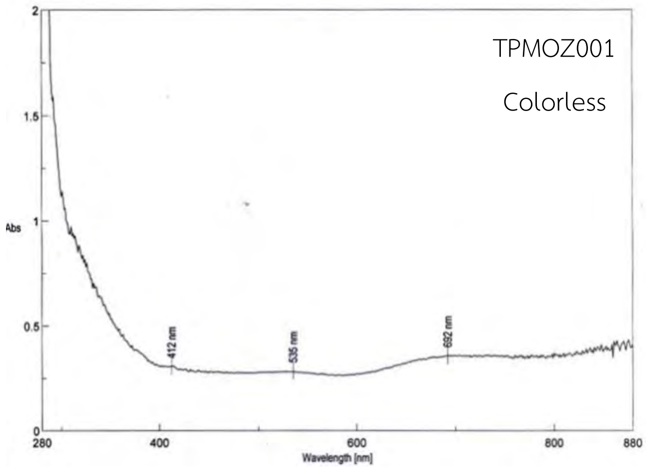

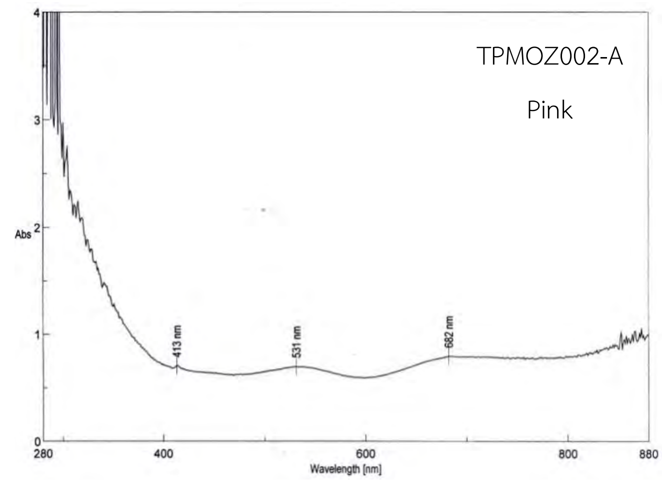

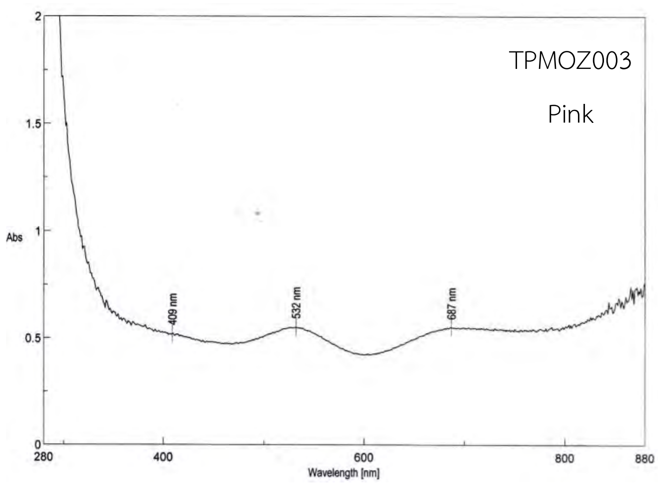

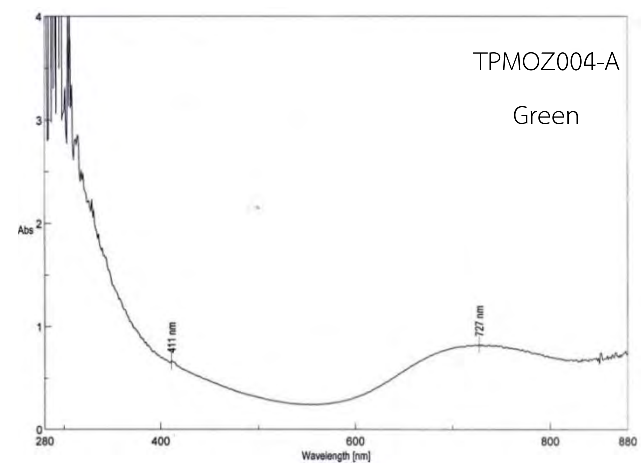

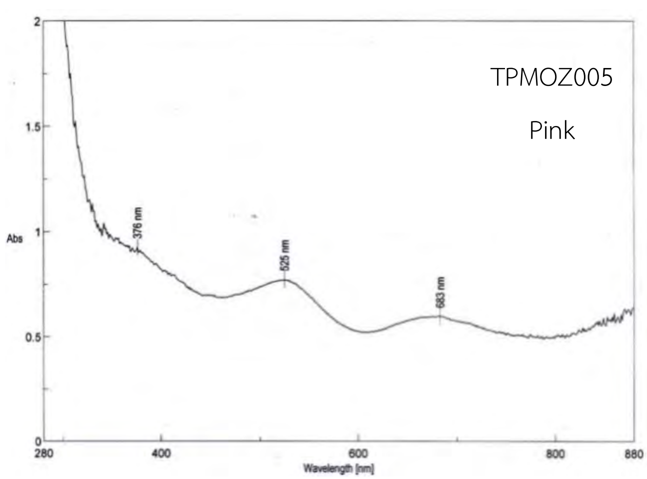

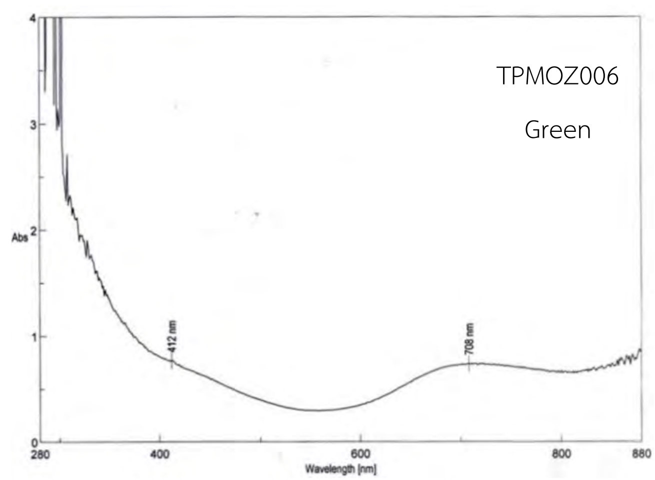

UV-VIS-NIR ABSORPTION SPECTRA OF NATURAL TOURMALINE SAMPLES FROM MOZAMBIQUE

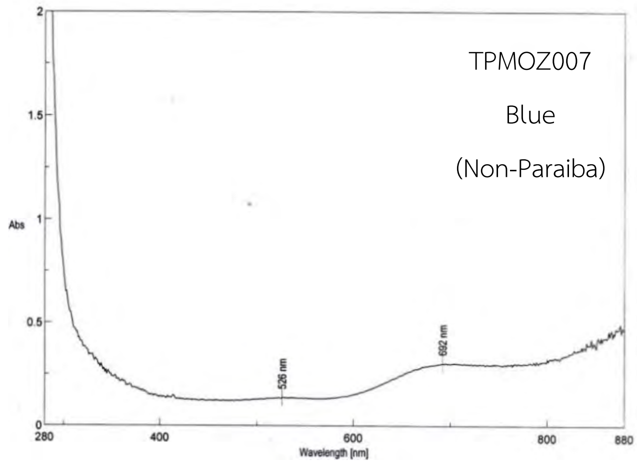

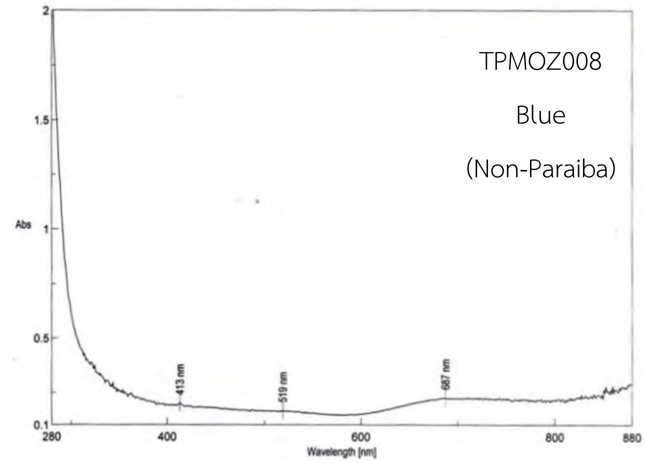

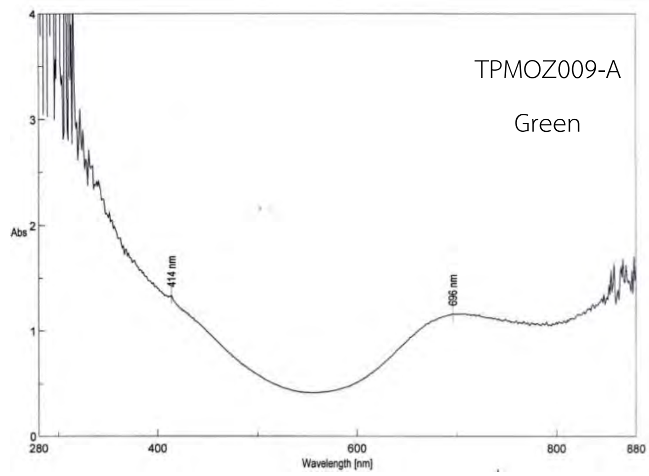

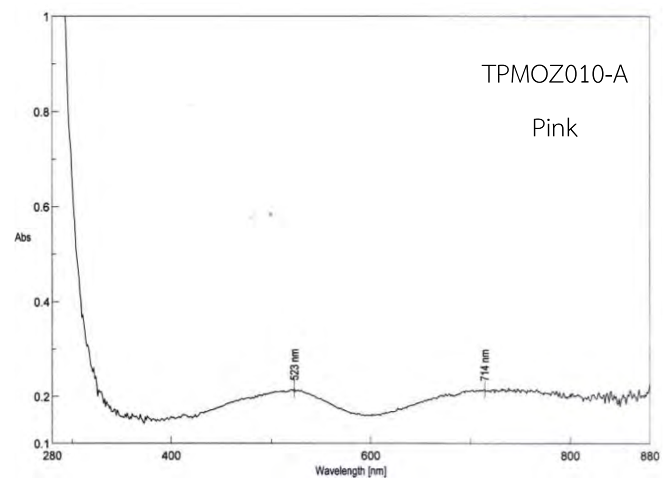

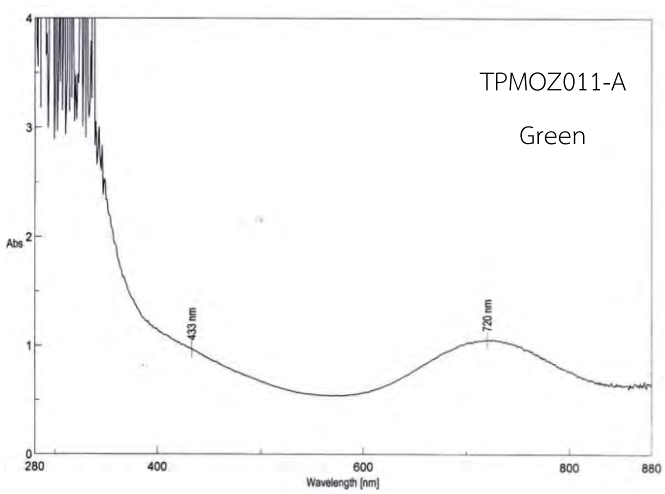

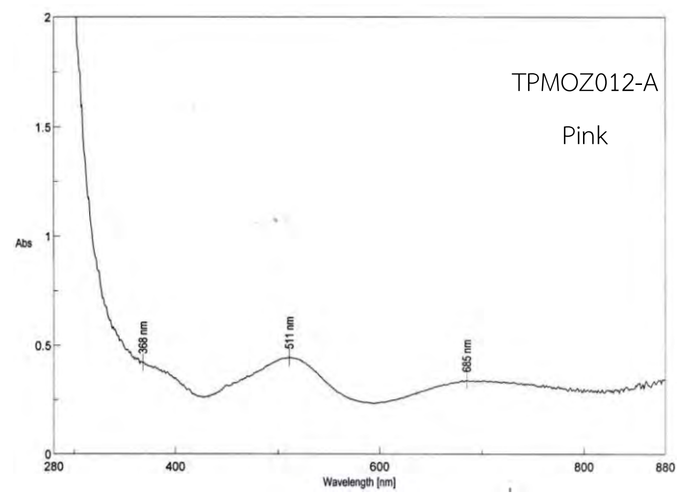

UV-VIS-NIR ABSORPTION SPECTRA OF NATURAL TOURMALINE SAMPLES FROM MOZAMBIQUE

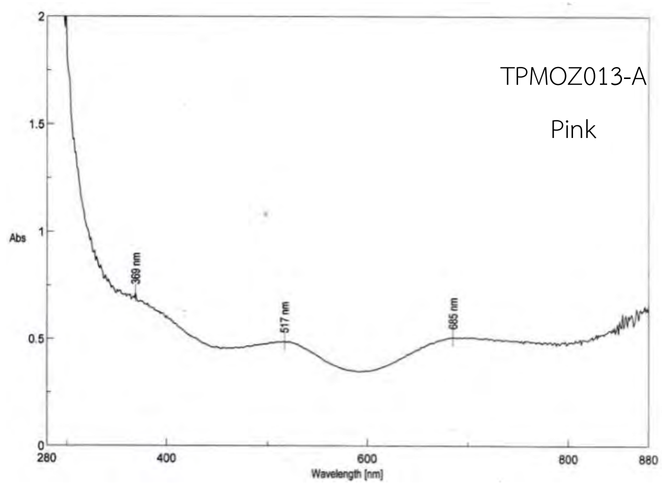

UV-VIS-NIR ABSORPTION SPECTRA OF NATURAL TOURMALINE SAMPLES FROM NIGERIA

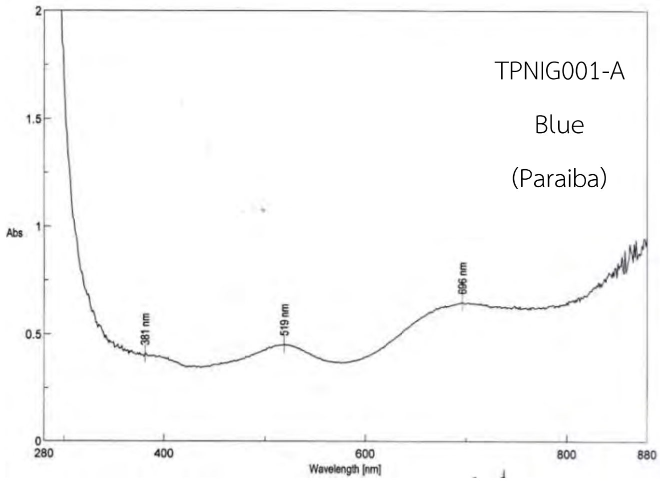

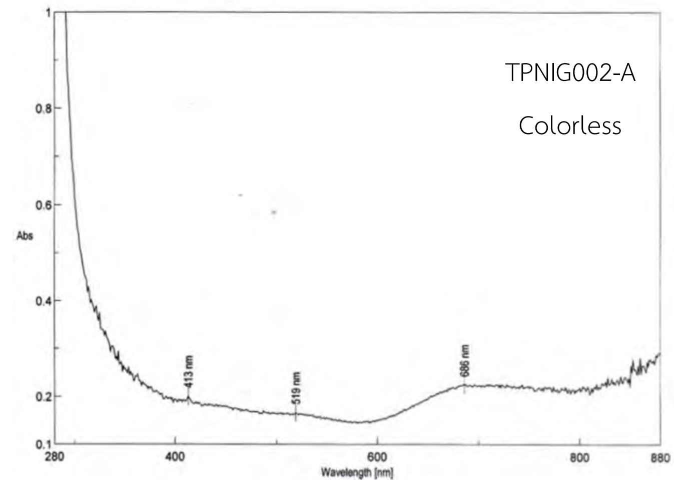

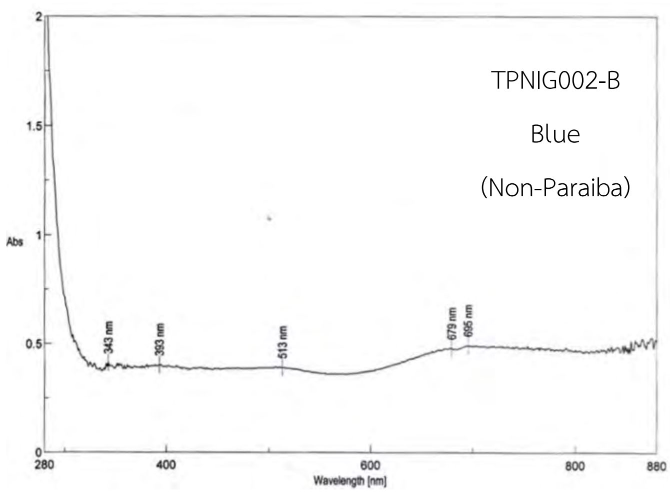

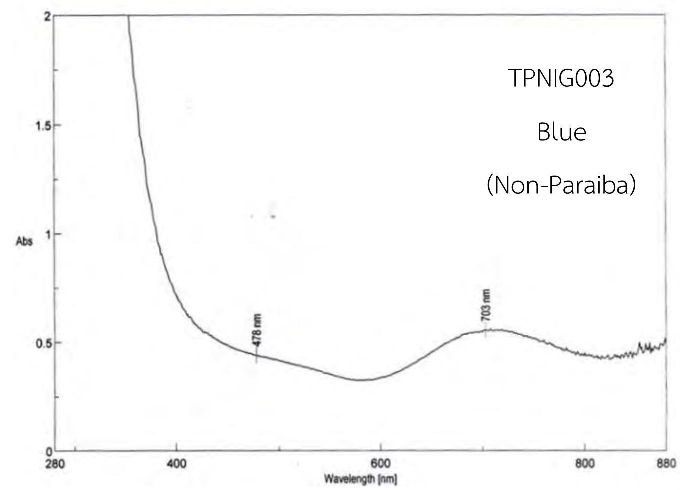

UV-VIS-NIR ABSORPTION SPECTRA OF NATURAL TOURMALINE SAMPLES FROM MADAGASCAR

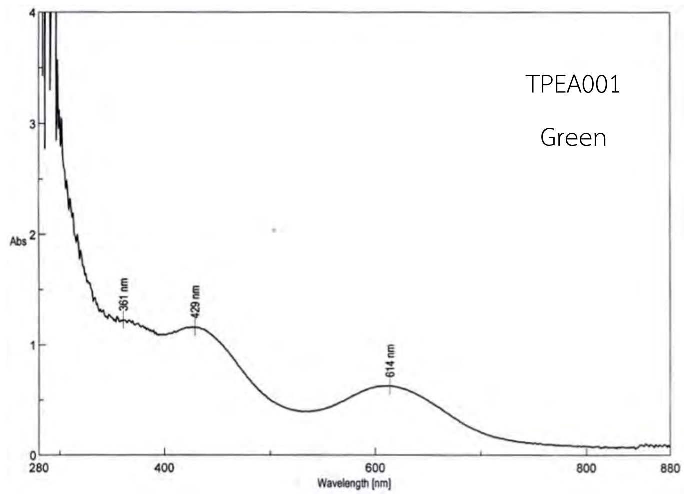

UV-VIS-NIR ABSORPTION SPECTRA OF NATURAL TOURMALINE SAMPLES FROM EAST AFRICA

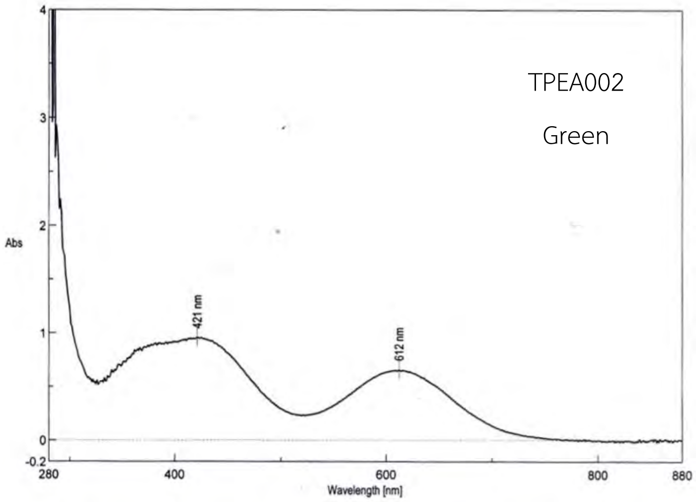

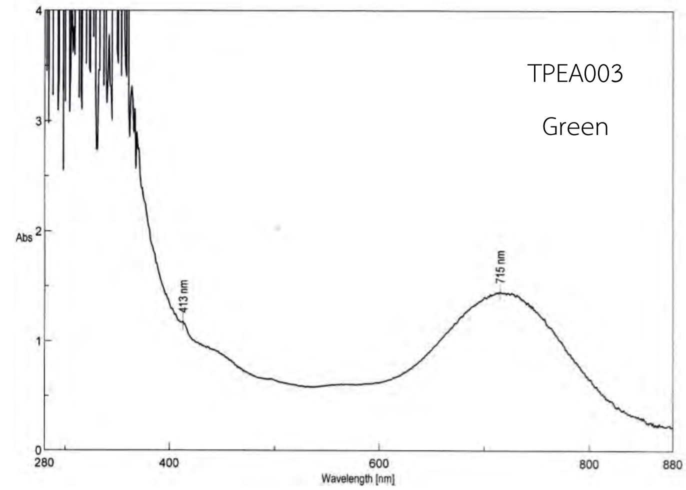

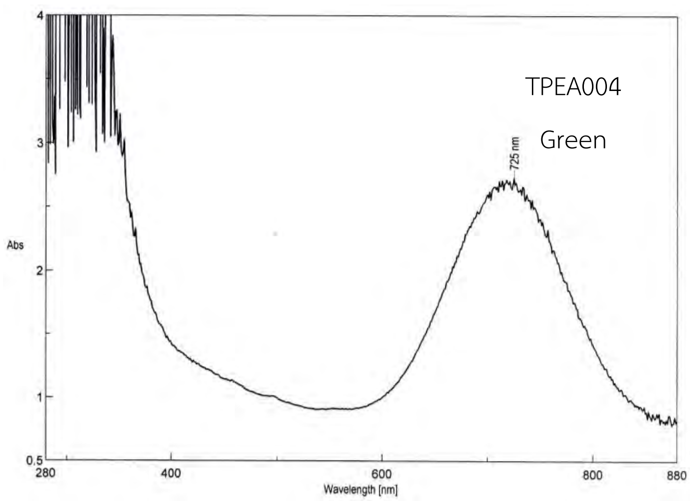

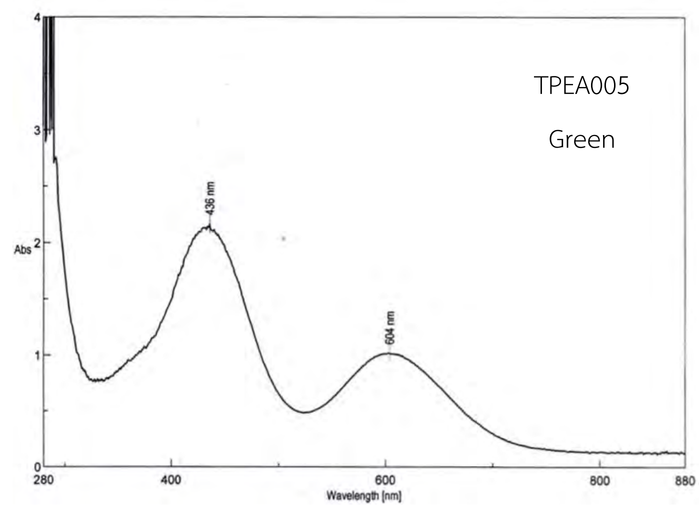

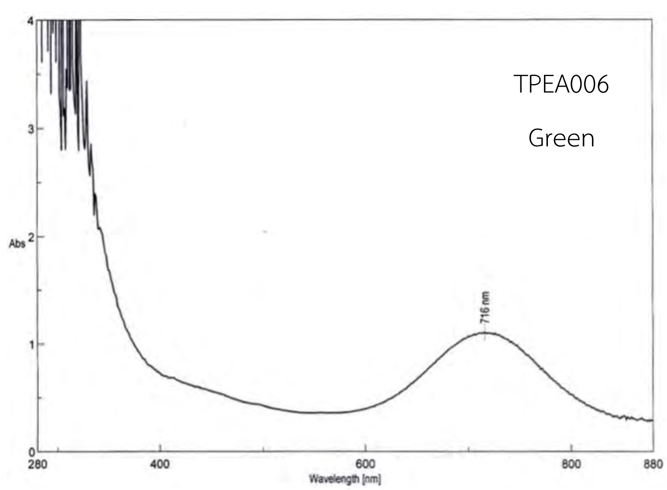

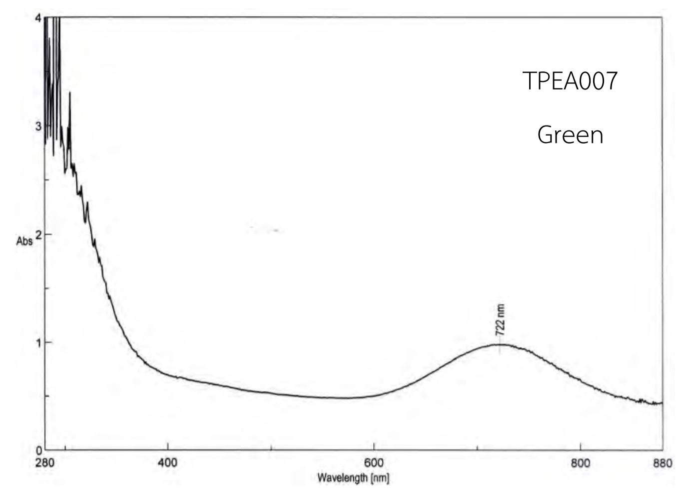

UV-VIS-NIR ABSORPTION SPECTRA OF NATURAL TOURMALINE SAMPLES FROM EAST AFRICA

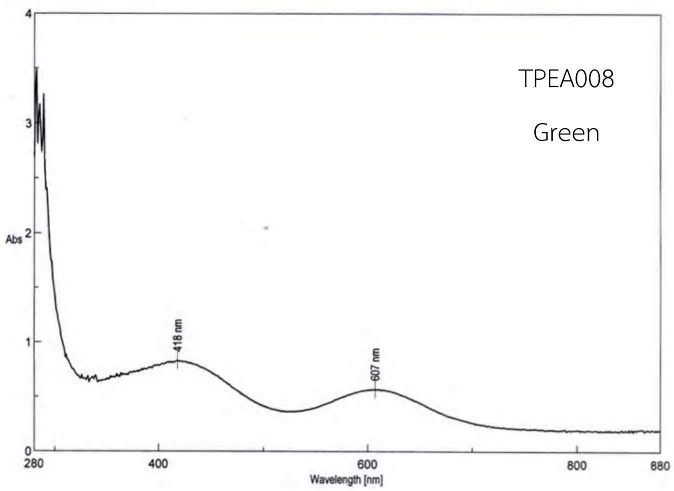

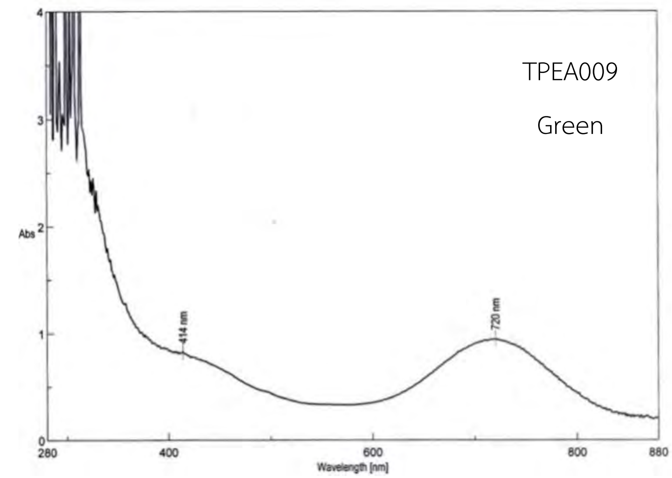

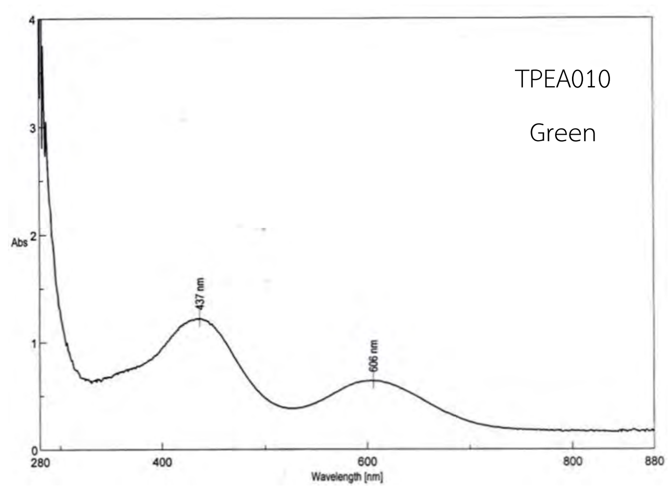

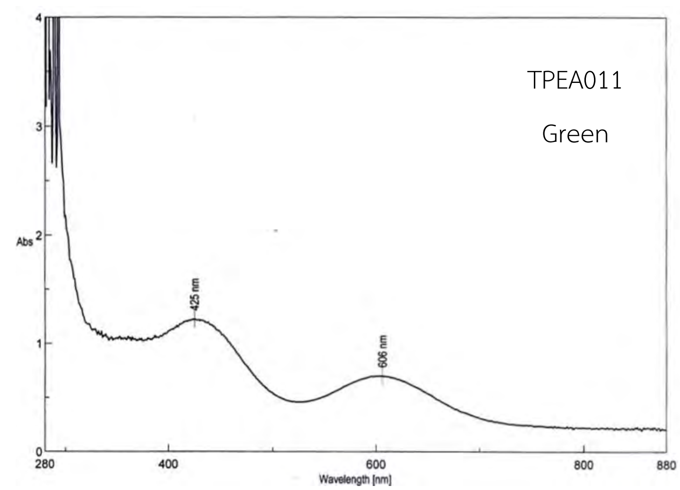

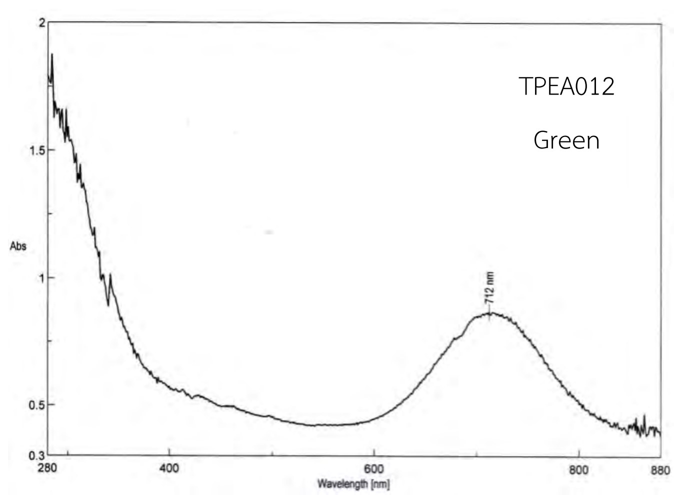

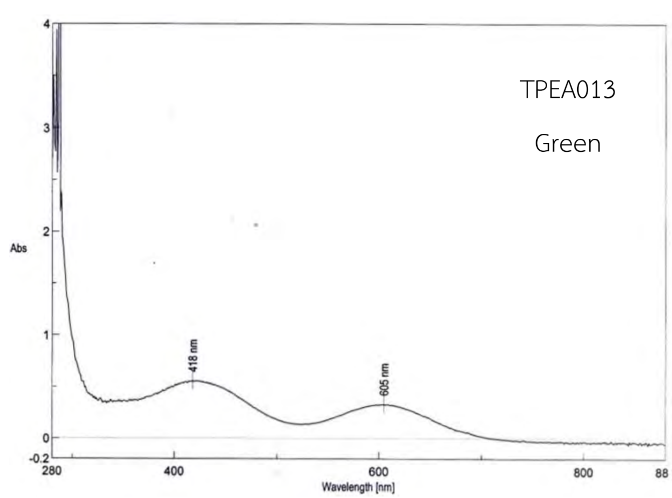

UV-VIS-NIR ABSORPTION SPECTRA OF NATURAL TOURMALINE SAMPLES FROM EAST AFRICA

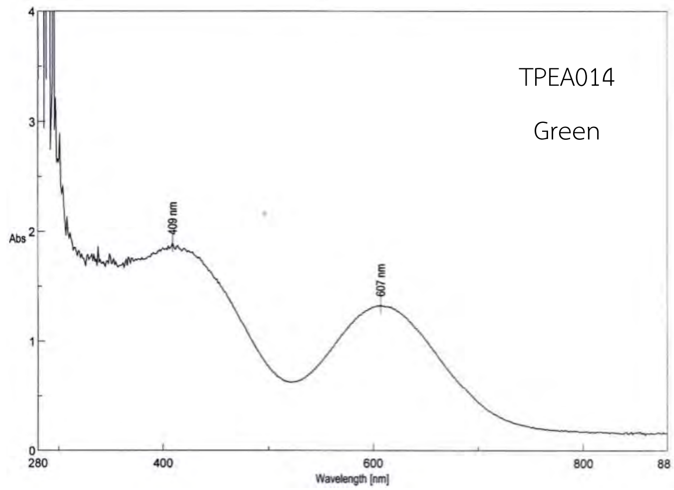

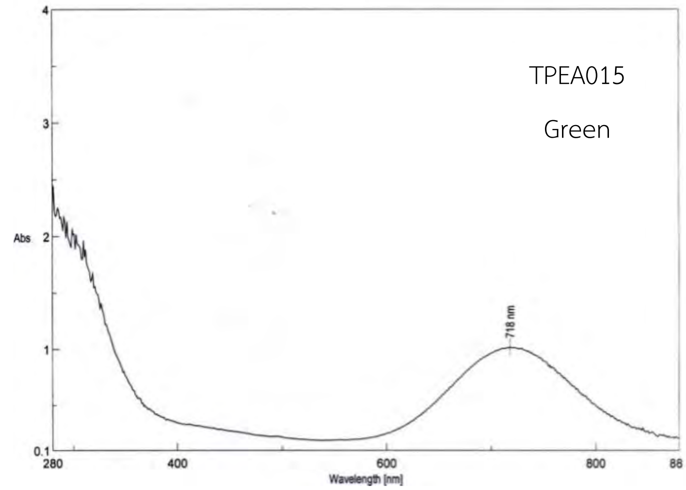

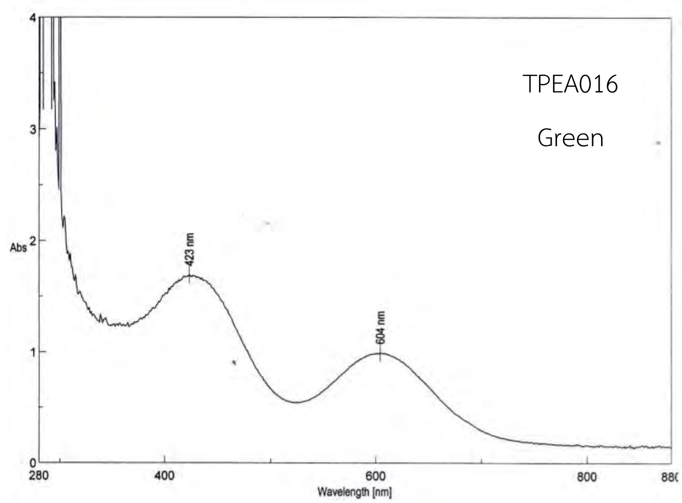

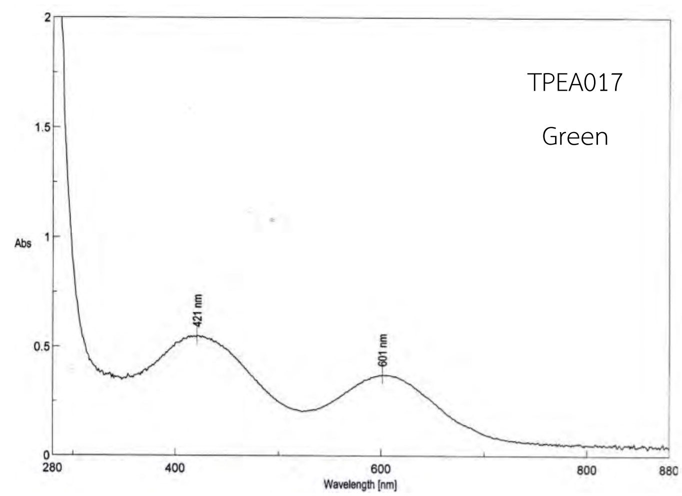

UV-VIS-NIR ABSORPTION SPECTRA OF FIRST GAMMA RAY IRRADIATED TOURMALINE SAMPLES

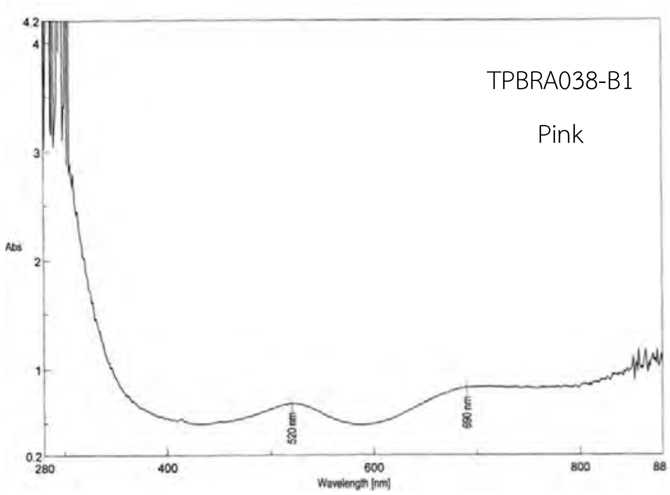

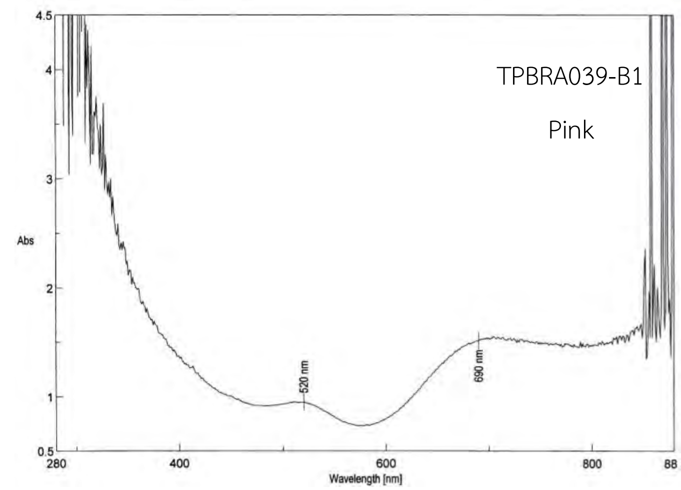

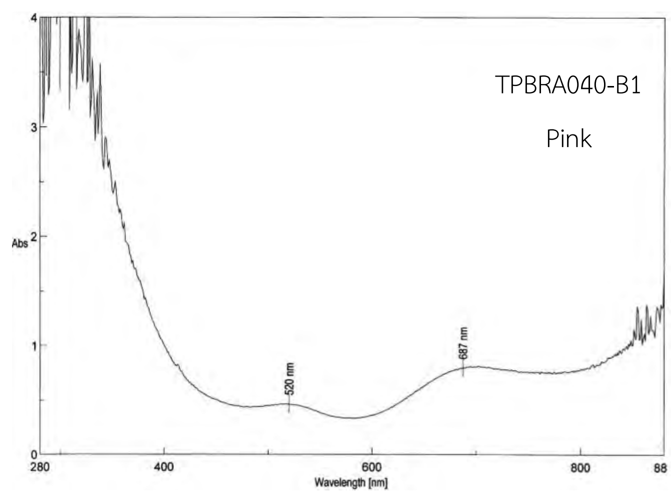

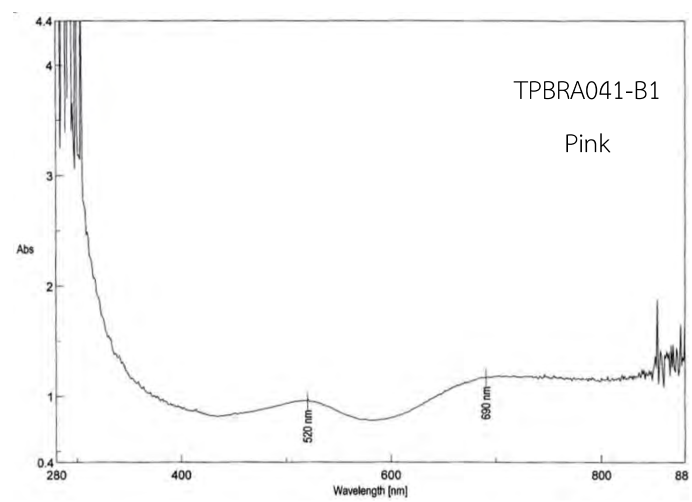

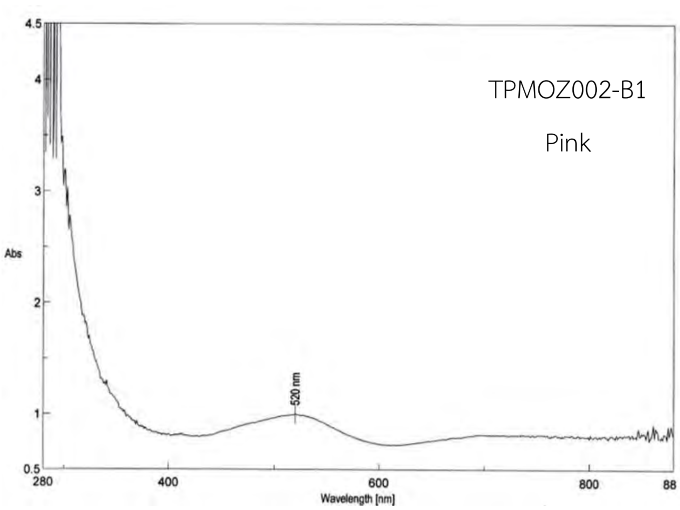

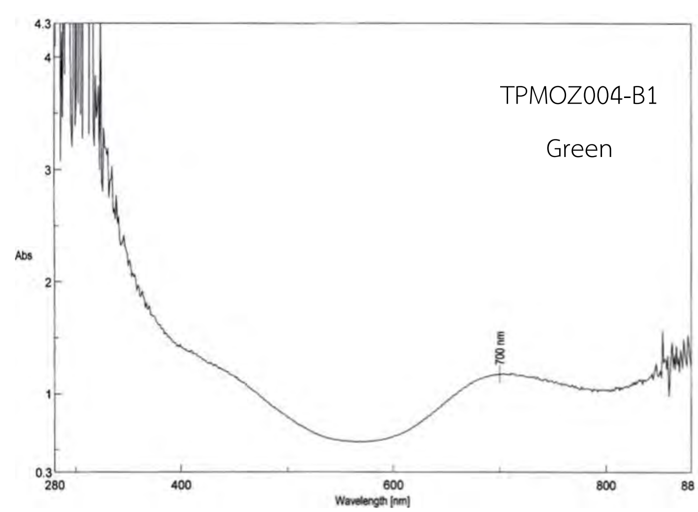

UV-VIS-NIR ABSORPTION SPECTRA OF FIRST GAMMA RAY IRRADIATED TOURMALINE SAMPLES

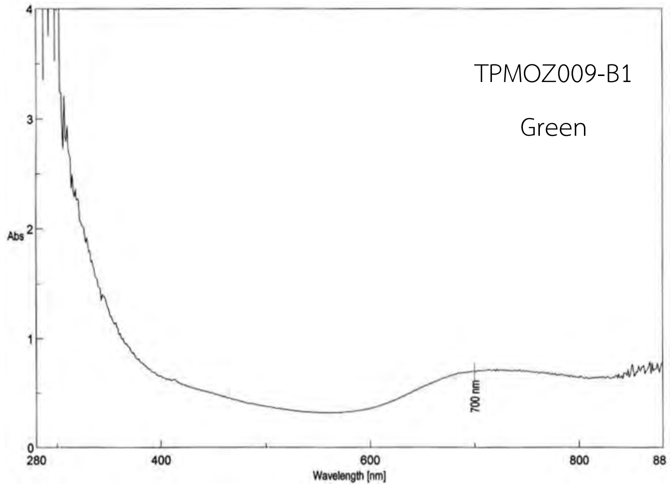

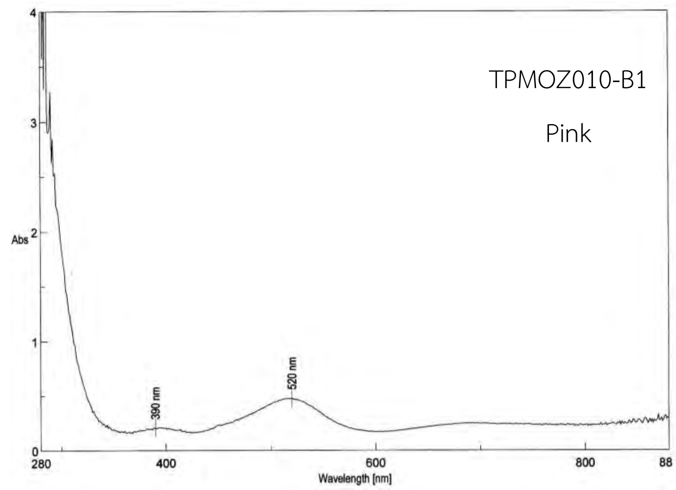

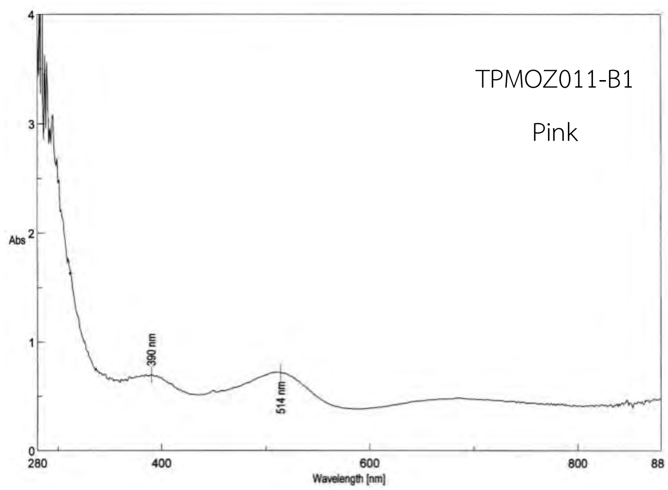

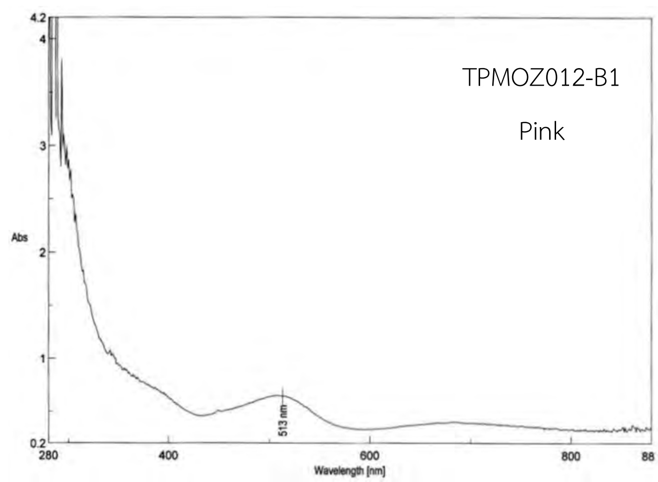

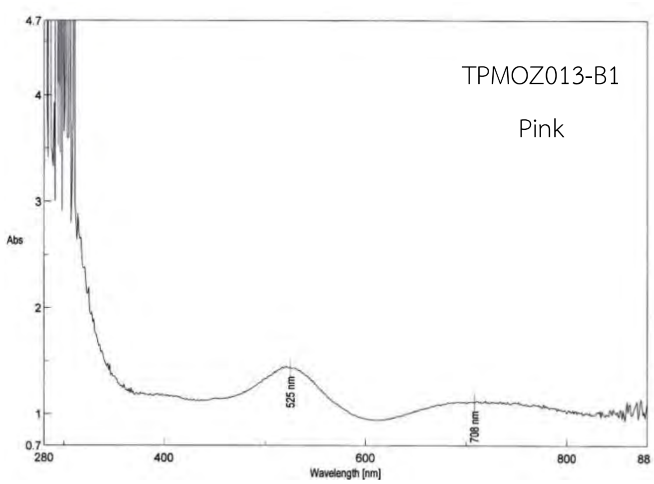

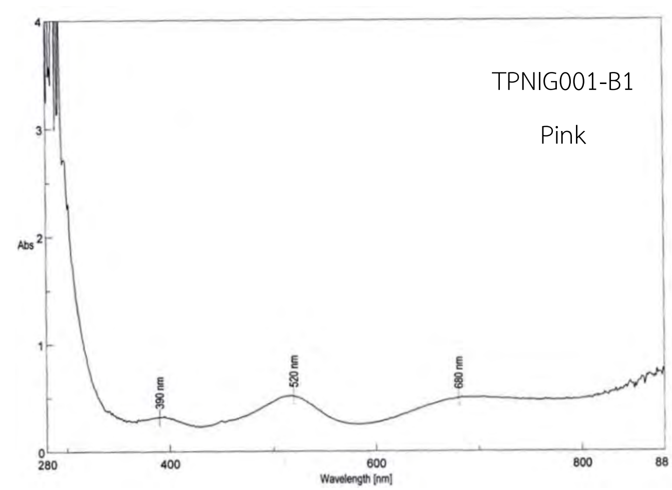

UV-VIS-NIR ABSORPTION SPECTRA OF SECOND GAMMA RAY IRRADIATED TOURMALINE SAMPLES

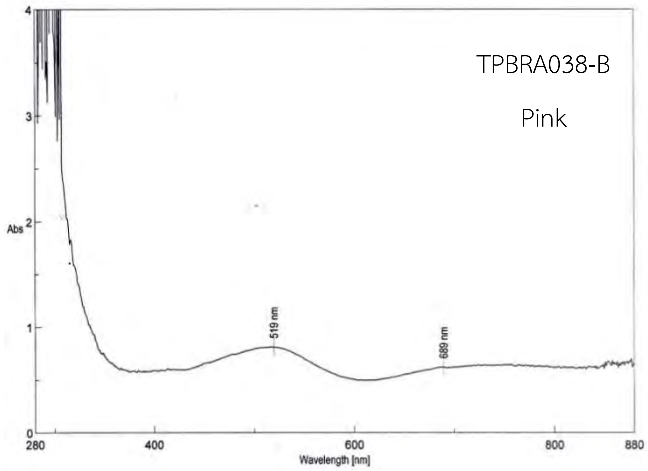

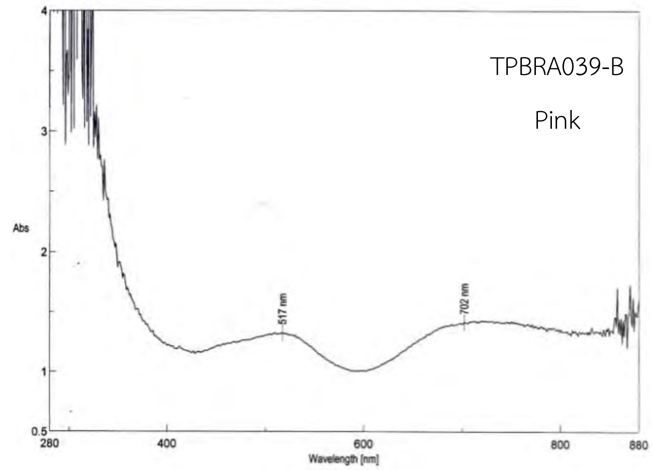

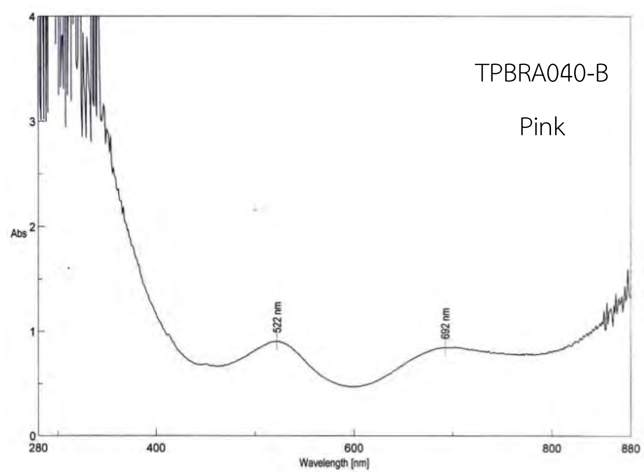

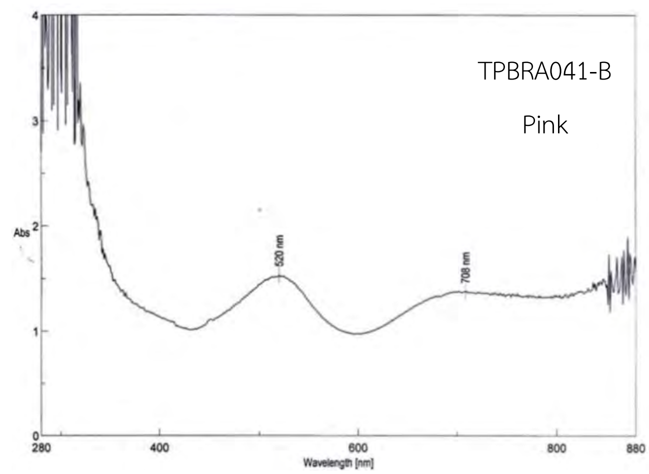

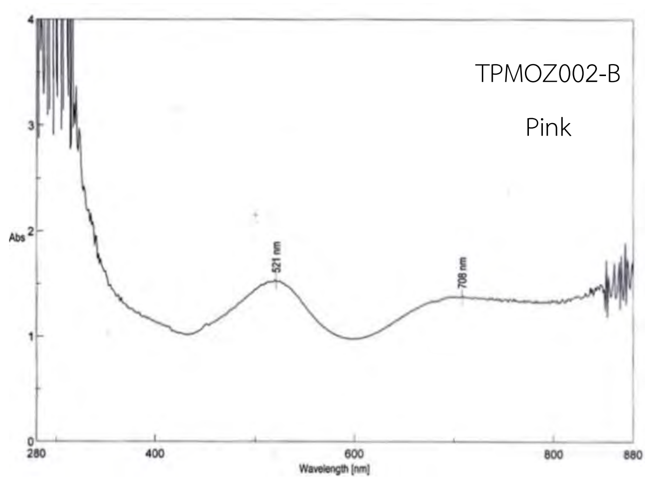

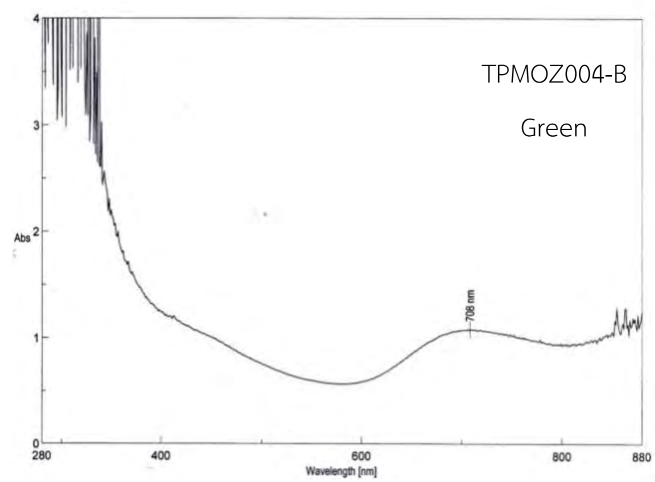

UV-VIS-NIR ABSORPTION SPECTRA OF SECOND GAMMA RAY IRRADIATED TOURMALINE SAMPLES

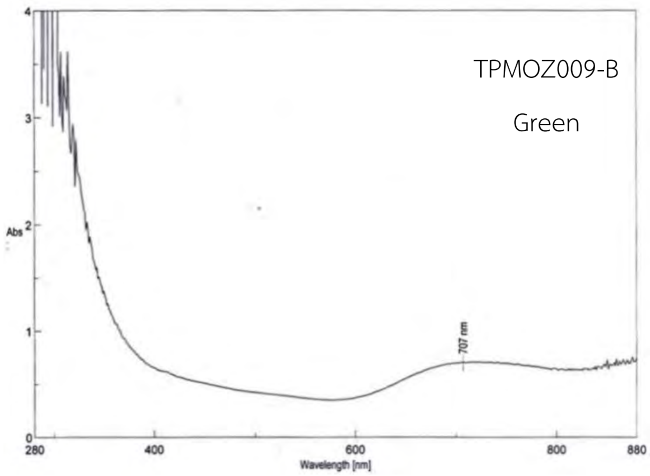

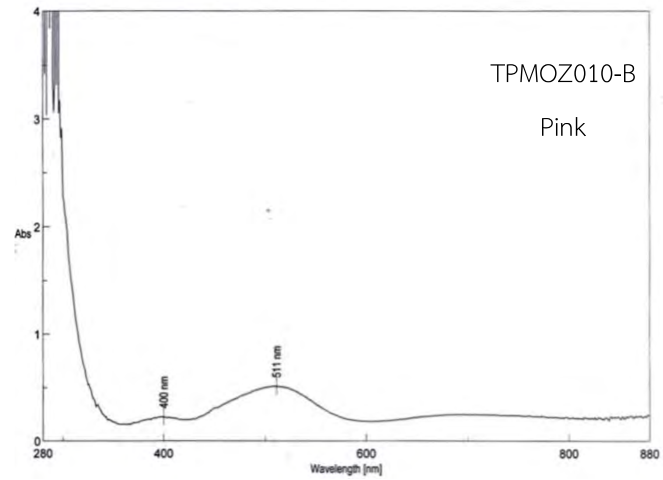

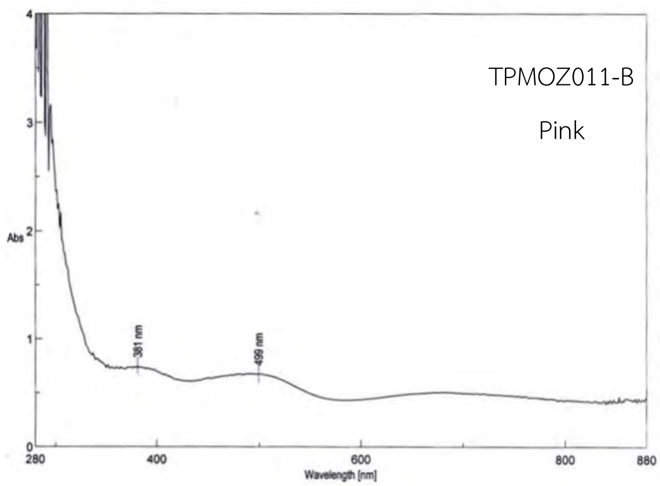

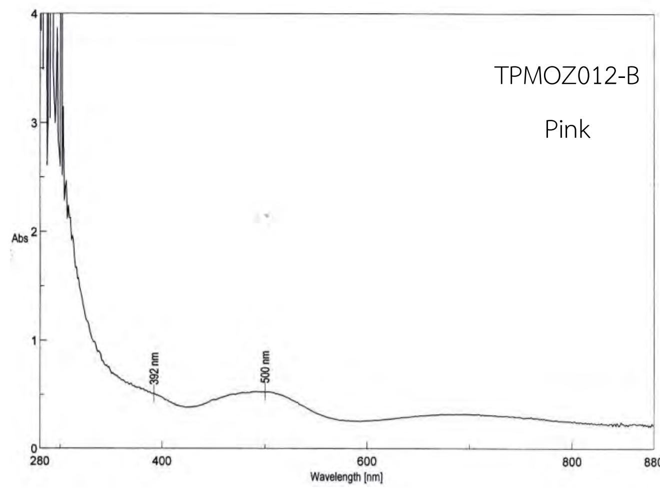

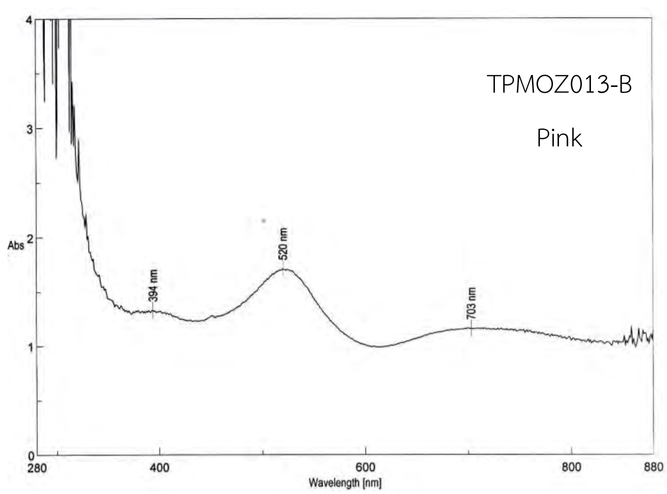

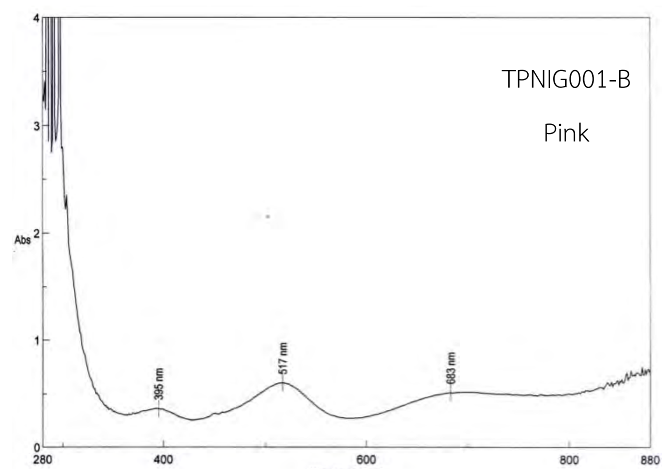

APPENDIX C

FTIR SPECTRA OF NATURAL TOURMALINE SAMPLES

AND COMPARISON OF BEFORE AND AFTER GAMMA RAY IRRADIATED TOURMALINE SAMPLES

FTIR SPECTRA OF NATURAL TOURMALINE SAMPLES

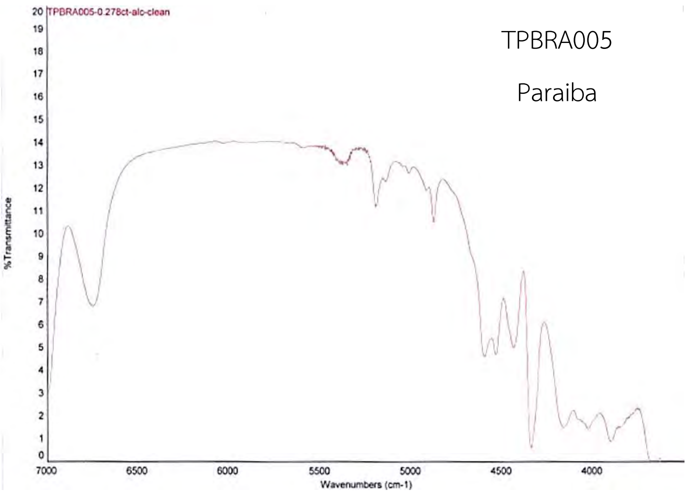

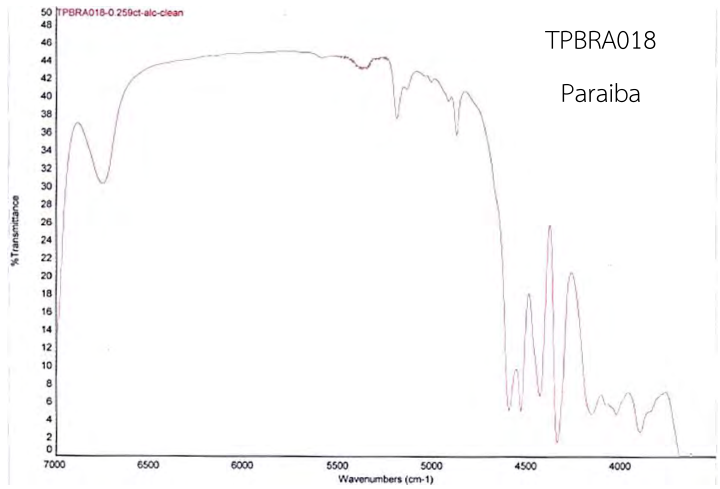

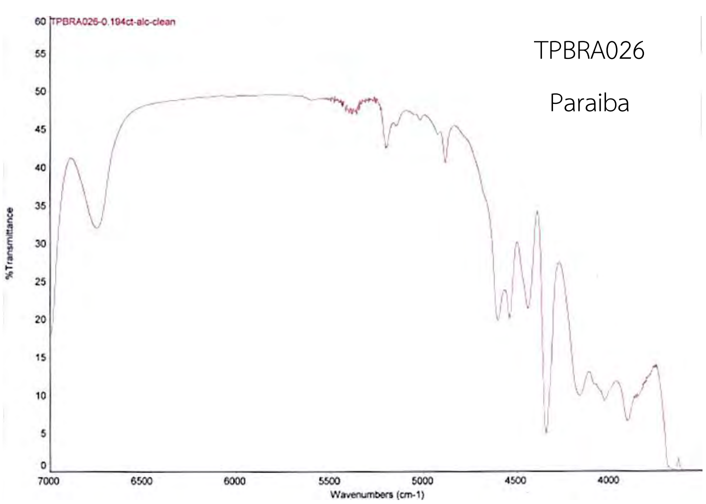

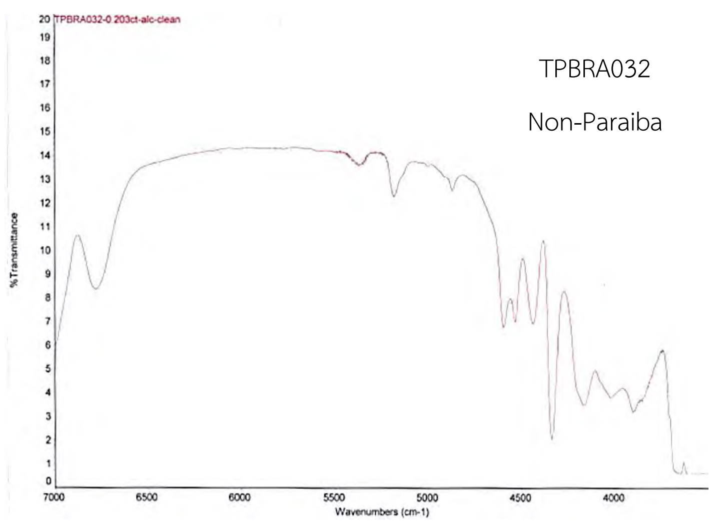

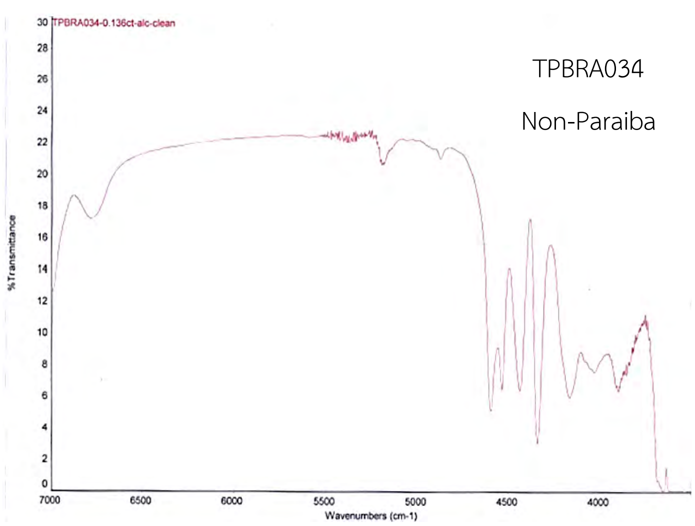

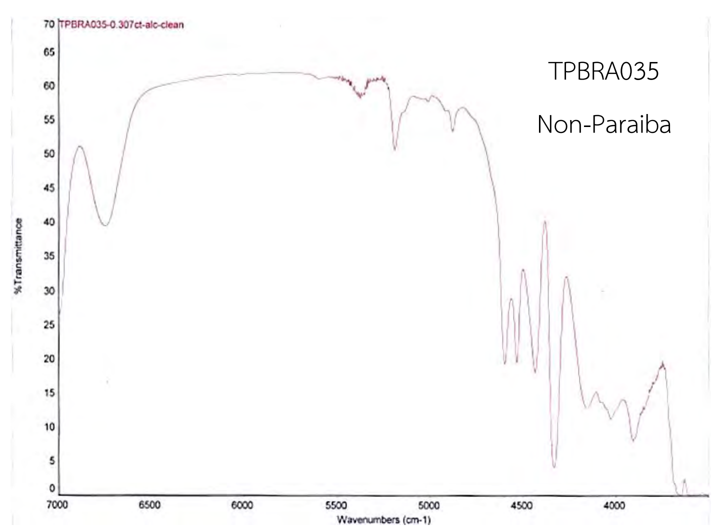

FTIR SPECTRA OF NATURAL TOURMALINE SAMPLES

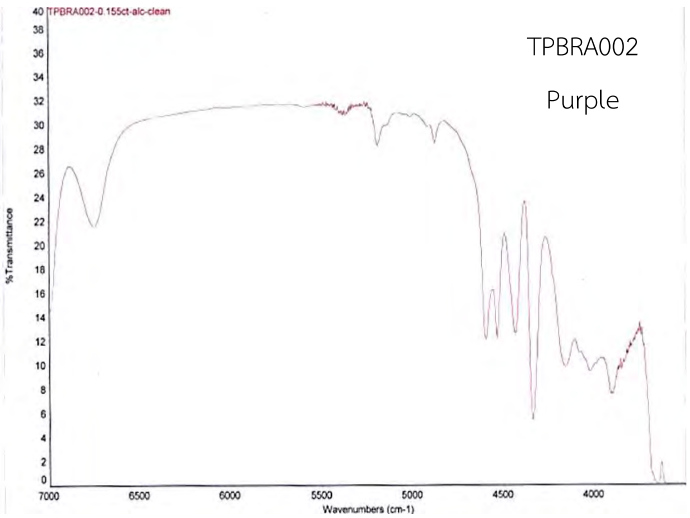

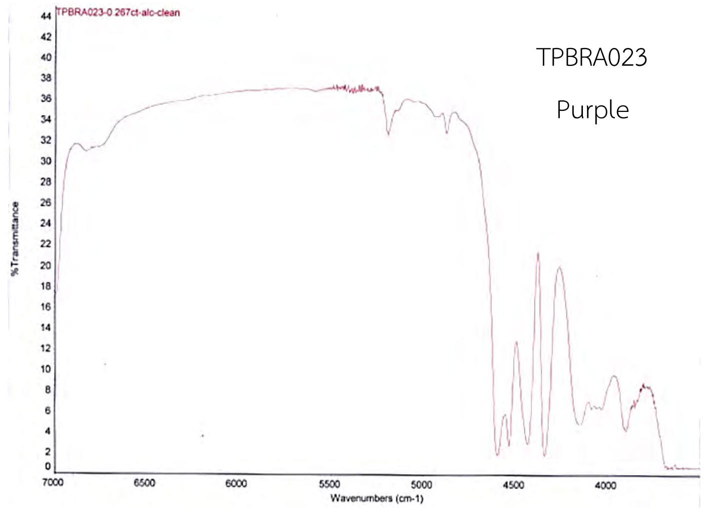

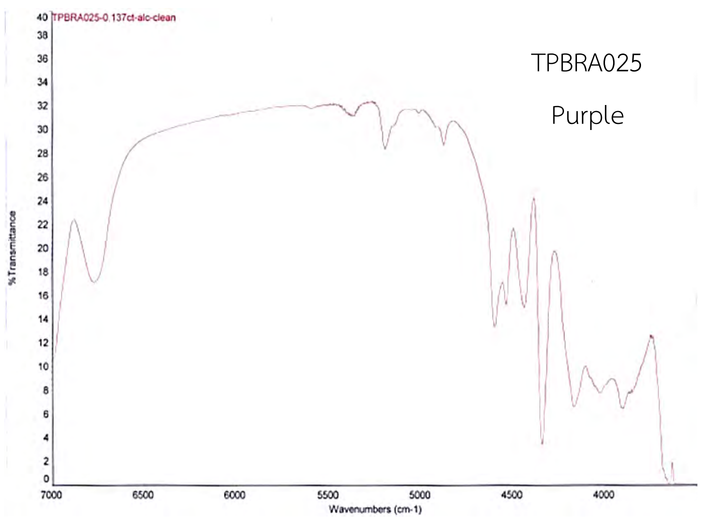

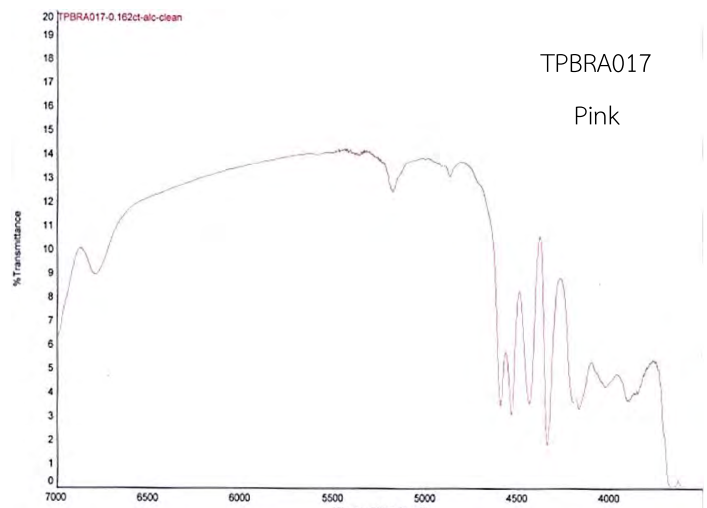

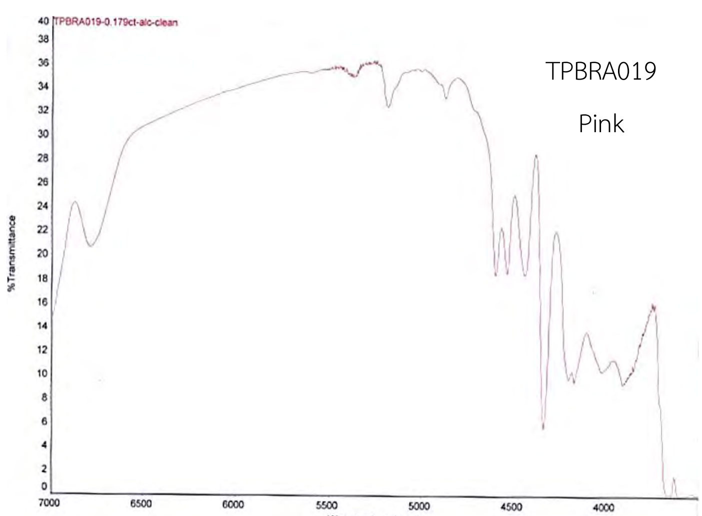

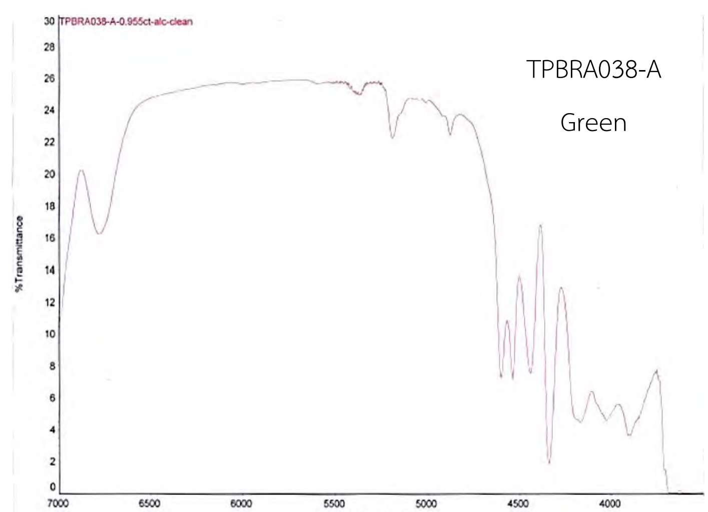

FTIR SPECTRA OF NATURAL TOURMALINE SAMPLES

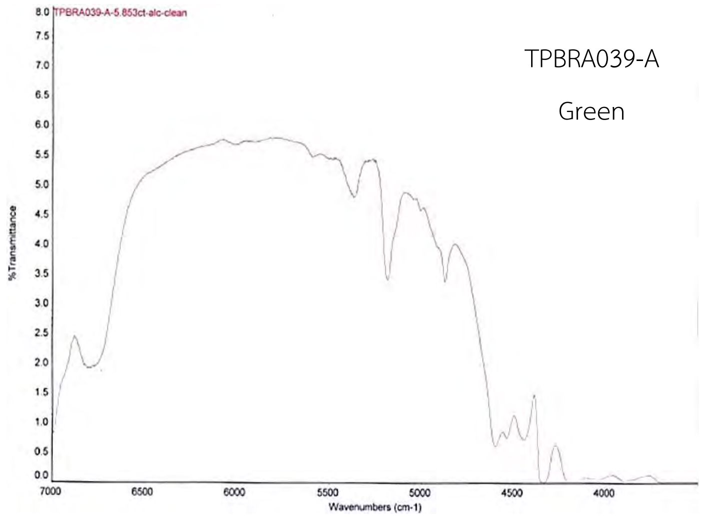

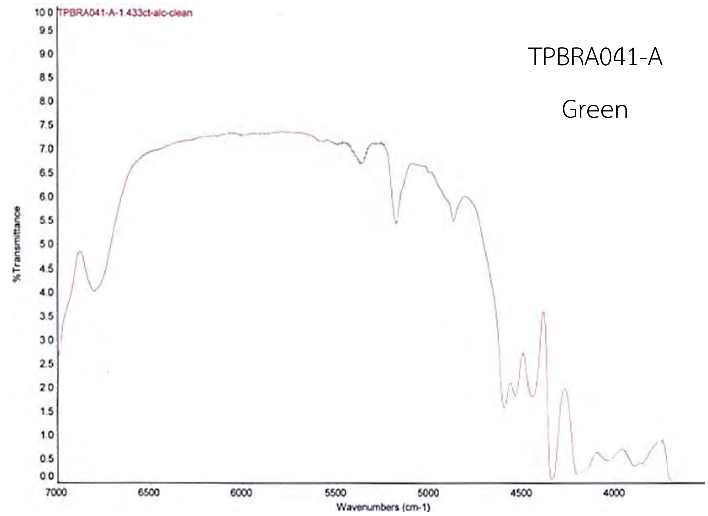

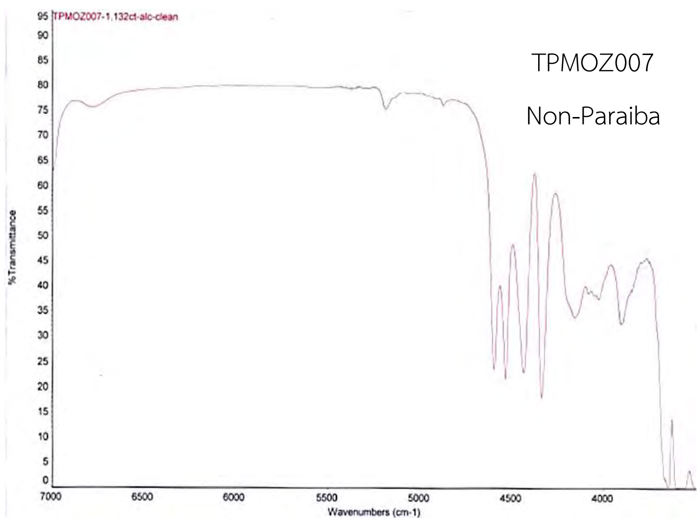

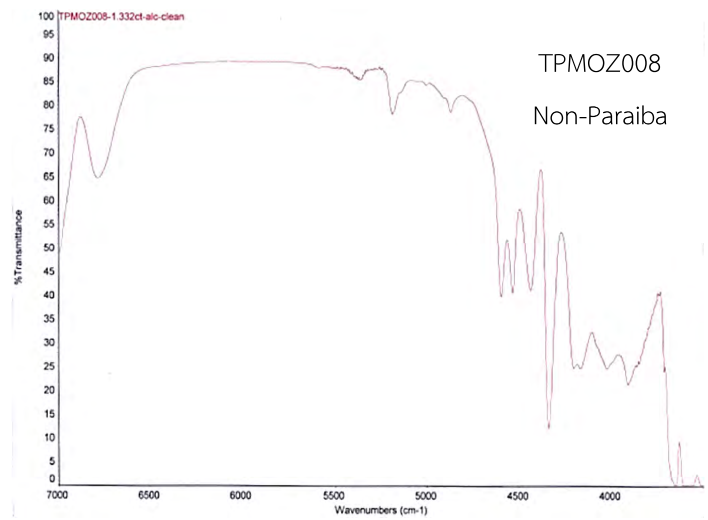

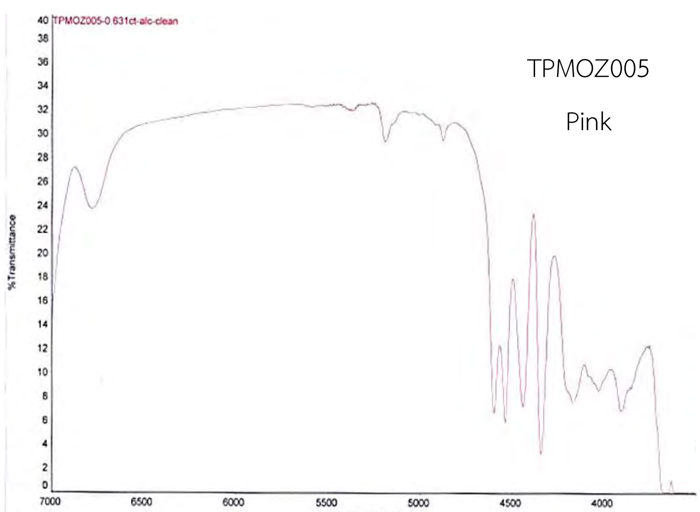

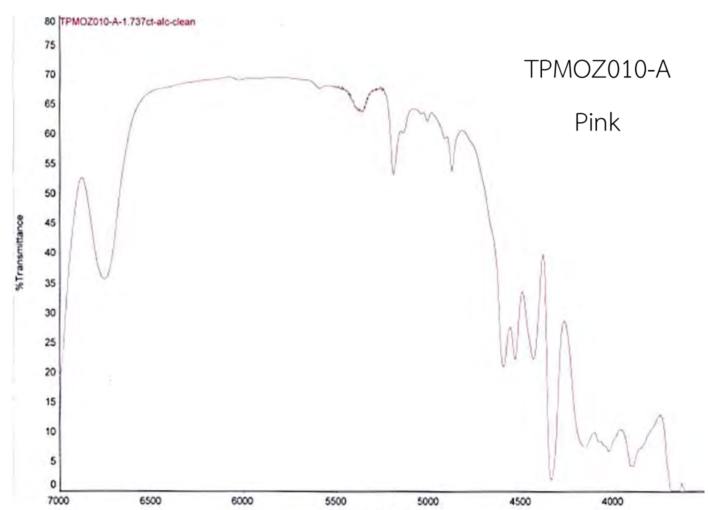

FTIR SPECTRA OF NATURAL TOURMALINE SAMPLES

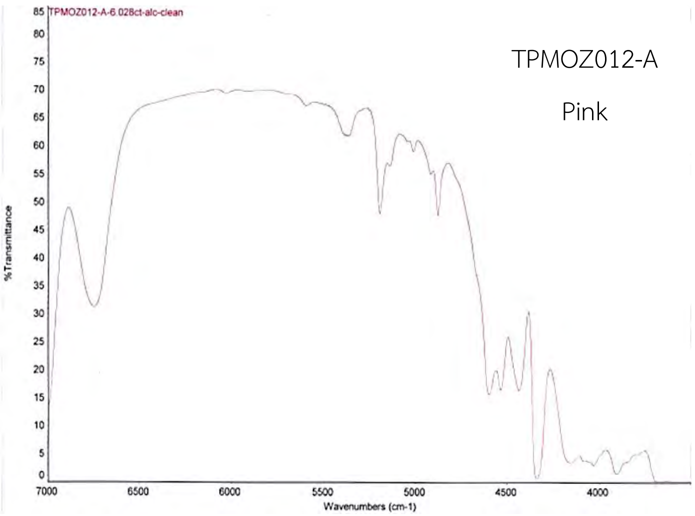

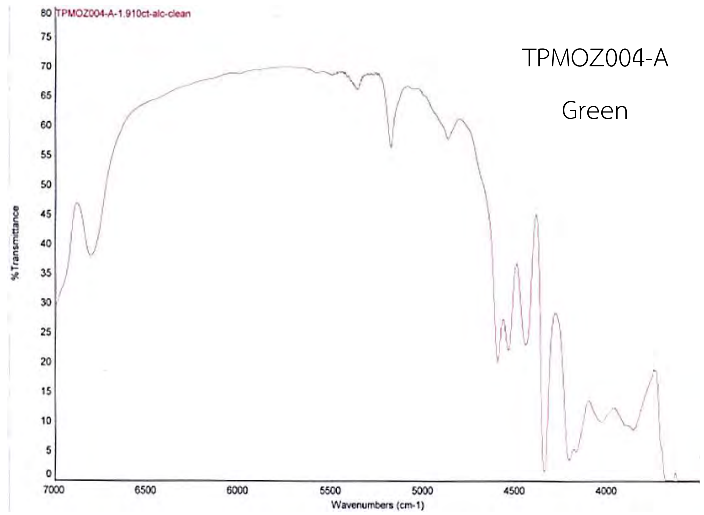

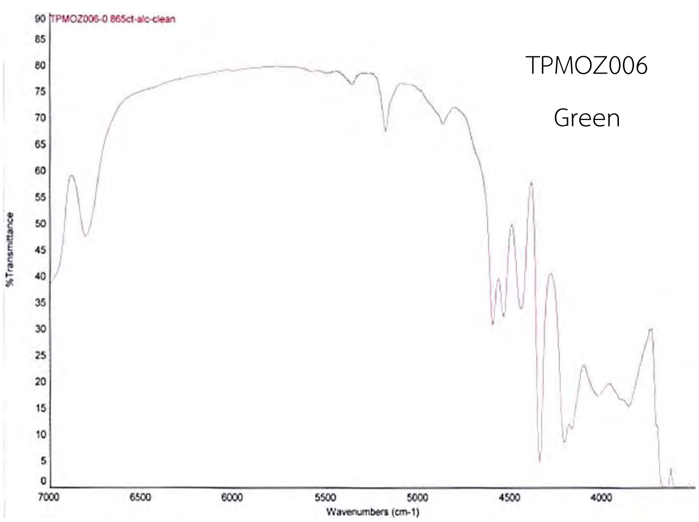

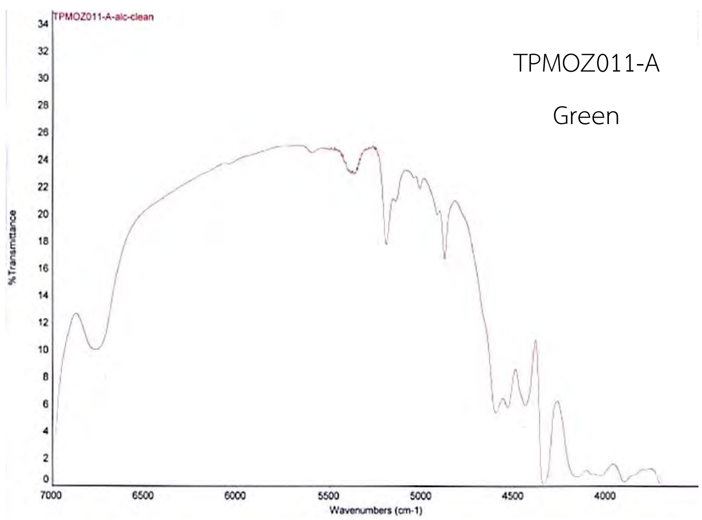

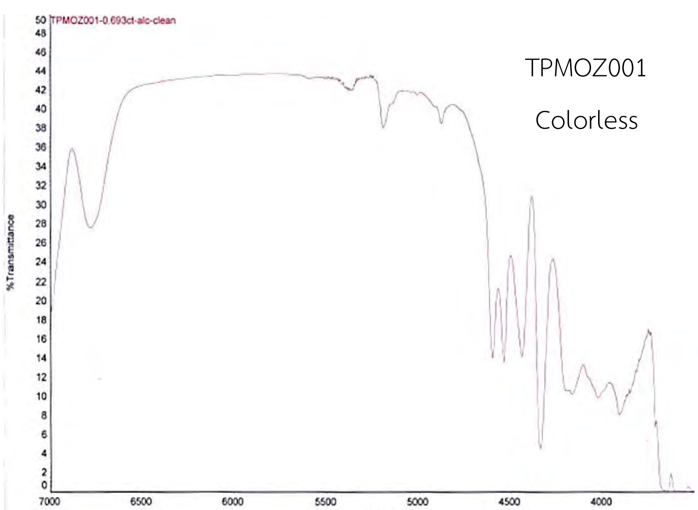

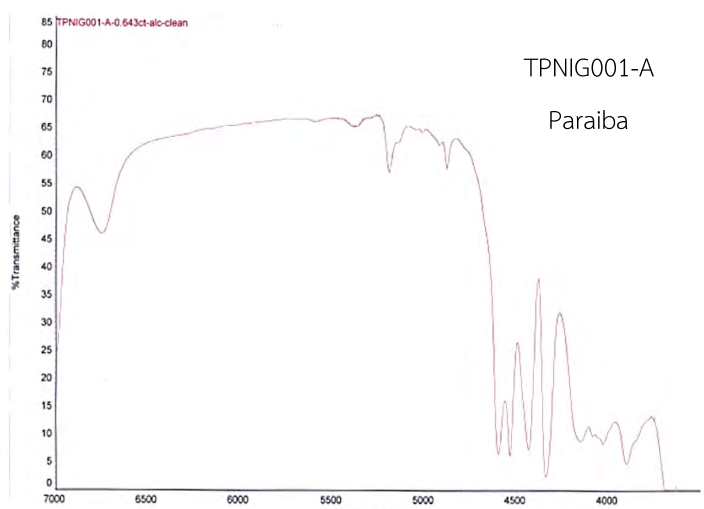

FTIR SPECTRA OF NATURAL TOURMALINE SAMPLES

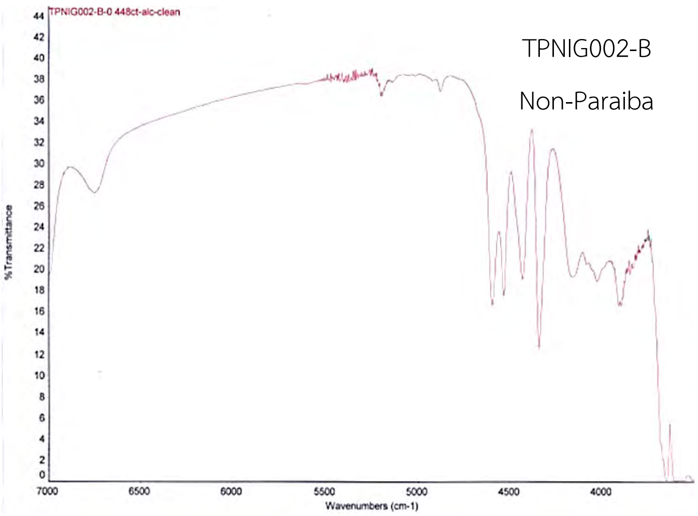

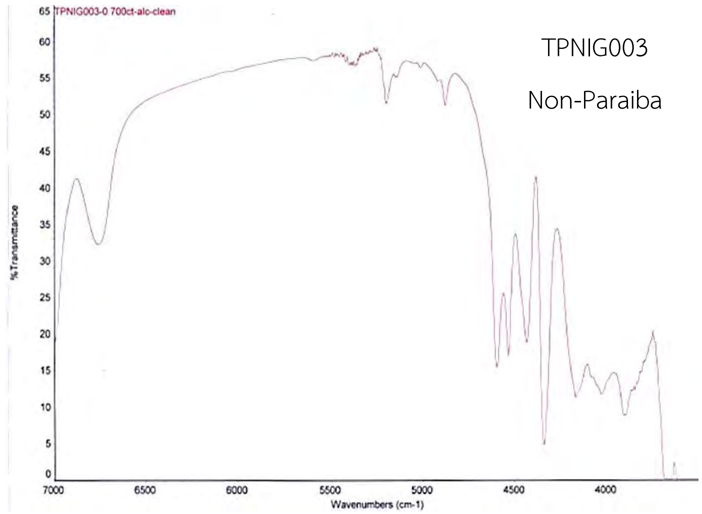

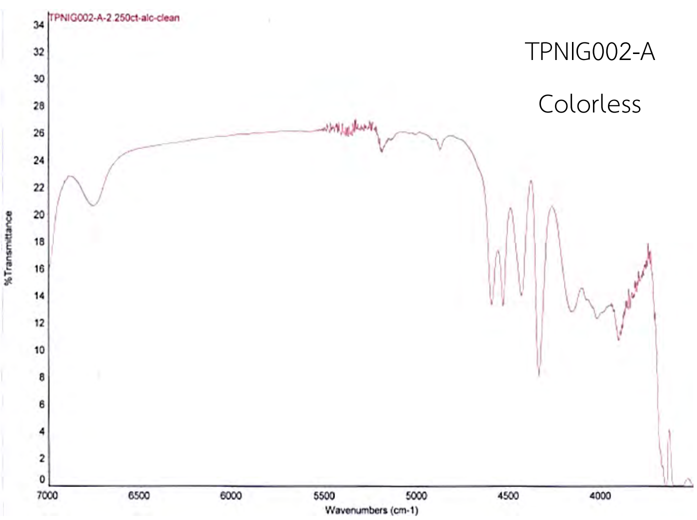

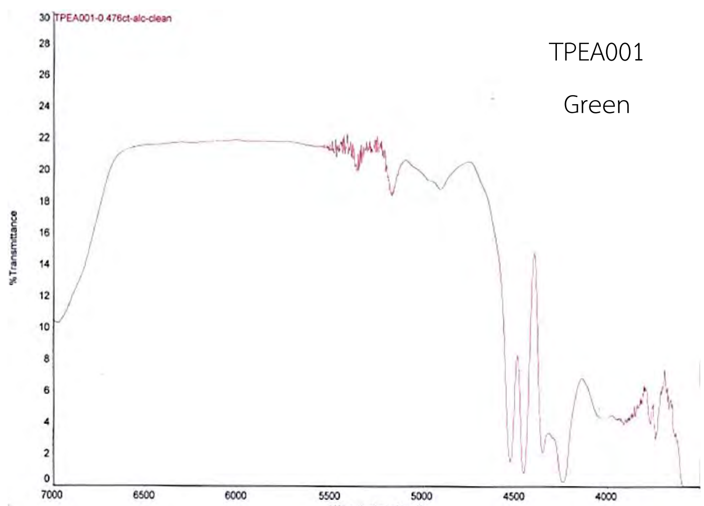

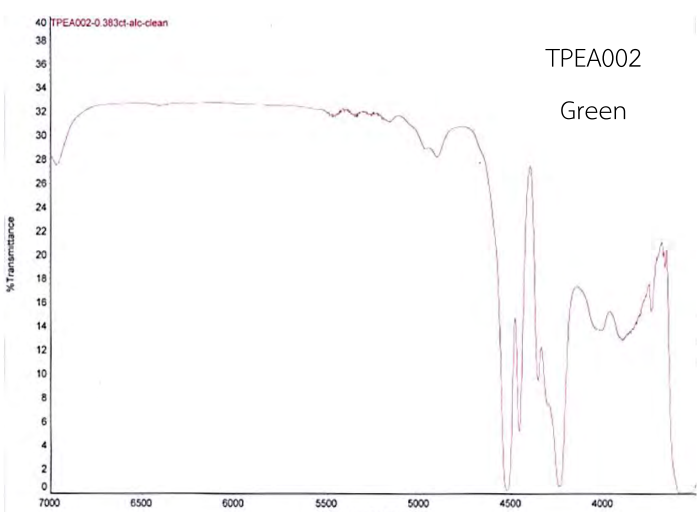

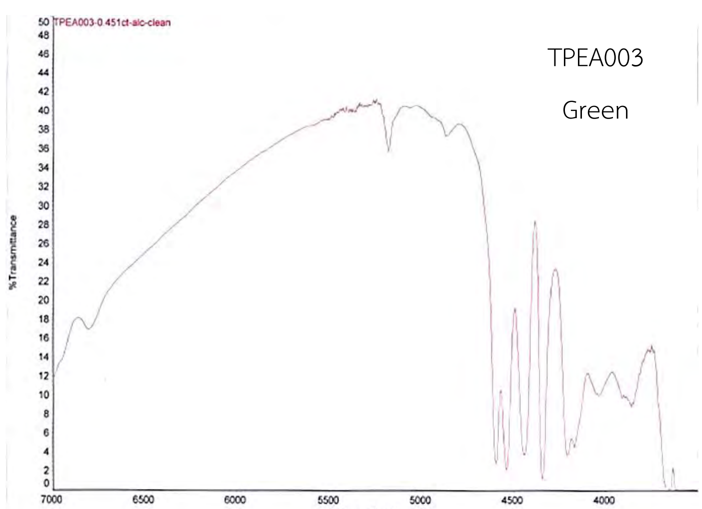

FTIR SPECTRA OF NATURAL TOURMALINE SAMPLES

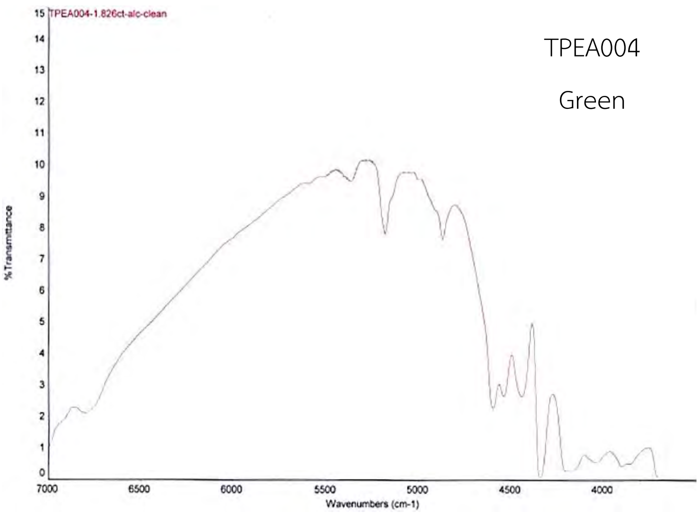

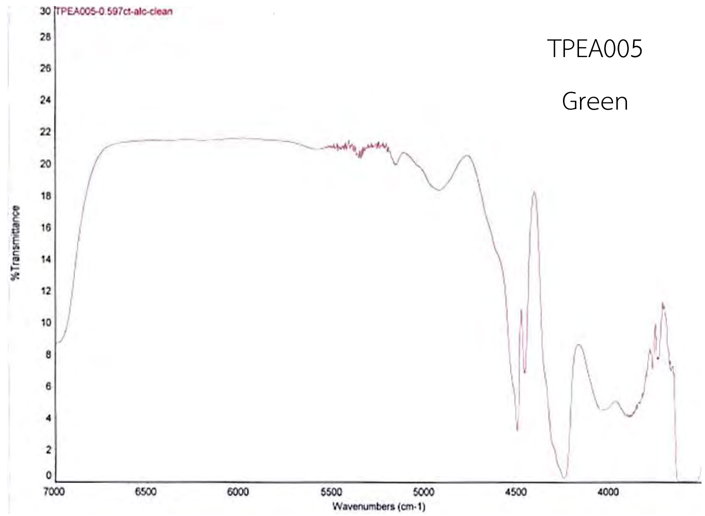

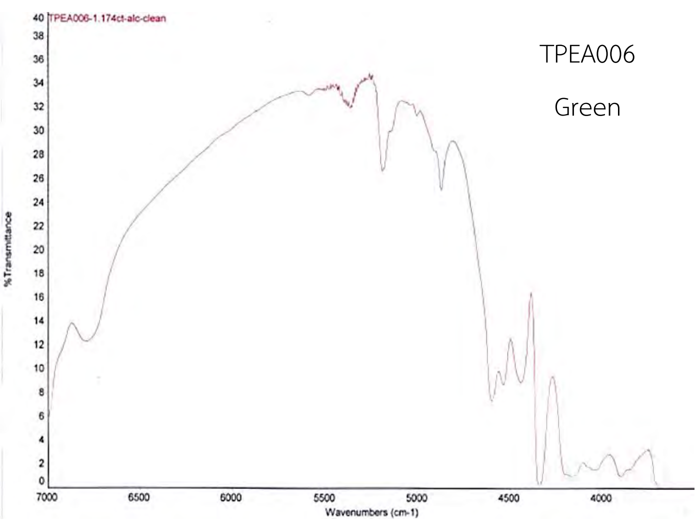

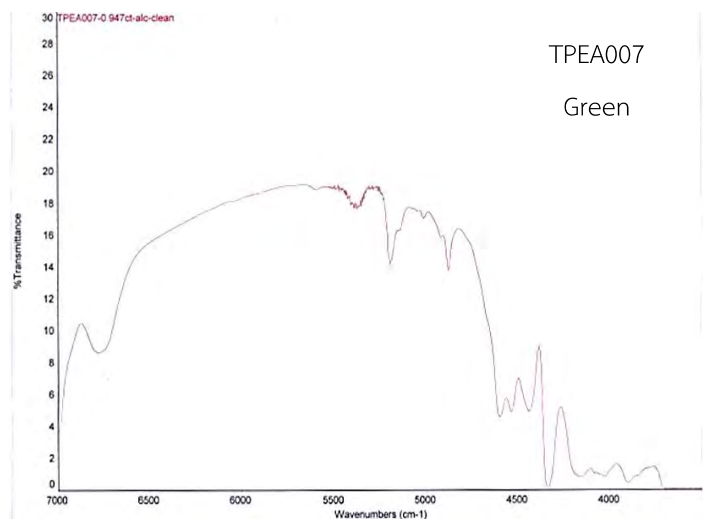

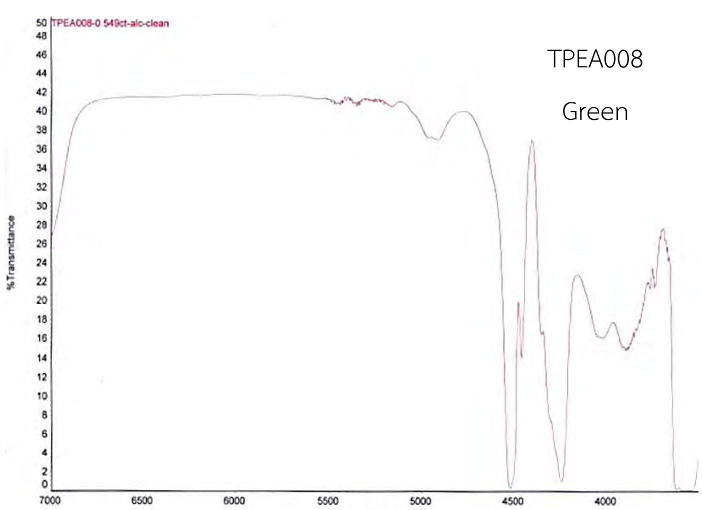

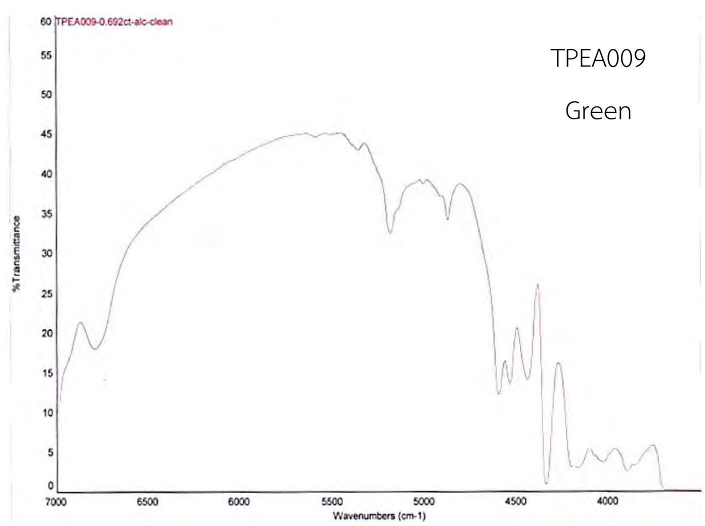

FTIR SPECTRA OF NATURAL TOURMALINE SAMPLES

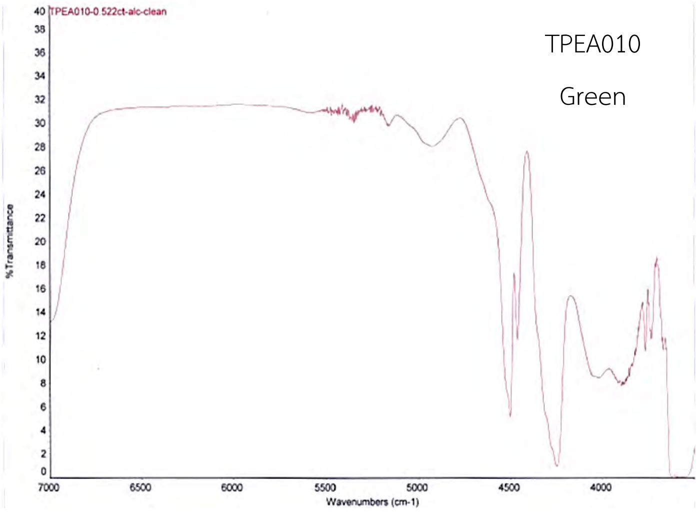

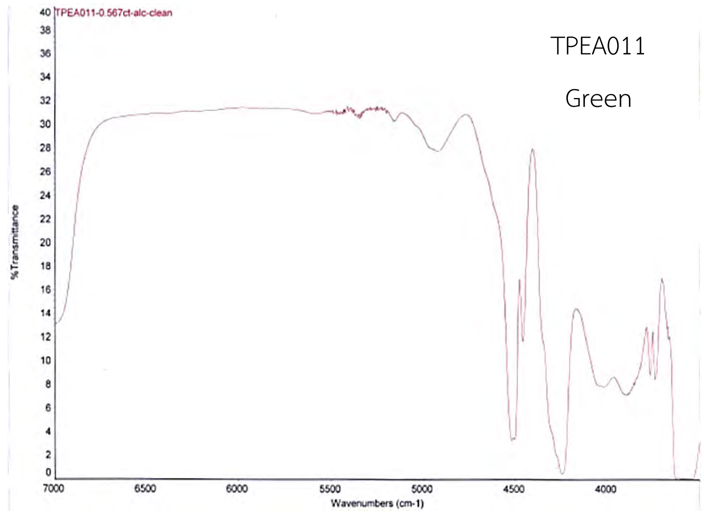

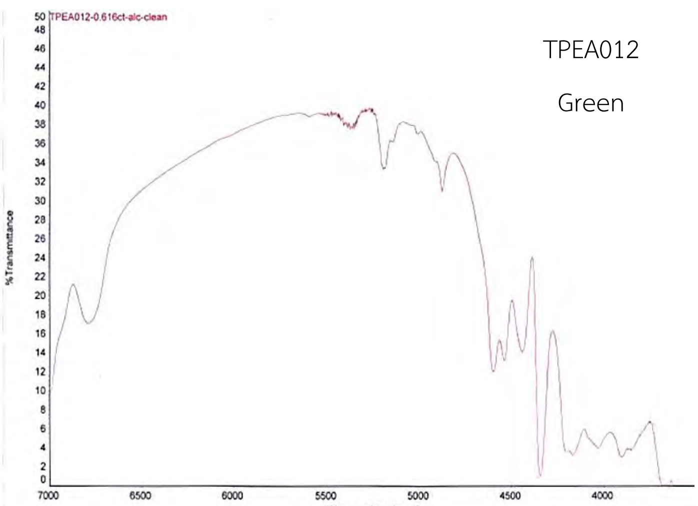

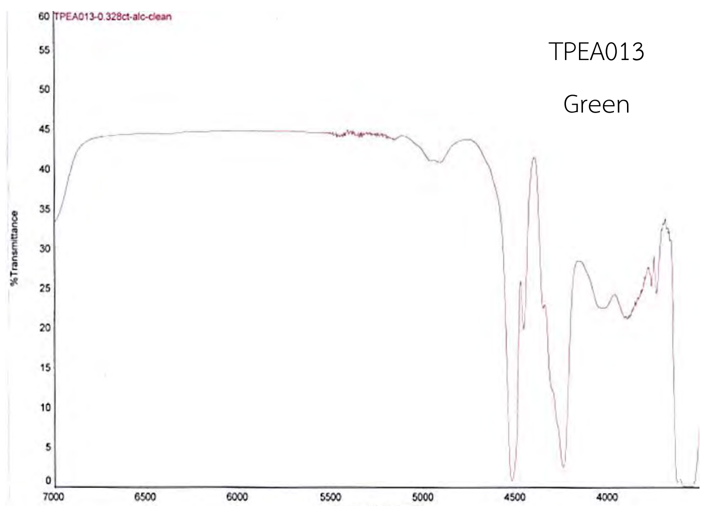

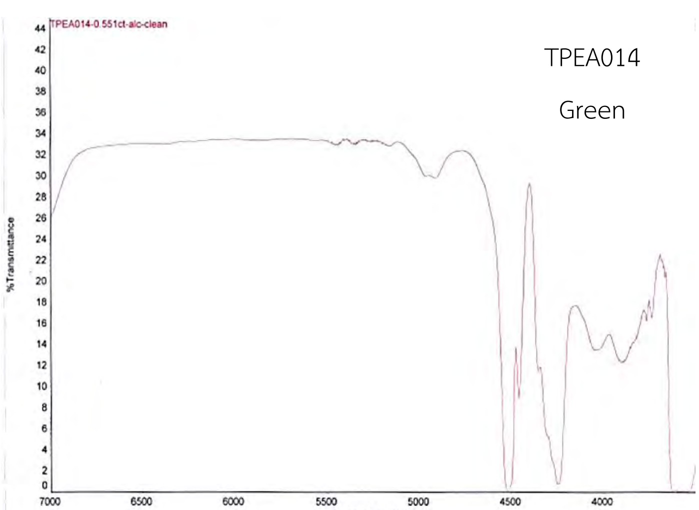

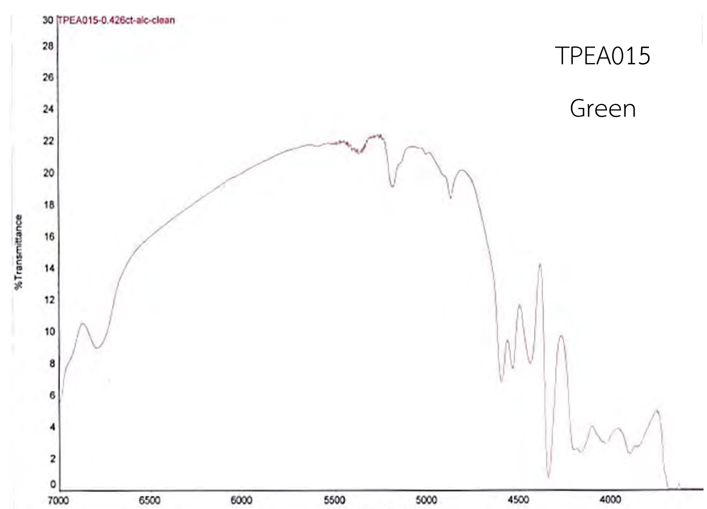

FTIR SPECTRA OF NATURAL TOURMALINE SAMPLES

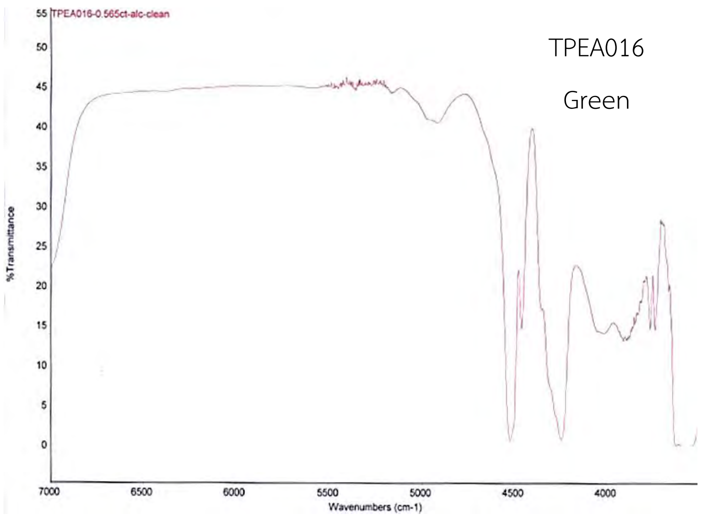

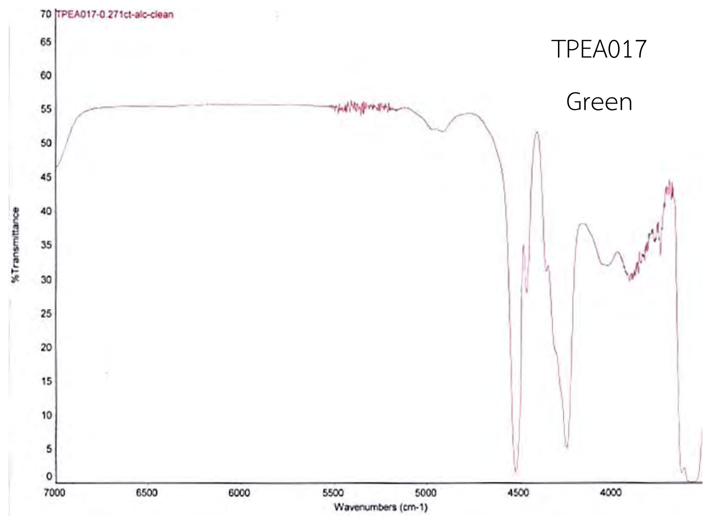

COMPARISON OF BEFORE AND AFTER GAMMA RAY IRRADIATED TOURMALINE SAMPLES

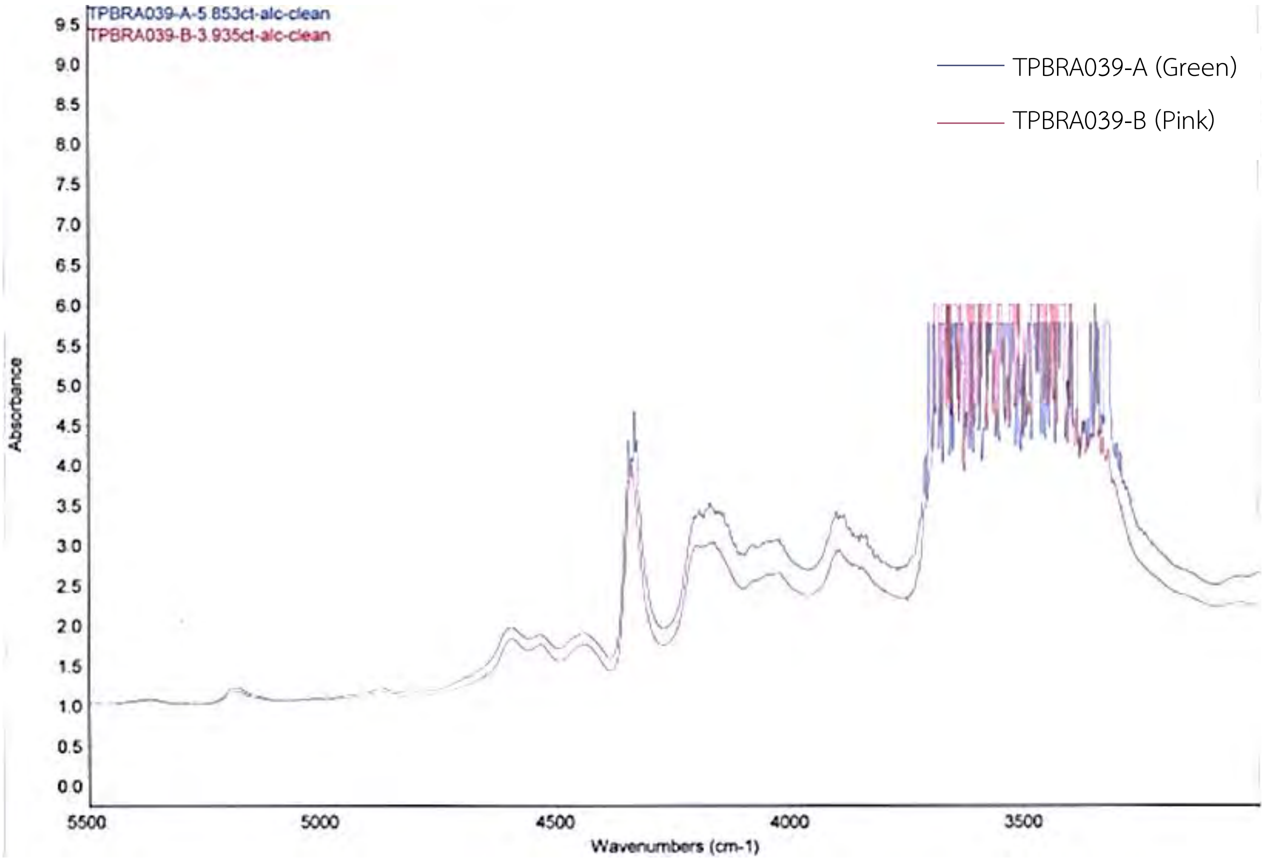

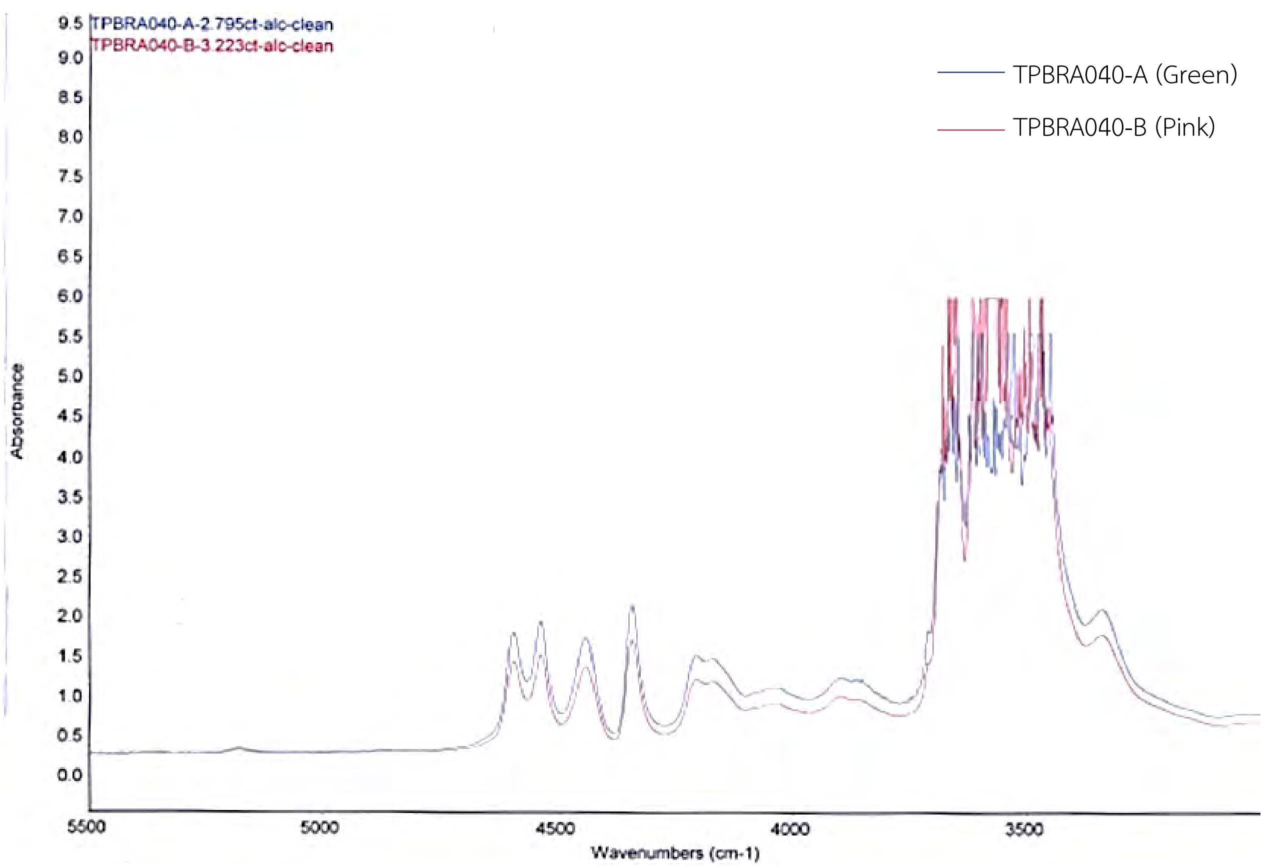

COMPARISON OF BEFORE AND AFTER GAMMA RAY IRRADIATED TOURMALINE SAMPLES

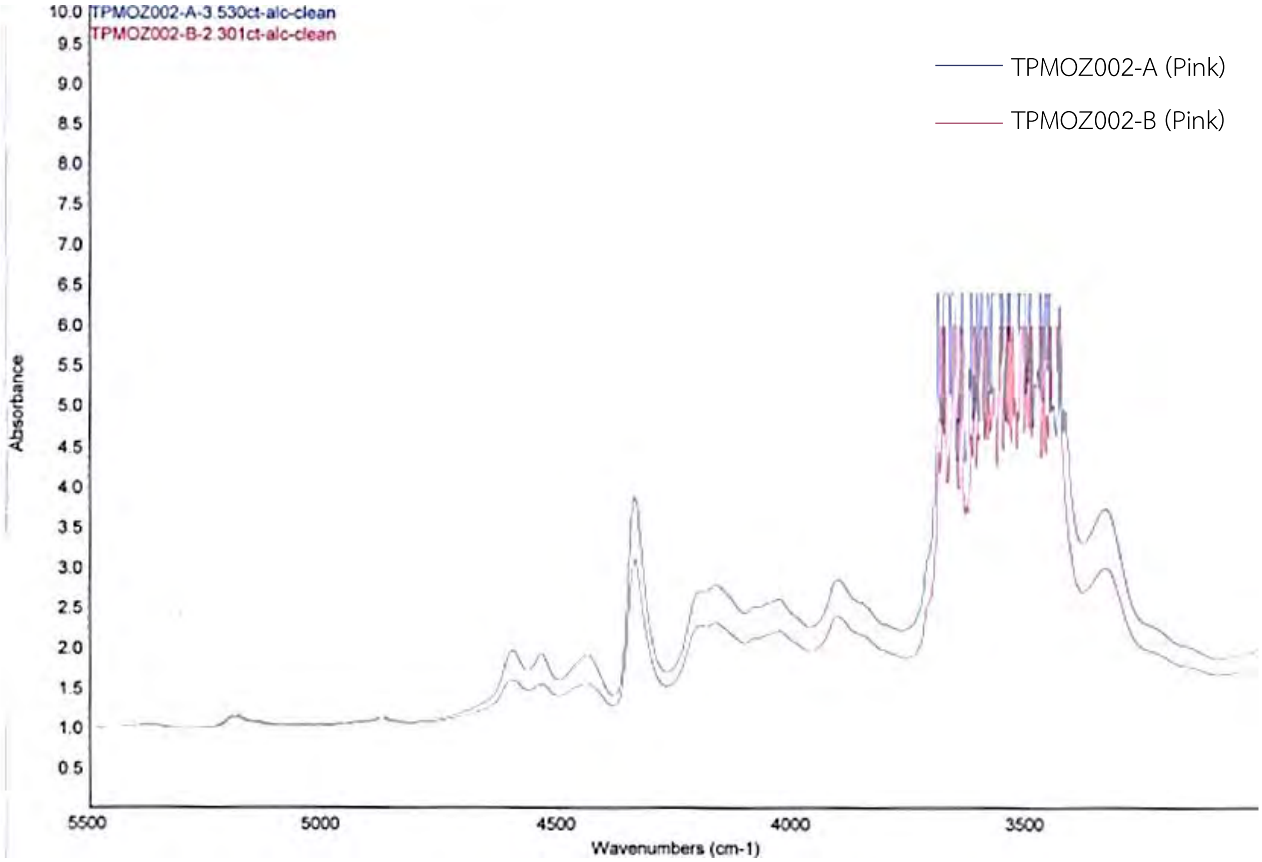

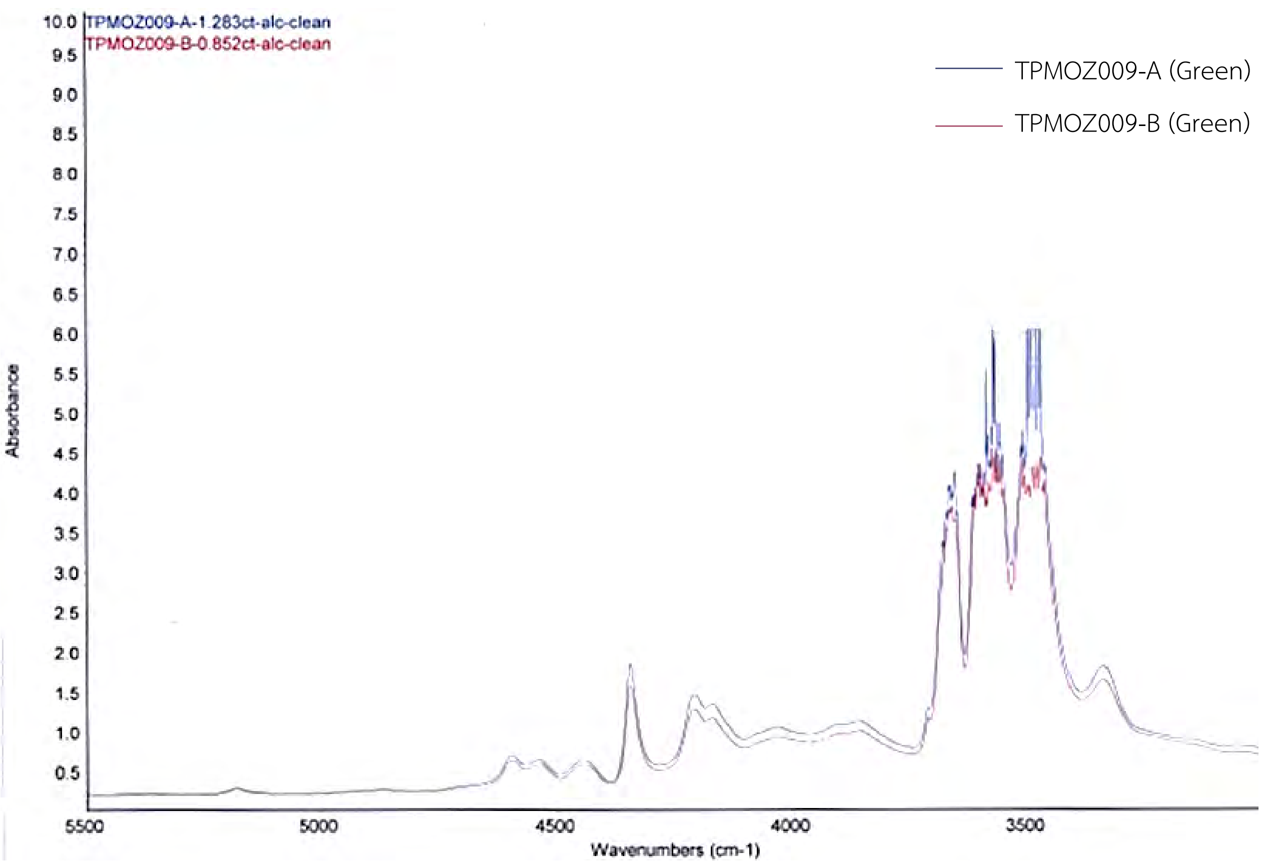

COMPARISON OF BEFORE AND AFTER GAMMA RAY IRRADIATED TOURMALINE SAMPLES

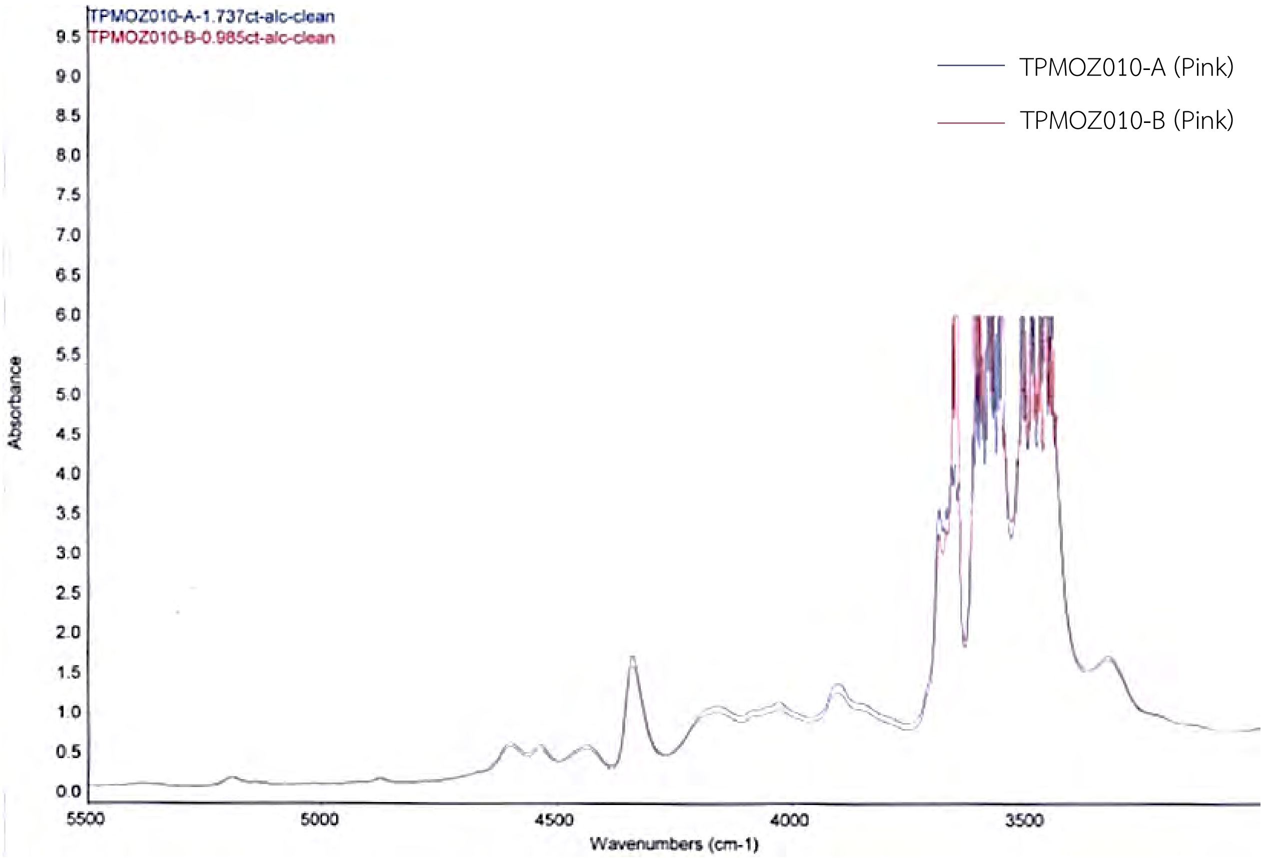

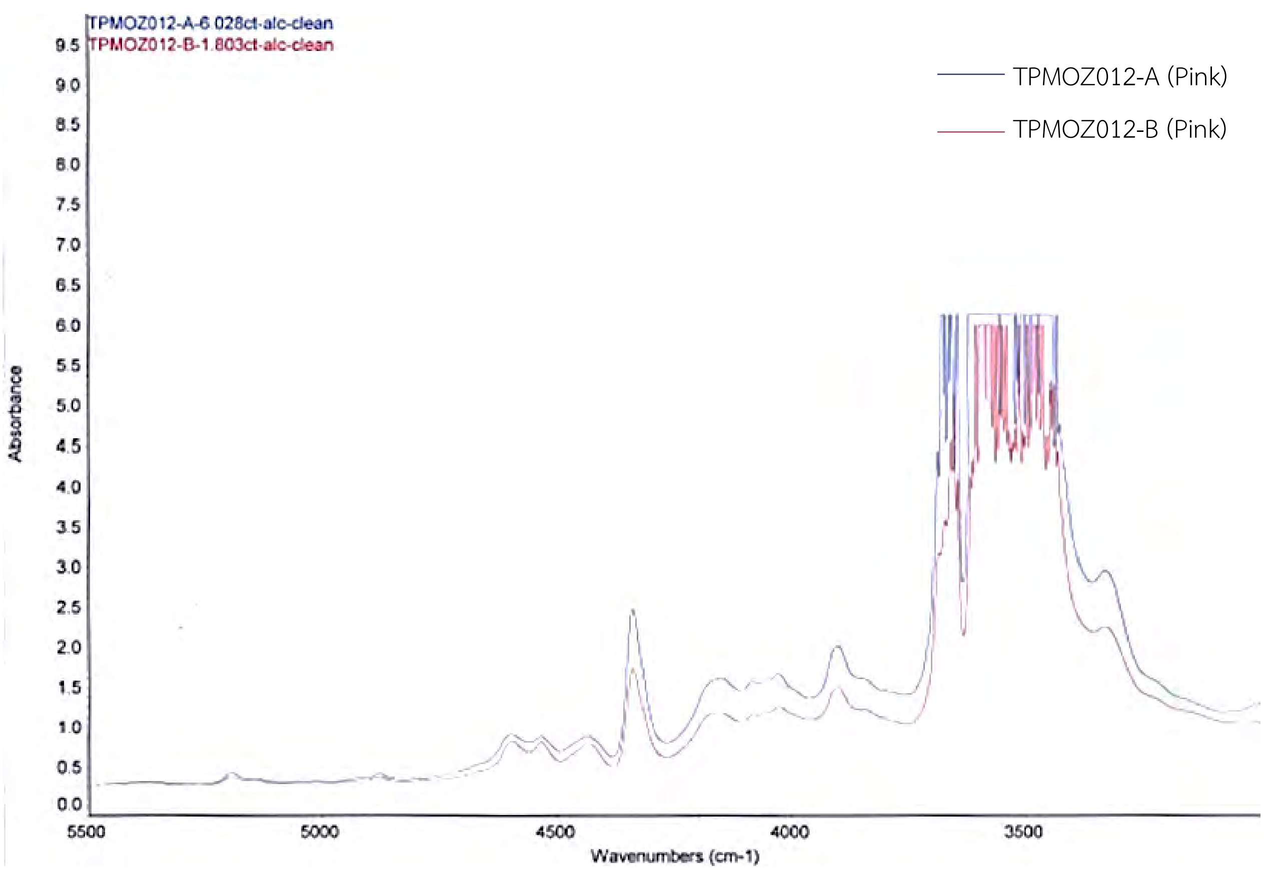

COMPARISON OF BEFORE AND AFTER GAMMA RAY IRRADIATED TOURMALINE SAMPLES

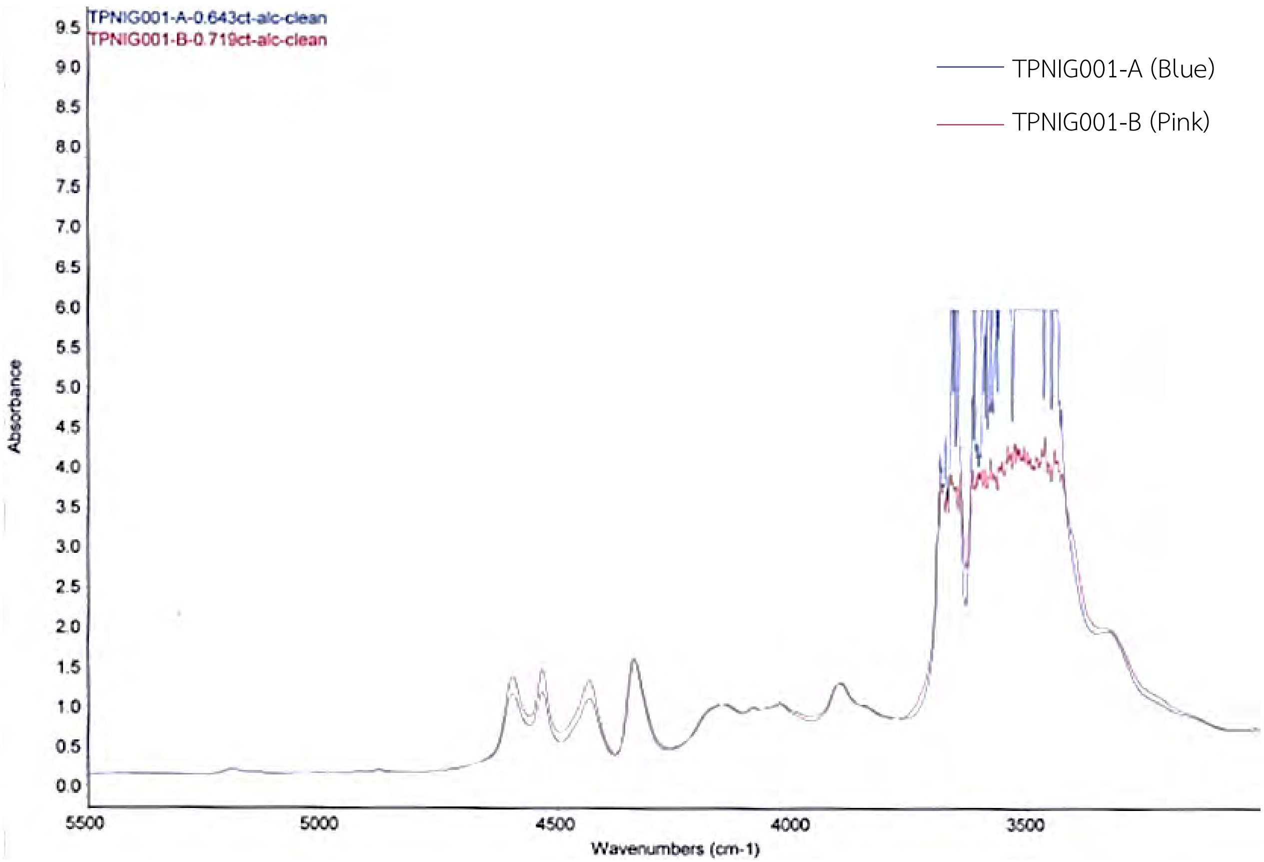

APPENDIX D

EDXRF RESULTS OF NATURAL TOURMALINE SAMPLES

AND EDXRF RESULTS OF AFTER FIRST GAMMA RAY IRRADIATED TOURMALINE SAMPLES

EDXRF RESULTS OF NATURAL BLUE (PARAIBA) TOURMALINE FROM BRAZIL (wt.%)

Sample	TPBRA004	TPBRA005	TPBRA006	TPBRA007	TPBRA008	TPBRA009	TPBRA012	TPBRA013	TPBRA014
Color	Blue (Raraiba)	Blue (Raraiba)	Blue (Raraiba)	Blue (Raraiba)	Blue (Raraiba)	Blue (Raraiba)	Blue (Raraiba)	Blue (Raraiba)	Blue (Raraiba)
SiO_2	36.55	34.57	34.20	34.62	34.65	34.22	33.85	34.10	34.04
TiO_2	0.02	0.01	0.01	0.05	0.02	0.09	0.05	0.09	0.06
Al_2O_3	41.57	42.79	43.05	43.21	43.80	42.11	42.97	41.89	41.89
Fe_2O_3	0.00	0.01	0.01	0.00	0.00	0.00	0.00	0.01	0.01
MnO	0.04	0.06	0.05	0.04	0.03	0.08	0.05	0.10	0.08
MgO	0.39	0.36	0.33	0.35	0.30	0.42	0.51	0.41	0.48
CaO	0.52	0.44	0.44	0.55	0.16	0.47	0.37	0.64	0.82
Na_2O	1.23	2.25	2.40	2.04	1.85	2.76	2.47	2.35	2.21
K_2O	0.08	0.05	0.08	0.04	0.07	0.12	0.06	0.15	0.10
P_2O_5	0.00	0.00	0.00	0.02	0.00	0.00	0.00	0.00	0.00
BaO	0.00	0.00	0.00	0.00	0.00	0.00	0.00	0.00	0.00
Rb_2O	0.00	0.00	0.00	0.00	0.00	0.00	0.00	0.00	0.00
SrO	0.00	0.00	0.00	0.00	0.00	0.00	0.00	0.00	0.00
Nb_2O_5	0.00	0.00	0.00	0.00	0.00	0.00	0.00	0.00	0.00
PbO_2	0.01	0.01	0.01	0.01	0.01	0.01	0.01	0.01	0.02
Ga_2O_3	0.07	0.04	0.06	0.05	0.06	0.12	0.06	0.09	0.07
ZnO	0.00	0.17	0.01	0.04	0.00	0.00	0.16	0.01	0.00
CuO	1.29	1.09	1.11	0.74	0.82	1.20	1.14	1.71	1.61
Ni_2O_3	0.00	0.00	0.00	0.00	0.00	0.00	0.00	0.00	0.00
V_2O_3	0.00	0.00	0.00	0.00	0.00	0.00	0.00	0.01	0.00
Cr_2O_3	0.00	0.00	0.00	0.00	0.00	0.00	0.00	0.00	0.00
CoO	0.00	0.00	0.00	0.00	0.00	0.00	0.00	0.00	0.00
W	0.00	0.00	0.00	0.00	0.00	0.00	0.00	0.00	0.00
SnO_2	0.00	0.00	0.00	0.00	0.00	0.01	0.00	0.00	0.00
Ce	0.01	0.00	0.00	0.00	0.00	0.00	0.00	0.01	0.01

EDXRF RESULTS OF NATURAL BLUE (PARAIBA) TOURMALINE FROM BRAZIL (wt.%)

Sample	TPBRA015	TPBRA016	TPBRA018	TPBRA020	TPBRA026	TPBRA027	TPBRA028	TPBRA029	TPBRA030
Color	Blue (Raraiba)	Blue (Raraiba)	Blue (Raraiba)	Blue (Raraiba)	Blue (Raraiba)	Blue (Raraiba)	Blue (Raraiba)	Blue (Raraiba)	Blue (Raraiba)
SiO_2	34.58	34.01	34.00	34.16	34.14	35.97	38.24	26.42	34.81
TiO_2	0.03	0.05	0.04	0.01	0.02	0.01	0.01	0.01	0.01
Al_2O_3	42.73	43.23	42.40	43.15	42.45	40.80	41.41	34.43	42.78
Fe_2O_3	0.00	0.00	0.00	0.01	0.01	0.00	0.00	0.00	0.00
MnO	0.04	0.06	0.08	0.06	0.08	0.03	0.00	0.00	0.05
MgO	0.42	0.36	0.30	0.45	0.47	0.30	0.37	0.39	0.39
CaO	0.32	0.47	0.57	0.46	0.79	0.23	0.35	0.04	0.37
Na_2O	2.18	2.03	1.90	1.76	2.29	1.09	1.43	0.94	2.27
K_2O	0.07	0.07	0.05	0.05	0.07	0.02	0.07	0.00	0.03
P_2O_5	0.00	0.00	0.19	0.00	0.00	0.10	0.00	0.00	0.00
BaO	0.00	0.00	0.00	0.00	0.00	0.00	0.00	0.01	0.00
Rb_2O	0.00	0.00	0.00	0.00	0.00	0.00	0.00	0.00	0.00
SrO	0.00	0.00	0.00	0.00	0.00	0.00	0.00	0.00	0.00
Nb_2O_5	0.00	0.00	0.00	0.00	0.00	0.00	0.00	0.00	0.00
PbO_2	0.01	0.01	0.01	0.01	0.01	0.01	0.00	0.00	0.01
Ga_2O_3	0.06	0.02	0.08	0.05	0.03	0.07	0.00	0.03	0.04
ZnO	0.37	0.16	0.01	0.14	0.00	0.00	0.00	2.98	0.01
CuO	0.96	1.20	2.01	1.47	1.16	0.78	0.00	1.14	1.05
Ni_2O_3	0.00	0.00	0.00	0.00	0.00	0.00	0.00	0.00	0.00
V_2O_3	0.00	0.00	0.00	0.00	0.00	0.00	0.00	0.00	0.00
Cr_2O_3	0.00	0.00	0.00	0.00	0.00	0.00	0.00	0.00	0.00
CoO	0.00	0.00	0.00	0.00	0.00	0.00	0.00	0.00	0.00
W	0.00	0.00	0.00	0.00	0.00	0.00	0.00	0.02	0.00
SnO_2	0.00	0.00	0.00	0.00	0.00	0.00	0.00	0.00	0.00
Ce	0.00	0.00	0.00	0.01	0.00	0.00	0.00	0.00	0.00

EDXRF RESULTS OF NATURAL BLUE (PARAIBA) TOURMALINE FROM BRAZIL (wt.%)

Sample	TPBRA042	TPBRA044	TPBRA046	TPBRA049	TPBRA050
Color	Blue (Raraiba)	Blue (Raraiba)	Blue (Raraiba)	Blue (Raraiba)	Blue (Raraiba)
SiO_2	33.81	33.96	33.92	32.93	34.14
TiO_2	0.00	0.00	0.01	0.01	0.00
Al_2O_3	42.07	43.79	42.27	43.02	43.56
Fe_2O_3	0.01	0.01	0.01	0.01	0.00
MnO	0.95	0.02	0.08	0.03	0.16
MgO	0.42	0.46	0.42	0.47	0.21
CaO	0.34	0.13	0.91	0.29	0.50
Na_2O	2.25	2.48	2.12	2.35	2.07
K_2O	0.04	0.08	0.04	0.05	0.00
P_2O_5	0.07	0.00	0.00	0.05	0.00
BaO	0.01	0.01	0.00	0.00	0.00
Rb_2O	0.00	0.00	0.00	0.00	0.00
SrO	0.00	0.00	0.00	0.00	0.00
Nb_2O_5	0.00	0.00	0.00	0.00	0.00
PbO_2	0.02	0.00	0.02	0.01	0.00
Ga_2O_3	0.03	0.09	0.07	0.10	0.06
ZnO	0.00	0.09	0.13	0.31	0.03
CuO	1.56	0.78	1.31	1.20	1.14
Ni_2O_3	0.00	0.00	0.00	0.00	0.00
V_2O_3	0.00	0.00	0.00	0.00	0.00
Cr_2O_3	0.00	0.00	0.00	0.00	0.00
CoO	0.00	0.00	0.00	0.00	0.00
W	0.00	0.00	0.00	0.00	0.00
SnO_2	0.00	0.00	0.00	0.00	0.00
Ce	0.00	0.00	0.00	0.00	0.00

EDXRF RESULTS OF NATURAL BLUE (NON-PARAIBA) TOURMALINE FROM BRAZIL (wt.%)

Sample	TPBRA032	TPBRA033	TPBRA034	TPBRA035	TPBRA036	TPBRA037	TPBRA043
Color	Blue (Non-Paraiba)	Blue (Non-Paraiba)	Blue (Non-Paraiba)	Blue (Non-Paraiba)	Blue (Non-Paraiba)	Blue (Non-Paraiba)	Blue (Non-Paraiba)
SiO_2	32.92	32.70	33.36	32.87	32.97	33.41	32.41
TiO_2	0.05	0.06	0.11	0.01	0.02	0.00	0.03
Al_2O_3	41.14	41.31	40.44	44.34	41.49	40.16	39.32
Fe_2O_3	0.08	0.17	0.04	0.13	0.07	0.02	0.22
MnO	2.91	3.17	2.28	0.42	2.82	3.59	1.32
MgO	0.44	0.42	0.30	0.53	0.43	0.39	0.33
CaO	0.41	0.41	0.95	0.19	0.45	0.58	0.26
Na_2O	2.58	2.35	1.94	2.55	2.55	2.62	2.25
K_2O	0.04	0.07	0.09	0.08	0.03	0.04	0.04
P_2O_5	0.00	0.00	0.04	0.00	0.00	0.00	0.00
BaO	0.00	0.00	0.00	0.01	0.00	0.00	0.00
Rb_2O	0.00	0.00	0.00	0.00	0.00	0.00	0.00
SrO	0.00	0.00	0.00	0.00	0.00	0.00	0.00
Nb_2O_5	0.00	0.00	0.00	0.00	0.00	0.00	0.00
PbO_2	0.00	0.00	0.01	0.00	0.01	0.02	0.09
Ga_2O_3	0.06	0.06	0.07	0.05	0.03	0.04	0.01
ZnO	0.05	0.14	0.01	0.07	0.09	0.07	0.02
CuO	1.22	1.09	2.03	0.70	0.92	0.95	3.49
Ni_2O_3	0.01	0.00	0.00	0.00	0.00	0.00	0.00
V_2O_3	0.00	0.00	0.00	0.00	0.00	0.00	0.00
Cr_2O_3	0.00	0.00	0.01	0.00	0.00	0.00	0.00
CoO	0.00	0.00	0.00	0.00	0.00	0.00	0.00
W	0.00	0.00	0.00	0.00	0.01	0.00	0.00
SnO_2	0.00	0.00	0.00	0.00	0.00	0.00	0.01
Ce	0.00	0.00	0.00	0.00	0.00	0.00	0.00

EDXRF RESULTS OF NATURAL PURPLE TOURMALINE FROM BRAZIL (wt.%)

Sample	TPBRA001	TPBRA002	TPBRA003	TPBRA010	TPBRA022	TPBRA023	TPBRA024	TPBRA025	TPBRA042
Color	Purple	Purple	Purple	Purple	Purple	Purple	Purple	Purple	Purple
SiO_2	32.85	37.03	34.93	34.98	33.72	33.34	34.59	32.72	32.88
TiO_2	0.09	0.01	0.02	0.01	0.02	0.05	0.03	0.14	0.01
Al_2O_3	39.82	40.14	43.17	42.07	43.03	42.46	42.75	40.39	42.14
Fe_2O_3	0.09	0.01	0.01	0.00	0.01	0.00	0.00	0.02	0.03
MnO	3.47	0.32	0.07	0.14	0.22	0.23	0.05	1.65	2.43
MgO	0.43	0.32	0.39	0.35	0.50	0.45	0.53	0.50	0.32
CaO	0.87	1.02	0.38	0.58	0.50	1.09	0.35	1.00	0.20
Na_2O	2.52	1.17	1.95	2.27	2.50	2.07	2.42	2.58	2.27
K_2O	0.13	0.07	0.06	0.05	0.05	0.07	0.06	0.10	0.06
P_2O_5	0.00	0.00	0.00	0.00	0.00	0.00	0.00	0.00	0.00
BaO	0.00	0.00	0.00	0.00	0.01	0.00	0.01	0.00	0.01
Rb_2O	0.00	0.00	0.00	0.00	0.00	0.00	0.00	0.01	0.00
SrO	0.00	0.00	0.00	0.00	0.00	0.00	0.00	0.00	0.00
Nb_2O_5	0.00	0.00	0.00	0.00	0.00	0.00	0.00	0.00	0.00
PbO_2	0.01	0.01	0.00	0.01	0.00	0.02	0.01	0.01	0.02
Ga_2O_3	0.07	0.07	0.06	0.07	0.06	0.07	0.07	0.07	0.05
ZnO	0.18	0.04	0.00	0.09	0.05	0.02	0.03	0.10	0.01
CuO	1.14	1.62	0.70	1.17	1.20	1.68	0.88	2.33	1.33
Ni_2O_3	0.00	0.00	0.00	0.00	0.00	0.00	0.00	0.00	0.00
V_2O_3	0.00	0.00	0.00	0.00	0.00	0.00	0.00	0.00	0.00
Cr_2O_3	0.00	0.00	0.02	0.00	0.00	0.00	0.00	0.00	0.00
CoO	0.00	0.00	0.00	0.00	0.00	0.00	0.00	0.00	0.00
W	0.00	0.00	0.00	0.00	0.00	0.00	0.00	0.00	0.00
SnO_2	0.00	0.00	0.01	0.00	0.00	0.00	0.00	0.00	0.00
Ce	0.00	0.00	0.00	0.00	0.00	0.00	0.00	0.00	0.00

EDXRF RESULTS OF NATURAL PURPLE TOURMALINE FROM BRAZIL (wt.%)

Sample	TPBRA051	TPBRA052	TPBRA053	TPBRA054	TPBRA055
Color	Purple	Purple	Purple	Purple	Purple
SiO_2	32.98	32.87	33.67	32.23	34.50
TiO_2	0.14	0.11	0.01	0.02	0.00
Al_2O_3	41.68	41.59	43.62	42.47	42.26
Fe_2O_3	0.01	0.01	0.00	0.02	0.00
MnO	0.35	0.47	0.18	0.10	0.32
MgO	0.49	0.48	0.45	0.62	0.42
CaO	0.73	0.80	0.52	0.53	0.91
Na_2O	2.35	2.25	2.20	2.96	1.98
K_2O	0.13	0.08	0.07	0.04	0.03
P_2O_5	0.00	0.00	0.00	0.00	0.00
BaO	0.00	0.00	0.01	0.00	0.01
Rb_2O	0.00	0.00	0.00	0.00	0.00
SrO	0.00	0.00	0.00	0.00	0.00
Nb_2O_5	0.00	0.00	0.00	0.00	0.00
PbO_2	0.01	0.02	0.01	0.01	0.01
Ga_2O_3	0.13	0.11	0.06	0.08	0.06
ZnO	0.04	0.35	0.01	1.14	0.01
CuO	2.00	1.76	1.05	1.28	1.29
Ni_2O_3	0.00	0.00	0.00	0.00	0.00
V_2O_3	0.00	0.00	0.00	0.00	0.00
Cr_2O_3	0.00	0.00	0.00	0.00	0.00
CoO	0.00	0.00	0.00	0.00	0.00
W	0.00	0.00	0.00	0.03	0.00
SnO_2	0.00	0.00	0.00	0.00	0.00
Ce	0.01	0.02	0.00	0.00	0.00

EDXRF RESULTS OF NATURAL PINK TOURMALINE FROM BRAZIL (wt.%)

Sample	TPBRA017	TPBRA019
Color	Pink	Pink
SiO_2	32.68	32.73
TiO_2	0.11	0.09
Al_2O_3	39.76	40.90
Fe_2O_3	0.69	0.50
MnO	3.35	3.29
MgO	0.35	0.42
CaO	0.27	0.20
Na_2O	3.08	2.59
K_2O	0.06	0.07
P_2O_5	0.00	0.00
BaO	0.01	0.00
Rb_2O	0.00	0.00
SrO	0.00	0.00
Nb_2O_5	0.00	0.00
PbO_2	0.00	0.00
Ga_2O_3	0.06	0.07
ZnO	0.97	0.67
CuO	0.43	0.30
Ni_2O_3	0.00	0.00
V_2O_3	0.01	0.00
Cr_2O_3	0.00	0.00
CoO	0.00	0.00
W	0.02	0.02
SnO_2	0.00	0.01
Ce	0.01	0.00

EDXRF RESULTS OF NATURAL GREEN TOURMALINE FROM BRAZIL (wt.%)

Sample	TPBRA031	TPBRA036	TPBRA037	TPBRA038-A	TPBRA039-A	TPBRA040-A	TPBRA041-A	TPBRA042	TPBRA043
Color	Green	Green	Green	Green	Green	Green	Green	Green	Green
SiO_2	30.61	34.62	33.49	33.78	33.07	32.95	33.41	33.40	32.46
TiO_2	0.14	0.02	0.04	0.10	0.12	0.13	0.07	0.09	0.10
Al_2O_3	37.25	41.45	40.80	40.32	39.75	39.67	40.41	40.01	39.97
Fe_2O_3	0.10	0.23	0.26	0.15	0.05	0.14	0.02	1.01	0.99
MnO	2.53	2.61	2.65	2.67	4.77	4.72	4.05	2.57	2.66
MgO	1.11	0.34	0.26	0.50	0.40	0.40	0.42	0.40	0.45
CaO	0.33	0.07	0.37	0.84	0.32	0.29	0.30	0.28	0.37
Na_2O	3.59	2..49	2.47	2.42	2.85	2.83	2.67	2.47	2.29
K_2O	0.12	0.04	0.02	0.08	0.03	0.03	0.03	0.03	0.02
P_2O_5	0.41	0.00	0.00	0.08	0.00	0.00	0.00	0.00	0.05
BaO	0.00	0.00	0.01	0.00	0.00	0.00	0.00	0.00	0.00
Rb_2O	0.00	0.00	0.00	0.00	0.00	0.00	0.00	0.00	0.00
SrO	0.00	0.00	0.00	0.00	0.00	0.00	0.00	0.00	0.00
Nb_2O_5	0.00	0.00	0.00	0.00	0.00	0.00	0.00	0.00	0.00
PbO_2	0.00	0.00	0.01	0.01	0.01	0.01	0.01	0.01	0.03
Ga_2O_3	0.03	0.00	0.03	0.04	0.03	0.03	0.04	0.03	0.04
ZnO	3.10	0.03	0.44	0.01	0.08	0.38	0.00	0.09	0.09
CuO	2.08	0.05	1.04	0.47	0.46	0.34	0.46	0.98	1.40
Ni_2O_3	0.00	0.00	0.00	0.00	0.00	0.01	0.00	0.00	0.00
V_2O_3	0.00	0.00	0.00	0.00	0.00	0.00	0.00	0.00	0.00
Cr_2O_3	0.12	0.00	0.00	0.00	0.00	0.00	0.00	0.00	0.01
CoO	0.00	0.00	0.00	0.00	0.00	0.00	0.00	0.00	0.00
W	0.04	0.00	0.00	0.00	0.00	0.02	0.00	0.00	0.00
SnO_2	0.00	0.00	0.00	0.00	0.00	0.00	0.00	0.00	0.00
Ce	0.00	0.00	0.00	0.00	0.00	0.00	0.00	0.01	0.01

EDXRF RESULTS OF NATURAL BLUE (NON-PARAIBA) TOURMALINE FROM NAMPULA IN MOZAMBIQUE (wt.%)

Sample	TPMOZ007	TPMOZ008
Color	Blue (Non-Paraiba)	Blue (Non-Paraiba)
SiO_2	33.83	33.62
TiO_2	0.02	0.02
Al_2O_3	42.15	41.80
Fe_2O_3	0.17	0.02
MnO	2.45	3.14
MgO	0.37	0.33
CaO	0.11	0.13
Na_2O	2.49	2.50
K_2O	0.02	0.02
P_2O_5	0.00	0.01
BaO	0.00	0.01
Rb_2O	0.00	0.00
SrO	0.00	0.00
Nb_2O_5	0.00	0.00
PbO_2	0.00	0.00
Ga_2O_3	0.07	0.11
ZnO	0.00	0.00
CuO	0.27	0.26
Ni_2O_3	0.00	0.00
V_2O_3	0.00	0.00
Cr_2O_3	0.00	0.00
CoO	0.00	0.00
W	0.00	0.00
SnO_2	0.00	0.00
Ce	0.00	0.00

EDXRF RESULTS OF NATURAL PINK TOURMALINE FROM NAMPULA IN MOZAMBIQUE (wt.%)

Sample	TPMOZ002-A	TPMOZ003	TPMOZ005	TPMOZ10-A	TPMOZ012-A	TPMOZ013-A
Color	Pink	Pink	Pink	Pink	Pink	Pink
SiO_2	33.89	34.09	33.51	34.10	34.47	34.17
TiO_2	0.01	0.00	0.01	0.00	0.00	0.00
Al_2O_3	41.99	43.83	41.05	42.93	43.67	43.06
Fe_2O_3	0.02	0.03	0.02	0.01	0.00	0.00
MnO	2.89	0.60	3.25	1.50	0.34	1.12
MgO	0.36	0.39	0.37	0.37	0.34	0.40
CaO	0.08	0.14	0.48	0.22	0.42	0.35
Na_2O	2.47	2.42	2.21	2.51	2.28	2.34
K_2O	0.03	0.05	0.06	0.03	0.03	0.03
P_2O_5	0.00	0.10	0.27	0.00	0.00	0.00
BaO	0.00	0.00	0.01	0.00	0.00	0.00
Rb_2O	0.00	0.00	0.00	0.00	0.00	0.00
SrO	0.00	0.00	0.00	0.00	0.00	0.00
Nb_2O_5	0.00	0.00	0.00	0.00	0.00	0.00
PbO_2	0.00	0.00	0.01	0.00	0.01	0.00
Ga_2O_3	0.07	0.08	0.07	0.11	0.10	0.07
ZnO	0.00	0.00	0.00	0.00	0.00	0.00
CuO	0.19	0.24	0.33	0.16	0.14	0.37
Ni_2O_3	0.00	0.00	0.00	0.00	0.00	0.00
V_2O_3	0.00	0.00	0.00	0.00	0.01	0.00
Cr_2O_3	0.00	0.00	0.03	0.00	0.00	0.00
CoO	0.00	0.00	0.00	0.00	0.00	0.00
W	0.00	0.00	0.00	0.00	0.00	0.00
SnO_2	0.00	0.00	0.00	0.00	0.01	0.00
Ce	0.00	0.00	0.00	0.01	0.00	0.00

EDXRF RESULTS OF NATURAL GREEN AND COLORLESS TOURMALINE FROM NAMPULA IN MOZAMBIQUE (wt.%)

Sample	TPMOZ004-A	TPMOZ006	TPMOZ009-A	TPMOZ011-A	TPMOZ001
Color	Green	Green	Green	Green	Colorless
SiO_2	32.53	32.54	33.52	34.68	33.80
TiO_2	0.19	0.18	0.17	0.01	0.01
Al_2O_3	38.62	38.97	38.25	43.05	42.29
Fe_2O_3	0.31	0.25	0.14	0.08	0.02
MnO	5.81	5.49	5.44	0.10	2.52
MgO	0.36	0.41	0.43	0.49	0.37
CaO	0.27	0.28	0.29	0.14	0.09
Na_2O	2.87	3.00	2.79	2.33	2.64
K_2O	0.03	0.03	0.01	0.05	0.03
P_2O_5	0.00	0.00	0.01	0.00	0.00
BaO	0.00	0.00	0.00	0.01	0.00
Rb_2O	0.00	0.00	0.00	0.00	0.00
SrO	0.00	0.00	0.00	0.00	0.00
Nb_2O_5	0.00	0.00	0.00	0.00	0.00
PbO_2	0.01	0.00	0.03	0.01	0.00
Ga_2O_3	0.07	0.05	0.06	0.04	0.07
ZnO	0.06	0.04	0.02	0.00	0.00
CuO	0.79	0.69	0.75	0.25	0.14
Ni_2O_3	0.00	0.00	0.00	0.00	0.00
V_2O_3	0.00	0.00	0.00	0.00	0.01
Cr_2O_3	0.00	0.00	0.00	0.00	0.00
CoO	0.00	0.00	0.00	0.00	0.00
W	0.00	0.00	0.00	0.00	0.00
SnO_2	0.00	0.00	0.01	0.00	0.00
Ce	0.00	0.00	0.00	0.00	0.00

EDXRF RESULTS OF NATURAL BLUE (PARIBA), BLUE (NON-PARAIBA),

AND COLORLESS TOURMALINE FROM JOS IN NIGERIA (wt.%)

Sample	TPNIG001-A	TPNIG002-B	TPNIG003	TPNIG002-A
Color	Blue (Paraiba)	Blue (Non-Paraiba)	Blue (Non-Paraiba)	Colorless
SiO_2	34.75	34.52	34.50	32.90
TiO_2	0.00	0.07	0.01	0.15
Al_2O_3	43.02	41.60	41.75	39.97
Fe_2O_3	0.01	0.88	0.77	2.62
MnO	0.36	0.25	0.68	1.90
MgO	0.39	0.49	0.32	0.44
CaO	0.63	0.52	0.56	1.10
Na_2O	2.05	2.29	2.37	2.24
K_2O	0.03	0.03	0.04	0.05
P_2O_5	0.00	0.00	0.00	0.01
BaO	0.00	0.00	0.00	0.01
Rb_2O	0.02	0.00	0.00	0.00
SrO	0.00	0.01	0.01	0.01
Nb_2O_5	0.00	0.00	0.00	0.00
PbO_2	0.17	0.02	0.25	0.02
Ga_2O_3	0.03	0.03	0.03	0.05
ZnO	0.00	0.00	0.12	0.01
CuO	0.45	0.32	0.45	0.32
Ni_2O_3	0.00	0.00	0.00	0.00
V_2O_3	0.00	0.01	0.00	0.01
Cr_2O_3	0.00	0.00	0.00	0.00
CoO	0.00	0.00	0.00	0.00
W	0.00	0.00	0.00	0.00
SnO_2	0.00	0.00	0.00	0.00
Ce	0.00	0.00	0.01	0.01

EDXRF RESULTS OF NATURAL GREEN TOURMALINE FROM MADAGASCAR (wt.%)

Sample	TPEA001
Color	Green
SiO_2	31.79
TiO_2	0.45
Al_2O_3	34.03
Fe_2O_3	0.03
MnO	0.04
MgO	11.32
CaO	1.50
Na_2O	2.18
K_2O	0.11
P_2O_5	0.00
BaO	0.00
Rb_2O	0.00
SrO	0.01
Nb_2O_5	0.00
PbO_2	0.00
Ga_2O_3	0.00
ZnO	0.01
CuO	0.00
Ni_2O_3	0.00
V_2O_3	0.36
Cr_2O_3	0.01
CoO	0.00
W	0.00
SnO_2	0.00
Ce	0.03

EDXRF RESULTS OF NATURAL GREEN TOURMALINE FROM EAST AFRICA (wt.%)

Sample	TPEA002	TPEA003	TPEA004	TPEA005	TPEA006	TPEA007	TPEA008	TPEA009
Color	Green	Green	Green	Green	Green	Green	Green	Green
SiO_2	35.03	32.82	32.70	34.02	36.08	32.23	34.84	33.57
TiO_2	0.66	0.02	0.02	0.62	0.02	0.89	0.04	0.02
Al_2O_3	29.44	38.26	38.37	26.68	39.40	25.41	38.25	40.45
Fe_2O_3	0.01	2.95	4.34	0.01	1.80	0.01	4.38	2.01
MnO	0.01	3.79	1.42	0.03	2.09	0.02	1.37	1.76
MgO	11.36	0.41	0.58	12.66	0.32	12.37	0.49	0.52
CaO	2.35	0.60	0.47	5.16	0.53	4.47	0.34	0.65
Na_2O	1.78	2.90	3.22	1.20	1.42	1.51	1.78	2.66
K_2O	0.11	0.05	0.04	0.11	0.05	0.09	0.04	0.03
P_2O_5	0.00	0.00	0.01	0.00	0.00	0.02	0.00	0.00
BaO	0.00	0.05	0.02	0.00	0.00	0.01	0.00	0.00
Rb_2O	0.00	0.00	0.00	0.00	0.00	0.00	0.00	0.00
SrO	0.40	0.00	0.00	0.33	0.00	0.29	0.00	0.00
Nb_2O_5	0.00	0.00	0.00	0.00	0.00	0.00	0.00	0.00
PbO_2	0.00	0.01	0.12	0.00	0.05	0.00	0.02	0.05
Ga_2O_3	0.00	0.03	0.03	0.01	0.05	0.01	0.05	0.05
ZnO	0.00	0.04	0.48	0.00	0.10	0.00	0.28	0.12
CuO	0.00	0.00	0.01	0.00	0.01	0.00	0.01	0.00
Ni_2O_3	0.00	0.00	0.00	0.00	0.00	0.00	0.00	0.00
V_2O_3	0.51	0.00	0.00	0.71	0.00	0.47	0.00	0.00
Cr_2O_3	0.08	0.00	0.00	0.18	0.00	0.17	0.00	0.00
CoO	0.00	0.01	0.00	0.00	0.00	0.00	0.00	0.00
W	0.00	0.00	0.01	0.00	0.00	0.00	0.00	0.01
SnO_2	0.00	0.00	0.02	0.00	0.01	0.00	0.01	0.02
Ce	0.05	0.01	0.01	0.08	0.01	0.08	0.01	0.00

EDXRF RESULTS OF NATURAL GREEN TOURMALINE FROM EAST AFRICA (wt.%)

Sample	TPEA010	TPEA011	TPEA012	TPEA013	TPEA014	TPEA015	TPEA016	TPEA017
Color	Green	Green	Green	Green	Green	Green	Green	Green
SiO_2	32.07	32.30	35.72	30.19	30.58	32.67	31.86	30.18
TiO_2	0.63	1.05	0.02	1.54	0.81	0.02	0.76	1.65
Al_2O_3	27.67	27.81	38.04	26.78	27.07	40.12	27.49	26.65
Fe_2O_3	0.00	0.01	2.01	0.02	0.01	2.97	0.03	0.02
MnO	0.02	0.01	2.02	0.02	0.02	1.55	0.02	0.02
MgO	15.65	15.65	0.45	15.75	15.91	0.36	15.48	15.64
CaO	3.21	2.29	0.44	3.81	4.19	0.65	3.65	3.54
Na_2O	1.56	1.95	2.76	2.08	1.83	2.79	1.65	2.23
K_2O	0.05	0.06	0.06	0.11	0.13	0.03	0.08	0.07
P_2O_5	0.00	0.00	0.00	0.00	0.00	0.40	0.00	0.04
BaO	0.00	0.05	0.00	0.11	0.05	0.00	0.09	0.12
Rb_2O	0.00	0.00	0.00	0.00	0.00	0.00	0.00	0.00
SrO	0.42	0.36	0.01	0.38	0.52	0.00	0.30	0.36
Nb_2O_5	0.00	0.00	0.00	0.00	0.00	0.00	0.00	0.00
PbO_2	0.00	0.00	0.16	0.00	0.00	0.09	0.00	0.00
Ga_2O_3	0.01	0.01	0.02	0.02	0.01	0.04	0.01	0.01
ZnO	0.00	0.00	0.16	0.00	0.00	0.24	0.01	0.01
CuO	0.00	0.00	0.00	0.01	0.00	0.00	0.00	0.01
Ni_2O_3	0.00	0.00	0.00	0.00	0.00	0.00	0.00	0.00
V_2O_3	0.39	0.20	0.01	0.14	0.45	0.01	0.24	0.00
Cr_2O_3	0.12	0.08	0.00	0.20	0.18	0.00	0.18	0.15
CoO	0.00	0.00	0.00	0.00	0.00	0.00	0.00	0.00
W	0.00	0.00	0.01	0.00	0.00	0.01	0.00	0.00
SnO_2	0.00	0.00	0.02	0.01	0.00	0.01	0.00	0.01
Ce	0.06	0.04	0.02	0.00	0.03	0.01	0.04	0.00

EDXRF RESULTS OF AFTER FIRST GAMMA RAY IRRADIATED TOURMALINE SAMPLES (wt.%)

Sample	TPBRA038-B1	TPBRA039-B1	TPBRA040-B1	TPBRA041-B1	TPMOZ002-B1	TPMOZ004-B1
Color	Pink	Pink	Pink	Pink	Pink	Green
SiO_2	33.64	33.13	32.30	33.08	34.02	33.54
TiO_2	0.01	0.08	0.12	0.07	0.01	0.13
Al_2O_3	41.19	39.72	38.63	39.77	41.93	39.60
Fe_2O_3	0.04	0.04	0.22	0.02	0.03	0.45
MnO	2.60	4.91	4.96	4.39	2.63	4.22
MgO	0.61	0.49	0.78	0.63	0.48	0.43
CaO	0.12	0.28	0.27	0.30	0.08	0.19
Na_2O	2.88	2.66	3.12	2.89	2.48	2.80
K_2O	0.06	0.03	0.04	0.04	0.04	0.00
P_2O_5	0.06	0.02	0.14	0.02	0.06	0.02
BaO	0.00	0.00	0.01	0.01	0.00	0.01
Rb_2O	0.00	0.00	0.00	0.00	0.00	0.00
SrO	0.00	0.00	0.00	0.00	0.00	0.00
Nb_2O_5	0.00	0.00	0.00	0.00	0.00	0.00
PbO_2	0.02	0.01	0.02	0.02	0.00	0.00
Ga_2O_3	0.06	0.03	0.06	0.05	0.06	0.04
ZnO	0.01	0.02	0.83	0.01	0.00	0.09
CuO	0.57	0.50	0.41	0.45	0.16	0.42
Ni_2O_3	0.00	0.00	0.00	0.00	0.00	0.00
V_2O_3	0.00	0.00	0.00	0.00	0.00	0.00
Cr_2O_3	0.00	0.00	0.00	0.00	0.00	0.00
CoO	0.00	0.00	0.00	0.00	0.00	0.00
W	0.00	0.00	0.01	0.00	0.00	0.00
SnO_2	0.01	0.00	0.00	0.01	0.00	0.00
Ce	0.00	0.00	0.01	0.01	0.00	0.00

EDXRF RESULTS OF AFTER FIRST GAMMA RAY IRRADIATED TOURMALINE SAMPLES (wt.%)

Sample	TPMOZ009-B1	TPMOZ010-B1	TPMOZ011-B1	TPMOZ012-B1	TPMOZ013-B1	TPNIG001-B1
Color	Green	Pink	Pink	Pink	Pink	Pink
SiO_2	32.08	34.58	35.75	34.96	34.68	34.42
TiO_2	0.15	0.00	0.01	0.00	0.00	0.01
Al_2O_3	38.30	42.55	42.23	43.29	43.08	42.79
Fe_2O_3	0.40	0.01	0.01	0.02	0.01	0.02
MnO	5.81	1.44	0.12	0.24	1.04	0.26
MgO	0.48	0.48	0.45	0.48	0.41	0.65
CaO	0.28	0.20	0.63	0.32	0.09	0.61
Na_2O	3.08	2.38	1.93	2.25	2.35	2.24
K_2O	0.04	0.03	0.03	0.03	0.01	0.07
P_2O_5	0.06	0.08	0.13	0.11	0.05	0.09
BaO	0.00	0.00	0.00	0.00	0.00	0.00
Rb_2O	0.00	0.00	0.00	0.00	0.00	0.00
SrO	0.00	0.00	0.00	0.00	0.00	0.01
Nb_2O_5	0.00	0.00	0.00	0.00	0.00	0.00
PbO_2	0.01	0.00	0.00	0.00	0.00	0.16
Ga_2O_3	0.10	0.08	0.05	0.06	0.07	0.03
ZnO	0.09	0.00	0.00	0.00	0.00	0.00
CuO	1.00	0.11	0.07	0.09	0.19	0.41
Ni_2O_3	0.00	0.00	0.00	0.00	0.00	0.00
V_2O_3	0.01	0.00	0.00	0.00	0.00	0.00
Cr_2O_3	0.00	0.02	0.00	0.00	0.00	0.06
CoO	0.00	0.00	0.00	0.00	0.00	0.00
W	0.00	0.00	0.00	0.00	0.00	0.00
SnO_2	0.00	0.00	0.00	0.00	0.00	0.00
Ce	0.00	0.00	0.00	0.01	0.00	0.01